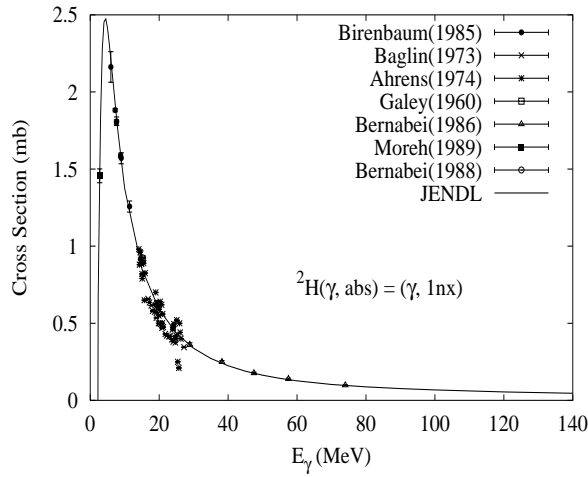


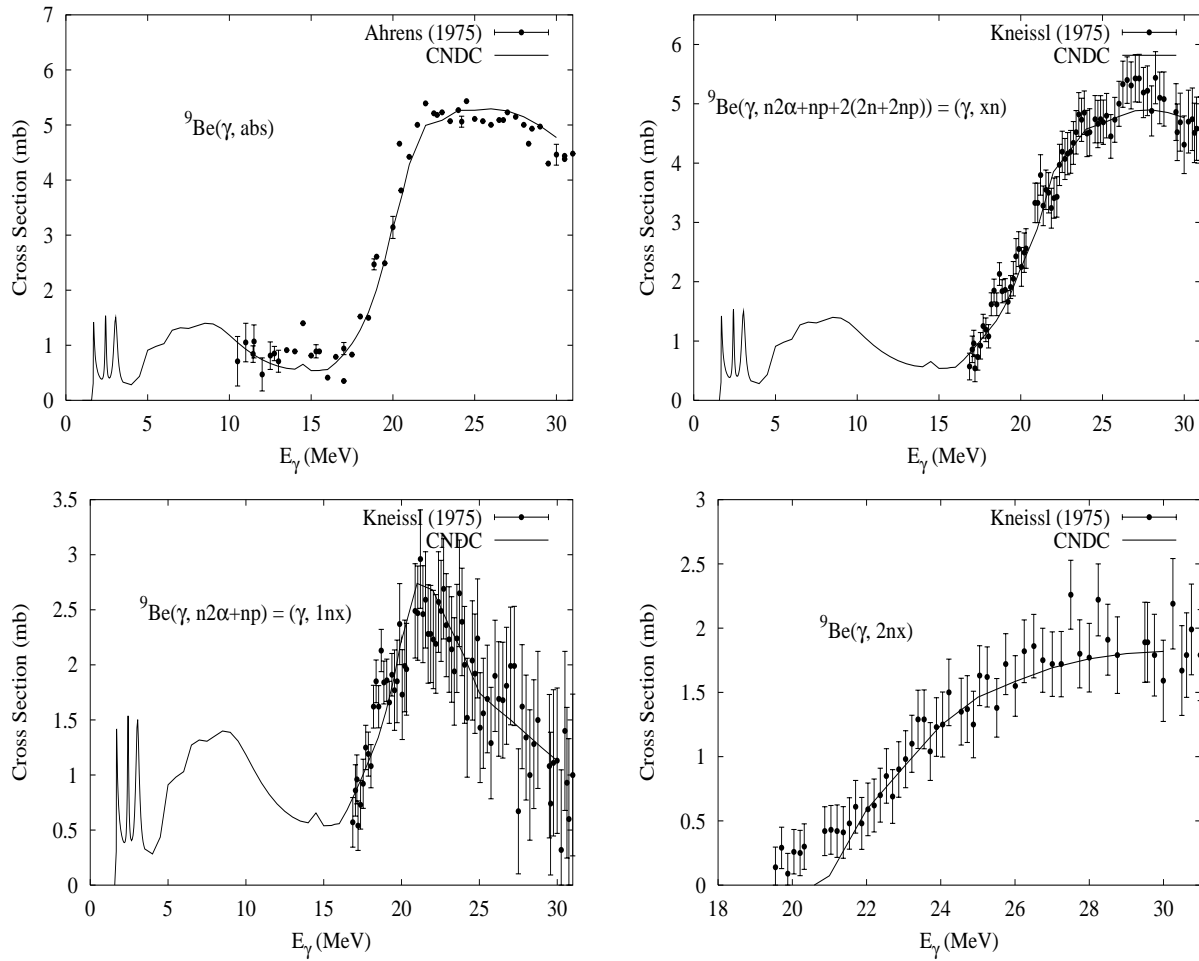
$\gamma + {}^2\text{H}$ 

Abundance (%)	Threshold Energies (MeV)								
	$\gamma, n$	$\gamma, p$	$\gamma, t$	$\gamma, \text{He-3}$	$\gamma, \alpha$	$\gamma, 2n$	$\gamma, np$	$\gamma, 2p$	$\gamma, 3n$
0.01	2.22	*	*	*	*	*	*	*	*



Deuteron's low photoneutron threshold (2.22 MeV) makes it an important potential neutron source in applications that include heavy water. Because of its light mass, the nuclear theories described in this report are unsuitable for modeling deuteron photodisintegration. Instead, use was made of models of Marshall + Guth [Mar50] and Partovi [Par64]. Furthermore, the evaluation was closely based on the measurements of [Ale68, All55, Bar52a, Bar52b, Bir85, Bis50, Deb92, Gal60, Hal53, Hou50, Kec56, McM55, Mor89, Phi50, Sne50, Waf51, Wha56]. Angular distributions of the photoneutrons are provided in the evaluation. Further details are given in [Mur94].

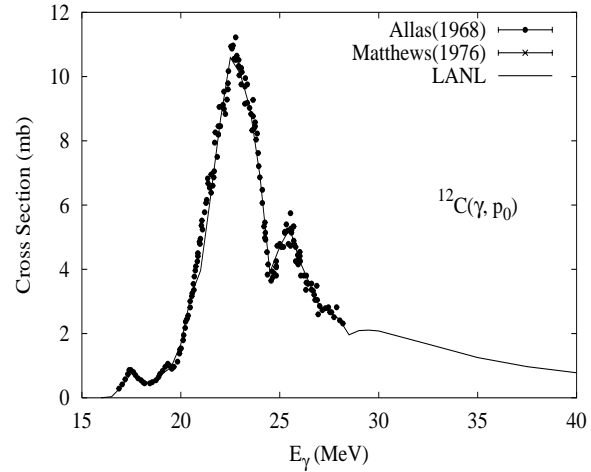
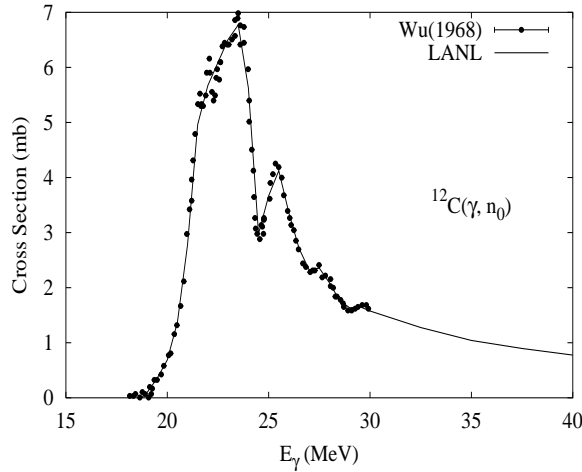
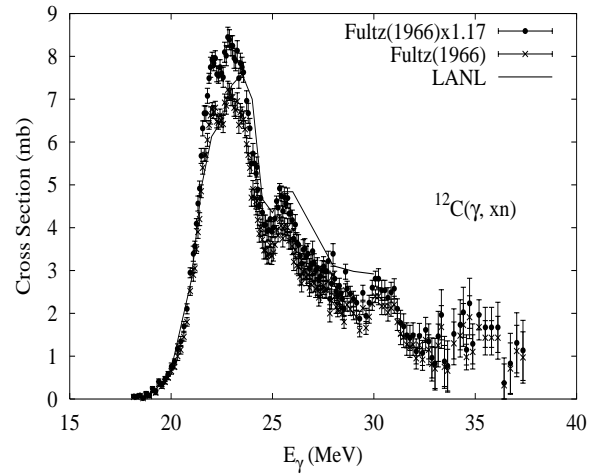
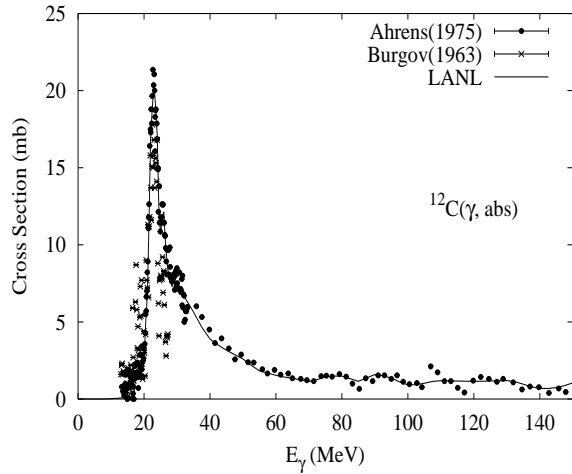
Abundance (%)	Threshold Energies (MeV)							
	$\gamma, n+2\alpha$	$\gamma, p$	$\gamma, t$	$\gamma, \text{He-3}$	$\gamma, 2n$	$\gamma, np$	$\gamma, 2p$	$\gamma, 3n$
100.00	1.67	16.89	17.69	21.18	20.56	18.92	29.34	31.24



The measured data of  $\sigma(\gamma, \text{abs})$  are taken from J.Ahrens [Ahr75] and the photonuclear data of  $(\gamma, 1n)$ ,  $(\gamma, 2n)$ ,  $(\gamma, np)$  reactions are taken from U.kneissl [Kne75], R.D.Edge [Edg57], J.H.Gibbons [Gib59], W.John [Joh62] and M.Fujishiro [Fuj82]. The experimental data were evaluated to guide the model calculation with code GLUNF [Zha99] up to 30 MeV, in which the file 6 in ENDF/B-VI format are given with full energy balance. However, below 16 MeV, the model calculation could not reproduce the experimental data of the  $(\gamma, 1n)$  reaction, while these data have been performed by T.Fukohari [Fuk99] by using GDR multiple Lorentzian fitting, which have been adopted in this work.

At low energy ( $< 30$  MeV), the giant-dipole resonance is the dominant excitation mechanism, in this energy region a simple isotropic approximation was used for the angular distribution of outgoing particles. The double differential cross sections include  $(\gamma, 1n)$ ,  $(\gamma, 2n)$  ${}^7\text{Be}$ ,  $(\gamma, np)$  ${}^7\text{Li}$  reaction channels. In the  $(\gamma, np)$  ${}^7\text{Li}^*$  reaction channel, the spectra of neutron, proton,  ${}^7\text{Li}$  and gamma as well as gamma-Multiplicity are involved in the file 6.

Abundance (%)	Threshold Energies (MeV)								
	$\gamma, n$	$\gamma, p$	$\gamma, t$	$\gamma, \text{He-3}$	$\gamma, \alpha$	$\gamma, 2n$	$\gamma, np$	$\gamma, 2p$	$\gamma, 3n$
98.89	18.72	15.96	27.37	26.28	7.37	31.84	27.41	27.19	53.13



Our evaluation of photonuclear reactions on carbon follows, to a large extent, the analysis described by Fuller [Ful85].

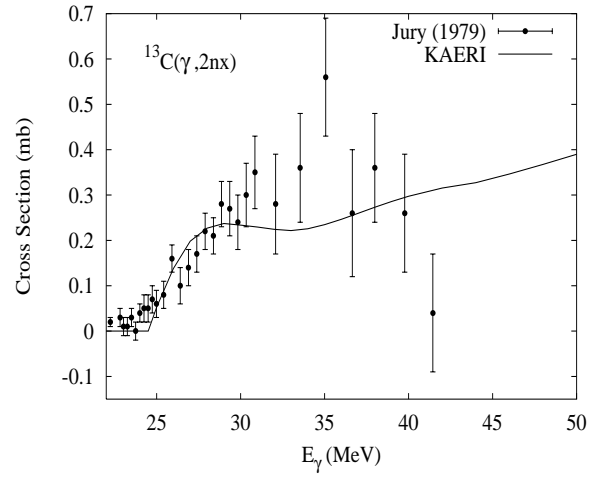
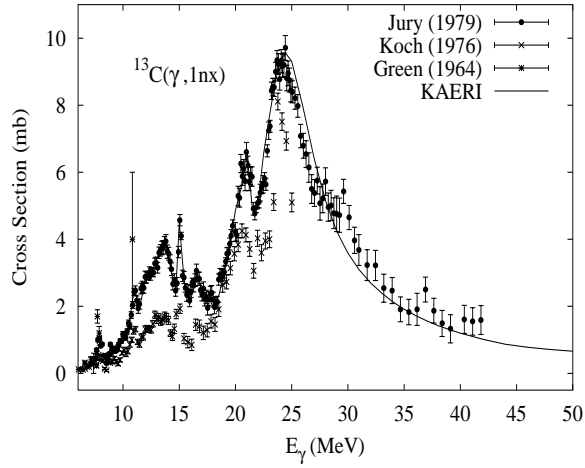
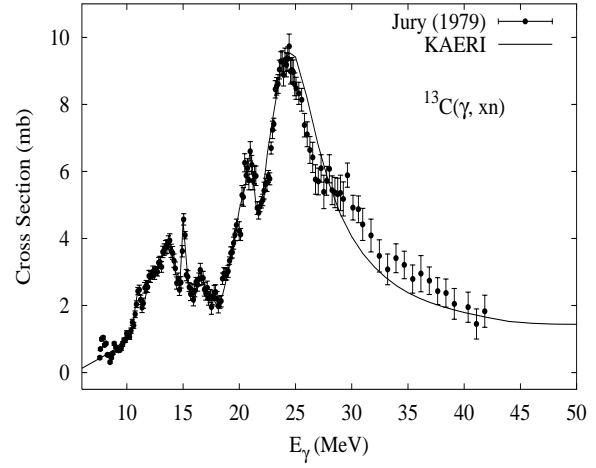
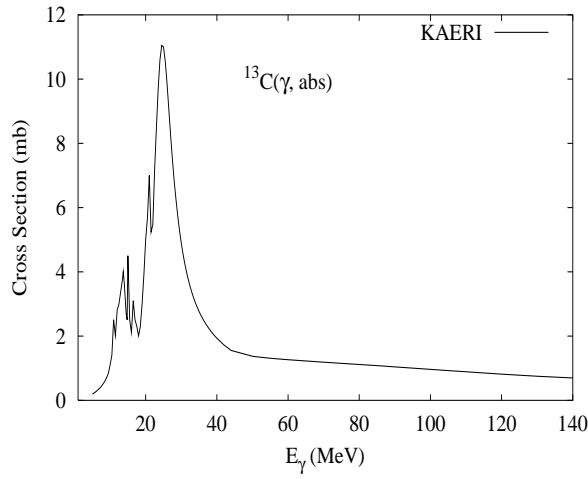
The photoabsorption cross section was evaluated based on the data of Ahrens [Ahr75], that extend up to 150 MeV. Below 30 MeV, a constant value of 0.7 mb was subtracted from these data, as recommended by Fuller.

The Hauser-Feshbach statistical theory cannot be immediately applied in the analysis of photonuclear reactions on carbon, since there are significant contributions from direct reactions. In particular the  $(\gamma, n_0)$  and  $(\gamma, p_0)$  processes, which result in the residual nucleus being left in its ground state, account for a significant fraction of the photonuclear cross section (particularly for incident energies below 30 MeV). Therefore we first evaluate the  $(\gamma, n_0)$  and  $(\gamma, p_0)$  cross sections from the available experimental data. We adopt Fuller's recommendations [Ful85] in the GDR region; at higher energies our evaluation is based on the Matthews [Mat76] data at 60, 80, and 100 MeV for  $(\gamma, p_0)$  reactions, and we assume an equal cross section for the  $(\gamma, n_0)$  reactions at these high energies motivated by the concept of QD reaction mechanism. We used dipole angular distribution shapes (the only non-zero Legendre coefficient being  $a_2$ ) taken from Fuller. This describes the angular distribution in the GDR region. Although it is not appropriate at higher energies, where forward peaking is observed [Cha95a], our present evaluation is probably adequate

for most applications since the  $(\gamma, n_0)$  and  $(\gamma, p_0)$  reactions become very small in magnitude at higher incident energies.

The remaining cross section after  $(\gamma, n_0)$  and  $(\gamma, p_0)$  processes have occurred is modeled with the GNASH code, and represented in the ENDF file using MT5. Preequilibrium and compound decay processes are included. The resulting neutron emission contribution, when added to the  $(\gamma, n_0)$  cross section, was compared with Fuller's evaluation based on a renormalization of Fultz's data [Ful66] by a factor 1.17. Reasonable agreement for neutron production was obtained in the GDR peak, though the calculations appeared to somewhat overpredict neutron production (by as much as 30%) by 30 MeV. This failing is due to the difficulties in using a Hauser-Feshbach code to model reactions on light nuclei. Finally, GNASH calculations [Cha95a] of proton emission spectra for 60 MeV incident photons agreed well with the DDX data of McGeorge [McG86].

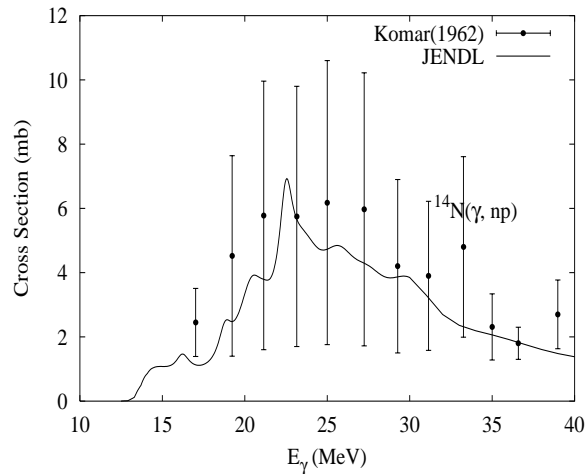
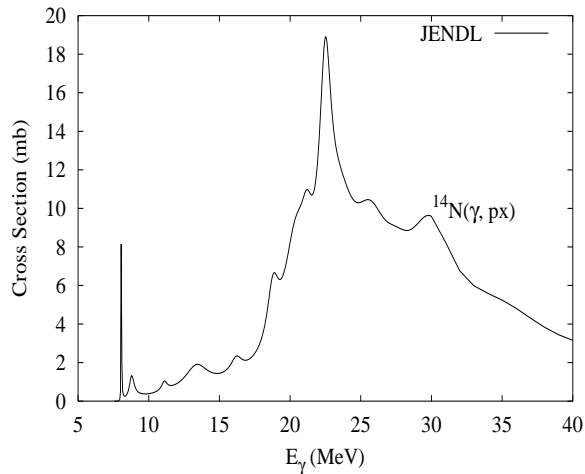
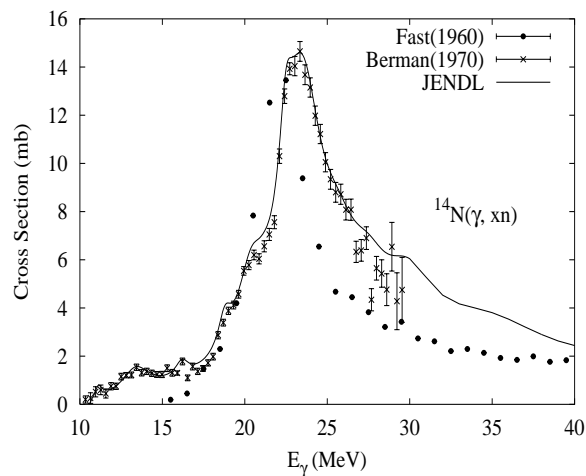
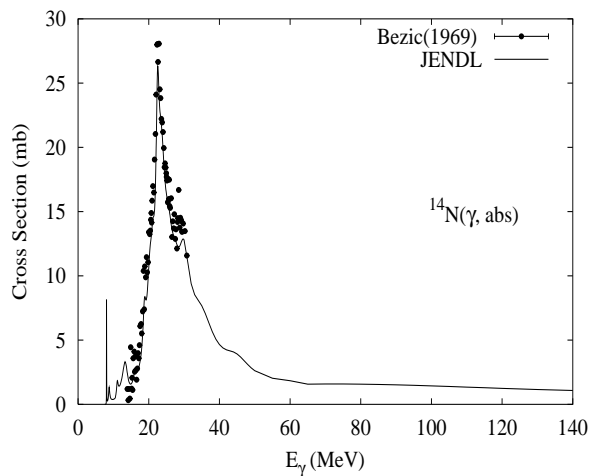
Abundance (%)	Threshold Energies (MeV)								
	$\gamma, n$	$\gamma, p$	$\gamma, t$	$\gamma, \text{He-3}$	$\gamma, \alpha$	$\gamma, 2n$	$\gamma, np$	$\gamma, 2p$	$\gamma, 3n$
1.11	4.95	17.53	23.88	24.41	10.65	23.67	20.90	31.63	36.79



The photoabsorption cross section has not been measured. However, there are experimental data for the  $(\gamma, 1nx)$ ,  $(\gamma, 2nx)$  and  $(\gamma, xn)$  reaction cross sections [Jur79, Koc76, Gre64]. We relied on the GUNF and GNASH codes to infer the photoabsorption cross section in the GDR regime, in order to model accurately Jury's  $(\gamma, 1nx)$  data. The photoabsorption cross section above the GDR, up to 140 MeV, was obtained from QD model calculations using the theory of Chadwick.

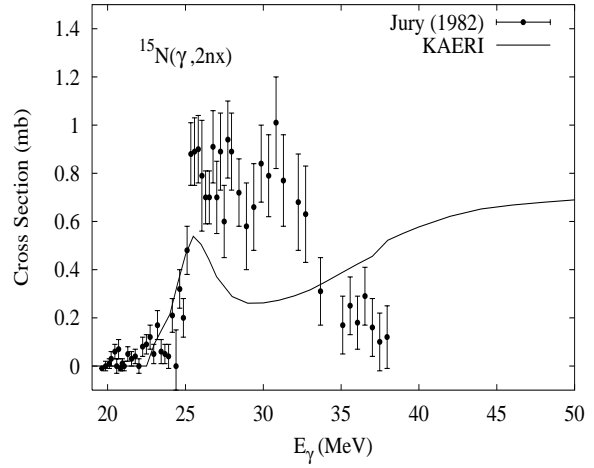
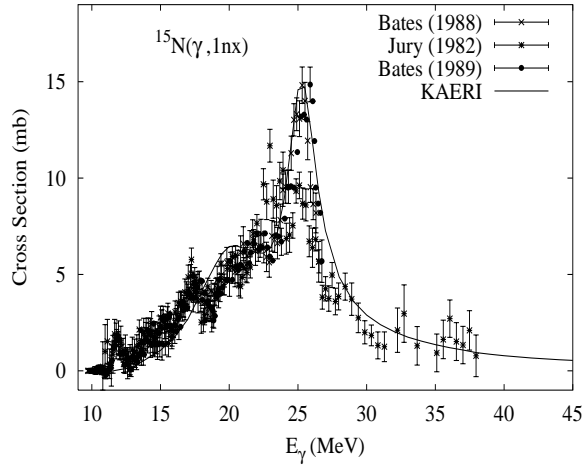
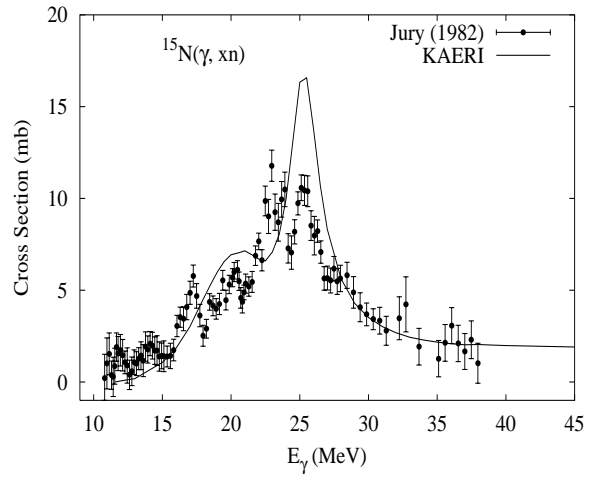
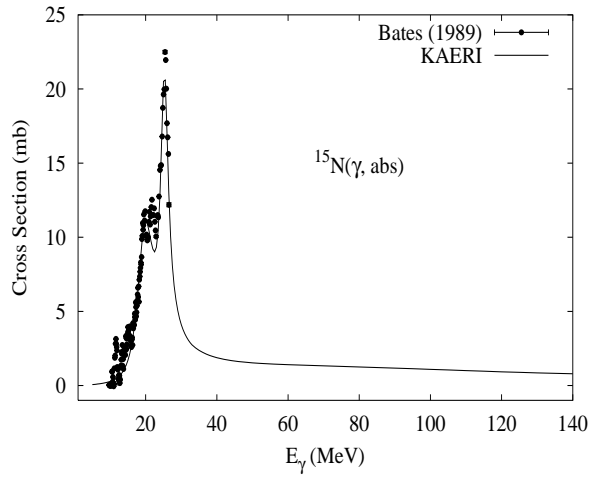
The calculated results of the emission channels by the GNASH code are in good agreement with the Jury data for the  $(\gamma, 1nx)$ ,  $(\gamma, 2nx)$  and  $(\gamma, xn)$  cross sections.

Abundance (%)	Threshold Energies (MeV)								
	$\gamma, n$	$\gamma, p$	$\gamma, t$	$\gamma, \text{He-3}$	$\gamma, \alpha$	$\gamma, 2n$	$\gamma, np$	$\gamma, 2p$	$\gamma, 3n$
99.63	10.55	7.55	22.74	20.74	11.61	30.62	12.50	25.08	46.24



The photoabsorption cross section was measured by Bezić et al. [Bez69] and was analyzed between 15 and 31 MeV. Above 31 MeV, the cross section was estimated based on measurements of  ${}^{16}\text{O}$  and  ${}^{12}\text{C}$ . Total photoneutron production data below 30 MeV [Ber70] were analyzed consistently together with other reaction channels [Kom62]. Above 30 MeV, the cross section was calculated with a GDR plus QD models [Mur91].

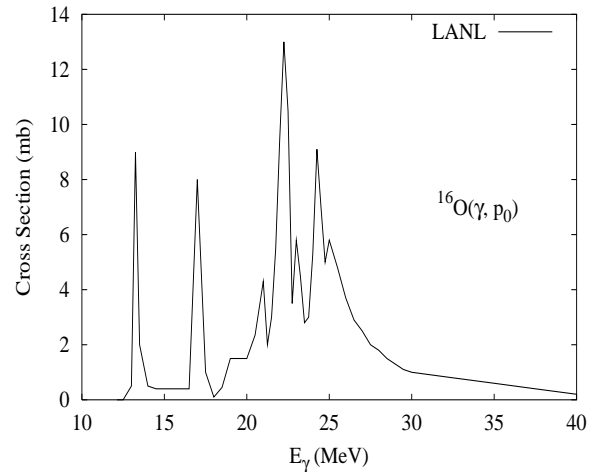
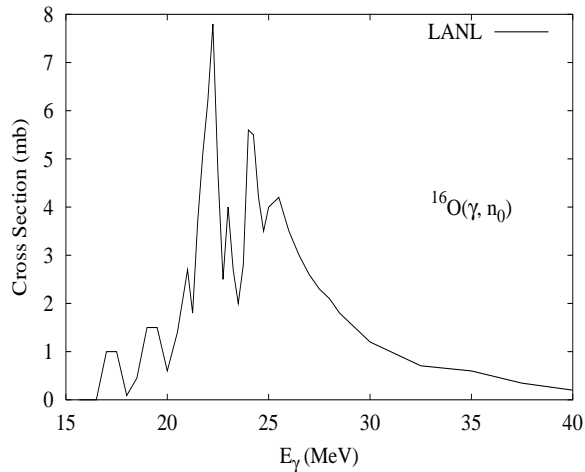
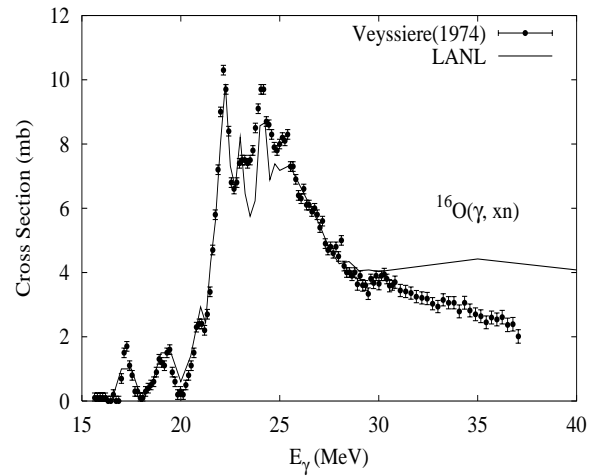
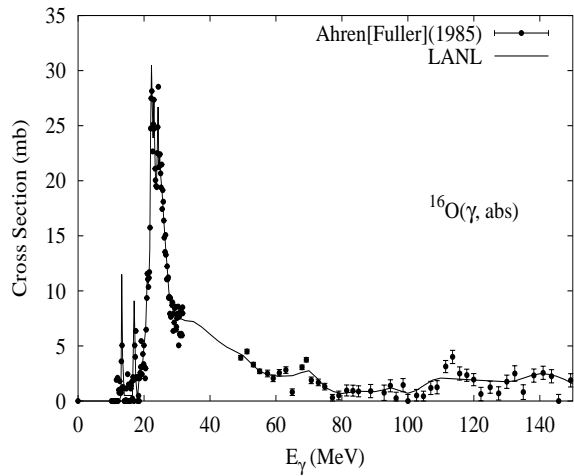
Abundance (%)	Threshold Energies (MeV)								
	$\gamma, n$	$\gamma, p$	$\gamma, t$	$\gamma, \text{He-3}$	$\gamma, \alpha$	$\gamma, 2n$	$\gamma, np$	$\gamma, 2p$	$\gamma, 3n$
0.37	10.83	10.21	14.85	28.20	10.99	21.39	18.38	31.04	41.45



The photoabsorption cross section was evaluated based on the experimental data of Bates [Bat89], up to 35 MeV. Above this energy, the absorption cross section was calculated from the QD model.

The calculated results of the emission channel by the GNASH code are in agreement with the experimental data of Bates [Bat88] for  $(\gamma, 1nx)$  reaction cross sections, but are larger than the measurements of Jury [Jur82] for the  $(\gamma, xn)$  and  $(\gamma, 2nx)$  reaction cross sections.

Abundance (%)	Threshold Energies (MeV)								
	$\gamma, n$	$\gamma, p$	$\gamma, t$	$\gamma, \text{He-3}$	$\gamma, \alpha$	$\gamma, 2n$	$\gamma, np$	$\gamma, 2p$	$\gamma, 3n$
99.76	15.66	12.13	25.03	22.79	7.16	28.89	22.96	22.34	52.06



Our evaluation of photonuclear reactions on oxygen follows, to a large extent, the analysis described by Fuller [Ful85].

The photoabsorption cross section was evaluated based on the data of Ahrens [Ahr75], that extend up to 150 MeV. Below 30 MeV, a constant value of 2.78 mb was subtracted from these data, as recommended by Fuller, in order to make these data consistent with the sum of other  $(\gamma, n)$ ,  $(\gamma, p)$ , *etc.* data. However, no such subtraction was made for energies above 50 MeV since this would result in negative cross sections, and a smooth transition was used for the absorption cross section from 30 to 50 MeV.

The Hauser-Feshbach statistical theory cannot be immediately applied in the analysis of photonuclear reactions on oxygen, since there are significant contributions from direct reactions. In particular the  $(\gamma, n_0)$  and  $(\gamma, p_0)$  processes, which result in the residual nucleus being left in its ground state, account for a significant fraction of the photonuclear cross section (particularly for incident energies below 30 MeV). Therefore we first evaluate the  $(\gamma, n_0)$  and  $(\gamma, p_0)$  cross sections from the available experimental data. We adopt Fuller's recommendations for these data. In the case of the  $p_0$  data, these are based on the inverse process of proton capture. These evaluations were extended to 45 MeV based on Phillips' [Phi79] measurements for  $n_0$  and the  $p_0$  results shown in this same paper which are of the same magnitude from 30-45 MeV. Above 45 MeV, because

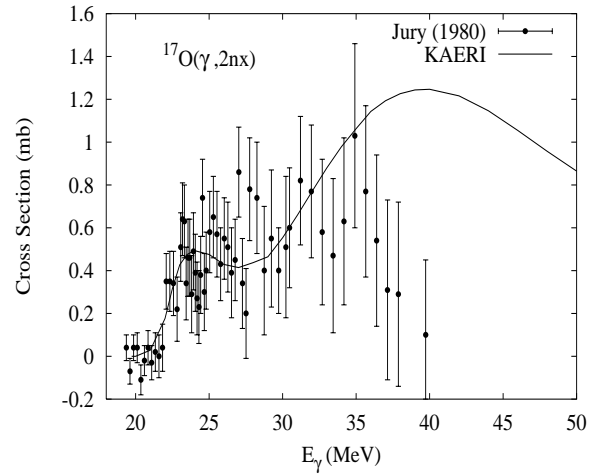
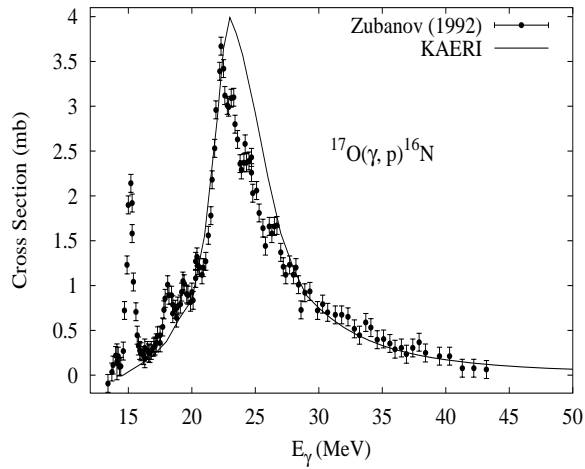
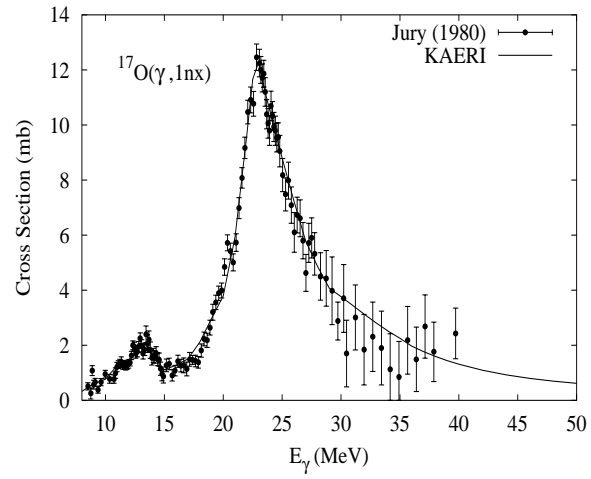
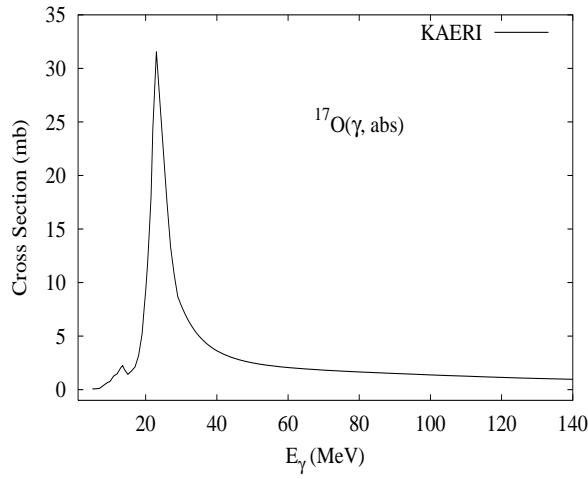


of a lack of other information, we based the  $n_0, p_0$  cross sections on those for carbon [Mat76], since the carbon and oxygen  $n_0, p_0$  data are of similar magnitude to oxygen at 30 MeV.

For the  $n_0$  and  $p_0$  cross sections we provide angular distributions using Legendre polynomials. These were obtained from Phillip's paper [Phi79], for both  $n_0$  and  $p_0$ . (Note that Phillips' text describing the  $p_0$  polynomials is not consistent with the data in his figure 7; Phillips advised us to use the graphical data rather than that based on the text.) Above 40 MeV, these angular distributions were simply extended, unmodified, up to 150 MeV. This is not physically correct [Cha95a], though its impact in transport calculations will be generally small due to the small magnitude of  $n_0, p_0$  cross sections above 40 MeV.

The remaining cross section after  $(\gamma, n_0)$  and  $(\gamma, p_0)$  processes have occurred is modeled with the GNASH code, and represented in the ENDF file using MT5. Preequilibrium and compound decay processes are included. The resulting neutron emission contribution, when added to the  $(\gamma, n_0)$  cross section, was compared with Fuller's evaluation, and other measurements [Vey74, Ber80, Kne75] and good agreement was obtained.

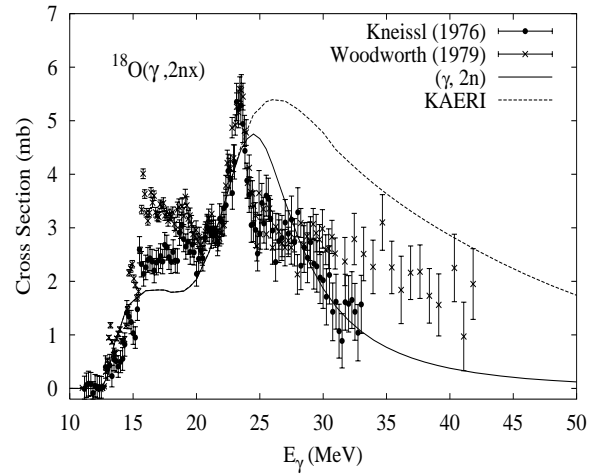
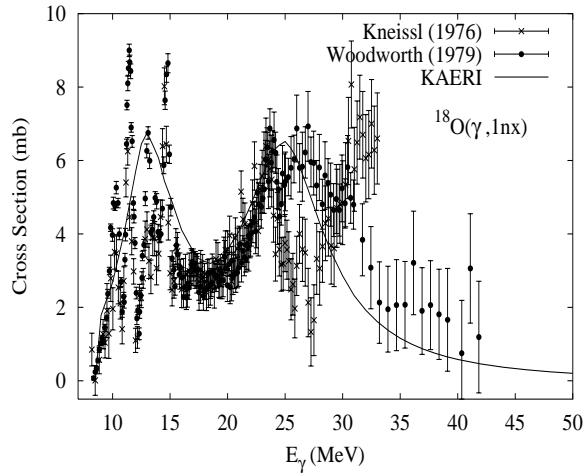
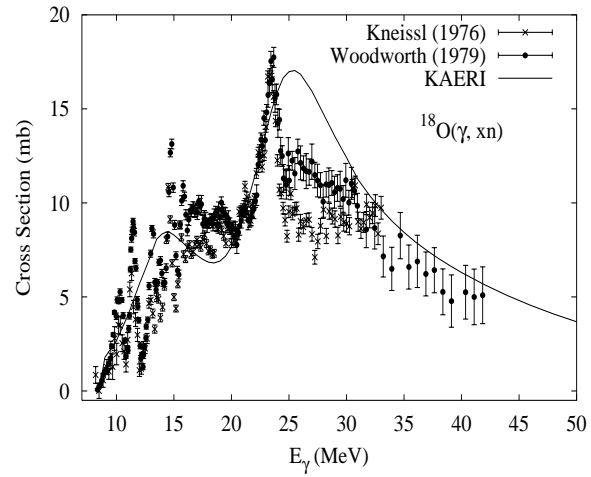
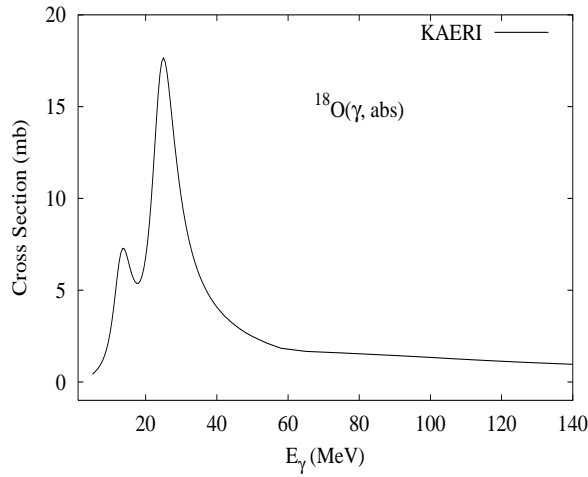
Abundance (%)	Threshold Energies (MeV)								
	$\gamma, n$	$\gamma, p$	$\gamma, t$	$\gamma, \text{He-3}$	$\gamma, \alpha$	$\gamma, 2n$	$\gamma, np$	$\gamma, 2p$	$\gamma, 3n$
0.04	4.14	13.78	18.62	18.76	6.36	19.81	16.27	25.26	33.03



The photoabsorption cross section has not been measured. However, there are experimental data for  $(\gamma, 1nx)$ ,  $(\gamma, p)$ ,  $(\gamma, 2nx)$  and  $(\gamma, xn)$  reaction cross sections by Jury [Jur80]. We relied on the GUNF and GNASH codes to infer the absorption cross section in the GDR regime, so as to model accurately the Jury's measured data. The absorption cross section above the GDR, up to 140 MeV, was taken from QD model calculations.

The calculated results for the emission channels by the GNASH code are in good agreement with the Jury data for  $(\gamma, 1nx)$ ,  $(\gamma, 2nx)$  and  $(\gamma, xn)$  reaction cross sections. Overall agreement was also seen for the calculated results for  $(\gamma, p)$  reaction cross sections with the experimental data of Zubanov [Zub92] except the sharp resonance at 15.2 MeV, which is due to the direct capture mechanism.

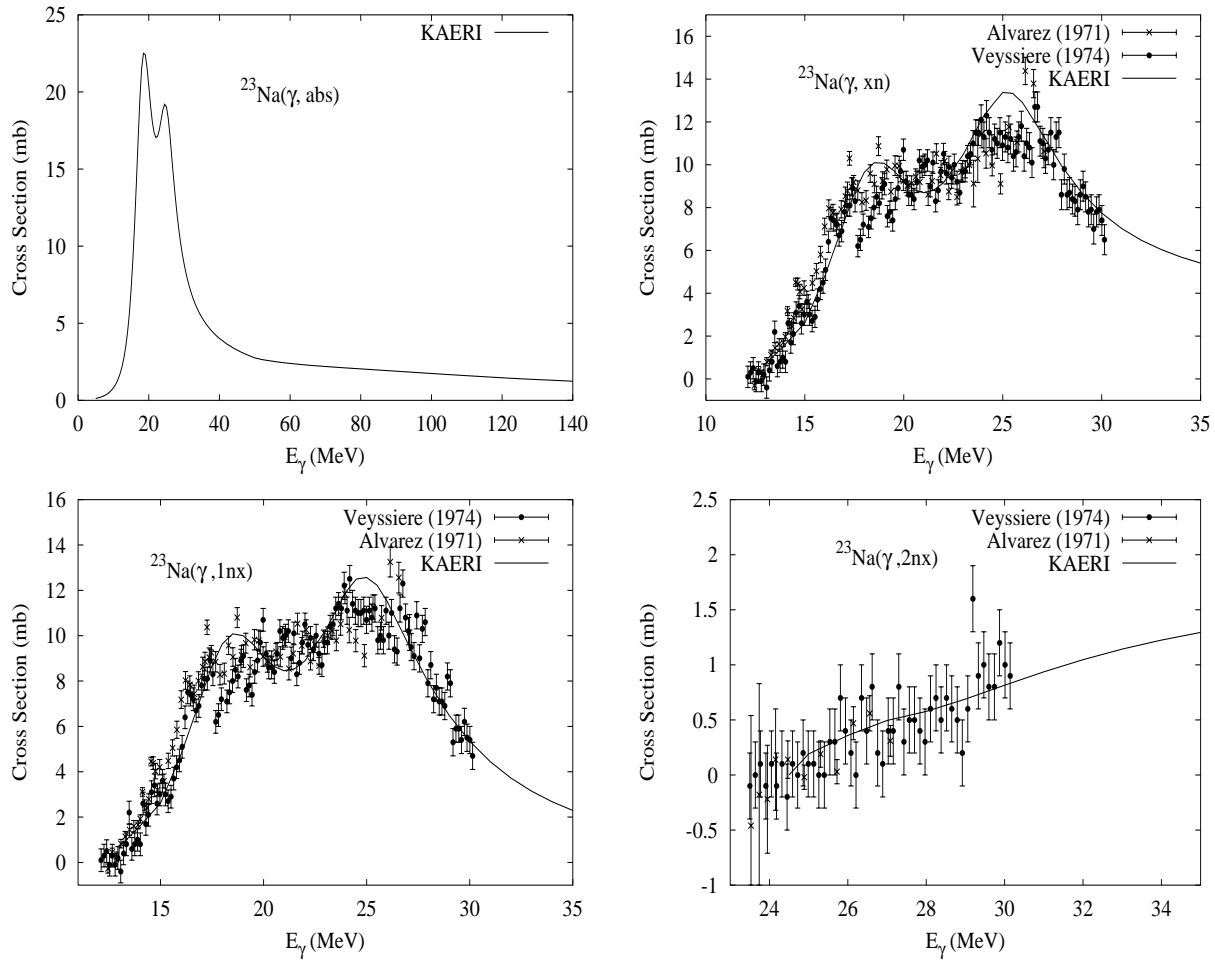
Abundance (%)	Threshold Energies (MeV)								
	$\gamma, n$	$\gamma, p$	$\gamma, t$	$\gamma, \text{He-3}$	$\gamma, \alpha$	$\gamma, 2n$	$\gamma, np$	$\gamma, 2p$	$\gamma, 3n$
0.20	8.04	15.94	15.83	25.59	6.23	12.19	21.82	29.05	27.85



The photoabsorption cross section has not been measured. However, there are experimental data for the  $(\gamma, 1nx)$ ,  $(\gamma, 1p)$ ,  $(\gamma, 2nx)$  and  $(\gamma, xn)$  reaction cross sections by Woodworth [Woo79] and Kneissl [Kne76]. We relied on the GUNF and GNASH codes to infer the photoabsorption cross section in the GDR regime, in order to reproduce the measured data of Woodworth and Kneissl consistently. The photoabsorption cross section above the GDR, up to 140 MeV, was obtained from QD model calculations using the theory of Chadwick. The calculated results are basically in agreement with the experimental data for  $(\gamma, 1nx)$ ,  $(\gamma, 1p)$ ,  $(\gamma, 2nx)$  and  $(\gamma, xn)$  reaction cross sections. However, as expected, the statistical approach is not adequate to represent the sharp resonance structures typically seen in light nuclei.

# $\gamma + {}^{23}\text{Na}$

Abundance (%)	Threshold Energies (MeV)								
	$\gamma, n$	$\gamma, p$	$\gamma, t$	$\gamma, \text{He-3}$	$\gamma, \alpha$	$\gamma, 2n$	$\gamma, np$	$\gamma, 2p$	$\gamma, 3n$
100.00	12.42	8.79	17.43	24.45	10.47	23.49	19.16	24.06	40.59

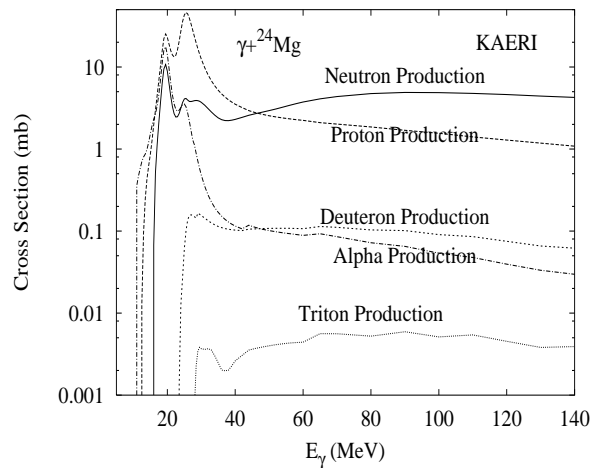
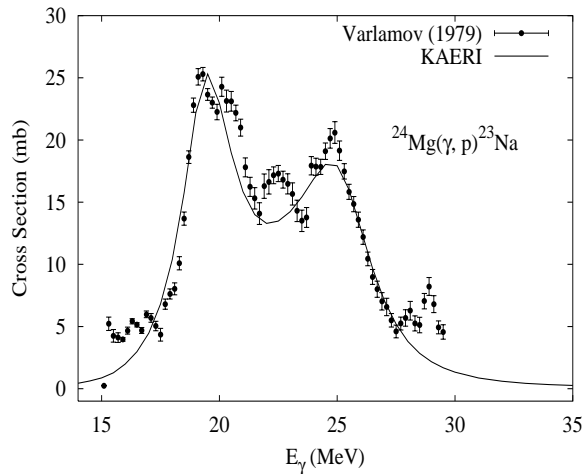
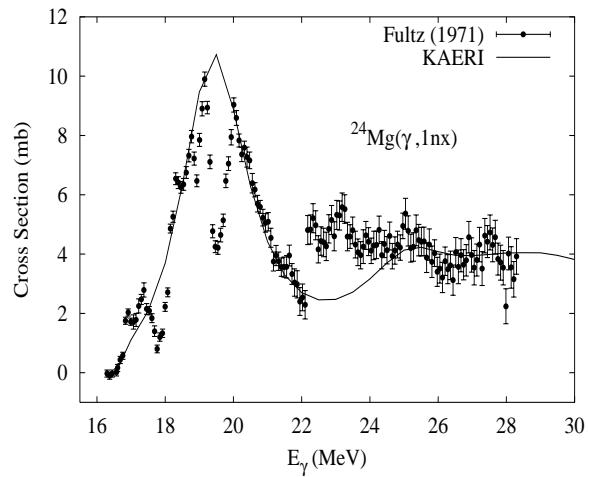
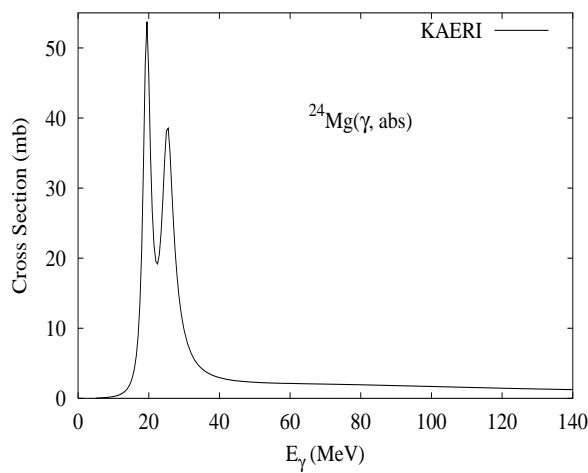


The photoabsorption cross section has not been measured. However, there are experimental data for the  $(\gamma, 1nx)$ ,  $(\gamma, 2nx)$ ,  $(\gamma, sn)$  and  $(\gamma, xn)$  reaction cross sections [Alv71, Vey74]. We relied on the GUNF and GNASH codes to infer the photoabsorption cross section in the GDR regime, in order to model accurately Veyssiere's  $(\gamma, 1nx)$  data. The photoabsorption cross section above the GDR, up to 140 MeV, was obtained from QD model calculations using the theory of Chadwick.

The calculated results of the emission channels by the GNASH code reproduce fairly well all the available experimental data for  $(\gamma, 1nx)$ ,  $(\gamma, 2nx)$ ,  $(\gamma, sn)$  and  $(\gamma, xn)$  reaction cross sections.

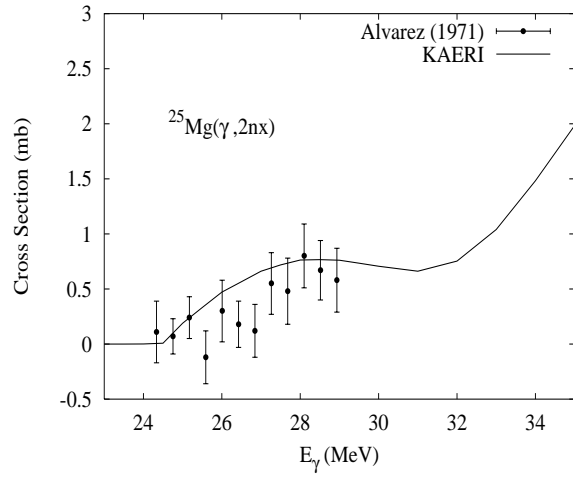
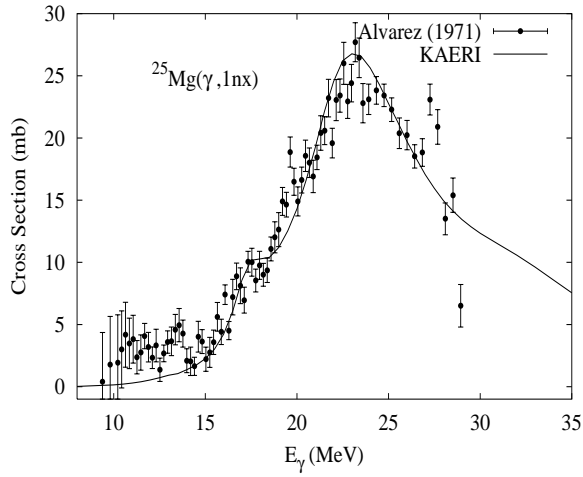
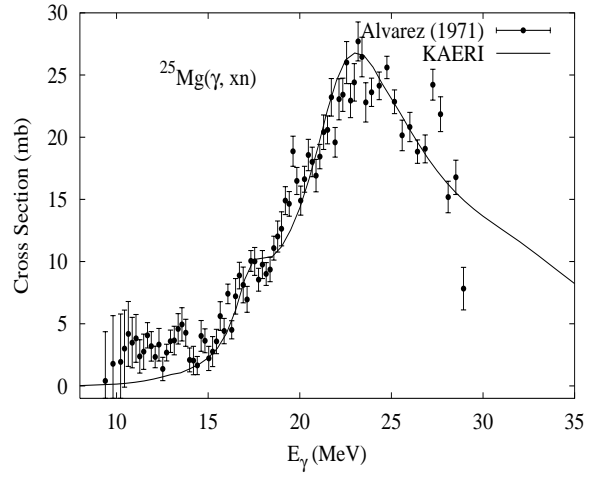
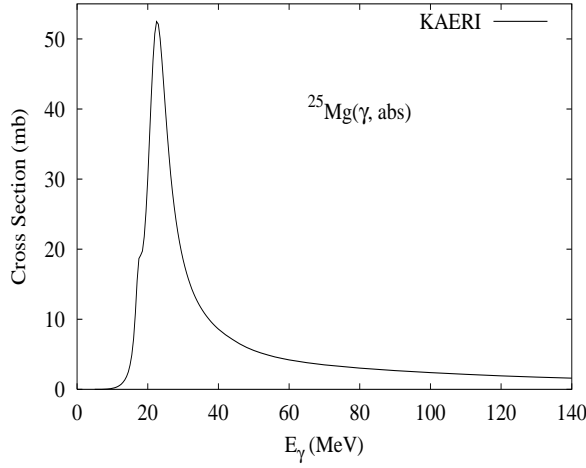
# $\gamma + {}^{24}\text{Mg}$

Abundance (%)	Threshold Energies (MeV)								
	$\gamma, n$	$\gamma, p$	$\gamma, t$	$\gamma, \text{He-3}$	$\gamma, \alpha$	$\gamma, 2n$	$\gamma, np$	$\gamma, 2p$	$\gamma, 3n$
78.99	16.53	11.69	26.69	23.13	9.31	29.68	24.11	20.48	49.06



The photoabsorption cross section has not been measured. However, there are experimental data for the  $(\gamma, 1n_x)$  [Ful71], and  $(\gamma, 1p)$  [Var79b] reaction cross sections. We relied on the GUNF and GNASH codes to infer the photoabsorption cross section in the GDR regime, in order to model accurately the  $(\gamma, 1n_x)$  and  $(\gamma, 1p)$  cross sections. The photoabsorption cross section above the GDR, up to 140 MeV, was obtained from QD model calculations using the theory of Chadwick. The calculated results of the emission channels by the GNASH code show reasonable agreement with both channels measured.

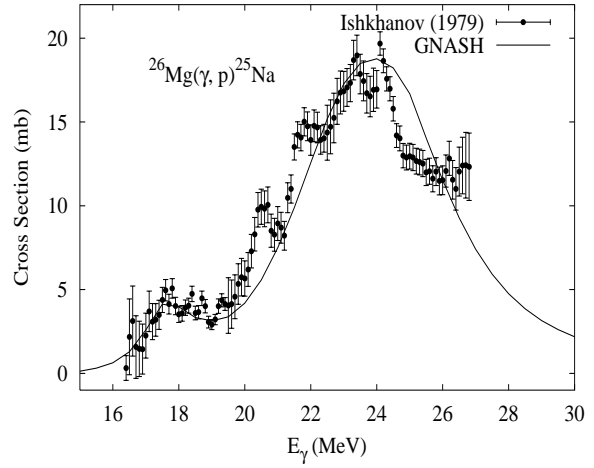
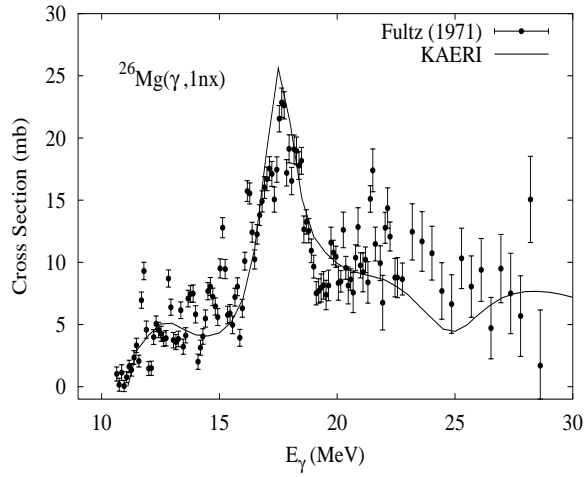
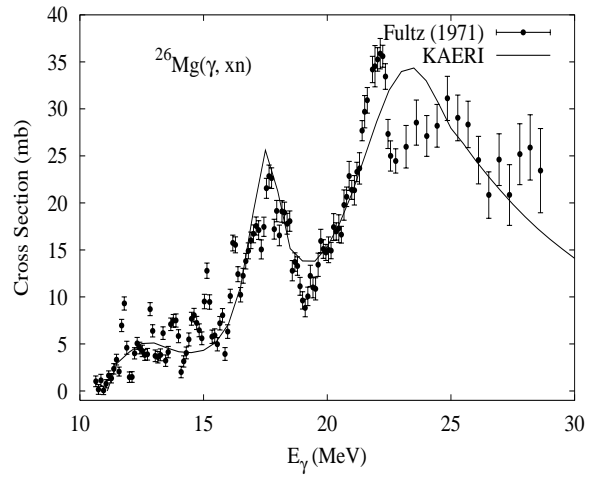
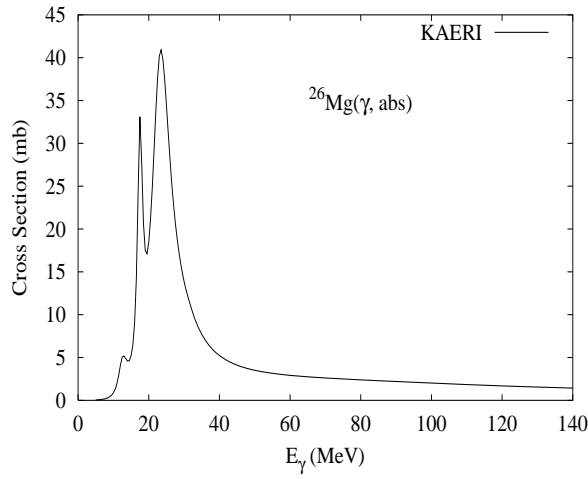
Abundance (%)	Threshold Energies (MeV)								
	$\gamma, n$	$\gamma, p$	$\gamma, t$	$\gamma, \text{He-3}$	$\gamma, \alpha$	$\gamma, 2n$	$\gamma, np$	$\gamma, 2p$	$\gamma, 3n$
10.00	7.33	12.06	22.96	20.10	9.88	23.86	19.02	22.61	37.01



The photoabsorption cross section has not been measured. However, there are experimental data for the  $(\gamma, 1nx)$ ,  $(\gamma, 2nx)$ ,  $(\gamma, sn)$  and  $(\gamma, xn)$  reaction cross sections [Alv71]. We relied on the GUNF and GNASH codes to infer the photoabsorption cross section in the GDR regime, in order to model accurately Alvarez's data. The photoabsorption cross section above the GDR, up to 140 MeV, was obtained from QD model calculations using the theory of Chadwick.

The calculated results of the emission channels by the GNASH code are in good agreement with the experimental data for all measured channels.

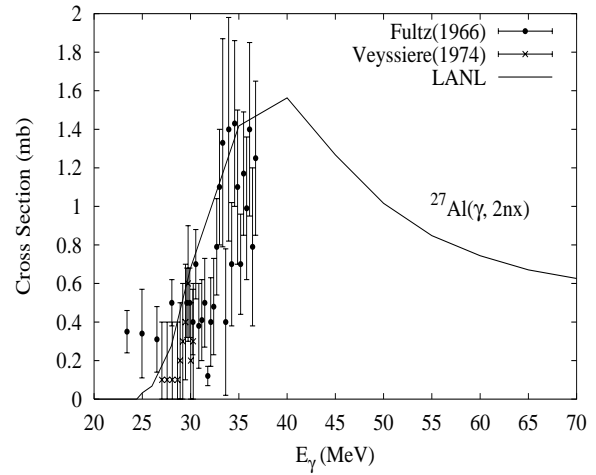
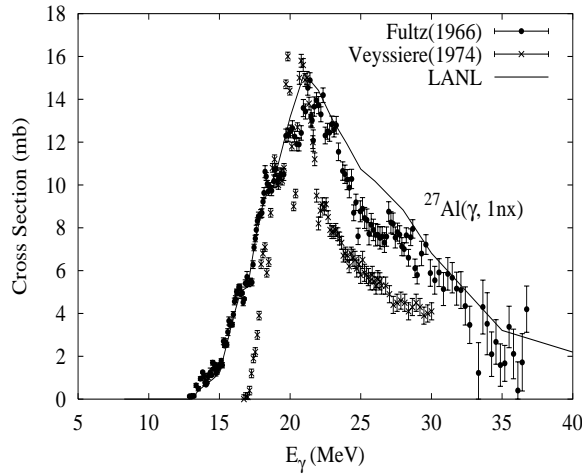
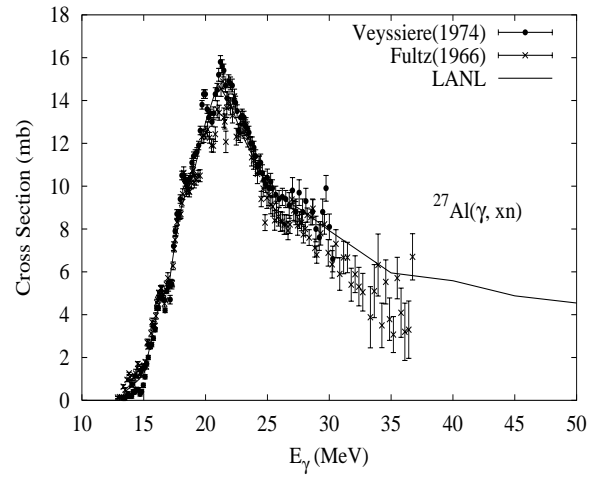
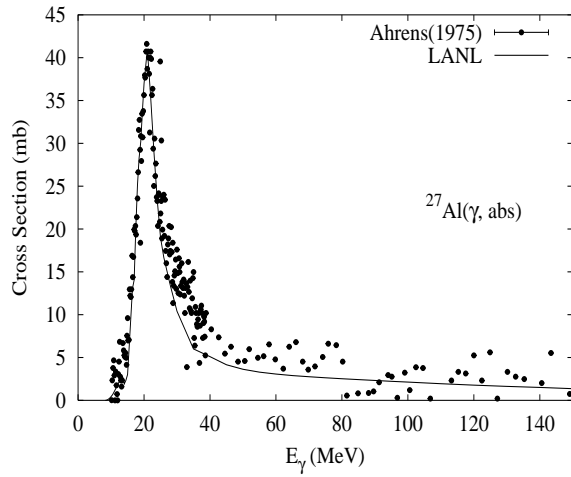
Abundance (%)	Threshold Energies (MeV)								
	$\gamma, n$	$\gamma, p$	$\gamma, t$	$\gamma, \text{He-3}$	$\gamma, \alpha$	$\gamma, 2n$	$\gamma, np$	$\gamma, 2p$	$\gamma, 3n$
11.01	11.09	14.14	21.63	25.99	10.61	18.42	23.15	24.84	34.95



The photoabsorption cross section has not been measured. However, there are experimental data for the  $(\gamma, 1nx)$ ,  $(\gamma, 1p)$ ,  $(\gamma, 2n)$ ,  $(\gamma, sn)$  and  $(\gamma, xn)$  reaction cross sections [Ful71, Ish79]. We relied on the GUNF and GNASH codes to infer the photoabsorption cross section in the GDR regime, in order to reproduce the overall shapes of the experimental data. The photoabsorption cross section above the GDR, up to 140 MeV, was obtained from QD model calculations using the theory of Chadwick.

The calculated results of the emission channels by the GNASH code are basically in agreement with the experimental data for the  $(\gamma, 1nx)$ ,  $(\gamma, 1p)$ ,  $(\gamma, 2n)$ ,  $(\gamma, sn)$  and  $(\gamma, xn)$  reaction cross sections.

Abundance (%)	Threshold Energies (MeV)								
	$\gamma, n$	$\gamma, p$	$\gamma, t$	$\gamma, \text{He-3}$	$\gamma, \alpha$	$\gamma, 2n$	$\gamma, np$	$\gamma, 2p$	$\gamma, 3n$
100.00	13.06	8.27	18.21	23.71	10.09	24.42	19.36	22.41	41.36

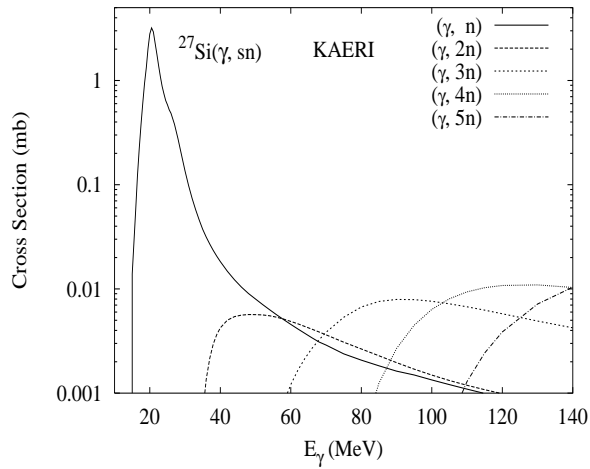
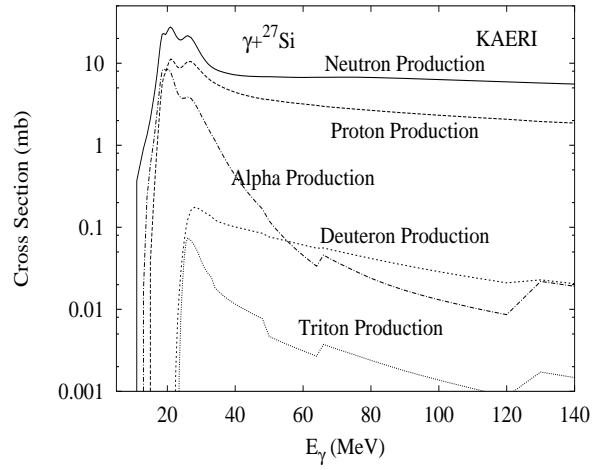
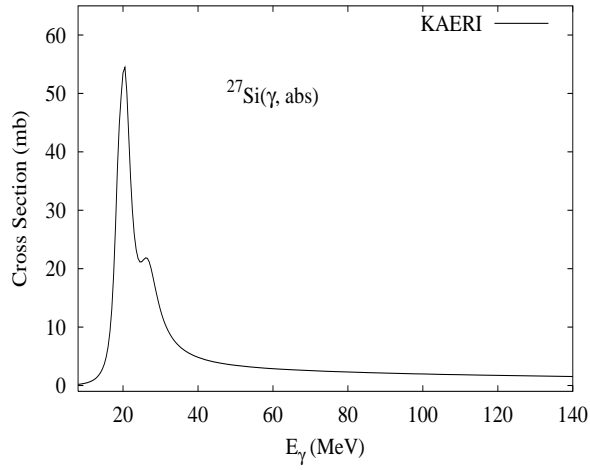


Available data are summarized by Varlamov [Var96]. The photoabsorption cross section was evaluated based on the data of Ahrens [Ahr75], that extend up to 150 MeV. However, above about 35 MeV, the evaluation used directly theoretical predictions from the QD model of Chadwick [Cha91]. Between approximately 30-40 MeV, the evaluation under-predicted the Ahrens absorption data. This was done since the evaluated neutron production in this energy range, based on GNASH predictions, somewhat over-predicted the photoneutron production measurements (see below), and it was felt that it is important to have as accurate as possible predictions of photoneutron production; increasing the absorption cross section here would lead to a worse discrepancy with the photoneutron production data.

Input level density parameters for the GNASH calculations were “tuned” so as to give an accurate representation of data at the GDR peak [i.e. at 21 MeV, a neutron production of about 15mb in agreement with [Ful66, Vey74]; a proton production about 16mb (experiment = 17.5 mb [Var96]); and an alpha production of 11 mb, with the sum adding up to 41 mb as predicted by Ahrens [Ahr75]].

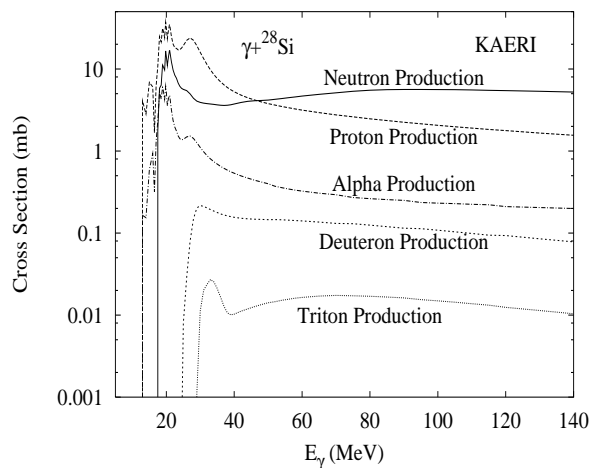
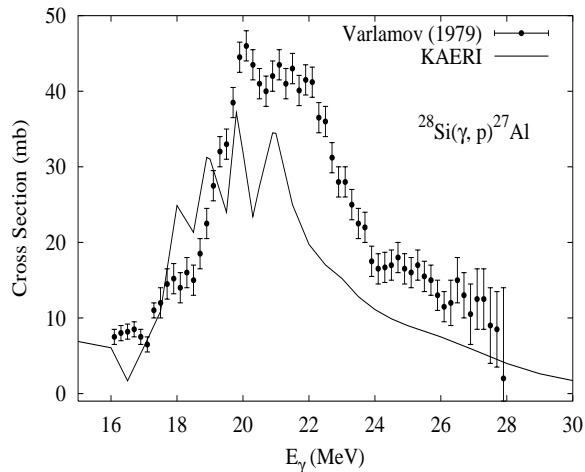
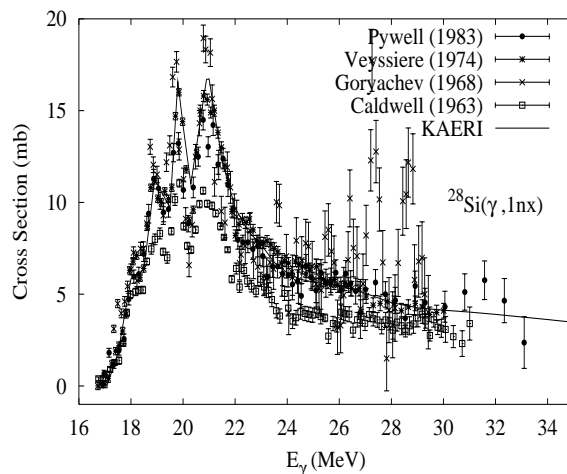
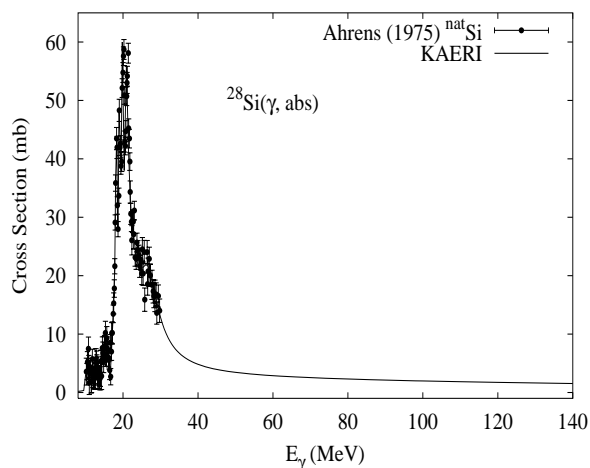


Abundance (%)	Threshold Energies (MeV)								
	$\gamma, n$	$\gamma, p$	$\gamma, t$	$\gamma, \text{He-3}$	$\gamma, \alpha$	$\gamma, 2n$	$\gamma, np$	$\gamma, 2p$	$\gamma, 3n$
0.00	13.31	7.46	27.28	13.38	9.34	32.36	18.83	13.77	47.35



There are no experimental data available. The photoabsorption cross section was obtained from GDR and QD model calculations, adopting the GDR parameters of  ${}^{28}\text{Si}$ . The neutron, proton, deuteron, triton and alpha emission cross sections, as well as production cross sections, were calculated by the GNASH code.

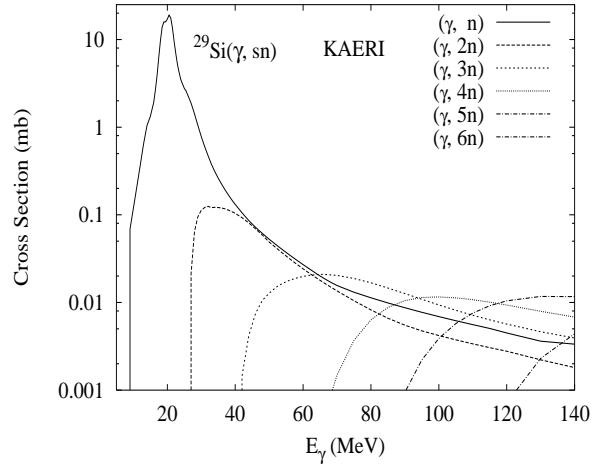
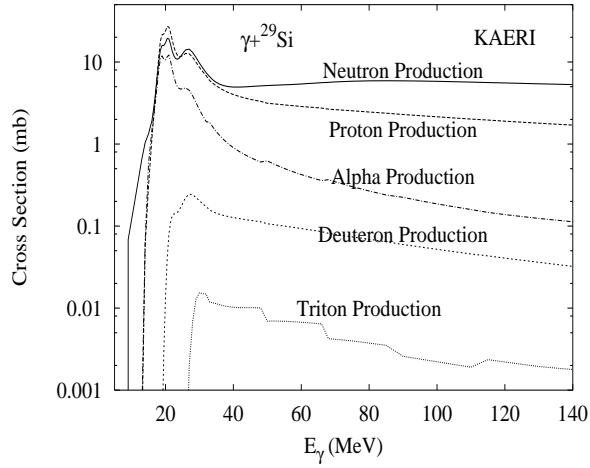
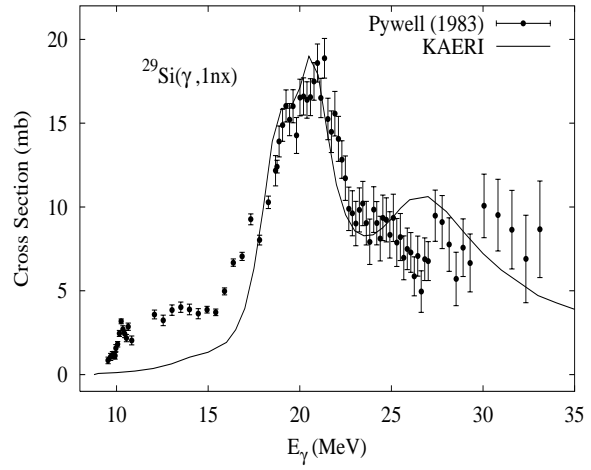
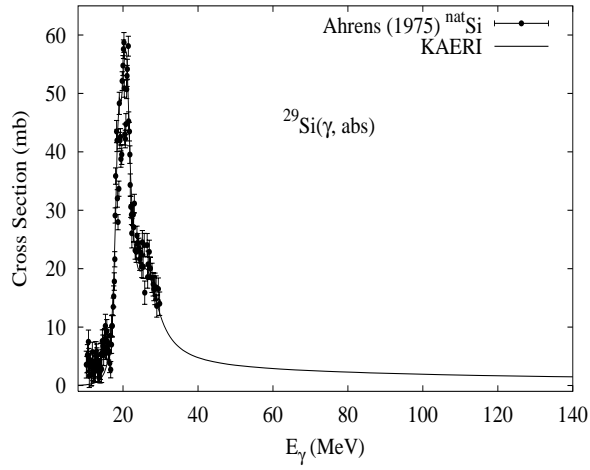
Abundance (%)	Threshold Energies (MeV)								
	$\gamma, n$	$\gamma, p$	$\gamma, t$	$\gamma, \text{He-3}$	$\gamma, \alpha$	$\gamma, 2n$	$\gamma, np$	$\gamma, 2p$	$\gamma, 3n$
92.23	17.18	11.58	27.53	23.23	9.98	30.49	24.64	19.86	49.53



The photoabsorption cross section was evaluated based on the measurements of Ahrens [Ahr75] for  ${}^{nat}\text{Si}$ . Above about 35 MeV, and up to 140 MeV, the absorption cross section was calculated from the QD model. Experimental data for  $(\gamma, 1nx)$  reaction cross section are available [Pyw83, Vey74, Cal63, Gor68].

The calculated results of the emission channels by the GNASH code are in good agreement with the experimental data of Pywell [Pyw83] and Veyssiere [Vey74] for the  $(\gamma, 1nx)$  reaction cross section, but are lower than the experimental data of Varlamov [Var79a] for the  $(\gamma, 1p)$  reaction cross section.

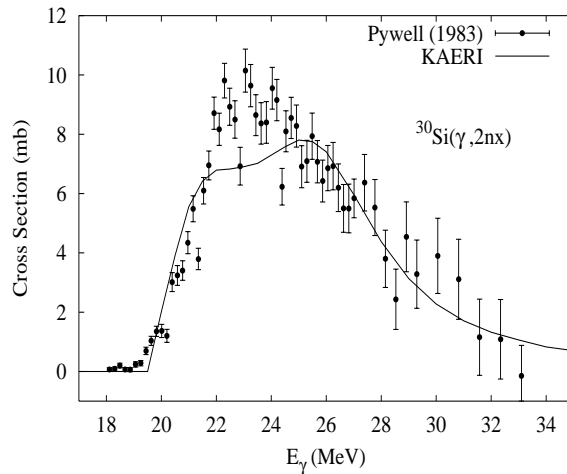
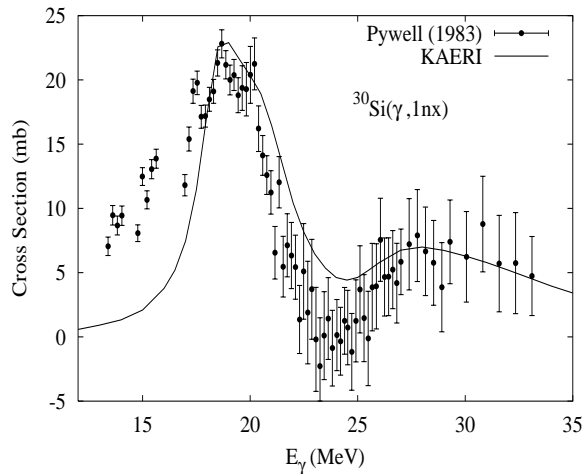
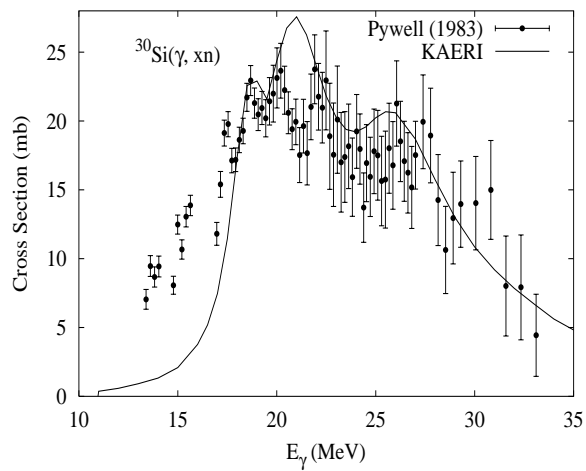
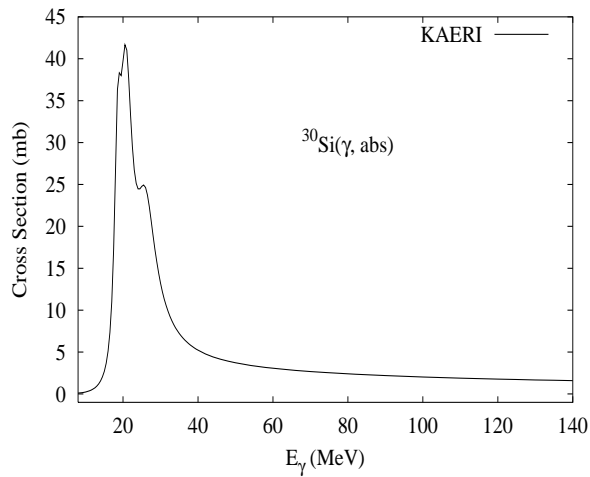
Abundance (%)	Threshold Energies (MeV)								
	$\gamma, n$	$\gamma, p$	$\gamma, t$	$\gamma, \text{He-3}$	$\gamma, \alpha$	$\gamma, 2n$	$\gamma, np$	$\gamma, 2p$	$\gamma, 3n$
4.67	8.47	12.33	24.63	20.61	11.13	25.65	20.06	21.89	38.96



The photoabsorption cross section was evaluated based on the measurements of Ahrens' [Ahr75] for  ${}^{nat}\text{Si}$ . Above about 35 MeV, and up to 140 MeV, the absorption cross section was calculated from the QD model.

The calculated results of the emission channels by the GNASH code reproduce fairly well the experimental data for the  $(\gamma, 1nx)$  reaction cross section [Pyw83].

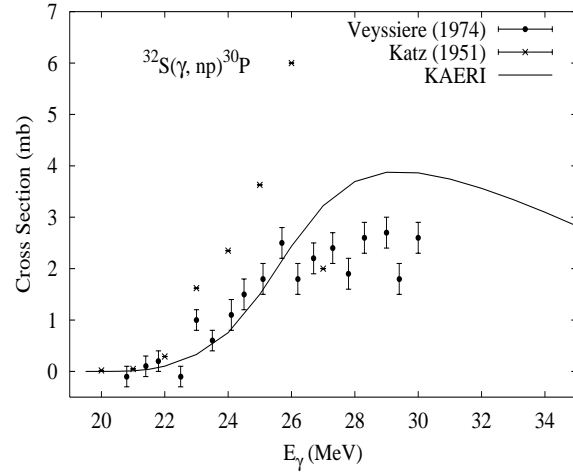
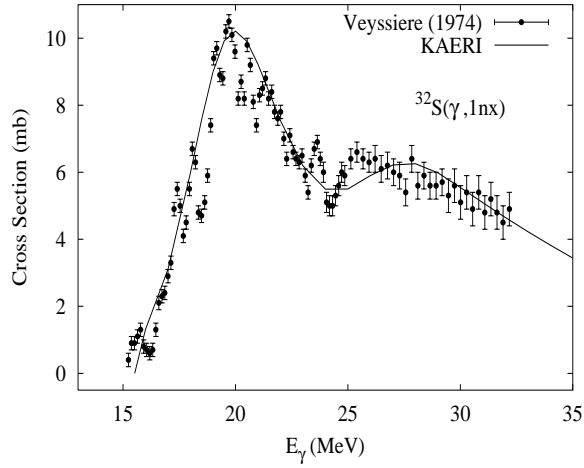
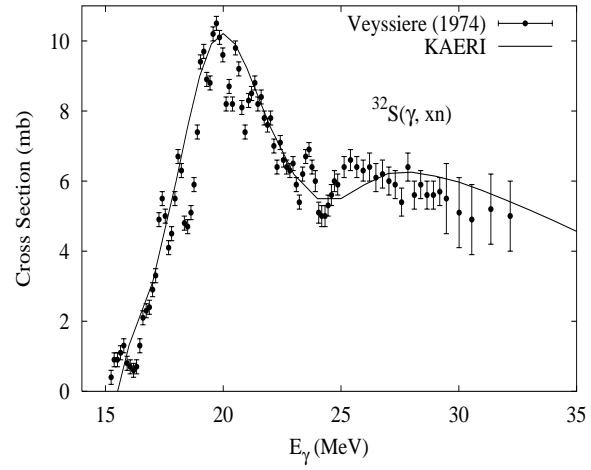
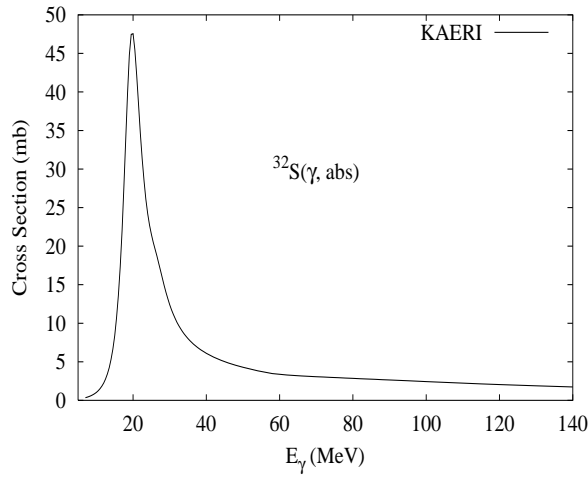
Abundance (%)	Threshold Energies (MeV)								
	$\gamma, n$	$\gamma, p$	$\gamma, t$	$\gamma, \text{He-3}$	$\gamma, \alpha$	$\gamma, 2n$	$\gamma, np$	$\gamma, 2p$	$\gamma, 3n$
3.10	10.61	13.51	22.19	24.78	10.64	19.08	22.94	23.99	36.26



The photoabsorption cross section has not been measured. However, there are experimental data [Pyw83] for the  $(\gamma, 1nx)$ ,  $(\gamma, 2nx)$  and  $(\gamma, xn)$  reaction cross sections. We relied on the GUNF and GNASH codes to infer the absorption cross section in the GDR regime, so as to reproduce the overall shapes of the Pywell's measurements. The absorption cross section above the GDR, up to 140 MeV, was taken from QD model calculations.

The calculated results of the emission channels by the GNASH code are basically in agreement with the experimental data for  $(\gamma, 1nx)$ ,  $(\gamma, 2nx)$  and  $(\gamma, xn)$  reaction cross sections.

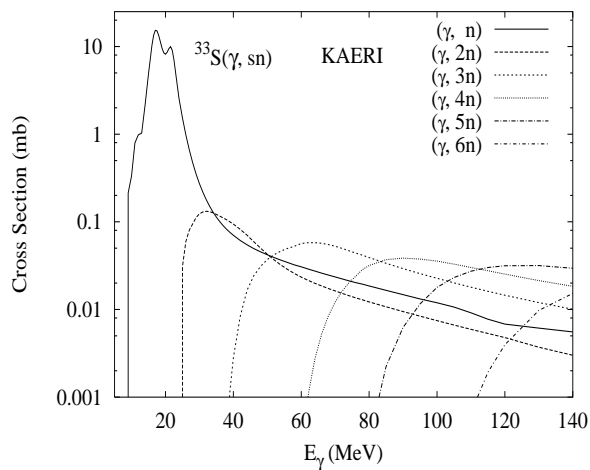
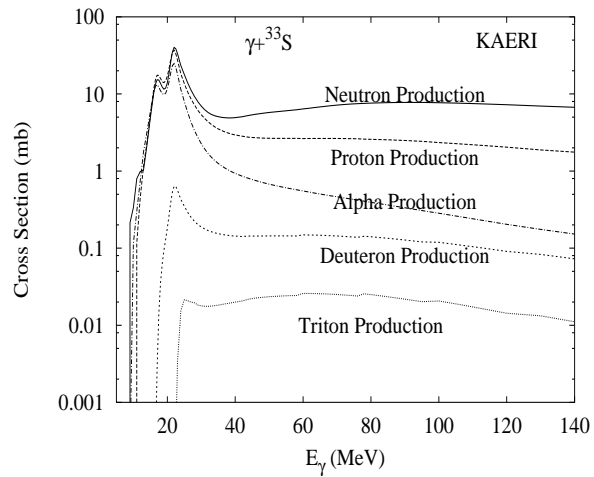
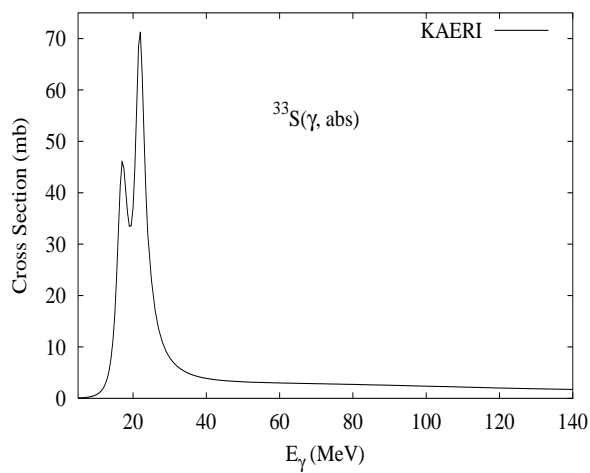
Abundance (%)	Threshold Energies (MeV)								
	$\gamma, n$	$\gamma, p$	$\gamma, t$	$\gamma, \text{He-3}$	$\gamma, \alpha$	$\gamma, 2n$	$\gamma, np$	$\gamma, 2p$	$\gamma, 3n$
95.02	15.04	8.86	24.01	19.05	6.95	28.10	21.18	16.16	47.07



The photoabsorption cross section has not been measured. However, there are experimental data for the  $(\gamma, 1nx)$ ,  $(\gamma, np)$ ,  $(\gamma, 2n)$  and  $(\gamma, xn)$  reaction cross sections [Vey74]. We relied on the GUNF and GNASH codes to infer the photoabsorption cross section in the GDR regime, in order to model accurately Veysiere's data. The photoabsorption cross section above the GDR, up to 140 MeV, was obtained from QD model calculations using the theory of Chadwick.

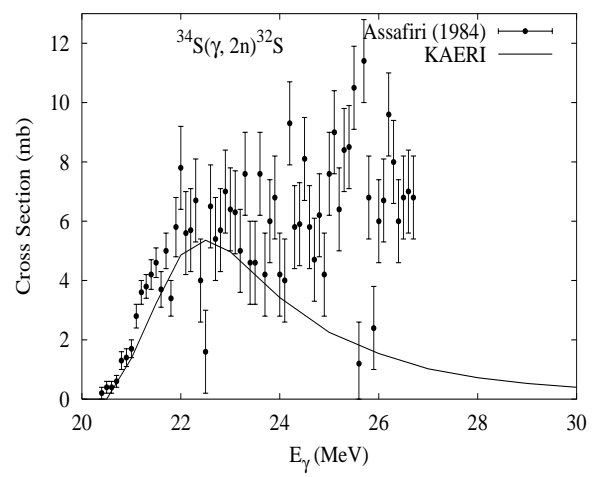
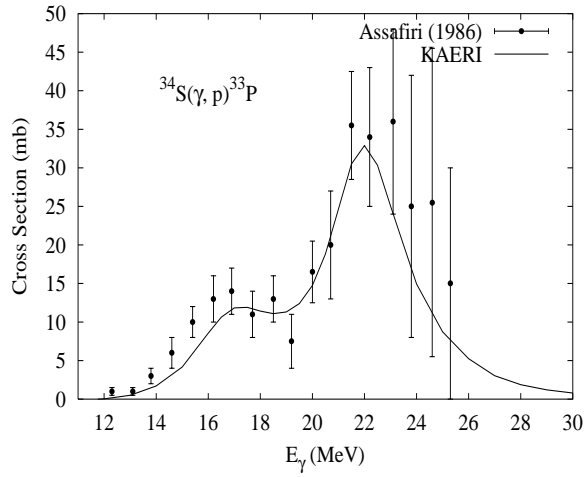
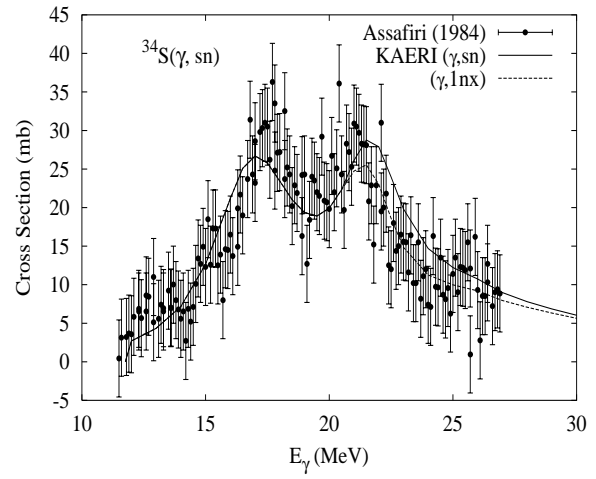
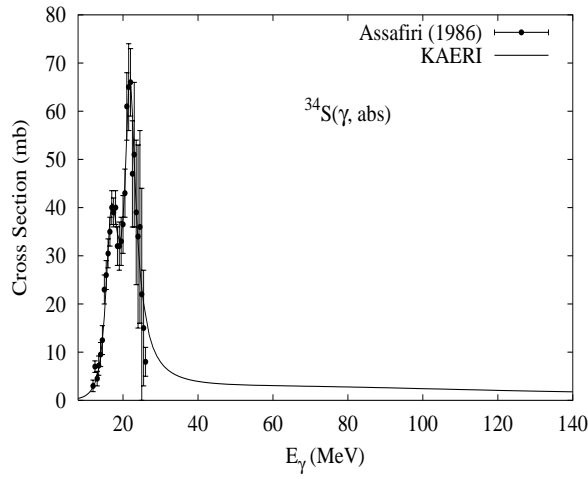
The calculated results of the emission channels by the GNASH code are in good agreement with the Veysiere data for  $(\gamma, 1nx)$ ,  $(\gamma, np)$ ,  $(\gamma, 2n)$  and  $(\gamma, xn)$  reaction cross sections.

Abundance (%)	Threshold Energies (MeV)								
	$\gamma, n$	$\gamma, p$	$\gamma, t$	$\gamma, \text{He-3}$	$\gamma, \alpha$	$\gamma, 2n$	$\gamma, np$	$\gamma, 2p$	$\gamma, 3n$
0.75	8.64	9.57	21.34	17.08	7.12	23.68	17.51	18.21	36.74



There are no experimental data available. The photoabsorption cross section was obtained from GDR and QD model calculations, adopting the GDR parameters of  ${}^{34}\text{S}$ . The neutron, proton, deuteron, triton and alpha emission cross sections, as well as production cross sections, were calculated by the GNASH code.

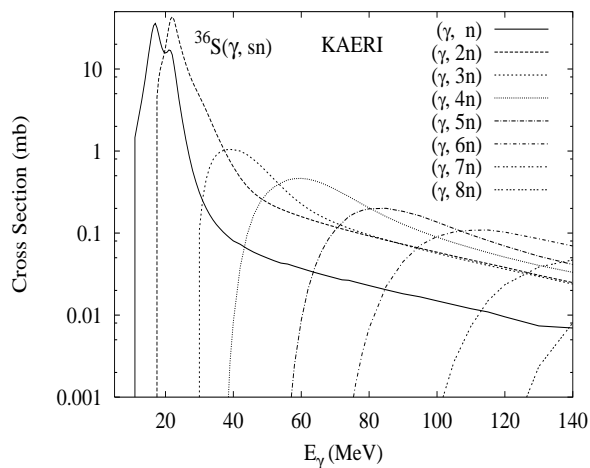
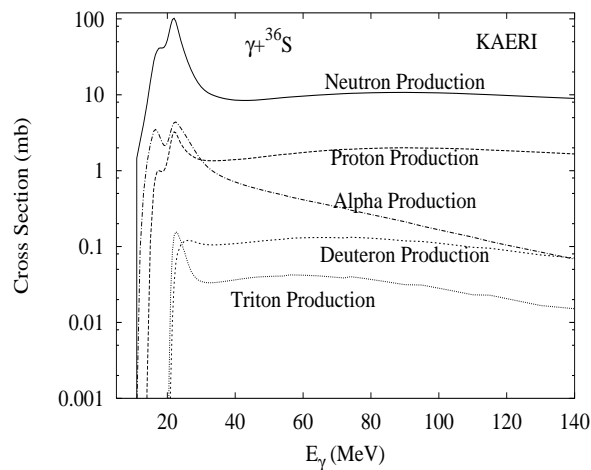
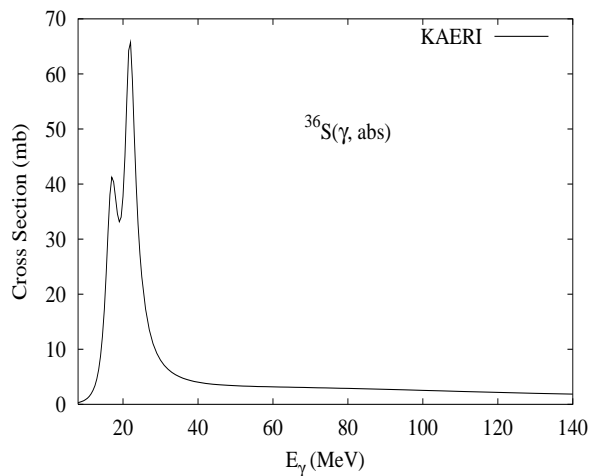
Abundance (%)	Threshold Energies (MeV)								
	$\gamma, n$	$\gamma, p$	$\gamma, t$	$\gamma, \text{He-3}$	$\gamma, \alpha$	$\gamma, 2n$	$\gamma, np$	$\gamma, 2p$	$\gamma, 3n$
4.21	11.42	10.88	20.44	21.91	7.92	20.06	20.99	20.43	35.10



The photoabsorption cross section was evaluated based on the experimental data of Assafiri [Ass86], up to 35 MeV. Above this energy, the absorption cross section was calculated from the QD model.

The calculated results of the emission channels by the GNASH code are in good agreement with the experimental data [Ass84] for the  $(\gamma, \text{sn})$  and  $(\gamma, p)$  reaction cross sections, but there are some gaps between calculations and measurements for  $(\gamma, 2n)$  reaction cross sections above around 25 MeV of photon energies.

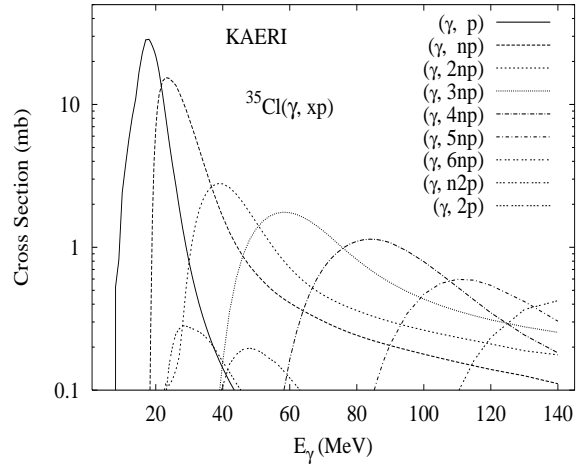
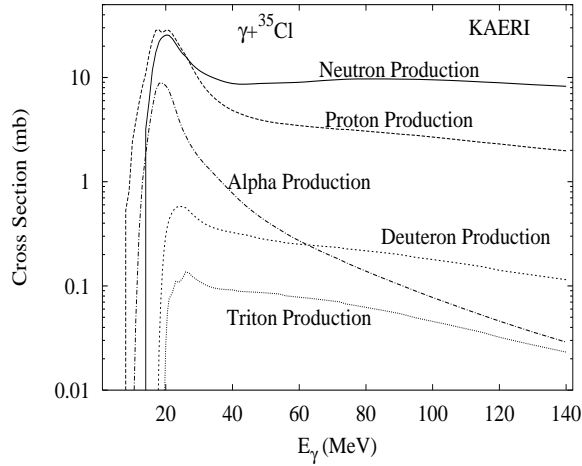
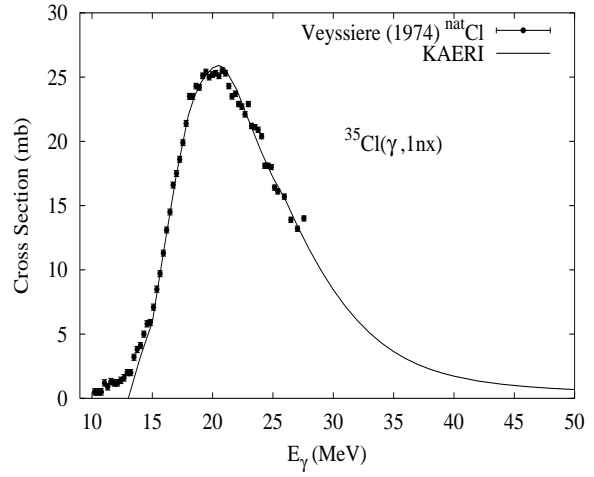
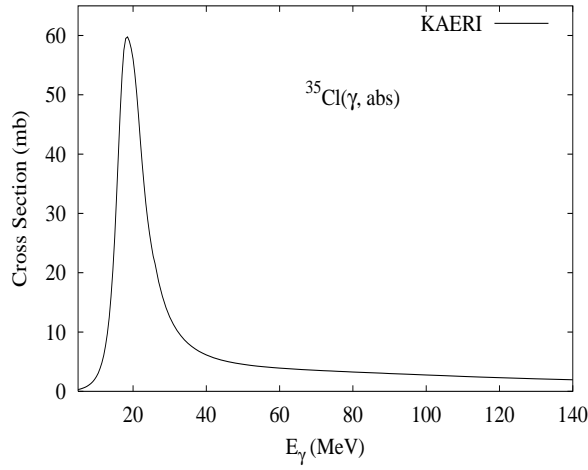
Abundance (%)	Threshold Energies (MeV)								
	$\gamma, n$	$\gamma, p$	$\gamma, t$	$\gamma, \text{He-3}$	$\gamma, \alpha$	$\gamma, 2n$	$\gamma, np$	$\gamma, 2p$	$\gamma, 3n$
0.02	9.89	13.10	19.28	25.10	9.01	16.87	21.47	25.28	28.29



There are no experimental data available. The photoabsorption cross section was obtained from GDR and QD model calculations, adopting the GDR parameters of  ${}^{34}\text{S}$ . The neutron, proton, deuteron, triton and alpha emission cross sections, as well as production cross sections, were calculated by the GNASH code.

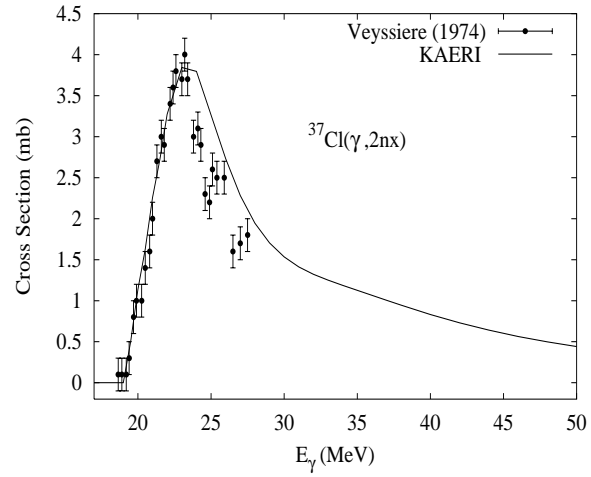
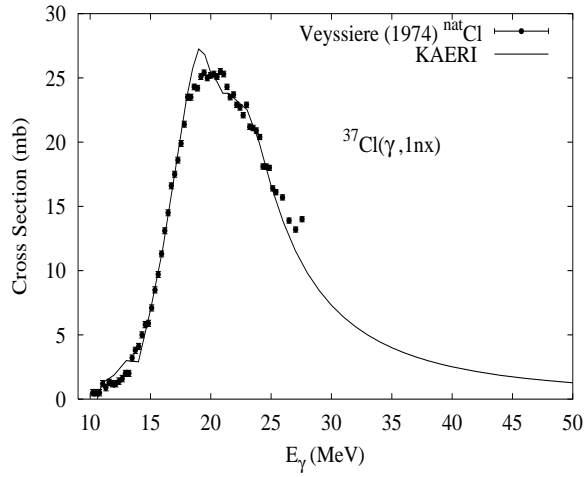
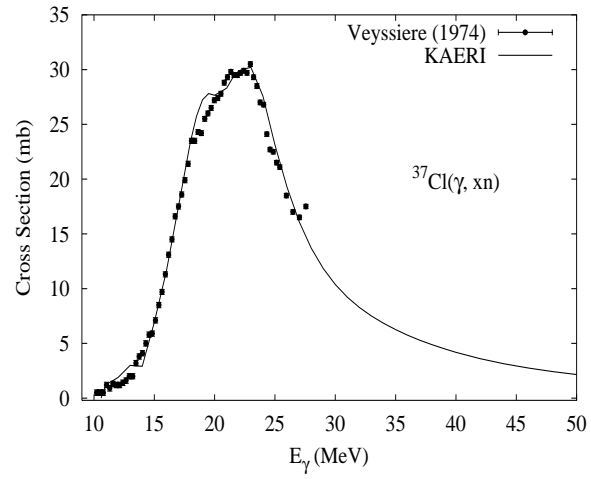
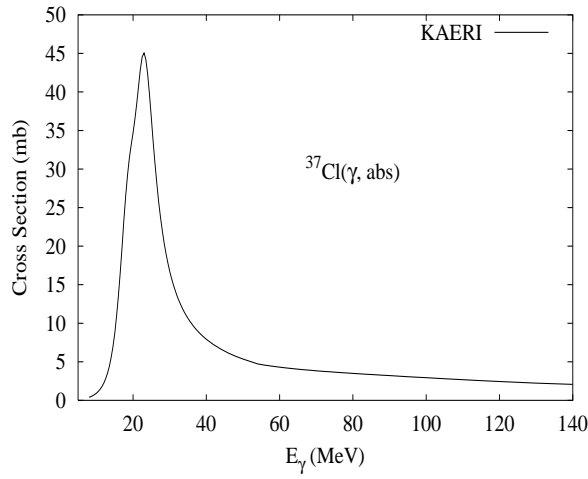


Abundance (%)	Threshold Energies (MeV)								
	$\gamma, n$	$\gamma, p$	$\gamma, t$	$\gamma, \text{He-3}$	$\gamma, \alpha$	$\gamma, 2n$	$\gamma, np$	$\gamma, 2p$	$\gamma, 3n$
75.77	12.65	6.37	17.95	19.64	7.00	24.15	17.79	17.25	39.90



The photoabsorption cross section has not been measured. However, for  ${}^{nat}\text{Cl}$ , there are experimental data for the  $(\gamma, 1nx)$ ,  $(\gamma, 2nx)$  and  $(\gamma, xn)$  reaction cross sections [Vey74]. We relied on the GUNF and GNASH codes to infer the photoabsorption cross section in the GDR regime, in order to model accurately the  $(\gamma, 1nx)$  data. The photoabsorption cross section above the GDR, up to 140 MeV, was obtained from QD model calculations using the theory of Chadwick. The neutron, proton, deuteron, triton and alpha emission cross sections, as well as production cross sections, were calculated by the GNASH code.

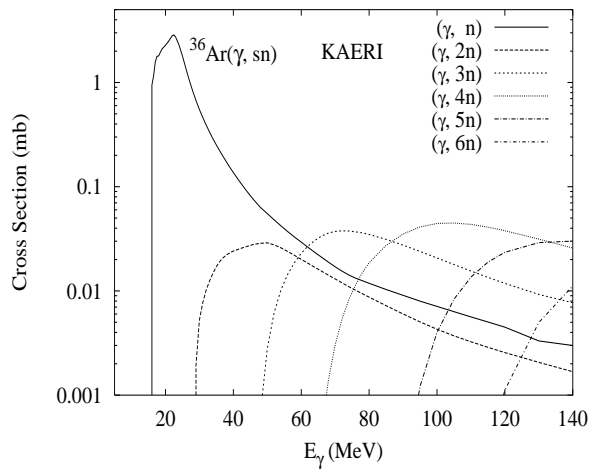
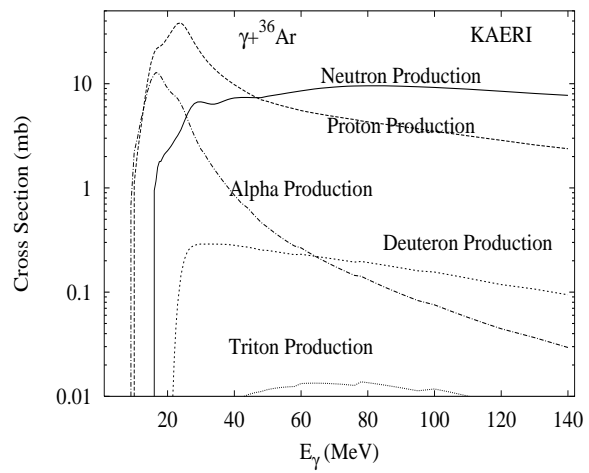
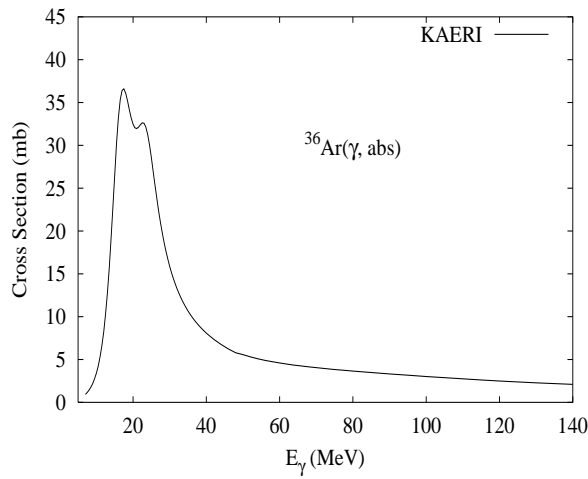
Abundance (%)	Threshold Energies (MeV)								
	$\gamma, n$	$\gamma, p$	$\gamma, t$	$\gamma, \text{He-3}$	$\gamma, \alpha$	$\gamma, 2n$	$\gamma, np$	$\gamma, 2p$	$\gamma, 3n$
24.23	10.31	8.39	16.78	22.14	7.85	18.89	18.28	21.48	31.54



The photoabsorption cross section has not been measured. However, for  ${}^{nat}\text{Cl}$ , there are experimental data for the  $(\gamma, 1nx)$ ,  $(\gamma, 2nx)$  and  $(\gamma, xn)$  reaction cross sections [Vey74]. We relied on the GUNF and GNASH codes to infer the photoabsorption cross section in the GDR regime, in order to model accurately the  $(\gamma, 1nx)$  data. The photoabsorption cross section above the GDR, up to 140 MeV, was obtained from QD model calculations using the theory of Chadwick.

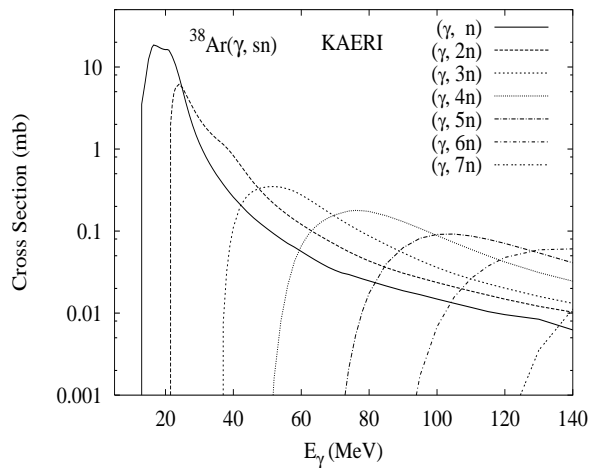
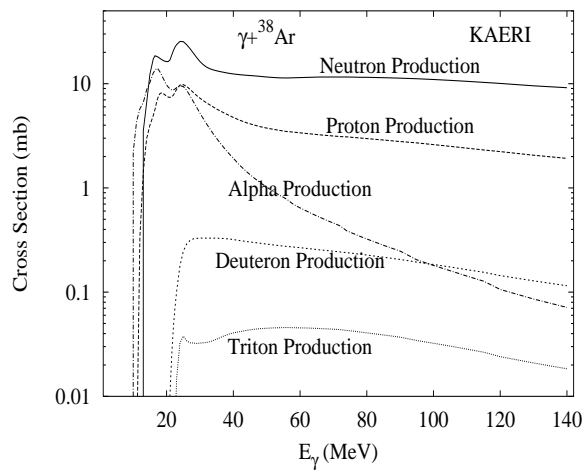
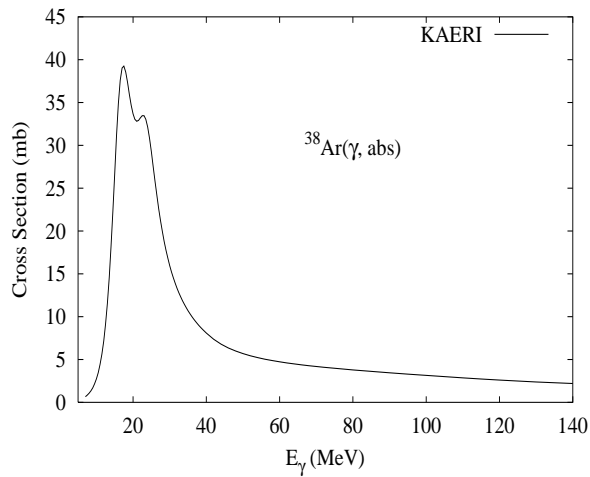
The calculated results of the emission channels by the GNASH are in agreement with the experimental data of  ${}^{nat}\text{Cl}$  for the  $(\gamma, 1nx)$ ,  $(\gamma, 2nx)$ , and  $(\gamma, xn)$  reaction cross sections.

Abundance (%)	Threshold Energies (MeV)								
	$\gamma, n$	$\gamma, p$	$\gamma, t$	$\gamma, \text{He-3}$	$\gamma, \alpha$	$\gamma, 2n$	$\gamma, np$	$\gamma, 2p$	$\gamma, 3n$
0.34	15.25	8.51	24.18	18.58	6.64	27.99	21.15	14.88	45.06



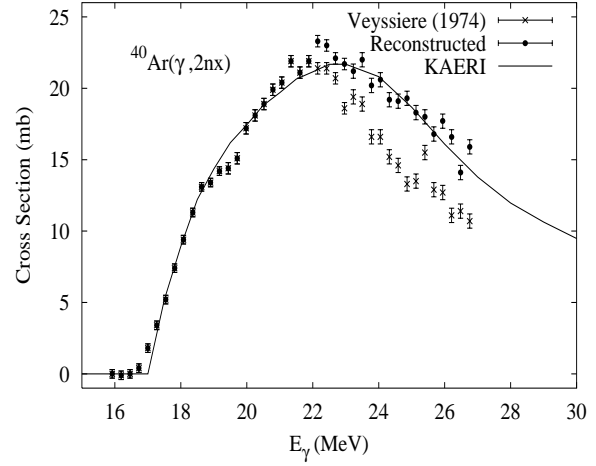
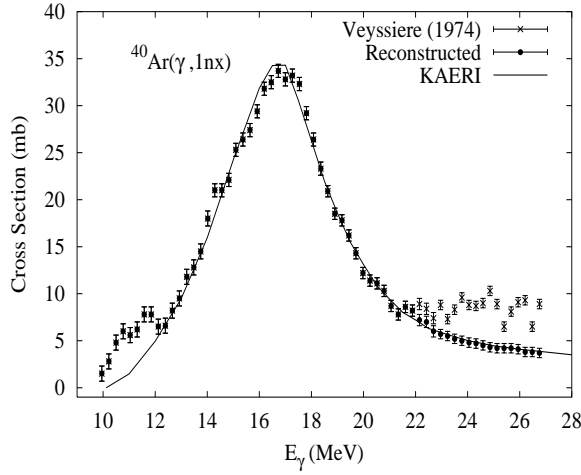
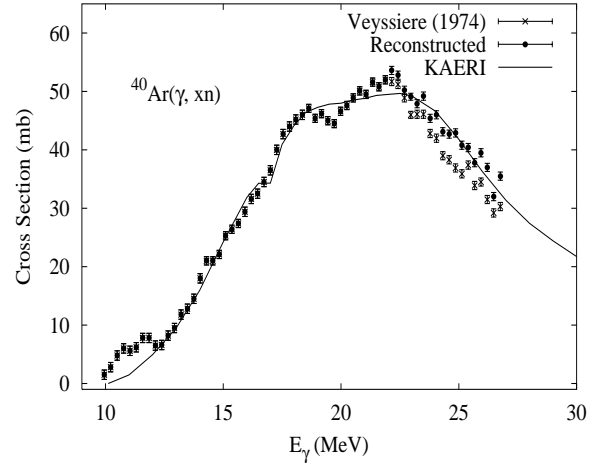
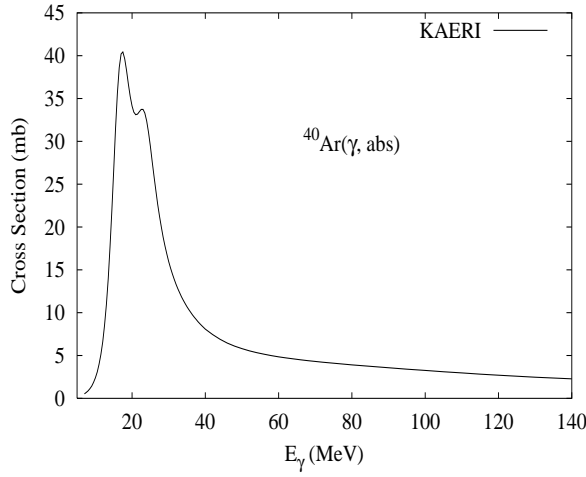
There are no experimental data available. The photoabsorption cross section was obtained from GDR and QD model calculations, adopting the GDR parameters of  ${}^{40}\text{Ar}$ . The neutron, proton, deuteron, triton and alpha emission cross sections, as well as production cross sections, were calculated by the GNASH code.

Abundance (%)	Threshold Energies (MeV)								
	$\gamma, n$	$\gamma, p$	$\gamma, t$	$\gamma, \text{He-3}$	$\gamma, \alpha$	$\gamma, 2n$	$\gamma, np$	$\gamma, 2p$	$\gamma, 3n$
0.06	11.84	10.24	20.65	20.80	7.21	20.63	20.55	18.63	35.88



There are no experimental data available. The photoabsorption cross section was obtained from GDR and QD model calculations, adopting the GDR parameters of  ${}^{40}\text{Ar}$ . The neutron, proton, deuteron, triton and alpha emission cross sections, as well as production cross sections, were calculated by the GNASH code.

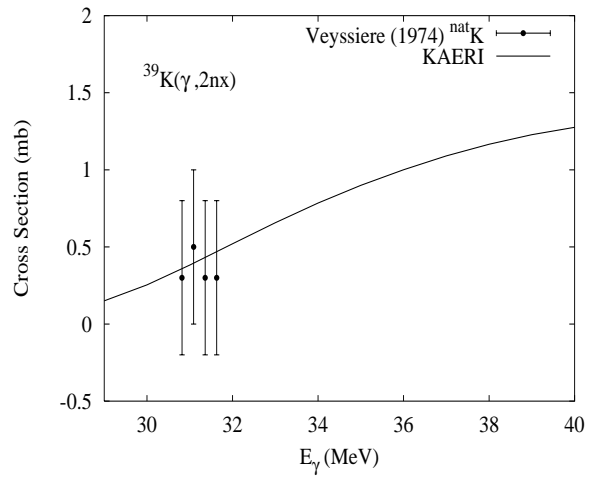
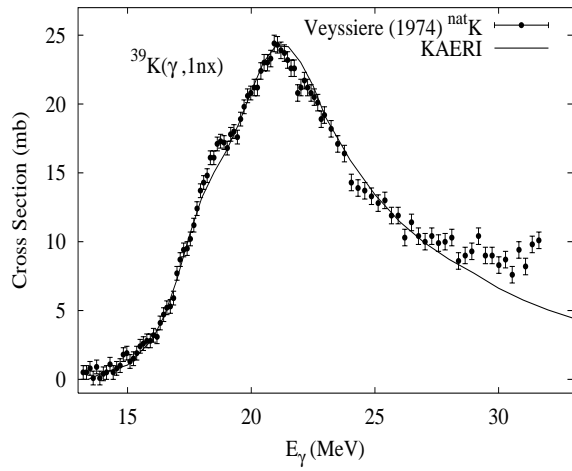
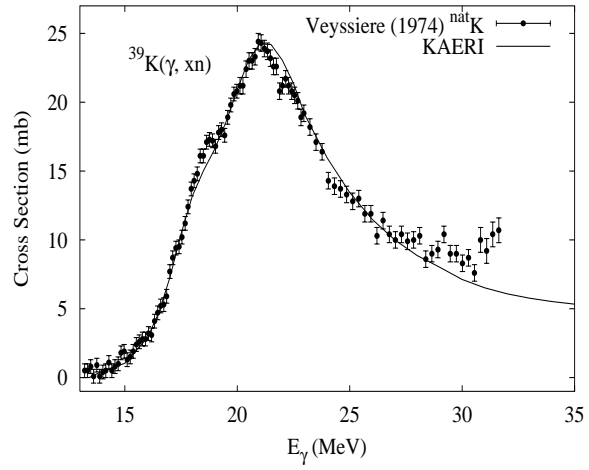
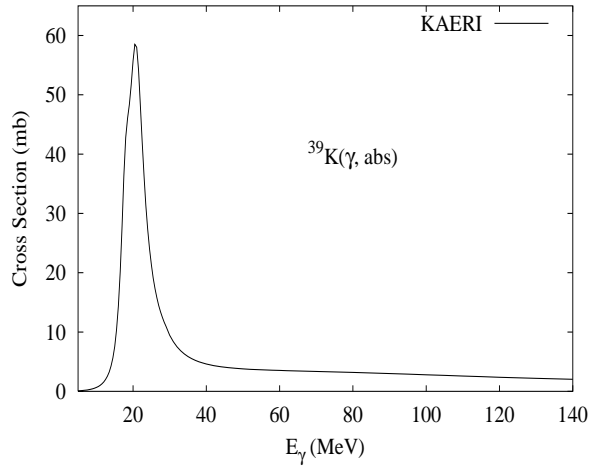
Abundance (%)	Threshold Energies (MeV)								
	$\gamma, n$	$\gamma, p$	$\gamma, t$	$\gamma, \text{He-3}$	$\gamma, \alpha$	$\gamma, 2n$	$\gamma, np$	$\gamma, 2p$	$\gamma, 3n$
99.60	9.87	12.53	18.23	23.07	6.80	16.47	20.60	22.76	28.30



There are no experimental data for the absorption cross section. However, experimental data are available for  $(\gamma, 1nx)$ ,  $(\gamma, 2nx)$ , and  $(\gamma, xn)$  reaction cross sections [Vey74]. We relied on the GUNF and GNASH codes to infer the photoabsorption cross section in the GDR regime, so as to model accurately the  $(\gamma, xn)$  data. The photoabsorption cross section above the GDR, up to 140 MeV, was obtained from QD model calculations using the theory of Chadwick.

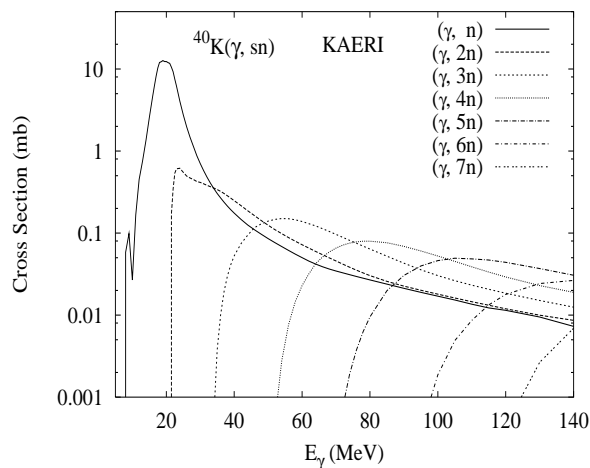
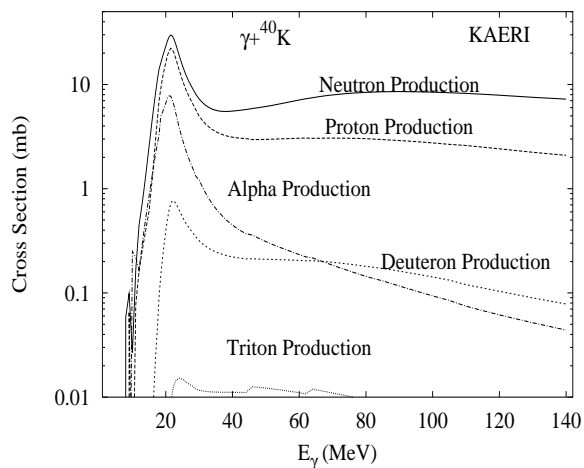
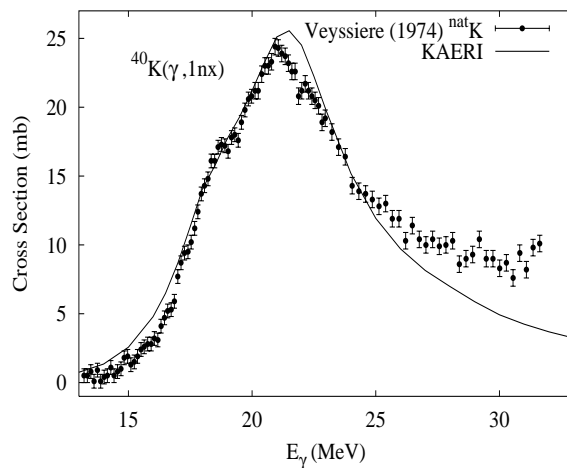
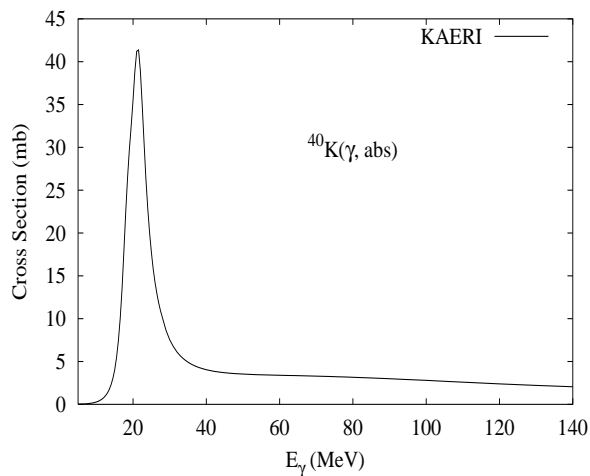
The calculated results of the emission channels by the GNASH code are in good agreement with all the photoneutron reaction data below 22 MeV. However, above 22 MeV the calculated cross section for the  $(\gamma, 1nx)$  channel is smaller, and that for the  $(\gamma, 2nx)$  channel is larger than the experimental data. New reference photoneutron cross sections were reconstructed by adding the excess of  $(\gamma, 1nx)$  cross section  $[(\gamma, 1nx)_{\text{expt}} - (\gamma, 1nx)_{\text{calc}}]$ , to the  $(\gamma, 2nx)$  cross section above 22 MeV.

Abundance (%)	Threshold Energies (MeV)								
	$\gamma, n$	$\gamma, p$	$\gamma, t$	$\gamma, \text{He-3}$	$\gamma, \alpha$	$\gamma, 2n$	$\gamma, np$	$\gamma, 2p$	$\gamma, 3n$
93.26	13.08	6.38	18.53	19.22	7.22	25.15	18.22	16.62	40.60



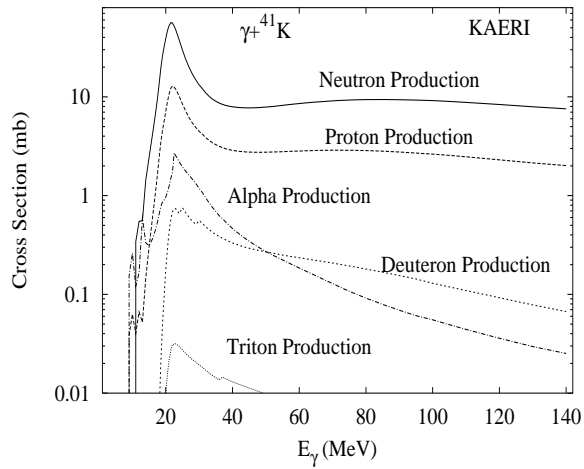
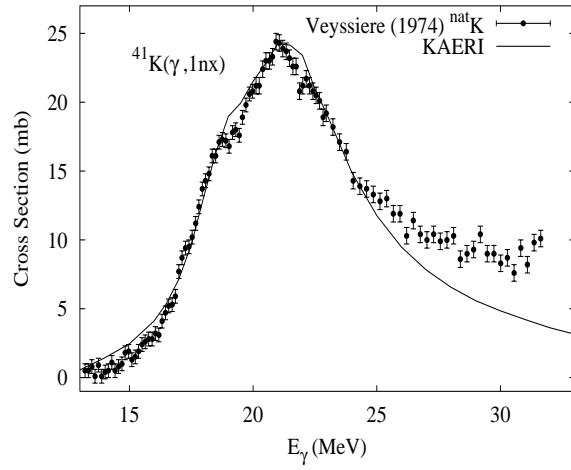
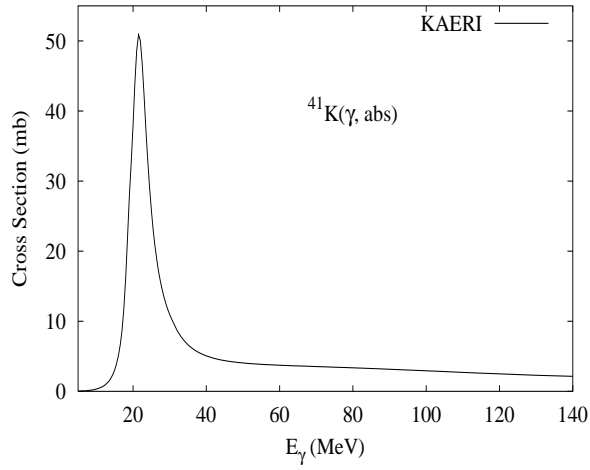
The photoabsorption cross section has not been measured. However, for  $^{nat}\text{K}$ , there are experimental data for the  $(\gamma, 1nx)$ ,  $(\gamma, 2nx)$  and  $(\gamma, xn)$  reaction cross sections [Vey74]. We relied on the GUNF and GNASH codes to infer the photoabsorption cross section in the GDR regime, in order to model accurately the  $(\gamma, 1nx)$  data. The photoabsorption cross section above the GDR, up to 140 MeV, was obtained from QD model calculations using the theory of Chadwick. The neutron, proton, deuteron, triton and alpha emission cross sections, as well as production cross sections, were calculated by the GNASH code.

Abundance (%)	Threshold Energies (MeV)								
	$\gamma, n$	$\gamma, p$	$\gamma, t$	$\gamma, \text{He-3}$	$\gamma, \alpha$	$\gamma, 2n$	$\gamma, np$	$\gamma, 2p$	$\gamma, 3n$
0.01	7.80	7.58	17.54	16.70	6.44	20.88	14.18	18.31	32.95



The photoabsorption cross section has not been measured. The photoabsorption cross section was obtained from GDR and QD model calculations, adopting the GDR parameters of  ${}^{39}\text{K}$ . The neutron, proton, deuteron, triton and alpha emission cross sections, as well as production cross sections, were calculated by the GNASH code. The calculated results for the  ${}^{40}\text{K}(\gamma, 1nx)$  are lower than the  ${}^{nat}\text{K}$  data above 25 MeV, where the  ${}^{39}\text{K}(\gamma, 2n)$  reaction channel opens.

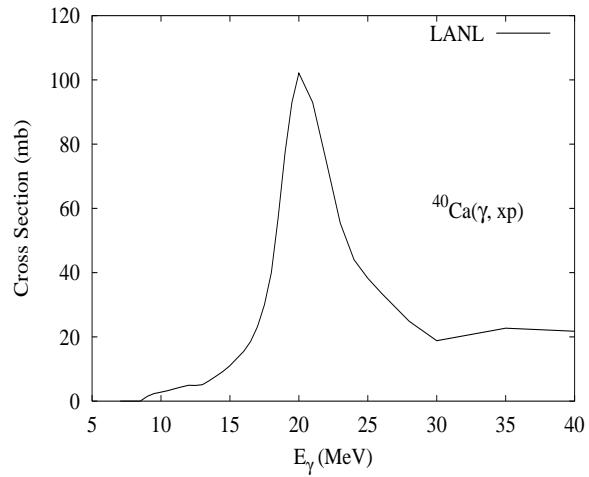
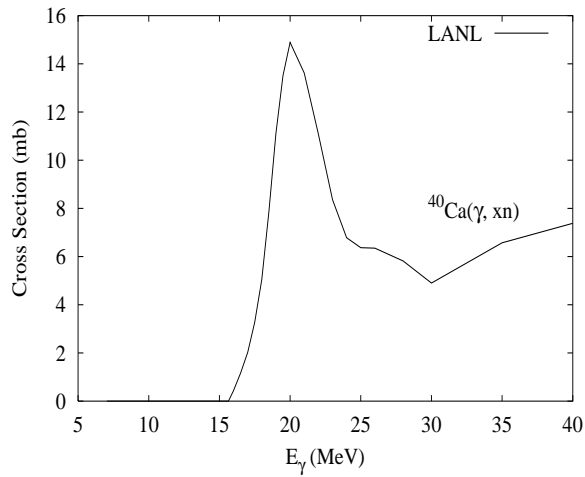
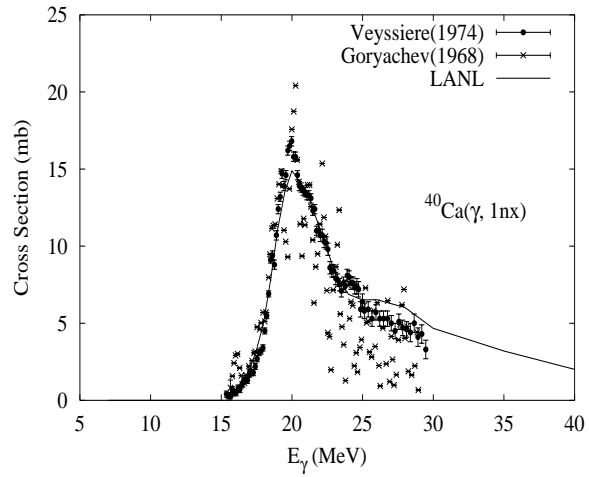
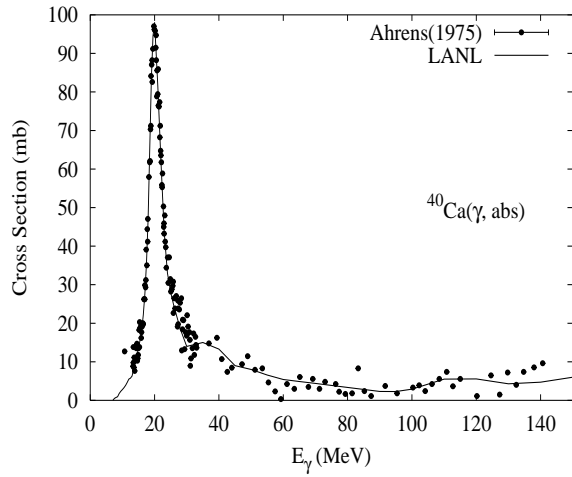
Abundance (%)	Threshold Energies (MeV)								
	$\gamma, n$	$\gamma, p$	$\gamma, t$	$\gamma, \text{He-3}$	$\gamma, \alpha$	$\gamma, 2n$	$\gamma, np$	$\gamma, 2p$	$\gamma, 3n$
6.73	10.10	7.81	15.79	20.69	6.22	17.89	17.68	20.33	30.97



The photoabsorption cross section has not been measured. The photoabsorption cross section was obtained from GDR and QD model calculations. The neutron, proton, deuteron, triton and alpha emission cross sections, as well as production cross sections, were calculated by the GNASH code. The calculated results for the  ${}^{41}\text{K}(\gamma, 1nx)$  are lower than the  ${}^{nat}\text{K}$  data above 25 MeV, where the  ${}^{39}\text{K}(\gamma, 2n)$  reaction channel opens.



Abundance (%)	Threshold Energies (MeV)								
	$\gamma, n$	$\gamma, p$	$\gamma, t$	$\gamma, \text{He-3}$	$\gamma, \alpha$	$\gamma, 2n$	$\gamma, np$	$\gamma, 2p$	$\gamma, 3n$
96.94	15.64	8.33	25.00	18.83	7.04	28.93	21.40	14.71	45.90



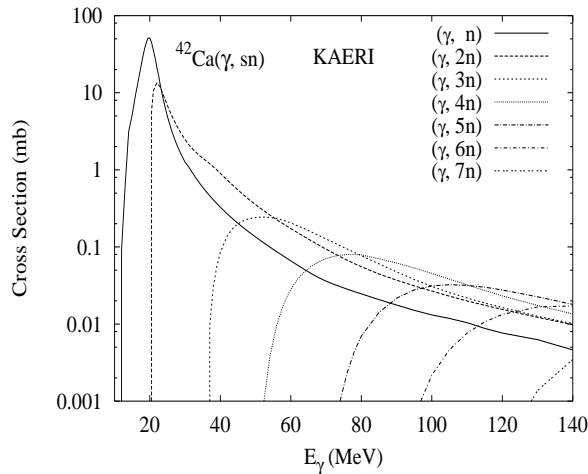
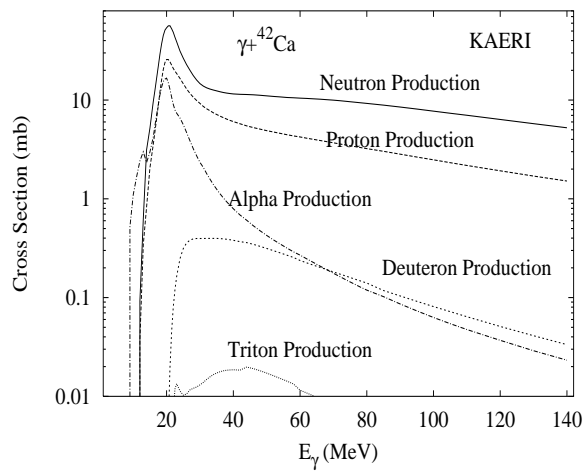
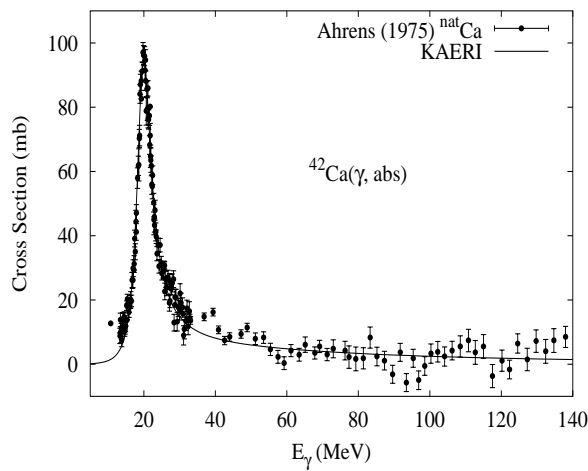
Available data are summarized by Varlamov [Var96]. The photoabsorption cross section was evaluated based on the data of Ahrens [Ahr75], that extend up to 150 MeV. At 60 MeV, the value for the absorption cross section was consistent with that used by Ryckbosch et al. [Ryc90].

The total photoabsorption cross section is used as an input into the GNASH calculations. These calculations then predict the branching to photoneutron, photoproton, etc. emission. The calculated photoneutron production was compared with measurements of Veyssiere [Vey74]. The calculations, after a level density adjustment for  ${}^{39}\text{Ca}$ , predicted the  $(\gamma, xn)$  data well, with the exception of the 25-30 MeV region where the calculated photoneutron production appears to be about 20% too high.

Measurement [Ryc90] of the inclusive photoproton spectrum for 62 MeV  $\text{Ca}(\gamma, xp)$  at  $90^\circ$  provide a useful test of the preequilibrium emission following QD absorption. These data are amongst the very few for essentially monochromatic photons. The calculations, in the preequilibrium region, agree very well with the measurements. This is important since the comparison tests not only the preequilibrium model, but also the angular distribution systematics [Cha95b]. In this particular case, where the systematics predict only a small forward peaking, the calculations at  $90^\circ$  account for the data.

# $\gamma + {}^{42}\text{Ca}$

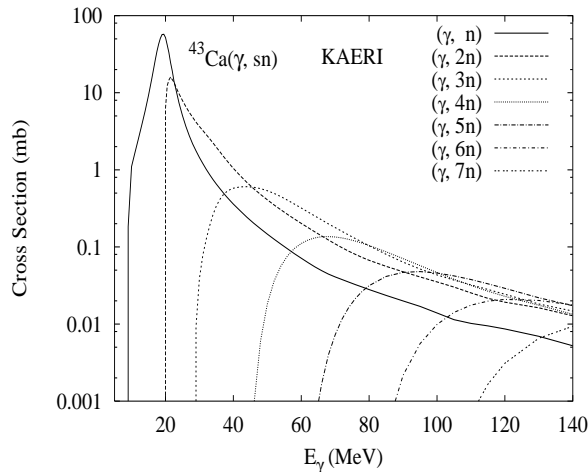
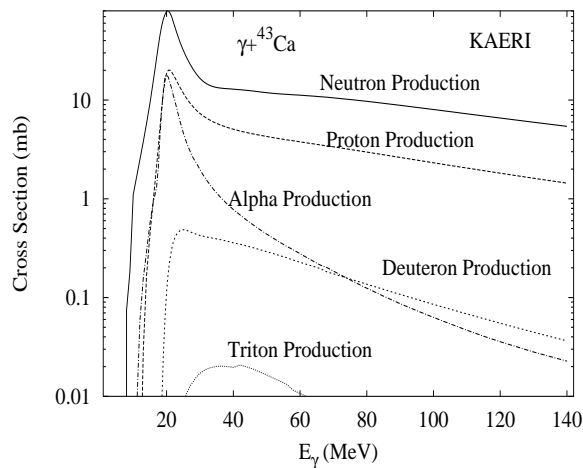
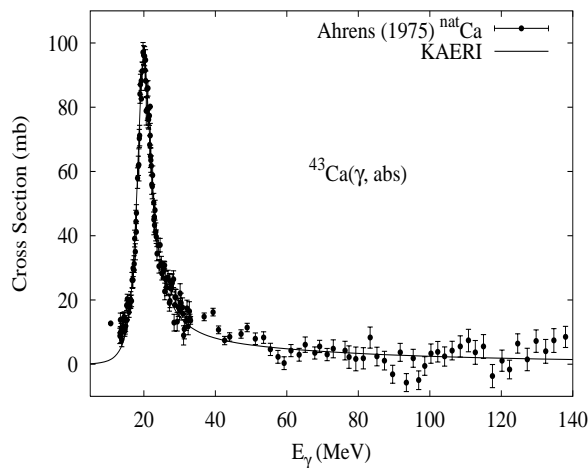
Abundance (%)	Threshold Energies (MeV)								
	$\gamma, n$	$\gamma, p$	$\gamma, t$	$\gamma, \text{He-3}$	$\gamma, \alpha$	$\gamma, 2n$	$\gamma, np$	$\gamma, 2p$	$\gamma, 3n$
0.65	11.48	10.28	19.69	20.24	6.26	19.84	20.37	18.09	35.49



There are no experimental data available. The photoabsorption cross section was obtained from GDR and QD model calculations, adopting the GDR parameters of  ${}^{40}\text{Ca}$ . The neutron, proton, deuteron, triton and alpha emission cross sections, as well as production cross sections, were calculated by the GNASH code.

# $\gamma + {}^{43}\text{Ca}$

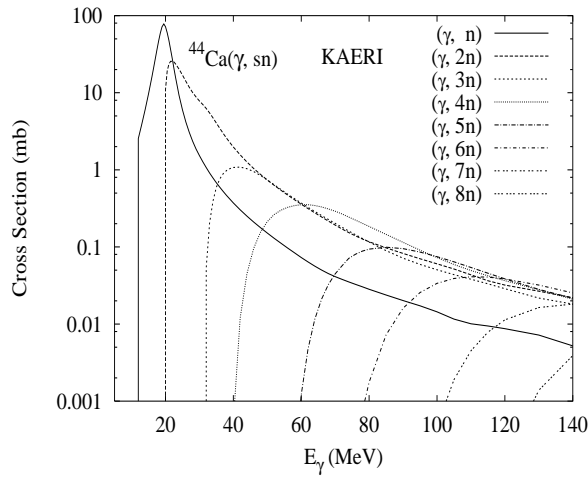
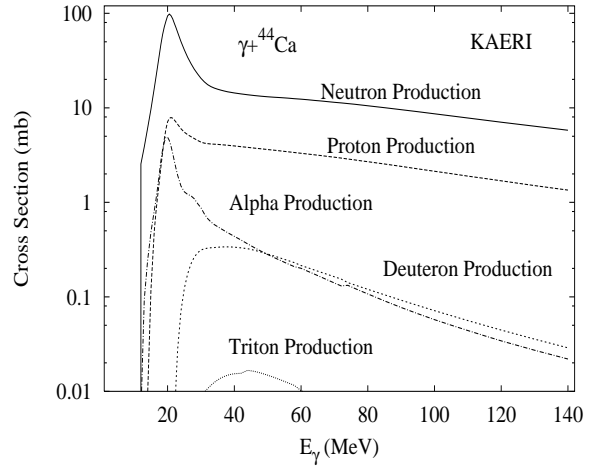
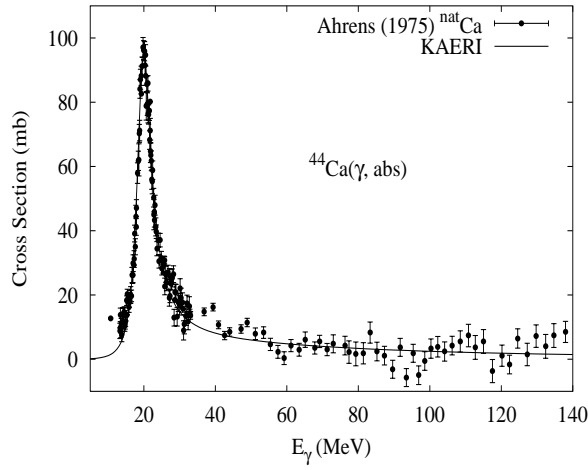
Abundance (%)	Threshold Energies (MeV)								
	$\gamma, n$	$\gamma, p$	$\gamma, t$	$\gamma, \text{He-3}$	$\gamma, \alpha$	$\gamma, 2n$	$\gamma, np$	$\gamma, 2p$	$\gamma, 3n$
0.14	7.93	10.68	19.82	18.30	7.59	19.41	18.21	19.92	27.78



There are no experimental data available. The photoabsorption cross section was obtained from GDR and QD model calculations, adopting the GDR parameters of  ${}^{40}\text{Ca}$ . The neutron, proton, deuteron, triton and alpha emission cross sections, as well as production cross sections, were calculated by the GNASH code.

# $\gamma + {}^{44}\text{Ca}$

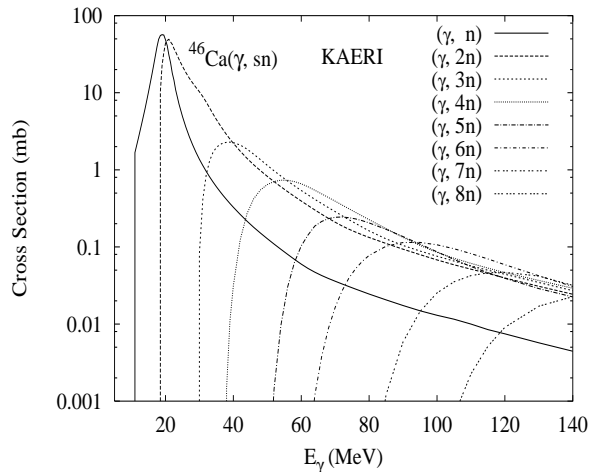
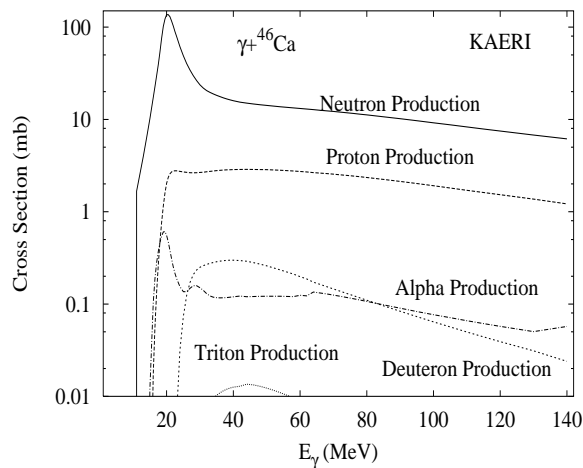
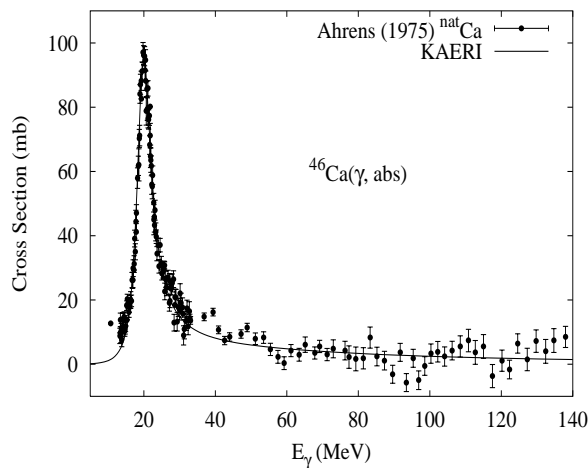
Abundance (%)	Threshold Energies (MeV)								
	$\gamma, n$	$\gamma, p$	$\gamma, t$	$\gamma, \text{He-3}$	$\gamma, \alpha$	$\gamma, 2n$	$\gamma, np$	$\gamma, 2p$	$\gamma, 3n$
2.09	11.13	12.17	20.86	23.33	8.86	19.06	21.81	21.63	30.55



There are no experimental data available. The photoabsorption cross section was obtained from GDR and QD model calculations, adopting the GDR parameters of  ${}^{40}\text{Ca}$ . The neutron, proton, deuteron, triton and alpha emission cross sections, as well as production cross sections, were calculated by the GNASH code.

# $\gamma + {}^{46}\text{Ca}$

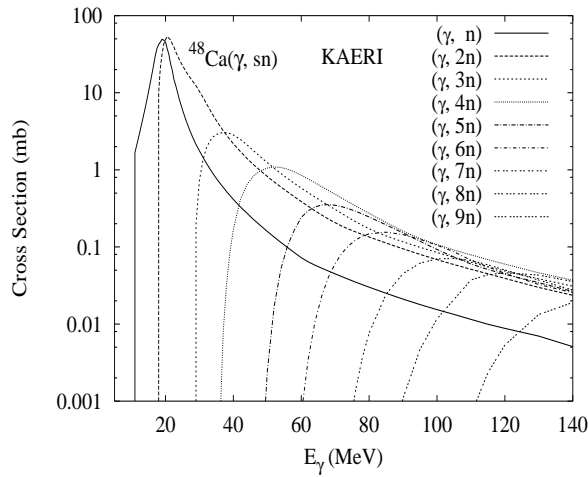
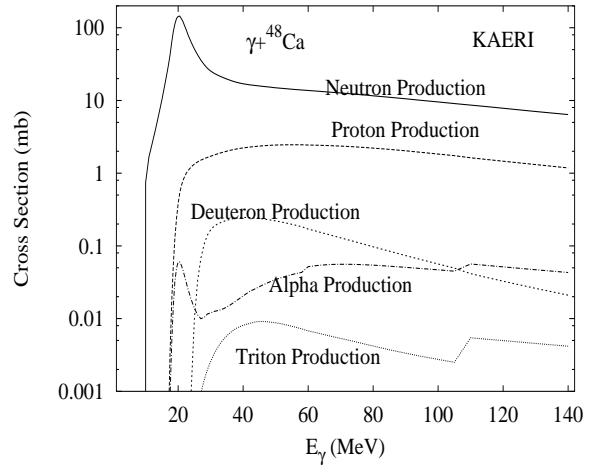
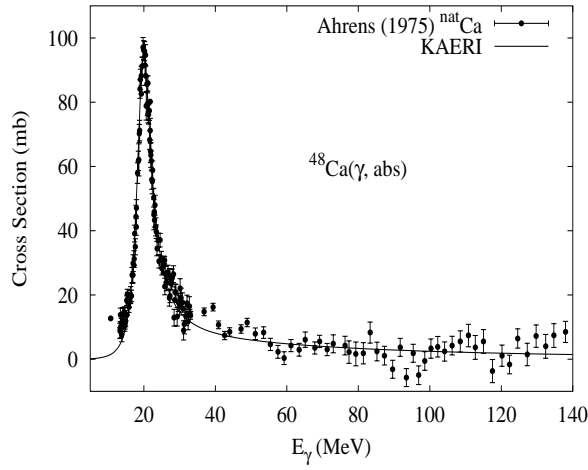
Abundance (%)	Threshold Energies (MeV)								
	$\gamma, n$	$\gamma, p$	$\gamma, t$	$\gamma, \text{He-3}$	$\gamma, \alpha$	$\gamma, 2n$	$\gamma, np$	$\gamma, 2p$	$\gamma, 3n$
0.00	10.40	13.82	21.50	26.09	11.15	17.81	22.69	25.46	28.95



There are no experimental data available. The photoabsorption cross section was obtained from GDR and QD model calculations, adopting the GDR parameters of  ${}^{40}\text{Ca}$ . The neutron, proton, deuteron, triton and alpha emission cross sections, as well as production cross sections, were calculated by the GNASH code.

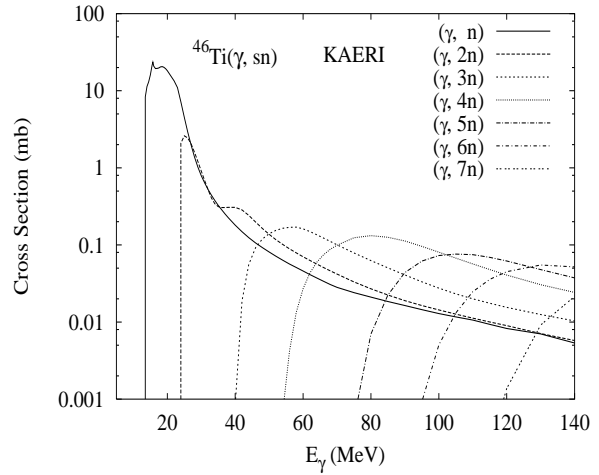
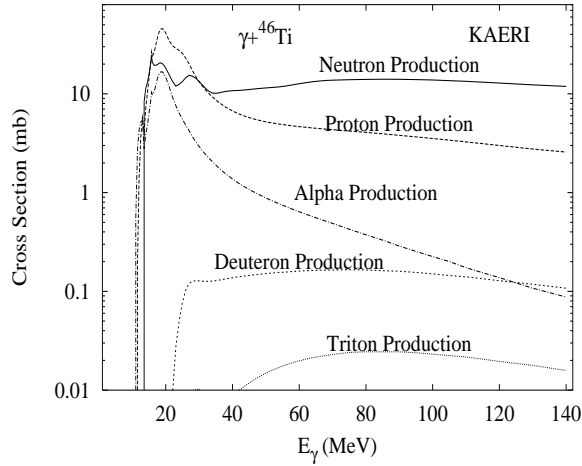
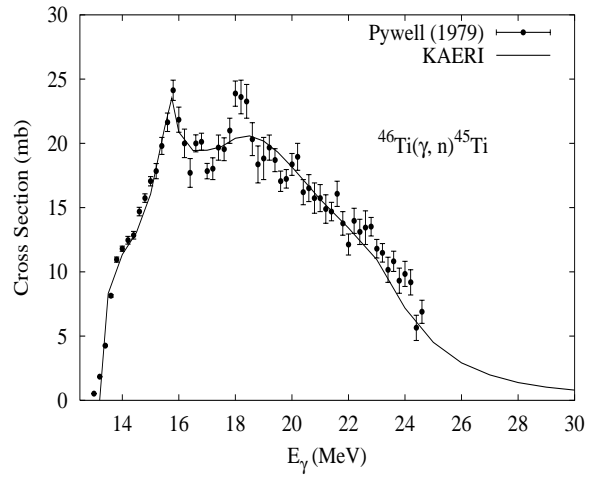
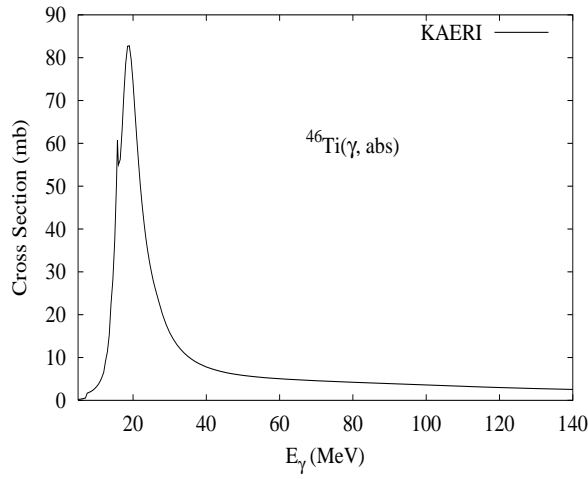
# $\gamma + {}^{48}\text{Ca}$

Abundance (%)	Threshold Energies (MeV)								
	$\gamma, n$	$\gamma, p$	$\gamma, t$	$\gamma, \text{He-3}$	$\gamma, \alpha$	$\gamma, 2n$	$\gamma, np$	$\gamma, 2p$	$\gamma, 3n$
0.19	9.94	15.81	22.55	29.43	14.38	17.22	24.16	29.07	27.62



There are no experimental data available. The photoabsorption cross section was obtained from GDR and QD model calculations, adopting the GDR parameters of  ${}^{40}\text{Ca}$ . The neutron, proton, deuteron, triton and alpha emission cross sections, as well as production cross sections, were calculated by the GNASH code.

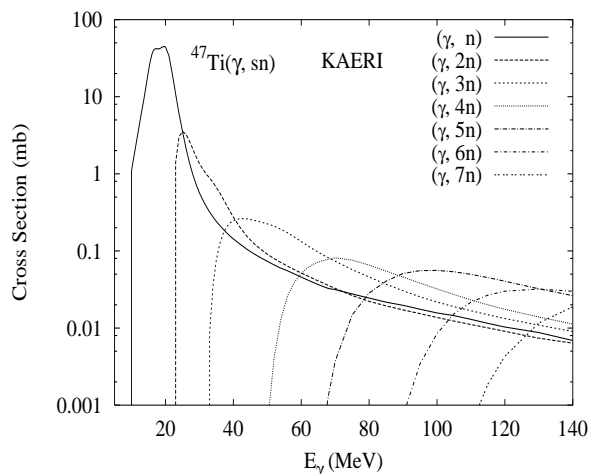
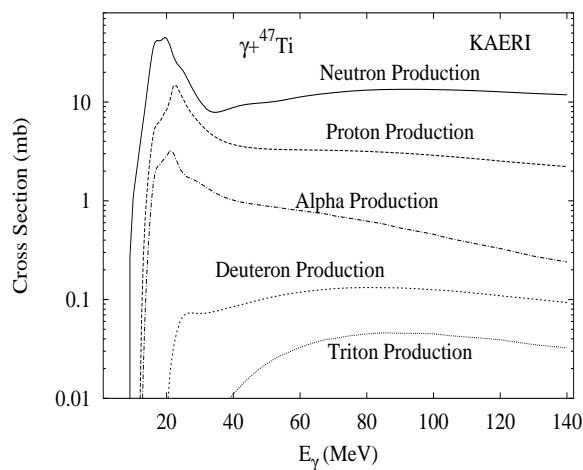
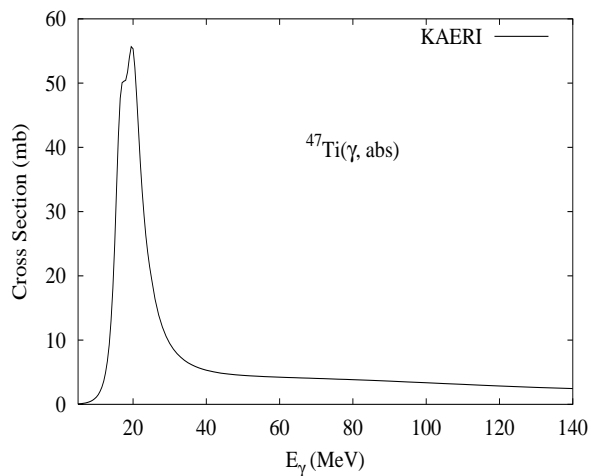
Abundance (%)	Threshold Energies (MeV)								
	$\gamma, n$	$\gamma, p$	$\gamma, t$	$\gamma, \text{He-3}$	$\gamma, \alpha$	$\gamma, 2n$	$\gamma, np$	$\gamma, 2p$	$\gamma, 3n$
8.00	13.19	10.34	22.89	20.65	8.00	22.72	21.67	17.23	39.02



The photoabsorption cross section has not been measured. However, there are experimental data for the  $(\gamma, 1n)$  reaction cross section [Pyw79a]. We relied on the GUNF and GNASH codes to infer the photoabsorption cross section in the GDR regime, in order to model accurately the  $(\gamma, 1n)$  data. The photoabsorption cross section above the GDR, up to 140 MeV, was obtained from QD model calculations using the theory of Chadwick. The neutron, proton, deuteron, triton and alpha emission cross sections, as well as production cross sections, were calculated by the GNASH code.

$\gamma + {}^{47}\text{Ti}$ 

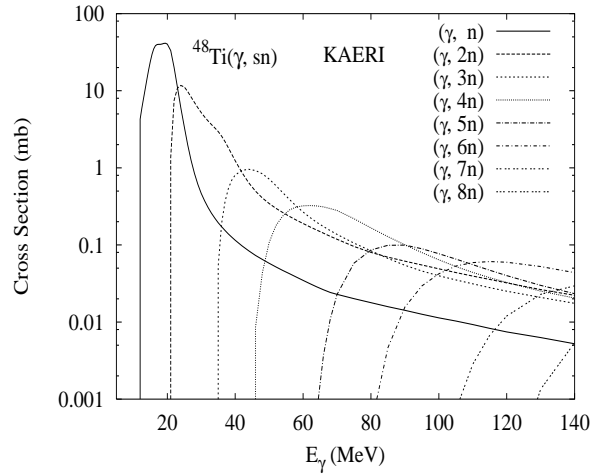
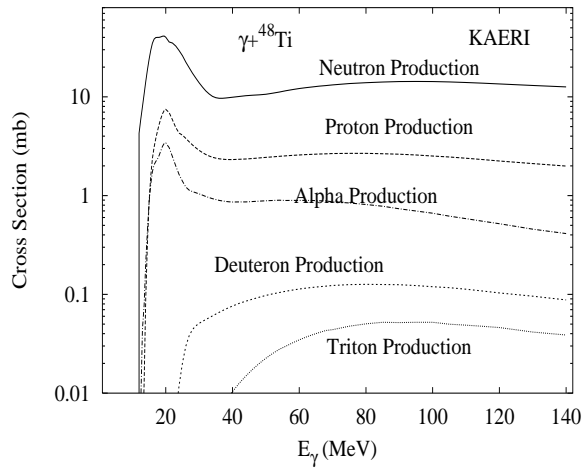
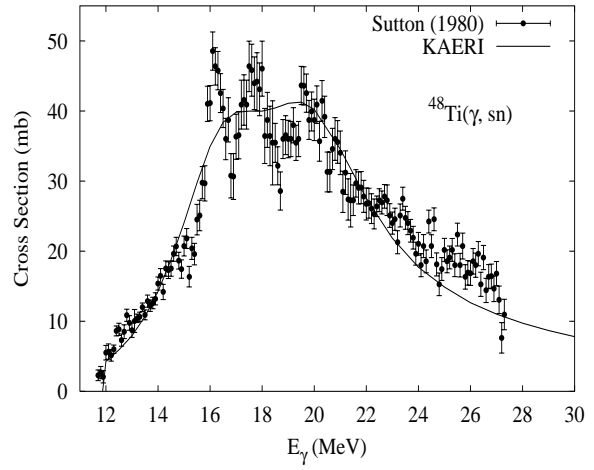
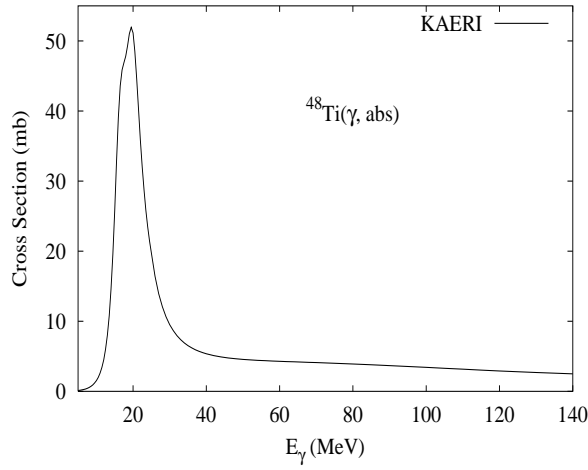
Abundance (%)	Threshold Energies (MeV)								
	$\gamma, n$	$\gamma, p$	$\gamma, t$	$\gamma, \text{He-3}$	$\gamma, \alpha$	$\gamma, 2n$	$\gamma, np$	$\gamma, 2p$	$\gamma, 3n$
7.30	8.88	10.46	22.07	18.39	8.95	22.07	19.22	18.70	31.60



There no experimental data available. The photoabsorption cross section was obtained from GDR and QD model calculations, adopting the GDR parameters of  ${}^{48}\text{Ti}$ . The neutron, proton, deuteron, triton and alpha emission cross sections, as well as production cross sections, were calculated by the GNASH code.



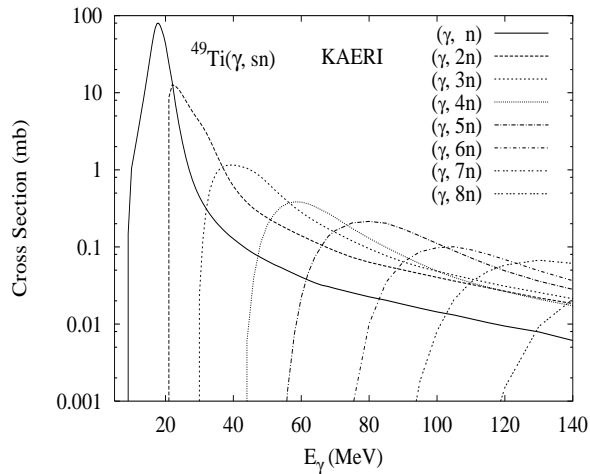
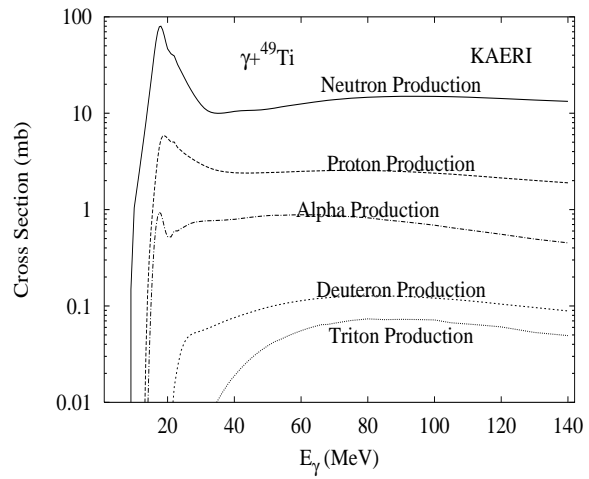
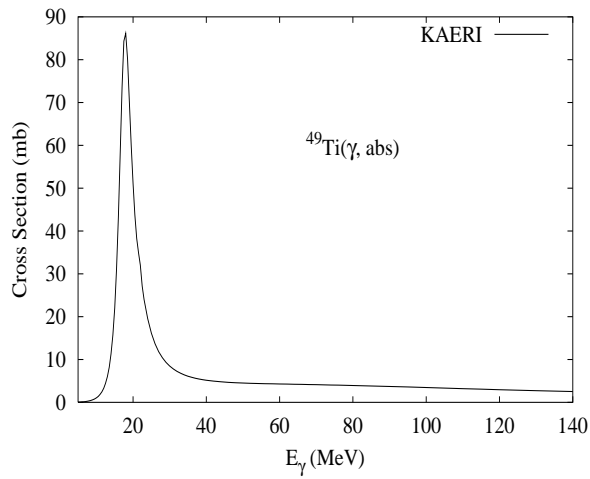
Abundance (%)	Threshold Energies (MeV)								
	$\gamma, n$	$\gamma, p$	$\gamma, t$	$\gamma, \text{He-3}$	$\gamma, \alpha$	$\gamma, 2n$	$\gamma, np$	$\gamma, 2p$	$\gamma, 3n$
73.80	11.63	11.45	22.37	22.61	9.44	20.50	22.09	19.92	33.69



The photoabsorption cross section has not been measured. However, there are experimental data for the  $(\gamma, xn)$  reaction cross section [Sut80]. We relied on the GUNF and GNASH codes to infer the photoabsorption cross section in the GDR regime, in order to model accurately the  $(\gamma, xn)$  data. The photoabsorption cross section above the GDR, up to 140 MeV, was obtained from QD model calculations using the theory of Chadwick. The neutron, proton, deuteron, triton and alpha emission cross sections, as well as production cross sections, were calculated by the GNASH code.

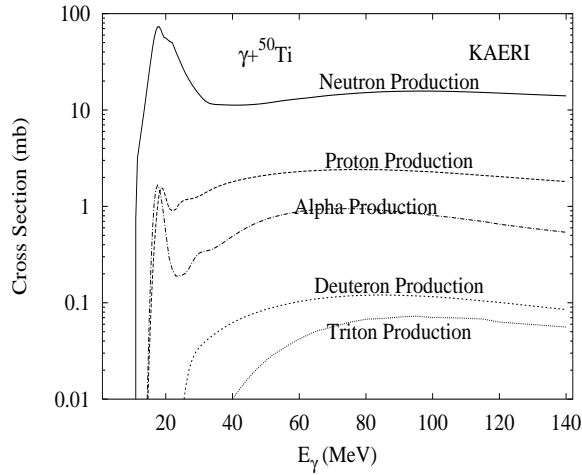
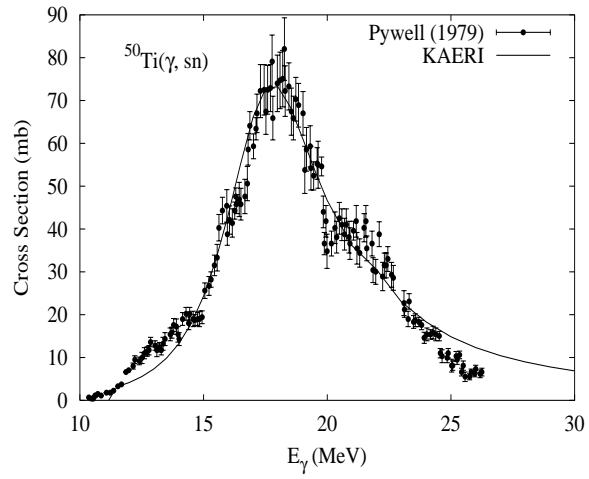
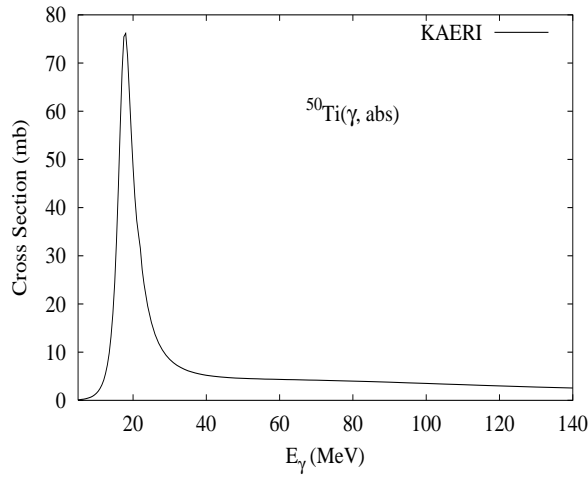
$\gamma + {}^{49}\text{Ti}$ 

Abundance (%)	Threshold Energies (MeV)								
	$\gamma, n$	$\gamma, p$	$\gamma, t$	$\gamma, \text{He-3}$	$\gamma, \alpha$	$\gamma, 2n$	$\gamma, np$	$\gamma, 2p$	$\gamma, 3n$
5.50	8.14	11.36	21.75	20.35	10.17	19.77	19.59	20.79	28.65



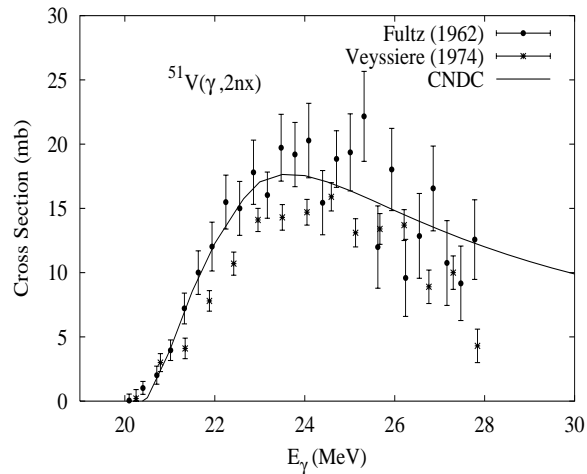
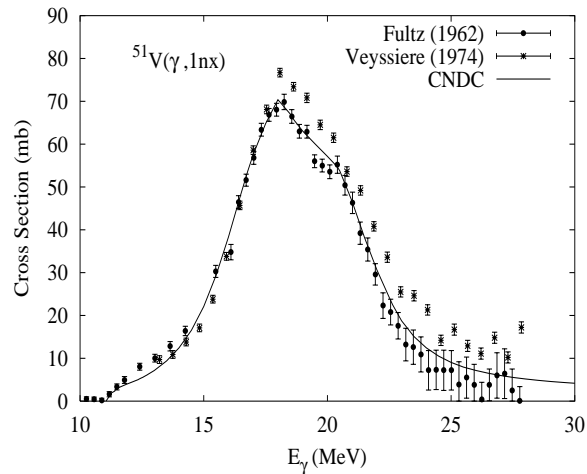
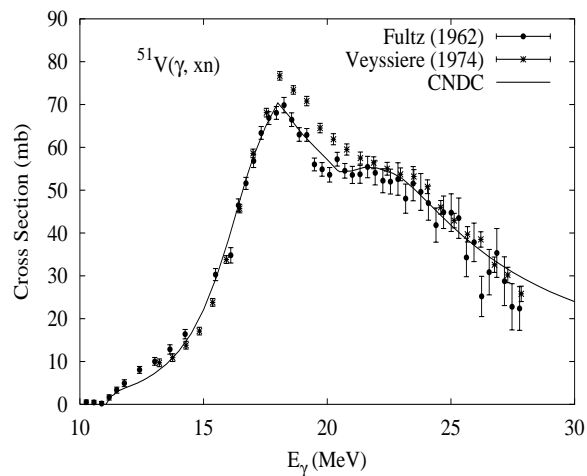
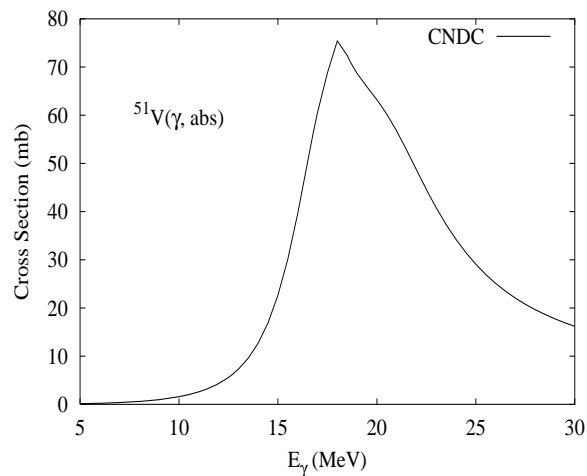
There no experimental data available. The photoabsorption cross section was obtained from GDR and QD model calculations, adopting the GDR parameters of  ${}^{48}\text{Ti}$ . The neutron, proton, deuteron, triton and alpha emission cross sections, as well as production cross sections, were calculated by the GNASH code.

Abundance (%)	Threshold Energies (MeV)								
	$\gamma, n$	$\gamma, p$	$\gamma, t$	$\gamma, \text{He-3}$	$\gamma, \alpha$	$\gamma, 2n$	$\gamma, np$	$\gamma, 2p$	$\gamma, 3n$
5.40	10.94	12.16	22.05	24.01	10.71	19.08	22.29	21.79	30.71



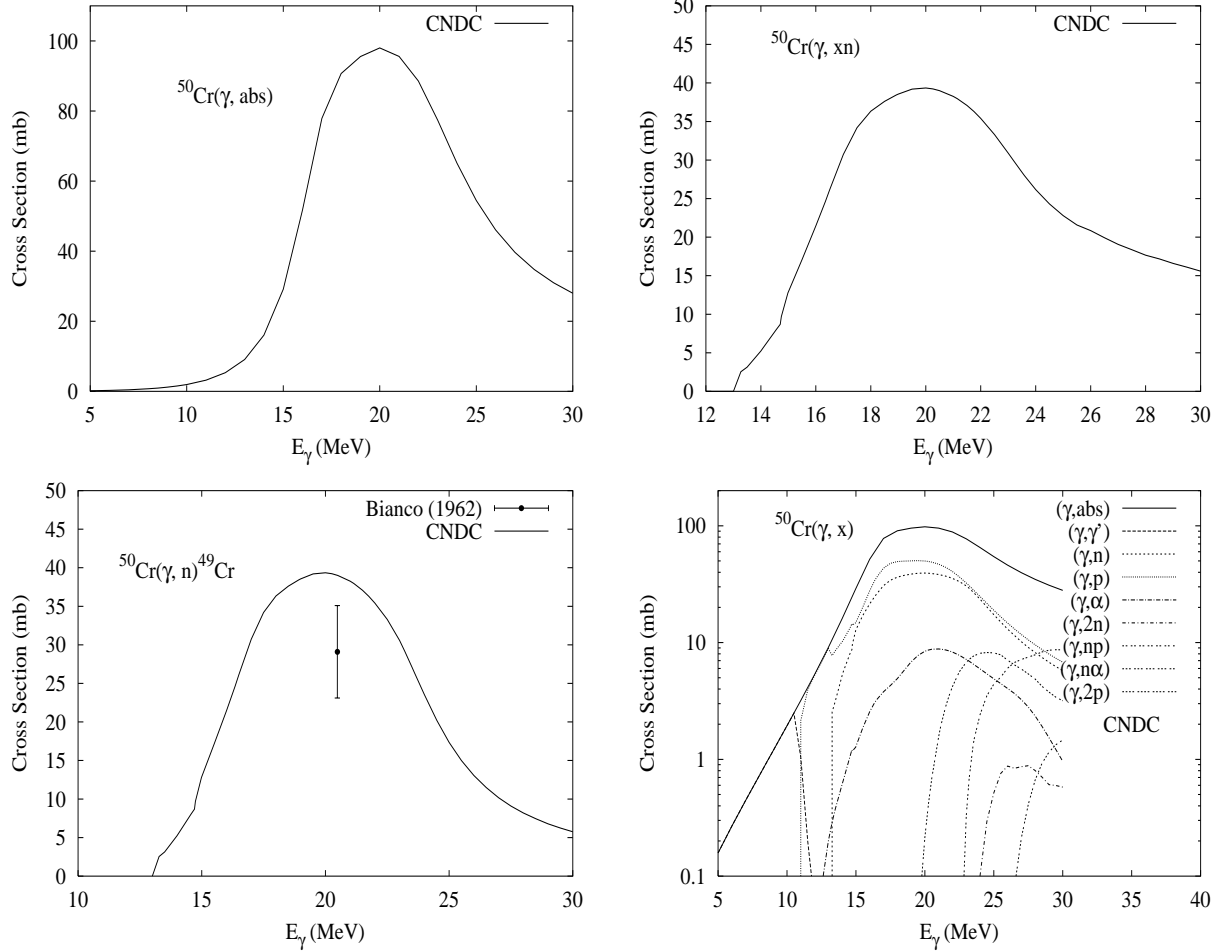
The photoabsorption cross section has not been measured. However, there are experimental data for the  $(\gamma, xn)$  reaction cross section [Pyw79b]. We relied on the GUNF and GNASH codes to infer the photoabsorption cross section in the GDR regime, in order to model accurately the  $(\gamma, xn)$  data. The photoabsorption cross section above the GDR, up to 140 MeV, was obtained from QD model calculations using the theory of Chadwick. The neutron, proton, deuteron, triton and alpha emission cross sections, as well as production cross sections, were calculated by the GNASH code.

Abundance (%)	Threshold Energies (MeV)								
	$\gamma, n$	$\gamma, p$	$\gamma, t$	$\gamma, \text{He-3}$	$\gamma, \alpha$	$\gamma, 2n$	$\gamma, np$	$\gamma, 2p$	$\gamma, 3n$
99.75	11.05	8.06	18.66	22.64	10.29	20.39	19.00	20.22	31.94



The photoabsorption cross section has not been measured. However, there are experimental data for the  $(\gamma, 1nx)$ ,  $(\gamma, 2nx)$  and  $(\gamma, xn)$  reaction cross sections [Ful62a, Vey74]. We relied on GUNF code [Zha98] to infer the photoabsorption cross section in the GDR regime, in order to model accurately the available experimental data [Ful62a, Vey74].

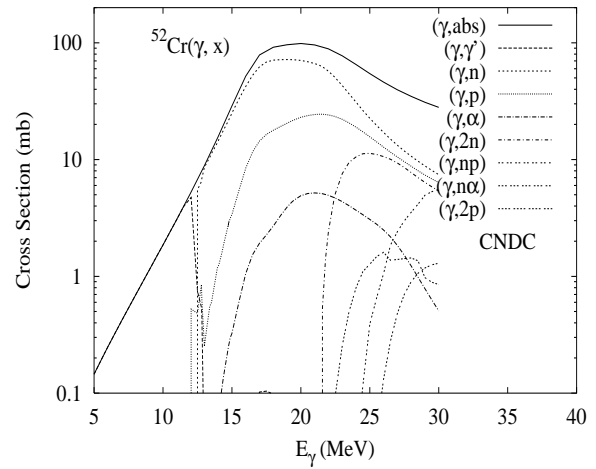
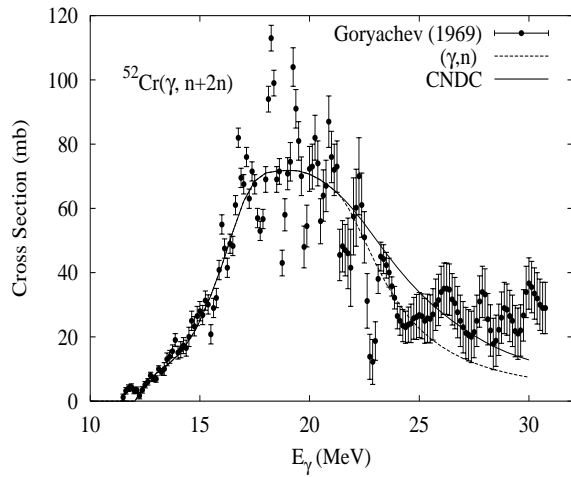
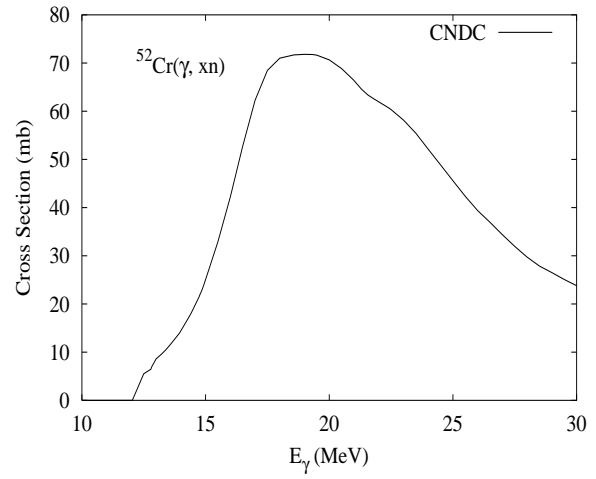
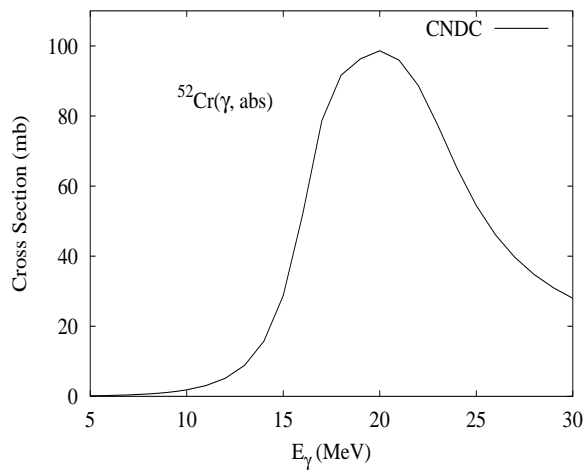
Abundance (%)	Threshold Energies (MeV)								
	$\gamma, n$	$\gamma, p$	$\gamma, t$	$\gamma, \text{He-3}$	$\gamma, \alpha$	$\gamma, 2n$	$\gamma, np$	$\gamma, 2p$	$\gamma, 3n$
4.34	13.00	9.59	23.20	20.26	8.56	23.58	21.14	16.35	39.92



The photoabsorption cross section has not been measured. However, the  $(\gamma, 1n)$  reaction was measured at 20.5 MeV [Bia62]. The experimental data for  ${}^{52}\text{Cr}(\gamma, xn)$  were also used to guide the model calculation.

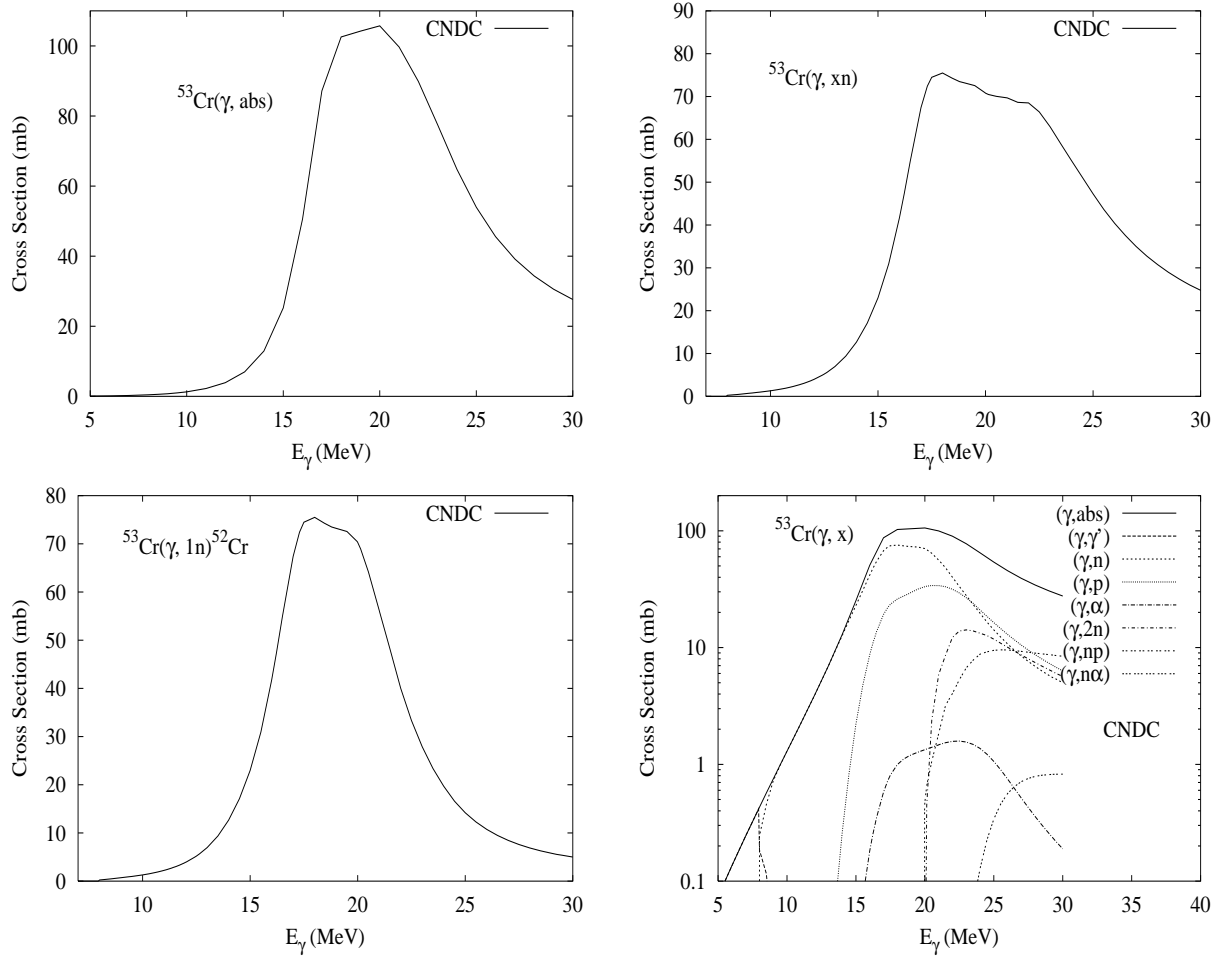
The APOM code [She92] is used to determine the optical potential parameters for neutrons. The optical potential parameters for charged particles  $p, \alpha, {}^3\text{He}, d,$  and  $t$ , were taken from [Per76]. We relied on GUNF code [Zha98] to infer the photoabsorption cross section in the GDR regime, in order to model accurately the available experimental data.

Abundance (%)	Threshold Energies (MeV)								
	$\gamma, n$	$\gamma, p$	$\gamma, t$	$\gamma, \text{He-3}$	$\gamma, \alpha$	$\gamma, 2n$	$\gamma, np$	$\gamma, 2p$	$\gamma, 3n$
83.79	12.04	10.50	22.41	21.79	9.35	21.30	21.56	18.57	34.30



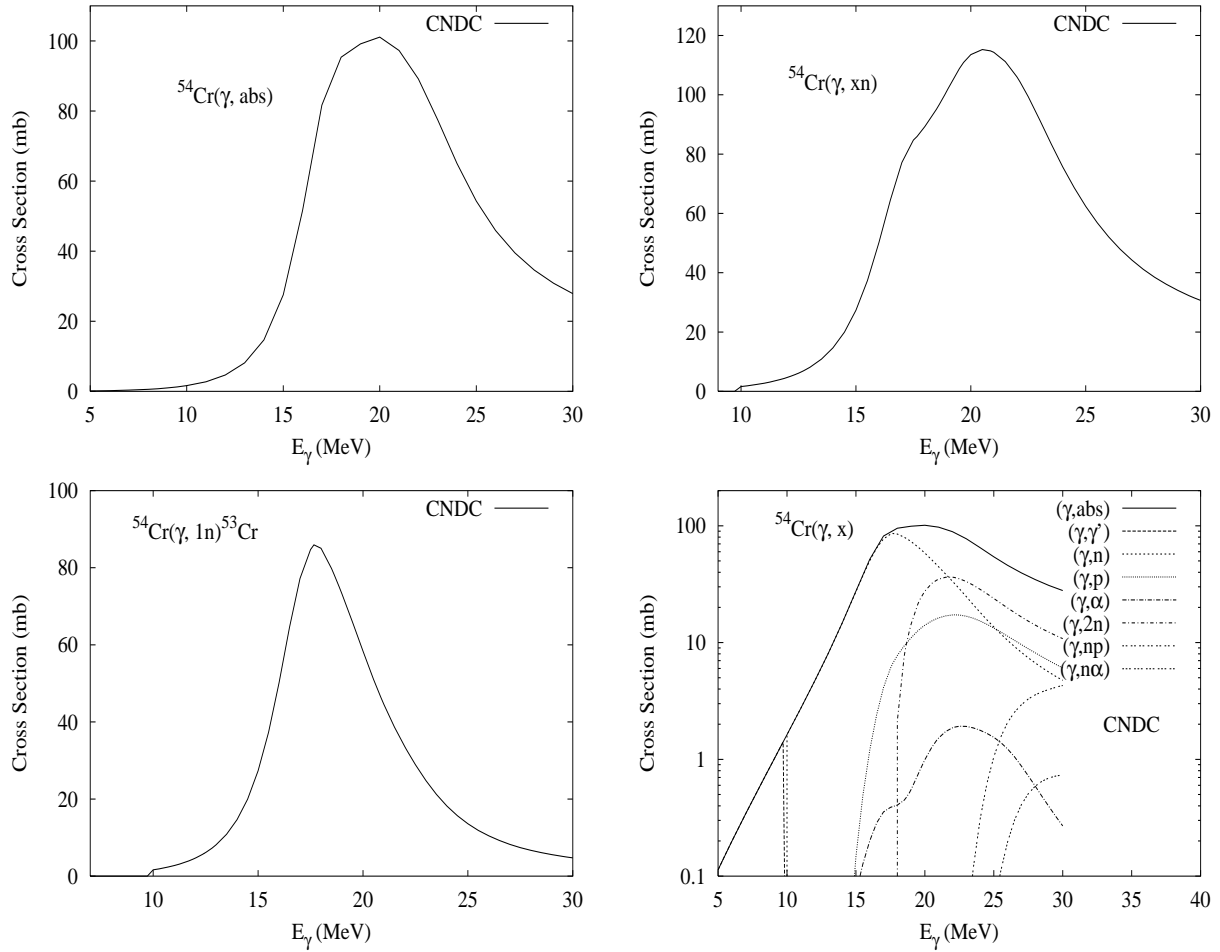
The photoabsorption cross section has not been measured. However, there are experimental data for the  $(\gamma, 1nx)$ , and  $(\gamma, 2nx)$  reaction cross sections [Gor69]. We relied on GUNF code [Zha98] to infer the photoabsorption cross section in the GDR regime, in order to model accurately the available experimental data. The APOM code [She92], was used to obtain the neutron optical potential parameters by fitting experimental data for the total and nonelastic scattering cross sections and for the elastic scattering angular distributions of  $n + {}^{nat,50,52,53,54}\text{Cr}$  reactions. The optical potential parameters for charged particles  $p$ ,  $\alpha$ ,  ${}^3\text{He}$ ,  $d$ , and  $t$ , were taken from [Per76].

Abundance (%)	Threshold Energies (MeV)								
	$\gamma, n$	$\gamma, p$	$\gamma, t$	$\gamma, \text{He-3}$	$\gamma, \alpha$	$\gamma, 2n$	$\gamma, np$	$\gamma, 2p$	$\gamma, 3n$
9.50	7.94	11.13	21.01	18.79	9.15	19.98	18.44	20.13	29.24



There are no experimental data available. The photoabsorption cross section was obtained from GDR model calculations using the GUNF code [Zha98]. Neutron optical potential parameters were determined from the APOM code [She92] fittings of neutron nuclear data for *nat*,<sup>50,52</sup>Cr. Optical potential parameters for charged particles, p,  $\alpha$ , <sup>3</sup>He, d, and t were obtained from [Per76].

Abundance (%)	Threshold Energies (MeV)								
	$\gamma, n$	$\gamma, p$	$\gamma, t$	$\gamma, \text{He-3}$	$\gamma, \alpha$	$\gamma, 2n$	$\gamma, np$	$\gamma, 2p$	$\gamma, 3n$
2.37	9.72	12.37	19.68	22.13	7.93	17.66	20.85	22.04	29.70

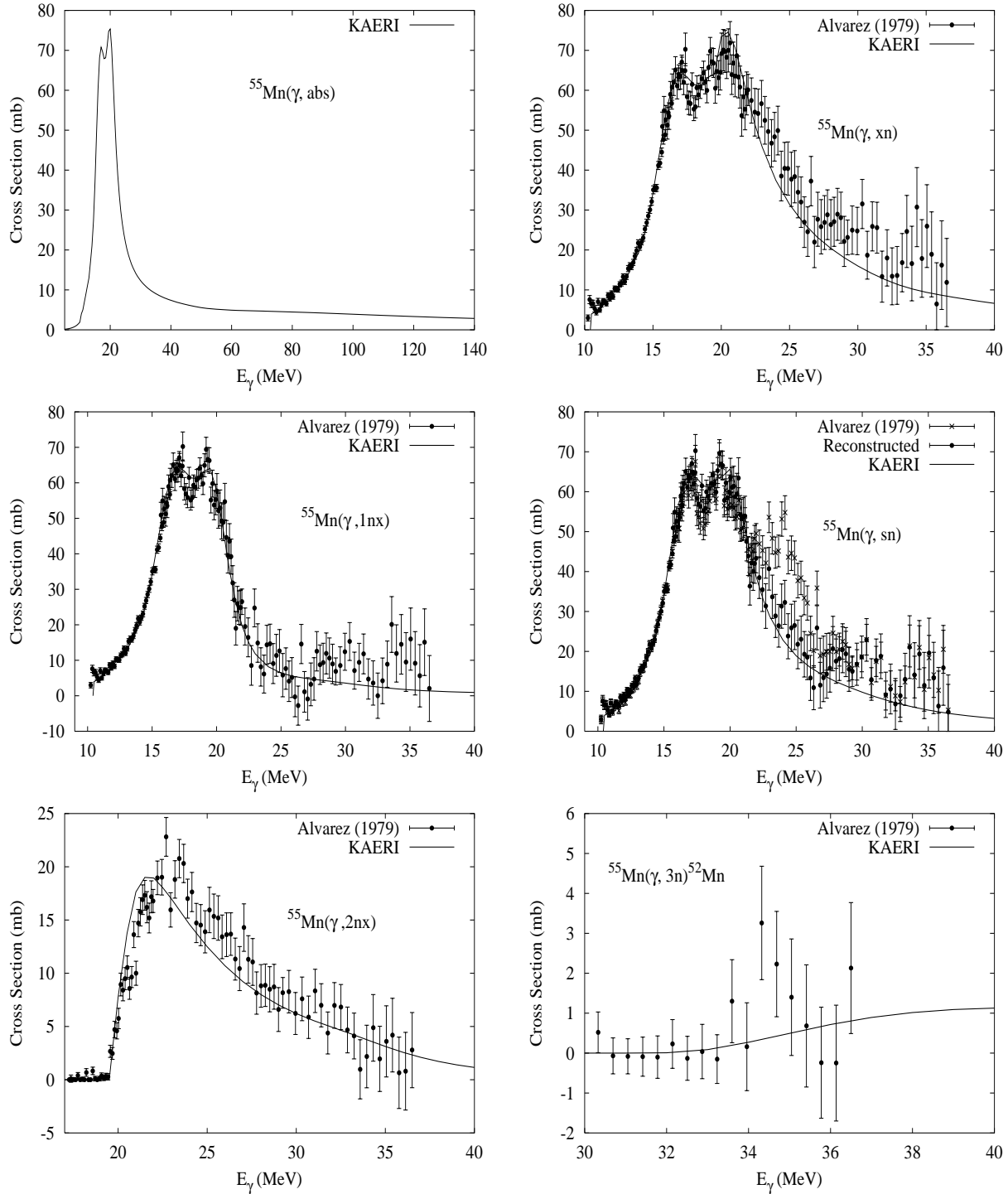


There are no experimental data available. The photoabsorption cross section was obtained from GDR model calculations using the GUNF code [Zha98]. Neutron optical potential parameters were determined from the APOM code [She92] fittings of neutron nuclear data for  $nat, {}^{50}, {}^{52}\text{Cr}$ . Optical potential parameters for charged particles,  $p$ ,  $\alpha$ ,  ${}^3\text{He}$ ,  $d$ , and  $t$  were obtained from [Per76].



# $\gamma + {}^{55}\text{Mn}$

Abundance (%)	Threshold Energies (MeV)								
	$\gamma, n$	$\gamma, p$	$\gamma, t$	$\gamma, \text{He-3}$	$\gamma, \alpha$	$\gamma, 2n$	$\gamma, np$	$\gamma, 2p$	$\gamma, 3n$
100.00	10.23	8.07	17.24	21.20	7.93	19.16	17.79	20.44	31.22

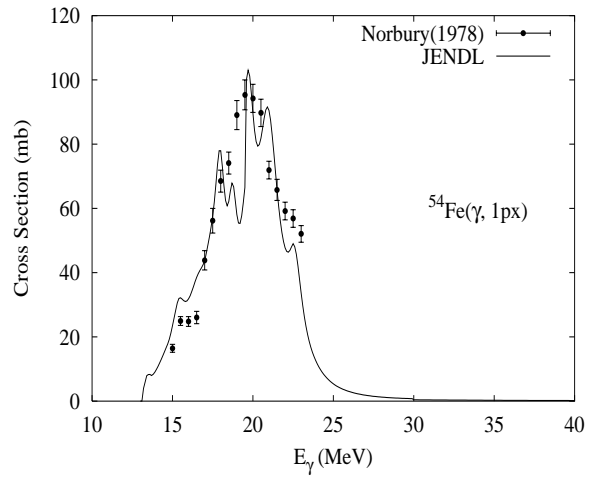
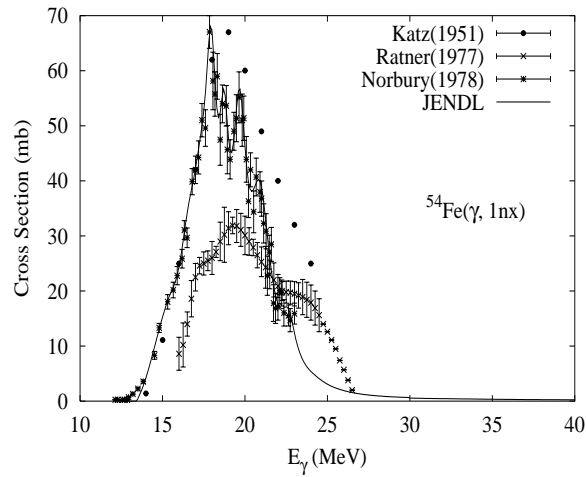
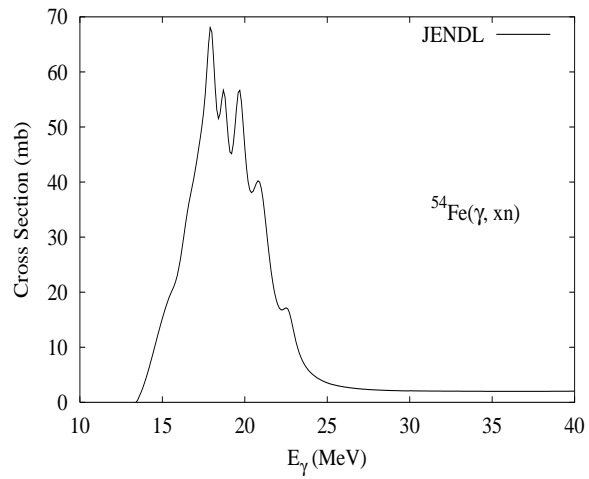
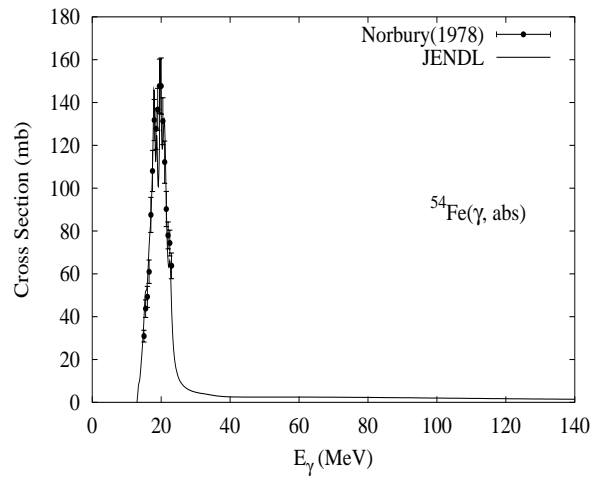


The photoabsorption cross section has not been measured. However, the experimental data [Alv79] were given for  $(\gamma, 1nx)$ ,  $(\gamma, 2nx)$ ,  $(\gamma, 3nx)$ ,  $(\gamma, sn)$  and  $(\gamma, xn)$  reaction cross sections. Since the original  $(\gamma, sn)$  data of Alvarez are not consistent with the  $(\gamma, 1nx)$  and  $(\gamma, 2nx)$  above 25 MeV, new  $(\gamma, sn)$  reference data were constructed by adding  $(\gamma, 1nx)$  and

$(\gamma, 2nx)$  data. We relied on the GUNF and GNASH codes to infer the photoabsorption cross section in the GDR regime, in order to model accurately the reconstructed  $(\gamma, sn)$  data. The photoabsorption cross section above the GDR, up to 140 MeV, was obtained from QD model calculations using the theory of Chadwick.

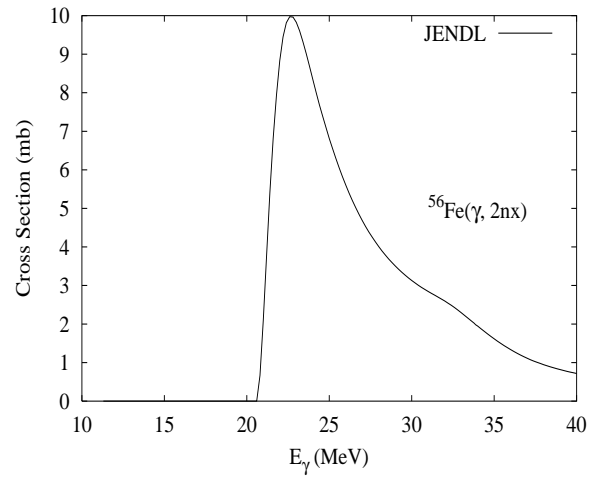
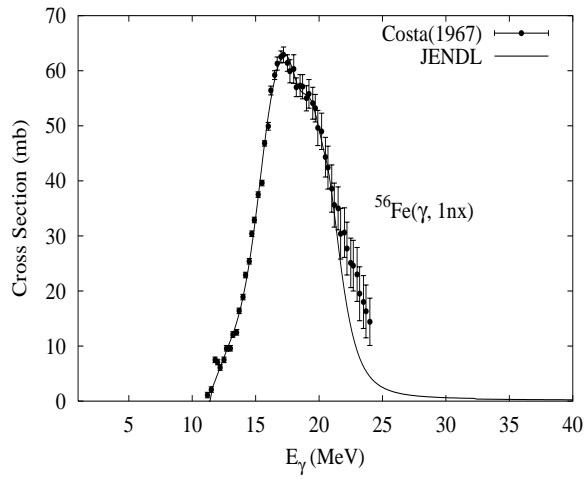
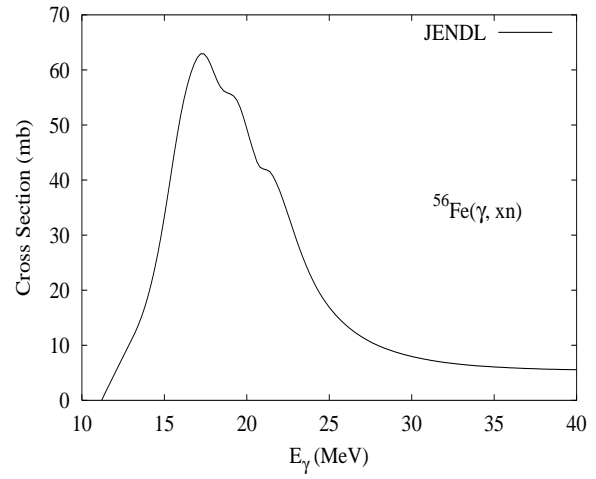
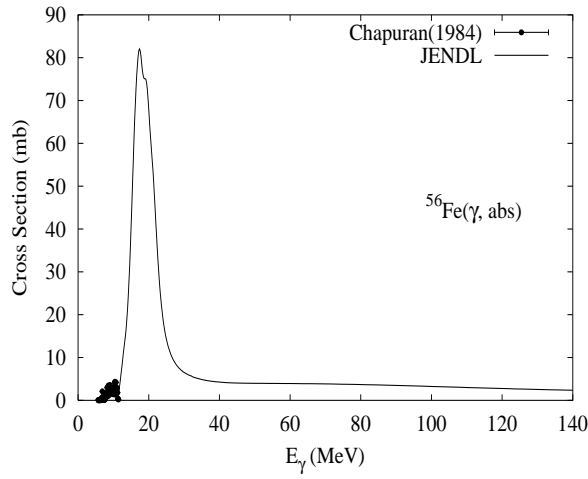
The calculated results of the emission channels by the GNASH code are basically in agreement with the experimental data for  $(\gamma, 1nx)$ ,  $(\gamma, 2nx)$ ,  $(\gamma, 3nx)$  and  $(\gamma, xn)$  as well as the reconstructed  $(\gamma, sn)$  reaction.

Abundance (%)	Threshold Energies (MeV)								
	$\gamma, n$	$\gamma, p$	$\gamma, t$	$\gamma, \text{He-3}$	$\gamma, \alpha$	$\gamma, 2n$	$\gamma, np$	$\gamma, 2p$	$\gamma, 3n$
5.90	13.38	8.85	22.96	19.73	8.42	24.06	20.91	15.41	40.25



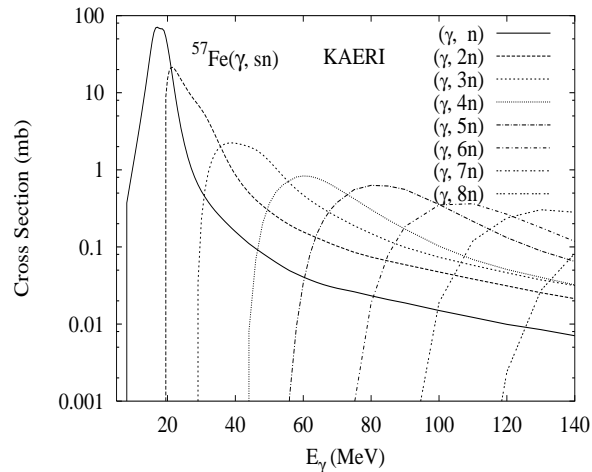
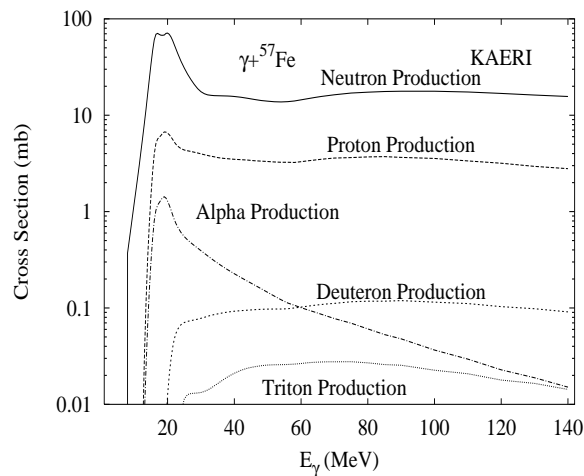
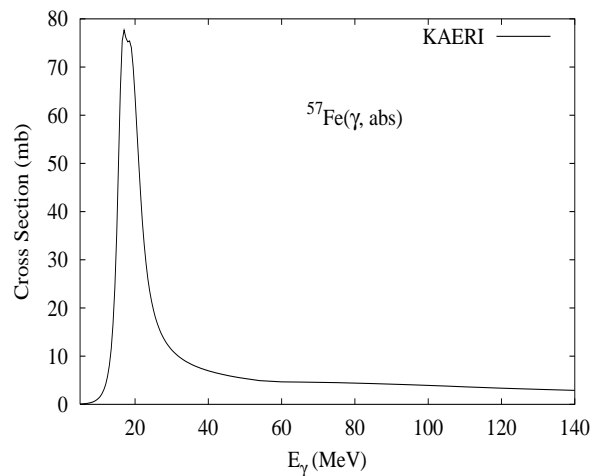
Photonuclear reactions were evaluated using ALICE-F [Fuk93] code calculations together with experimental data. Input model parameters were adjusted so as to improve the quality of the calculated results compared with data [Nor78]. Photoabsorption was modeled as a sum of GDR and QD components [Cha91].

Abundance (%)	Threshold Energies (MeV)								
	$\gamma, n$	$\gamma, p$	$\gamma, t$	$\gamma, \text{He-3}$	$\gamma, \alpha$	$\gamma, 2n$	$\gamma, np$	$\gamma, 2p$	$\gamma, 3n$
91.72	11.20	10.18	20.87	20.25	7.61	20.50	20.41	18.25	33.87



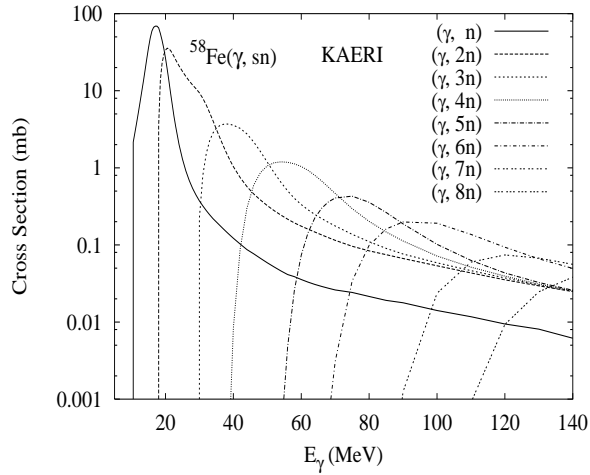
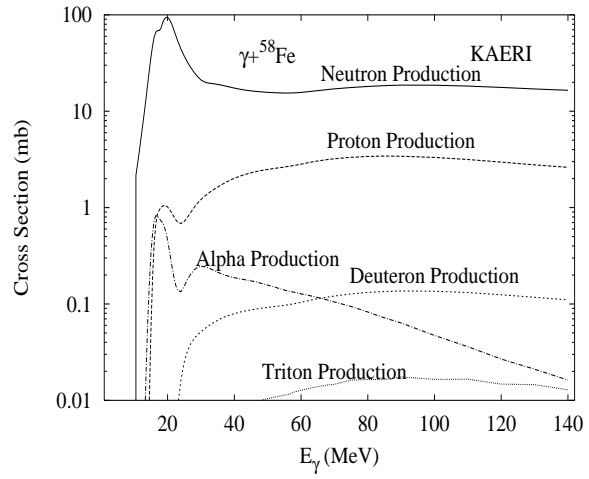
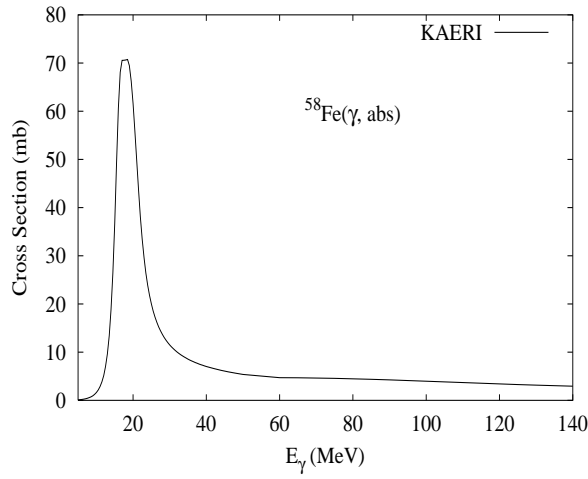
Photonuclear reactions were evaluated using ALICE-F [Fuk93] code calculations together with experimental data. Input model parameters were adjusted so as to improve the quality of the calculated results compared with data [Cos67]. Photoabsorption was modeled as a sum of GDR and QD components [Cha91].

Abundance (%)	Threshold Energies (MeV)								
	$\gamma, n$	$\gamma, p$	$\gamma, t$	$\gamma, \text{He-3}$	$\gamma, \alpha$	$\gamma, 2n$	$\gamma, np$	$\gamma, 2p$	$\gamma, 3n$
2.10	7.65	10.56	19.58	18.18	7.32	18.84	17.83	19.65	28.14



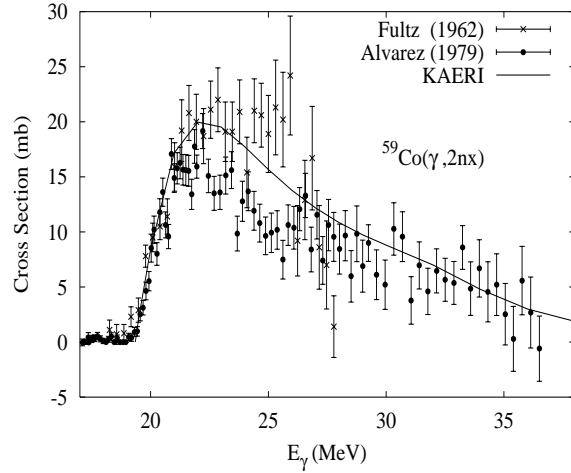
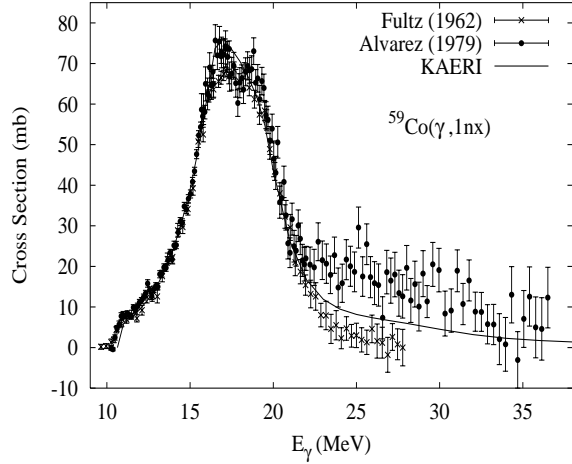
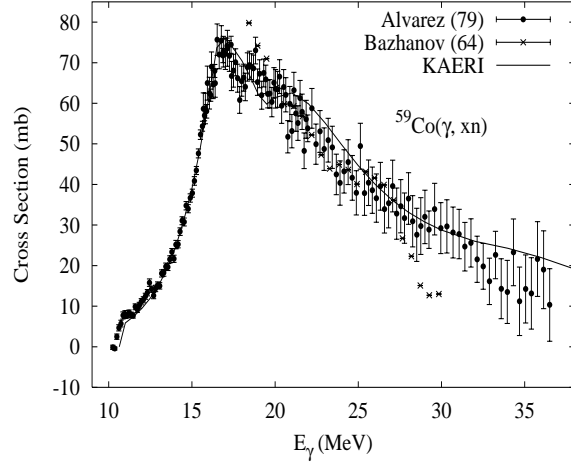
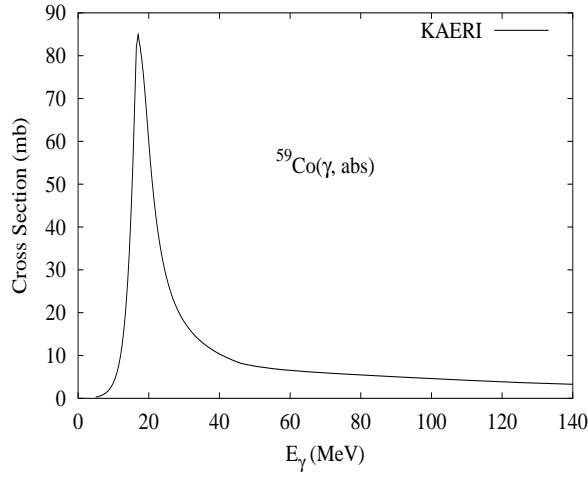
There are no experimental data available. The photoabsorption cross section was obtained from GDR and QD model calculations, adopting the GDR parameters of  ${}^{56}\text{Fe}$ . The neutron, proton, deuteron, triton and alpha emission cross sections, as well as production cross sections, were calculated by the GNASH code.

Abundance (%)	Threshold Energies (MeV)								
	$\gamma, n$	$\gamma, p$	$\gamma, t$	$\gamma, \text{He-3}$	$\gamma, \alpha$	$\gamma, 2n$	$\gamma, np$	$\gamma, 2p$	$\gamma, 3n$
0.28	10.04	11.95	19.39	21.98	7.65	17.69	20.60	21.44	28.89



There are no experimental data available. The photoabsorption cross section was obtained from GDR and QD model calculations, adopting the GDR parameters of  ${}^{56}\text{Fe}$ . The neutron, proton, deuteron, triton and alpha emission cross sections, as well as production cross sections, were calculated by the GNASH code.

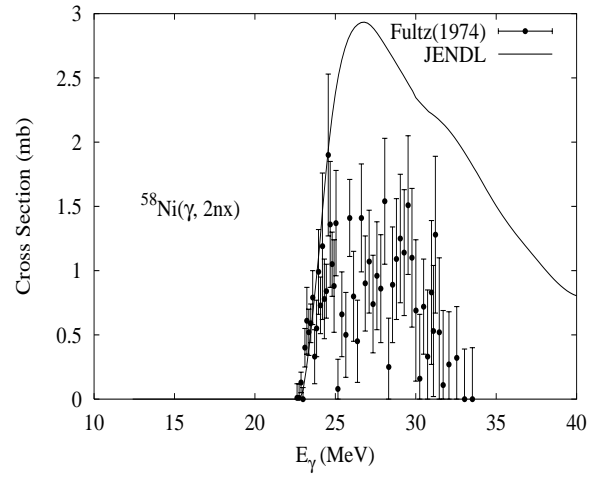
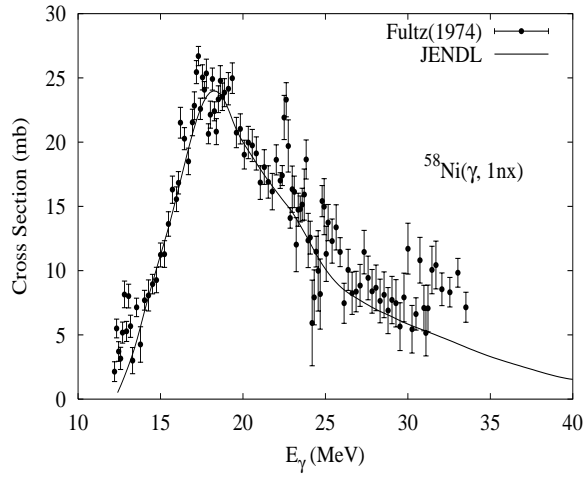
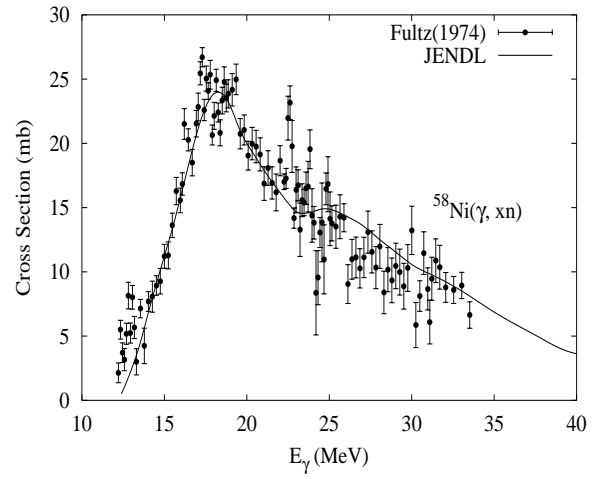
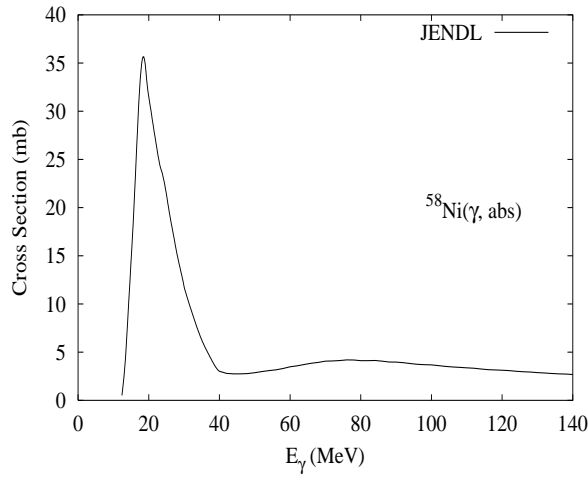
Abundance (%)	Threshold Energies (MeV)								
	$\gamma, n$	$\gamma, p$	$\gamma, t$	$\gamma, \text{He-3}$	$\gamma, \alpha$	$\gamma, 2n$	$\gamma, np$	$\gamma, 2p$	$\gamma, 3n$
100.00	10.45	7.36	16.57	20.25	6.94	19.03	17.41	19.32	30.40



The photoabsorption cross section has not been measured. However, there are experimental data for the  $(\gamma, 1nx)$  and  $(\gamma, 2nx)$  reaction cross sections by Fultz and Alvarez [Ful62a, Alv79],  $(\gamma, 3nx)$  cross section by Alvarez [Alv79], and  $(\gamma, xn)$  reaction cross section by [Baz64, Alv79]. We relied on the GUNF and GNASH codes to infer the photoabsorption cross section in the GDR regime, in order to model accurately the  $(\gamma, xn)$  data of Alvarez. The photoabsorption cross section above the GDR, up to 140 MeV, was obtained from QD model calculations using the theory of Chadwick.

The calculated results of the emission channels by the GNASH code are in good agreement with the experimental data.

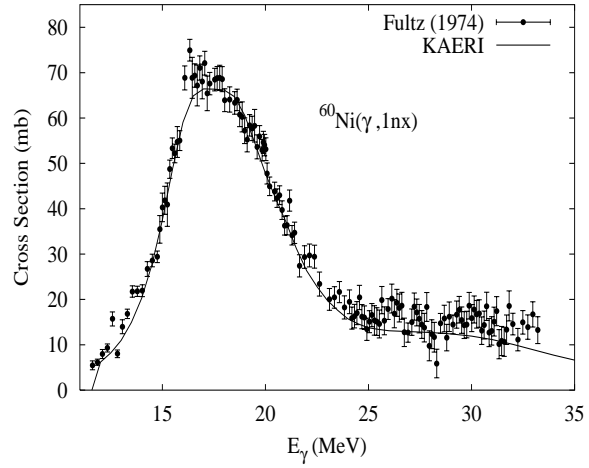
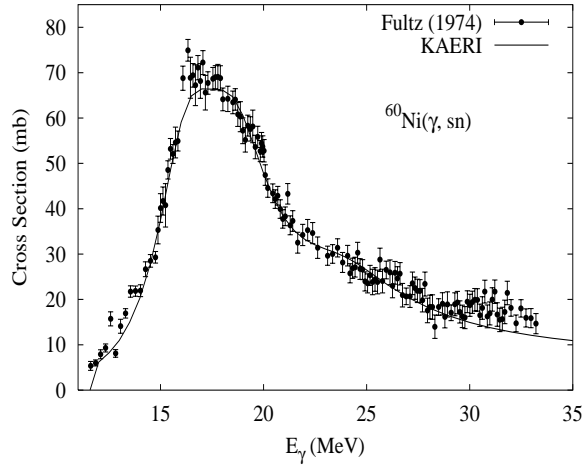
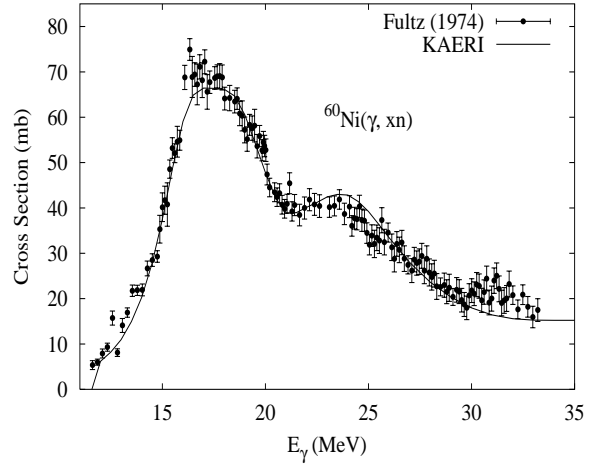
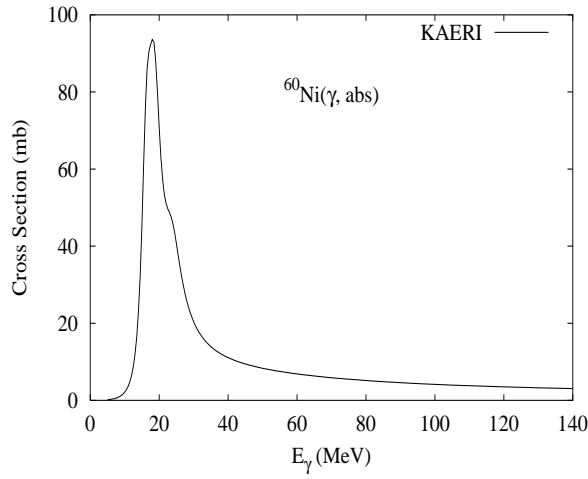
Abundance (%)	Threshold Energies (MeV)								
	$\gamma, n$	$\gamma, p$	$\gamma, t$	$\gamma, \text{He-3}$	$\gamma, \alpha$	$\gamma, 2n$	$\gamma, np$	$\gamma, 2p$	$\gamma, 3n$
68.08	12.22	8.17	21.15	17.68	6.40	22.47	19.55	14.20	39.11



Photonuclear reactions were evaluated using ALICE-F [Fuk93] code calculations together with experimental data. Input model parameters were adjusted so as to improve the quality of the calculated results compared with data [Ful74]. Photoabsorption was modeled as a sum of GDR and QD components [Cha91].



Abundance (%)	Threshold Energies (MeV)								
	$\gamma, n$	$\gamma, p$	$\gamma, t$	$\gamma, \text{He-3}$	$\gamma, \alpha$	$\gamma, 2n$	$\gamma, np$	$\gamma, 2p$	$\gamma, 3n$
26.22	11.39	9.53	20.08	19.22	6.29	20.39	19.99	16.90	32.61

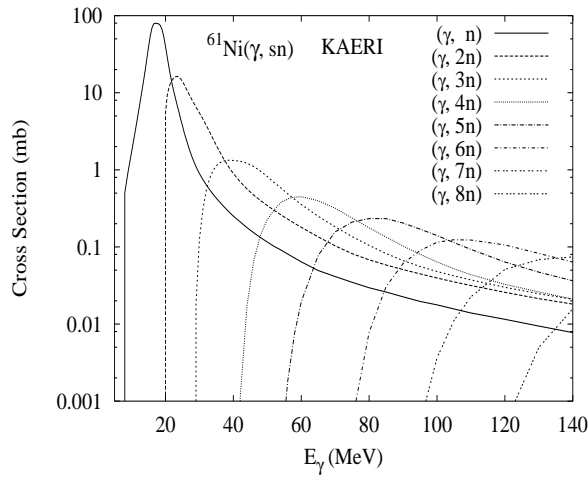
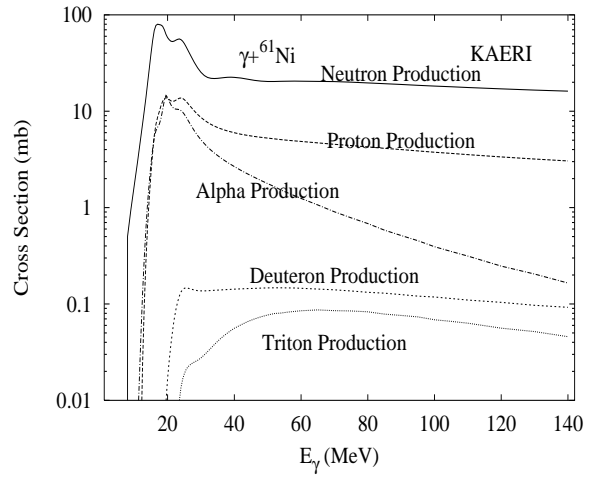
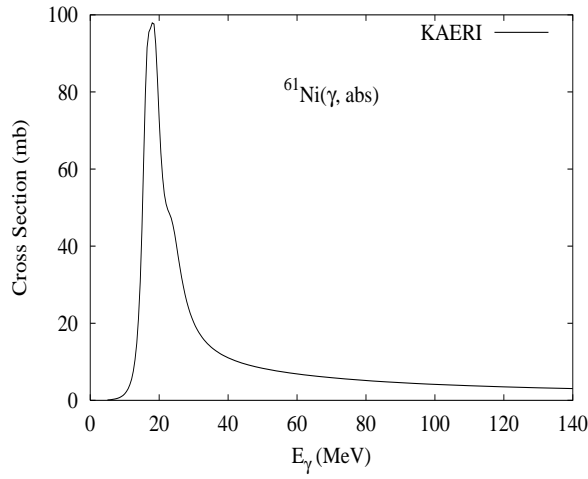


The photoabsorption cross section has not been measured. However, there are experimental data for the  $(\gamma, 1nx)$ ,  $(\gamma, 2nx)$ ,  $(\gamma, sn)$  and  $(\gamma, xn)$  reaction cross sections [Ful74]. We relied on the GUNF and GNASH codes to infer the photoabsorption cross section in the GDR regime, in order to model accurately the  $(\gamma, sn)$  data. The photoabsorption cross section above the GDR, up to 140 MeV, was obtained from QD model calculations using the theory of Chadwick.

The calculated results of the emission channels by the GNASH code are in good agreement with the experimental data.

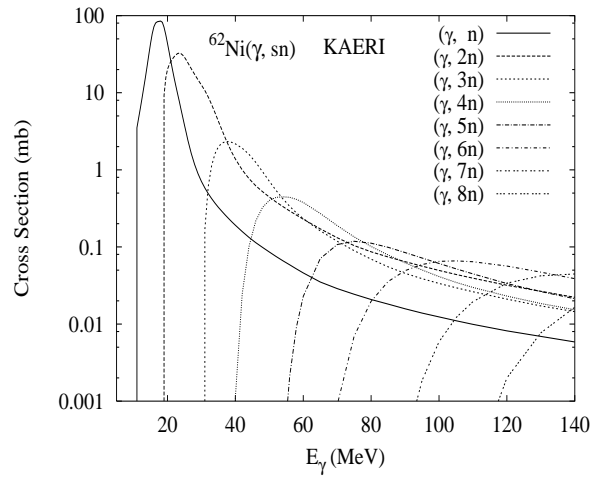
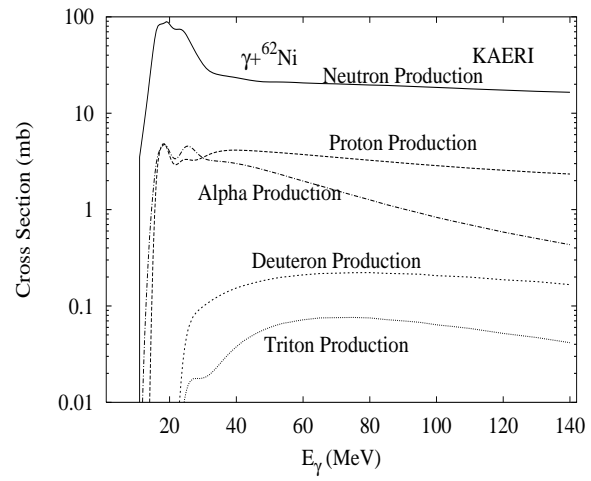
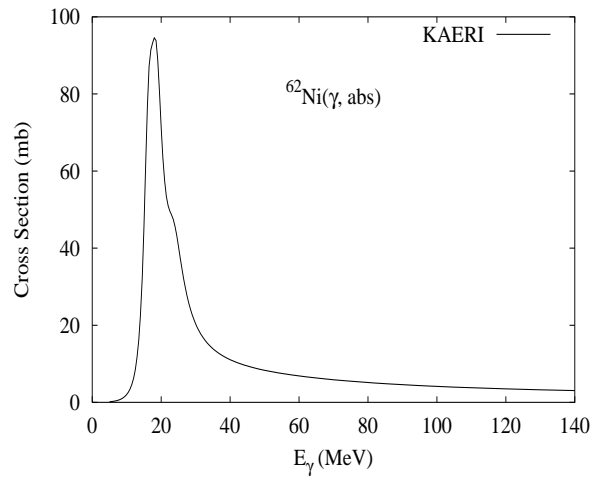
# $\gamma + {}^{61}\text{Ni}$

Abundance (%)	Threshold Energies (MeV)								
	$\gamma, n$	$\gamma, p$	$\gamma, t$	$\gamma, \text{He-3}$	$\gamma, \alpha$	$\gamma, 2n$	$\gamma, np$	$\gamma, 2p$	$\gamma, 3n$
1.14	7.82	9.86	19.33	17.00	6.47	19.21	17.35	18.14	28.21



There are no experimental data available. The photoabsorption cross section was obtained from GDR and QD model calculations, adopting the GDR parameters of  ${}^{60}\text{Ni}$ . The neutron, proton, deuteron, triton and alpha emission cross sections, as well as production cross sections, were calculated by the GNASH code.

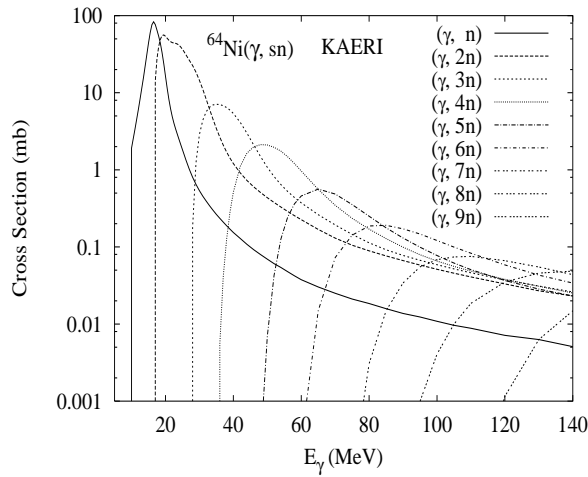
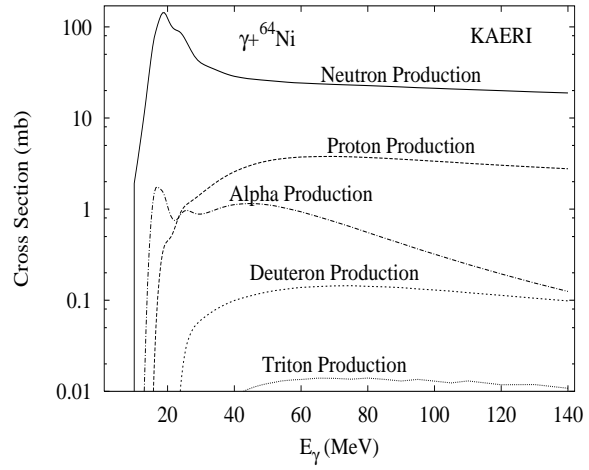
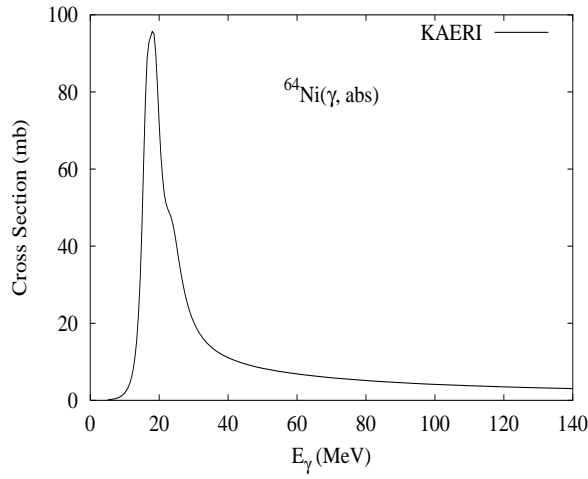
Abundance (%)	Threshold Energies (MeV)								
	$\gamma, n$	$\gamma, p$	$\gamma, t$	$\gamma, \text{He-3}$	$\gamma, \alpha$	$\gamma, 2n$	$\gamma, np$	$\gamma, 2p$	$\gamma, 3n$
3.63	10.60	11.14	19.47	21.02	7.02	18.42	20.46	19.92	29.81



There are no experimental data available. The photoabsorption cross section was obtained from GDR and QD model calculations, adopting the GDR parameters of  ${}^{60}\text{Ni}$ . The neutron, proton, deuteron, triton and alpha emission cross sections, as well as production cross sections, were calculated by the GNASH code.

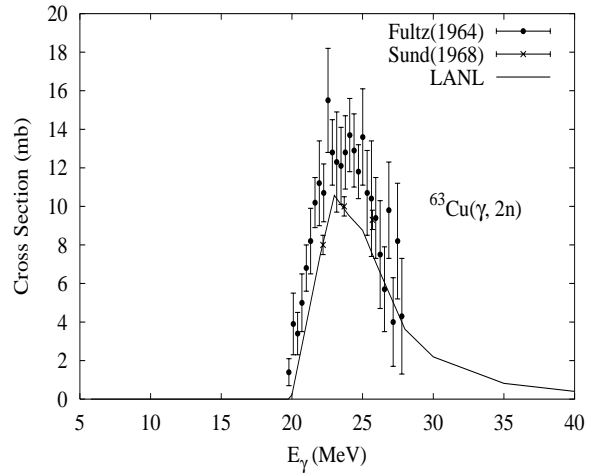
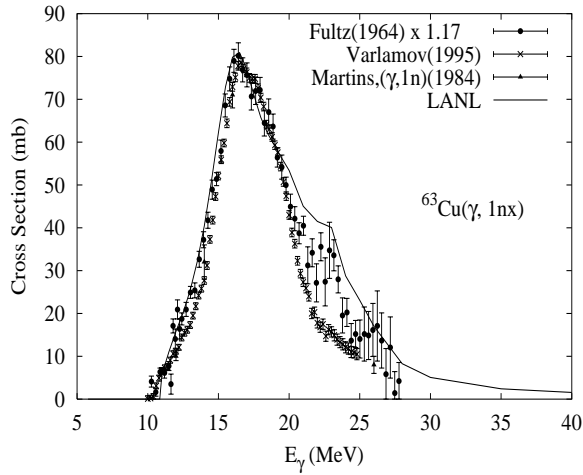
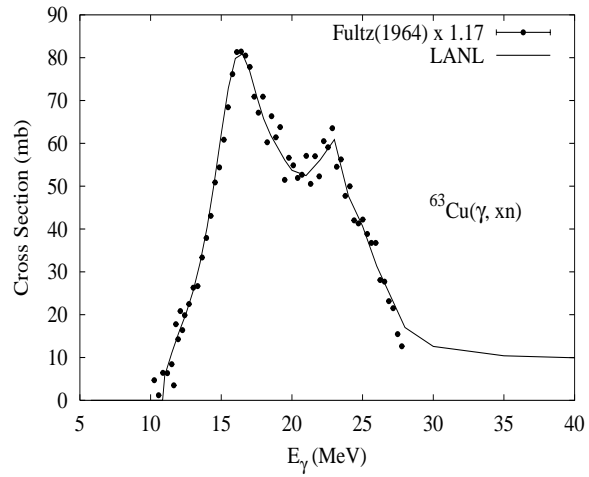
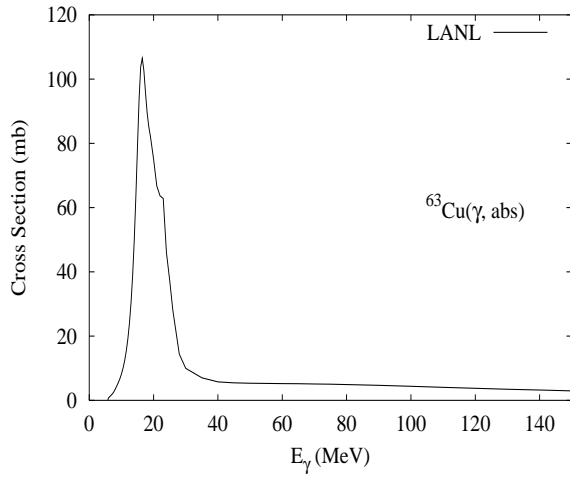
# $\gamma + {}^{64}\text{Ni}$

Abundance (%)	Threshold Energies (MeV)								
	$\gamma, n$	$\gamma, p$	$\gamma, t$	$\gamma, \text{He-3}$	$\gamma, \alpha$	$\gamma, 2n$	$\gamma, np$	$\gamma, 2p$	$\gamma, 3n$
0.93	9.66	12.55	19.15	23.11	8.12	16.50	21.04	22.78	27.09



There are no experimental data available. The photoabsorption cross section was obtained from GDR and QD model calculations, adopting the GDR parameters of  ${}^{60}\text{Ni}$ . The neutron, proton, deuteron, triton and alpha emission cross sections, as well as production cross sections, were calculated by the GNASH code.

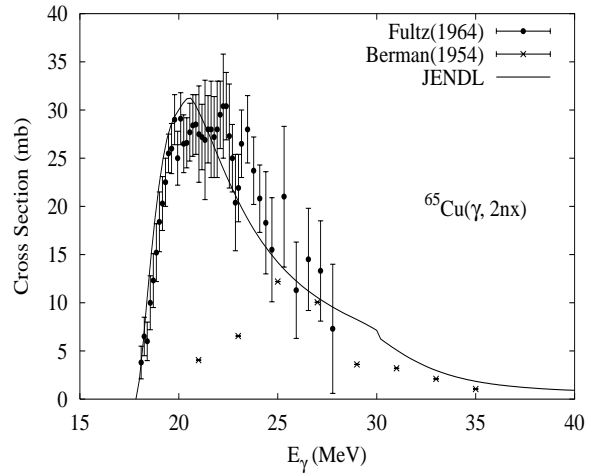
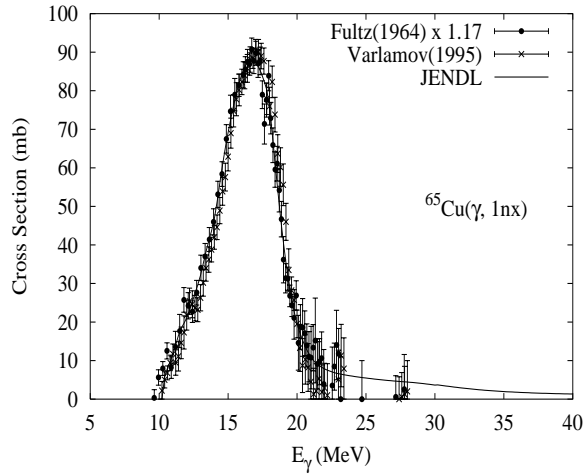
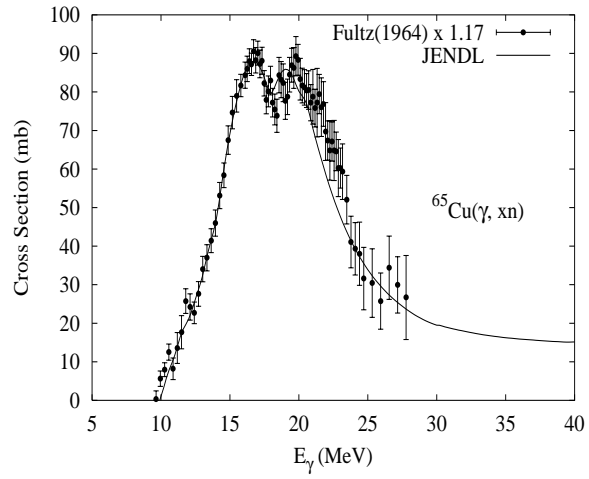
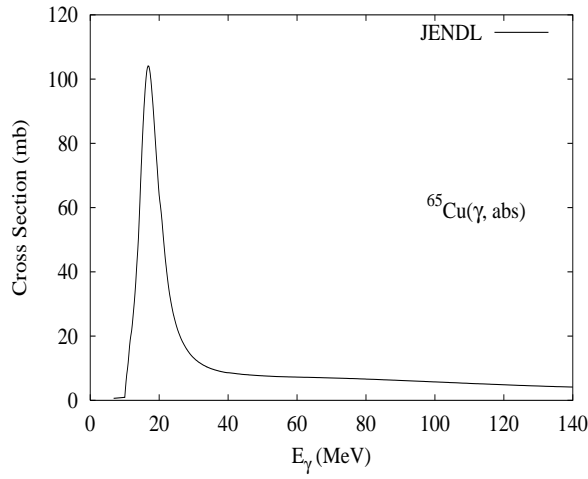
Abundance (%)	Threshold Energies (MeV)								
	$\gamma, n$	$\gamma, p$	$\gamma, t$	$\gamma, \text{He-3}$	$\gamma, \alpha$	$\gamma, 2n$	$\gamma, np$	$\gamma, 2p$	$\gamma, 3n$
69.17	10.85	6.12	16.06	18.86	5.78	19.74	16.72	17.26	31.45



Available data are summarized by Varlamov [Var96]. No data exist for the total absorption cross section, for  ${}^{63}\text{Cu}$ . However, data do exist for the photoneutron cross section [Ful64], and the GNASH code predicts the ratio of  $(\gamma, \text{abs})$  to  $(\gamma, n)$  and  $(\gamma, p)$ , etc. Thus, we relied on the GNASH code to infer the absorption cross section in the GDR regime, so as to model accurately the Fultz  $(\gamma, xn)$  measured data [Ful64]. We followed recommendations from IAEA CRP members at the JAERI CRP to renormalize the Livermore Fultz data and absorption cross section by 1.17. This led to agreement with Varlamov [Var95]. The total absorption cross section above the GDR, up to 150 MeV, was taken from QD model calculations using the theory of Chadwick [Cha91]. The  $(\gamma, xn)$  data agreed with Fultz [Ful64] x1.17. The  $(\gamma, 1nx)$  data were in fairly good agreement with those of Fultz x 1.17 [Ful64], Varlamov [Var95], and Martins [Mar84], though were on the high side of the data near 23 MeV. Likewise, the  $(\gamma, 2n)$  were low at 23 MeV compared to the Fultz x 1.17 data, but these 2 defects compensated each other and  $(\gamma, xn)$  agreed with data.

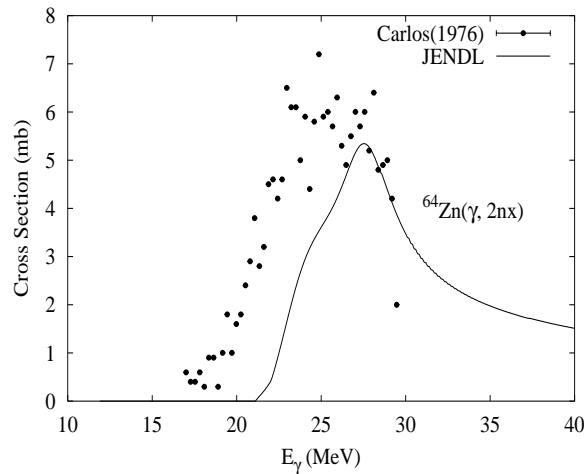
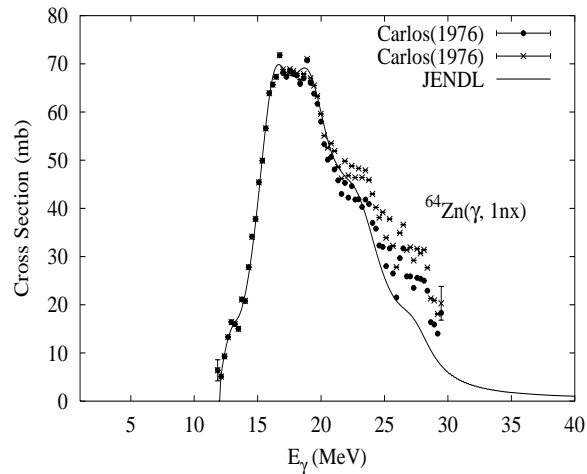
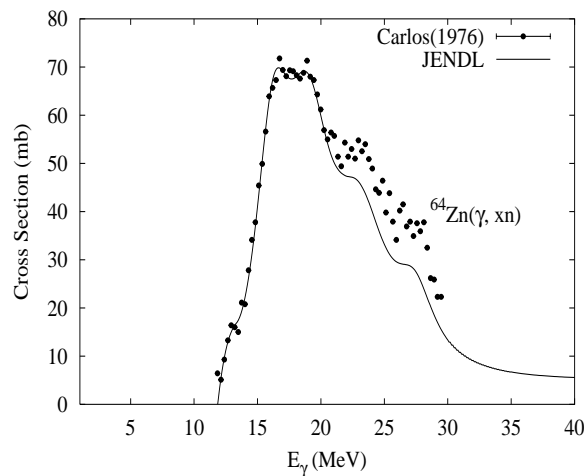
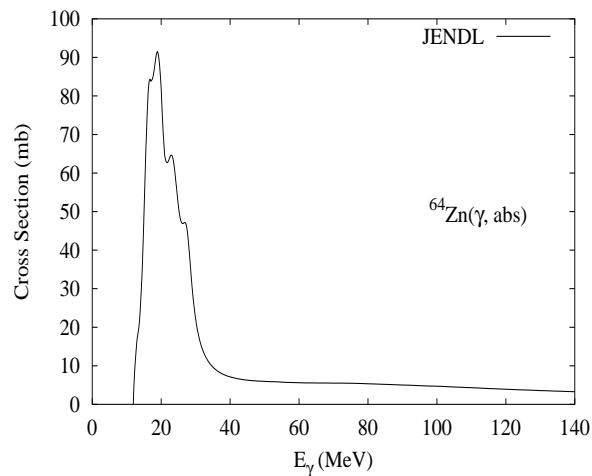
$\gamma + {}^{65}\text{Cu}$ 

Abundance (%)	Threshold Energies (MeV)								
	$\gamma, n$	$\gamma, p$	$\gamma, t$	$\gamma, \text{He-3}$	$\gamma, \alpha$	$\gamma, 2n$	$\gamma, np$	$\gamma, 2p$	$\gamma, 3n$
30.83	9.91	7.45	15.47	20.77	6.79	17.83	17.11	20.00	28.68



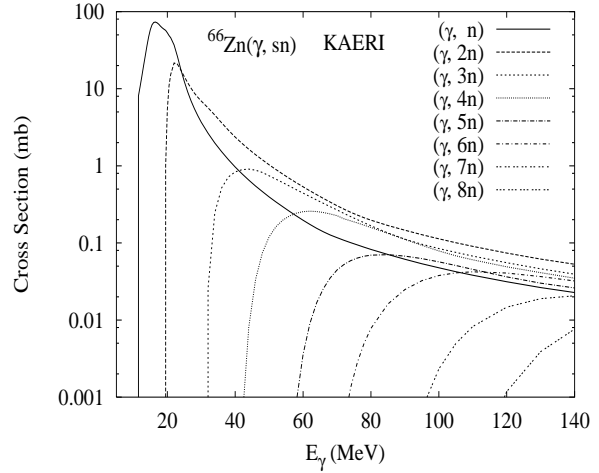
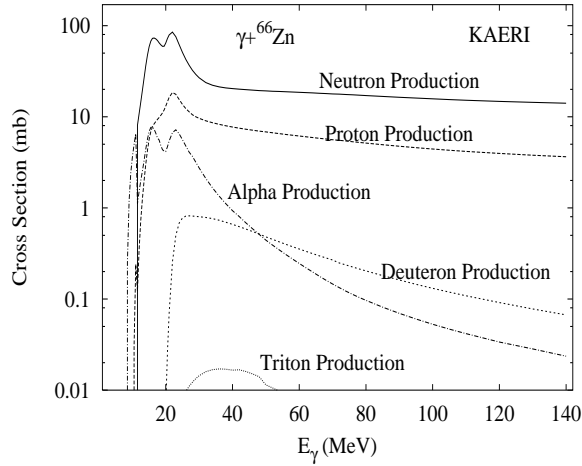
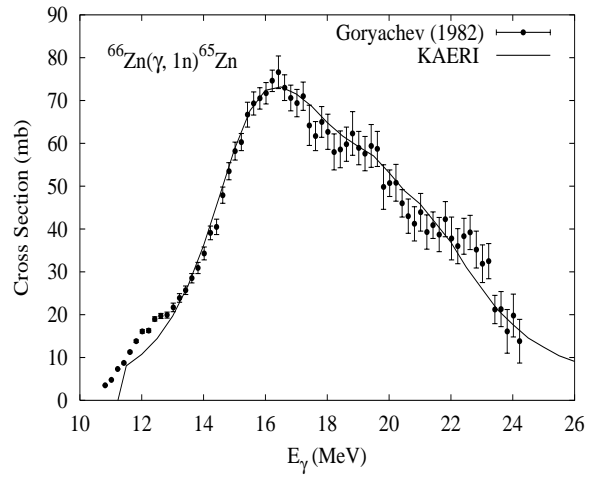
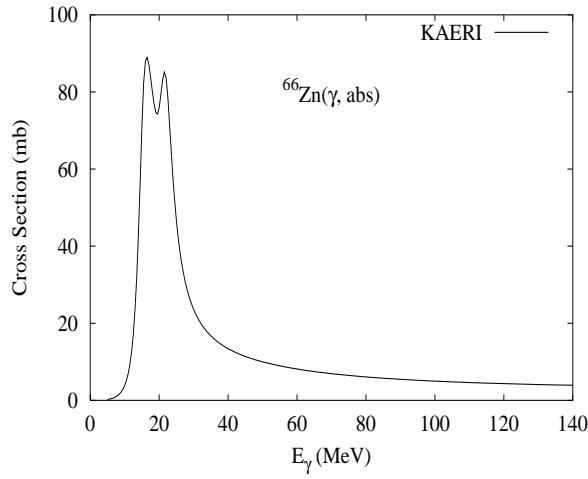
Photonuclear reactions were evaluated using ALICE-F [Fuk93] code calculations together with experimental data [Ful64, Var95]. Renormalization was applied to the Livermore Fultz's data up by 17% in accordance with a suggestion of IAEA Third Research Co-ordination Meeting on Compilation and Evaluation of Photonuclear Data for Applications on 25-29 October 1999. This led to agreement with the Varlamov's ( $\gamma, 1nx$ ) reaction cross section [Var95]. Photoabsorption was modeled as a sum of GDR and QD components [Cha91].

Abundance (%)	Threshold Energies (MeV)								
	$\gamma, n$	$\gamma, p$	$\gamma, t$	$\gamma, \text{He-3}$	$\gamma, \alpha$	$\gamma, 2n$	$\gamma, np$	$\gamma, 2p$	$\gamma, 3n$
48.60	11.86	7.71	18.97	16.71	3.96	20.97	18.57	13.83	33.87



Photonuclear reactions were evaluated using ALICE-F [Fuk93] code calculations together with experimental data. Input model parameters were adjusted so as to improve the quality of the calculated results compared with data [Car76]. Photoabsorption was modeled as a sum of GDR and QD components [Cha91].

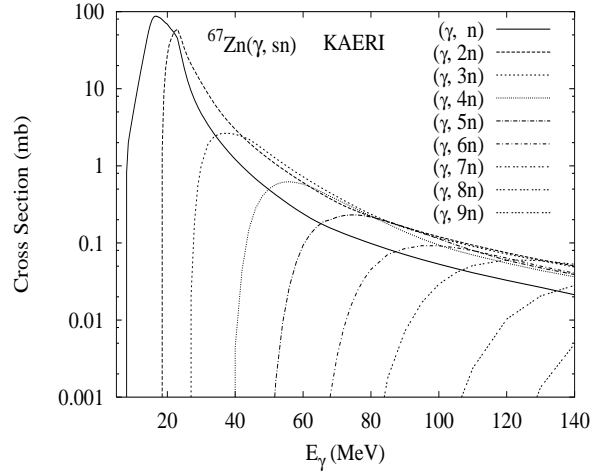
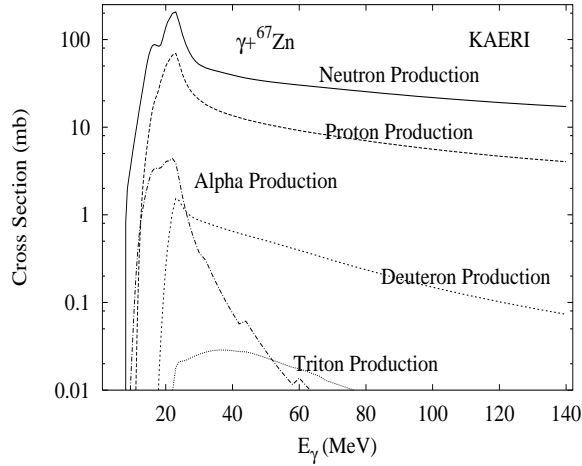
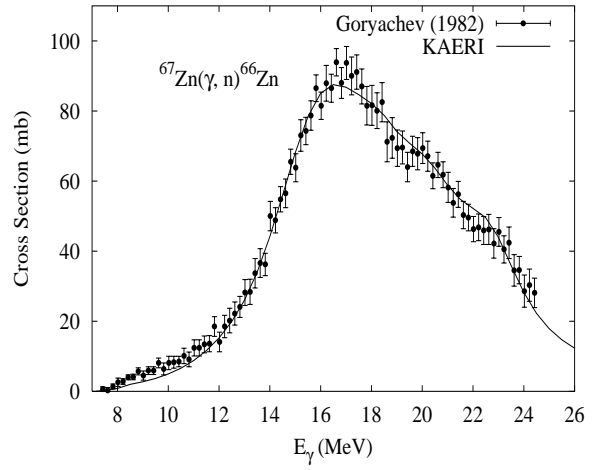
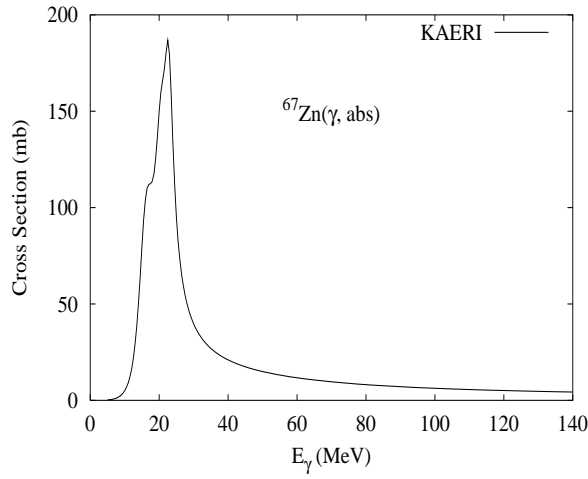
Abundance (%)	Threshold Energies (MeV)								
	$\gamma, n$	$\gamma, p$	$\gamma, t$	$\gamma, \text{He-3}$	$\gamma, \alpha$	$\gamma, 2n$	$\gamma, np$	$\gamma, 2p$	$\gamma, 3n$
27.90	11.06	8.93	18.27	18.32	4.58	19.04	18.84	16.38	30.90



The photoabsorption cross section has not been measured. However, there are experimental data for the  $(\gamma, 1n)$  reaction cross section [Gor82]. We relied on the GUNF and GNASH codes to infer the photoabsorption cross section in the GDR regime, in order to model accurately the  $(\gamma, 1n)$  data. The photoabsorption cross section above the GDR, up to 140 MeV, was obtained from QD model calculations using the theory of Chadwick. The neutron, proton, deuteron, triton and alpha emission cross sections, as well as production cross sections, were calculated by the GNASH code.

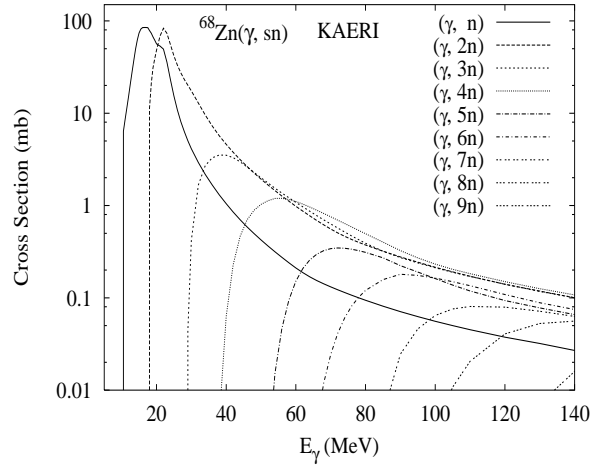
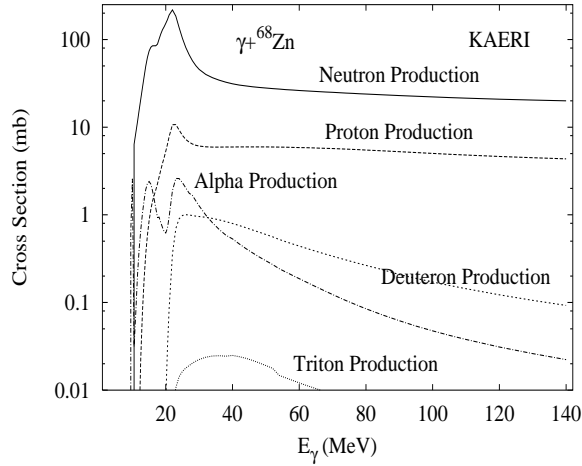
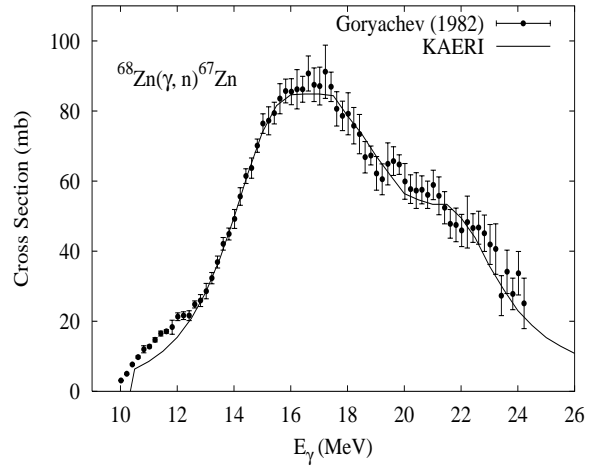
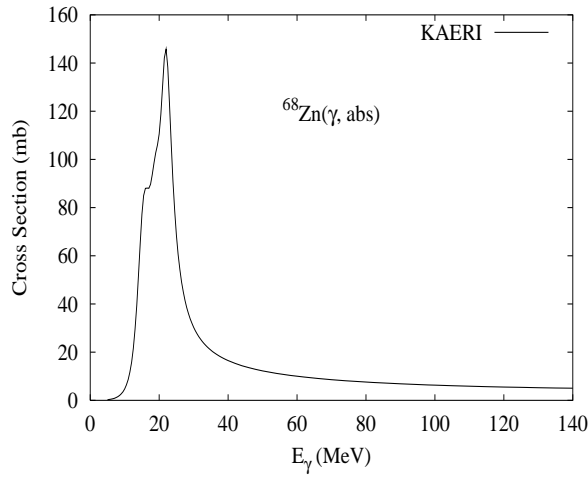


Abundance (%)	Threshold Energies (MeV)								
	$\gamma, n$	$\gamma, p$	$\gamma, t$	$\gamma, \text{He-3}$	$\gamma, \alpha$	$\gamma, 2n$	$\gamma, np$	$\gamma, 2p$	$\gamma, 3n$
4.10	7.05	8.91	17.41	15.71	4.79	18.11	15.98	17.33	26.09



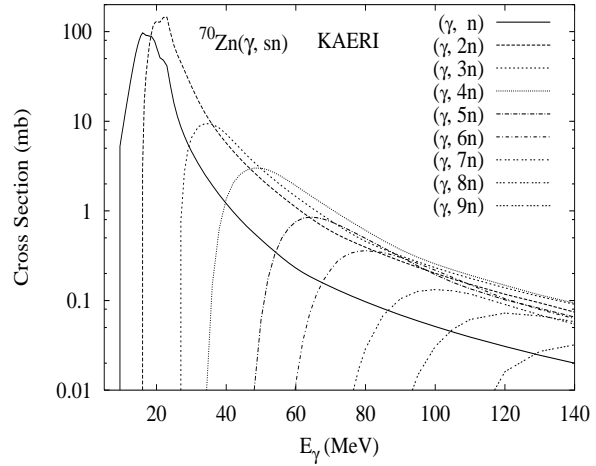
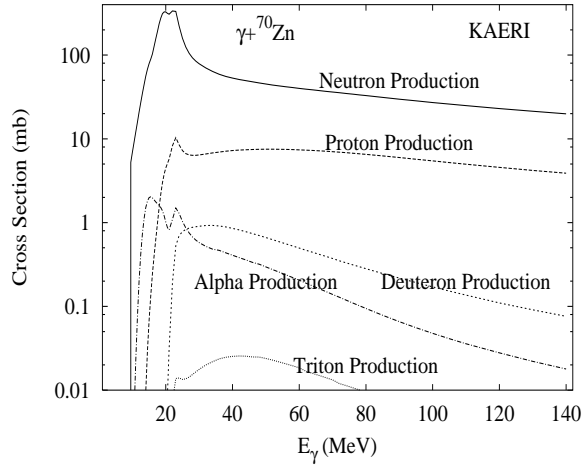
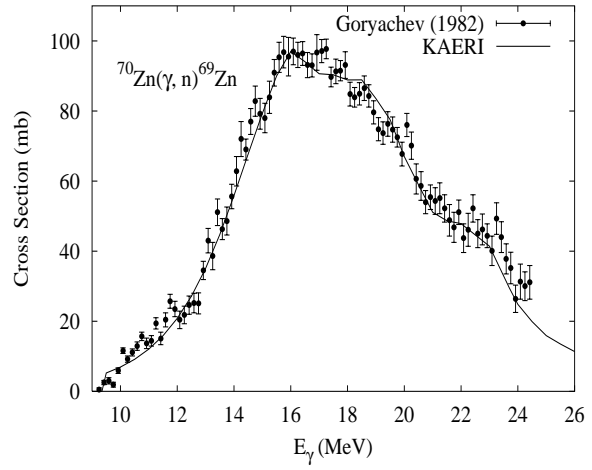
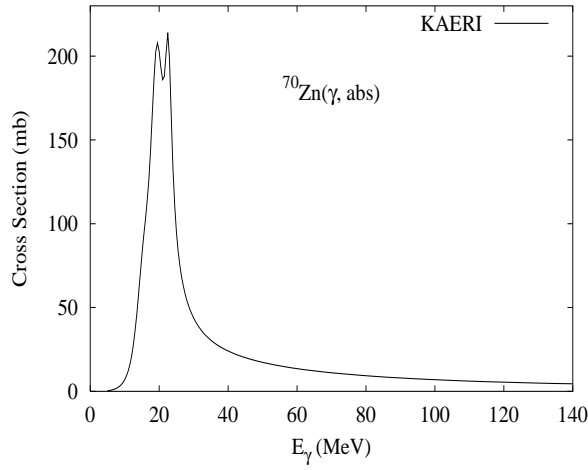
The photoabsorption cross section has not been measured. However, there are experimental data for the  $(\gamma, 1n)$  reaction cross section [Gor82]. We relied on the GUNF and GNASH codes to infer the photoabsorption cross section in the GDR regime, in order to model accurately the  $(\gamma, 1n)$  data. The photoabsorption cross section above the GDR, up to 140 MeV, was obtained from QD model calculations using the theory of Chadwick. The neutron, proton, deuteron, triton and alpha emission cross sections, as well as production cross sections, were calculated by the GNASH code.

Abundance (%)	Threshold Energies (MeV)								
	$\gamma, n$	$\gamma, p$	$\gamma, t$	$\gamma, \text{He-3}$	$\gamma, \alpha$	$\gamma, 2n$	$\gamma, np$	$\gamma, 2p$	$\gamma, 3n$
18.80	10.20	9.99	17.69	19.81	5.33	17.25	19.11	18.56	28.31



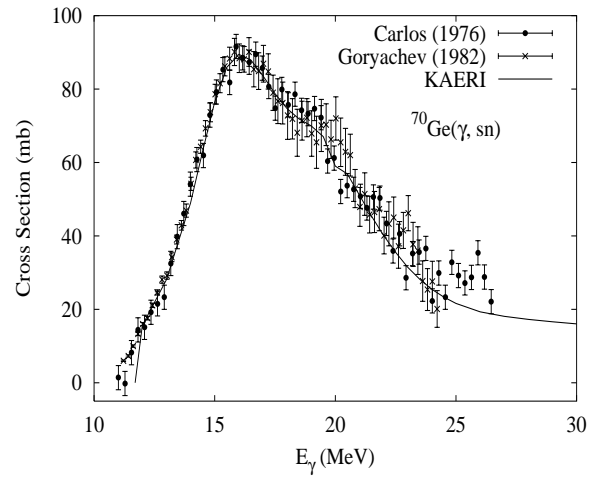
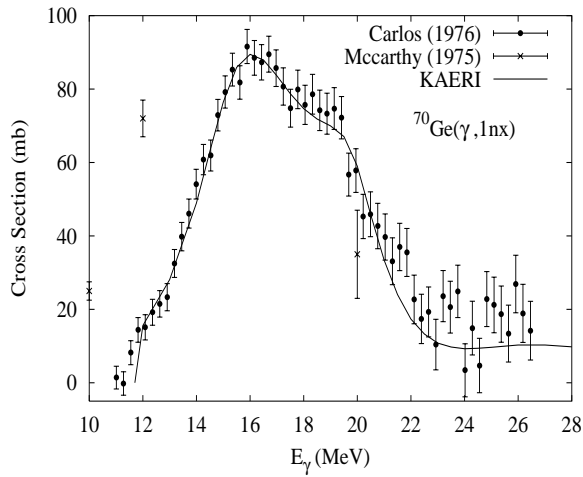
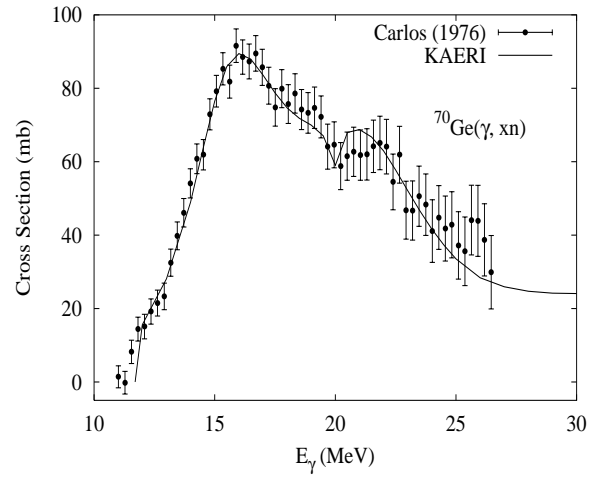
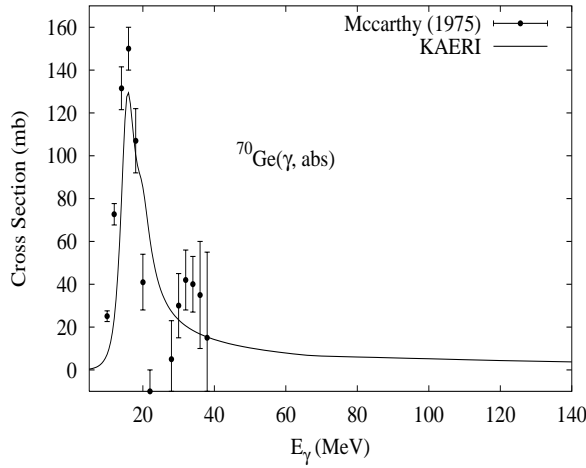
The photoabsorption cross section has not been measured. However, there are experimental data for the  $(\gamma, 1n)$  reaction cross section [Gor82]. We relied on the GUNF and GNASH codes to infer the photoabsorption cross section in the GDR regime, in order to model accurately the  $(\gamma, 1n)$  data. The photoabsorption cross section above the GDR, up to 140 MeV, was obtained from QD model calculations using the theory of Chadwick. The neutron, proton, deuteron, triton and alpha emission cross sections, as well as production cross sections, were calculated by the GNASH code.

Abundance (%)	Threshold Energies (MeV)								
	$\gamma, n$	$\gamma, p$	$\gamma, t$	$\gamma, \text{He-3}$	$\gamma, \alpha$	$\gamma, 2n$	$\gamma, np$	$\gamma, 2p$	$\gamma, 3n$
0.60	9.22	11.11	17.21	20.75	5.96	15.70	19.38	20.66	25.90



The photoabsorption cross section has not been measured. However, there are experimental data for the  $(\gamma, 1n)$  reaction cross section [Gor82]. We relied on the GUNF and GNASH codes to infer the photoabsorption cross section in the GDR regime, in order to model accurately the  $(\gamma, 1n)$  data. The photoabsorption cross section above the GDR, up to 140 MeV, was obtained from QD model calculations using the theory of Chadwick. The neutron, proton, deuteron, triton and alpha emission cross sections, as well as production cross sections, were calculated by the GNASH code.

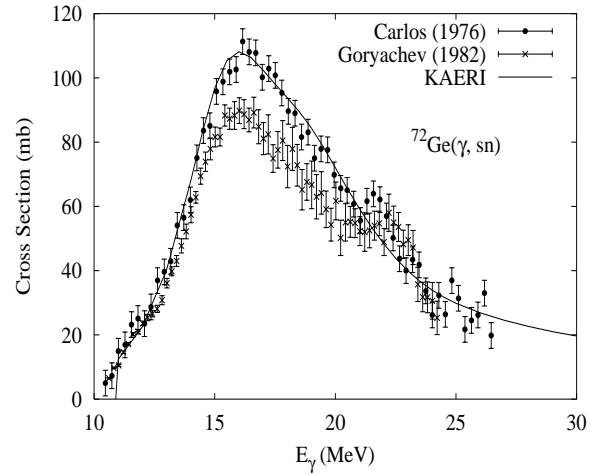
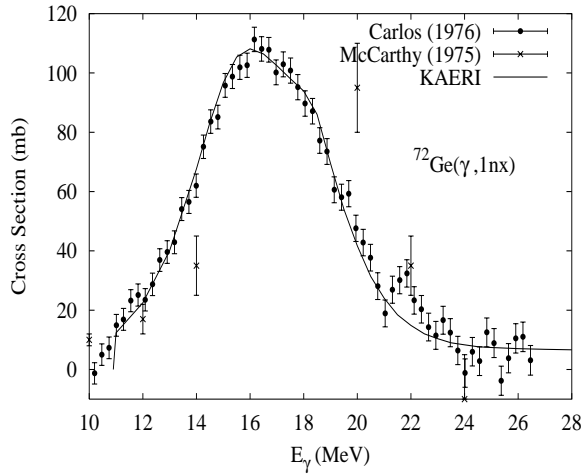
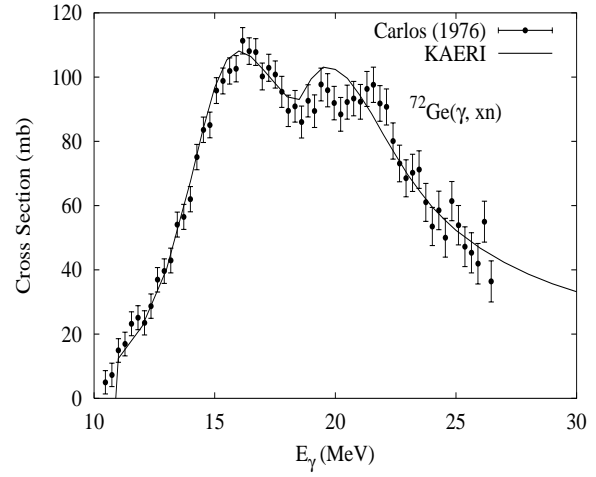
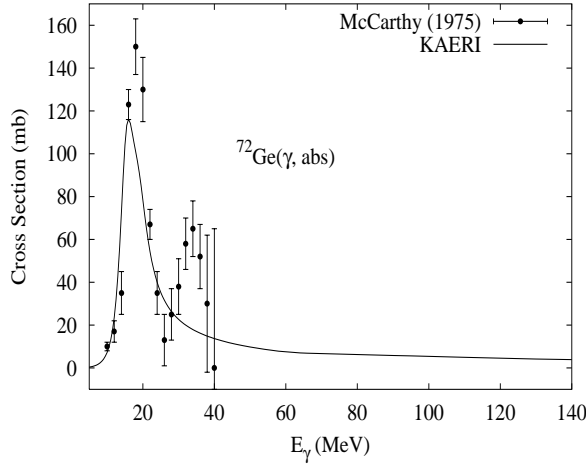
Abundance (%)	Threshold Energies (MeV)								
	$\gamma, n$	$\gamma, p$	$\gamma, t$	$\gamma, \text{He-3}$	$\gamma, \alpha$	$\gamma, 2n$	$\gamma, np$	$\gamma, 2p$	$\gamma, 3n$
21.23	11.54	8.53	18.63	17.61	4.09	19.73	18.84	15.13	32.12



The experimental data of absorption cross section and  $(\gamma, 1nx)$ ,  $(\gamma, 1p)$ ,  $(\gamma, np)$ ,  $(\gamma, 2nx)$  reaction cross sections were given by McCarthy [McC75]. However, his absorption cross section has a small number of data points and a peak with large errors above 30 MeV, and his  $(\gamma, 1nx)$  cross section has different threshold, shape, and magnitude than the others. The experimental data of Carlos [Car76] and Goryachev [Gor82] were also given for  $(\gamma, 1nx)$ ,  $(\gamma, 2nx)$ ,  $(\gamma, sn)$  and  $(\gamma, xn)$  reaction cross sections. We relied on the GUNF and GNASH codes to infer the absorption cross section in the GDR regime, so as to model accurately the  $(\gamma, sn)$  reaction measured data of Carlos. The absorption cross section above the GDR, up to 140 MeV, was taken from QD model calculations.

The calculated results of the emission channels by the GNASH code are in good agreement with all the measured reaction data of Carlos and Goryachev.

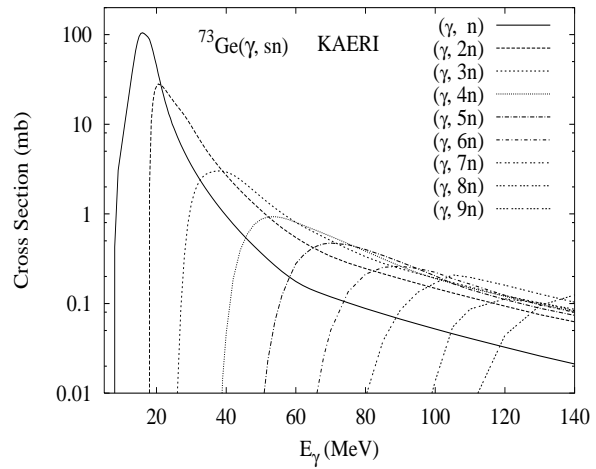
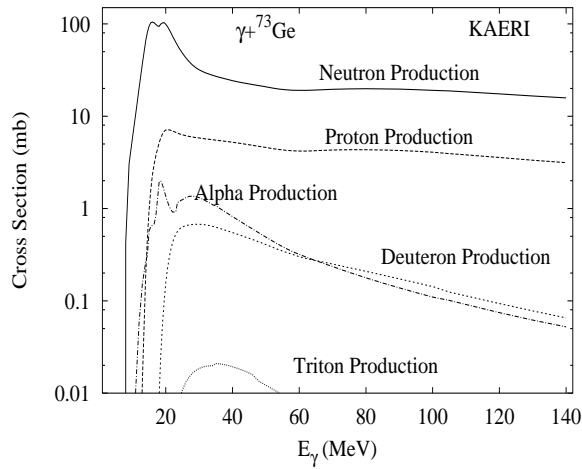
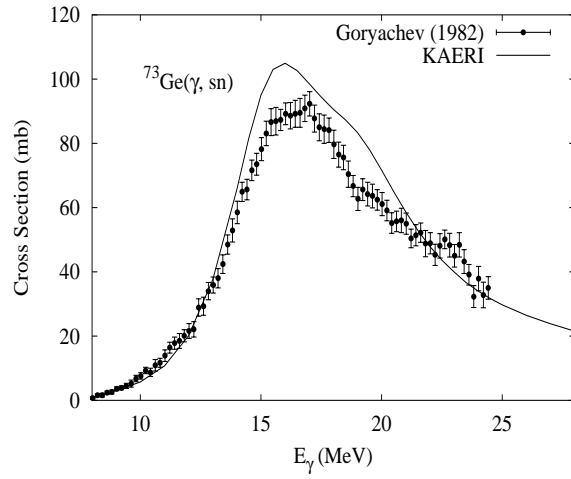
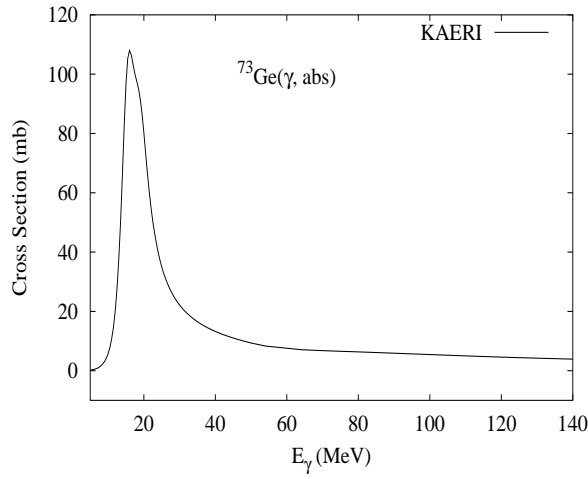
Abundance (%)	Threshold Energies (MeV)								
	$\gamma, n$	$\gamma, p$	$\gamma, t$	$\gamma, \text{He-3}$	$\gamma, \alpha$	$\gamma, 2n$	$\gamma, np$	$\gamma, 2p$	$\gamma, 3n$
27.66	10.75	9.73	18.21	19.10	5.00	18.16	19.04	17.60	29.70



The experimental data of absorption cross section and  $(\gamma, 1nx)$ ,  $(\gamma, 1p)$ ,  $(\gamma, np)$ ,  $(\gamma, 2nx)$  reaction cross sections were given by McCarthy [McC75]. However, his absorption cross section has a small number of data points and a peak with large errors above 30 MeV, and his  $(\gamma, 1nx)$  cross section has different threshold, shape, and magnitude than the others. The experimental data of Carlos [Car76] and Goryachev [Gor82] were also given for  $(\gamma, 1nx)$ ,  $(\gamma, 2nx)$ ,  $(\gamma, sn)$  and  $(\gamma, xn)$  reaction cross sections. We relied on the GUNF and GNASH codes to infer the absorption cross section in the GDR regime, so as to model accurately the  $(\gamma, sn)$  reaction measured data. The absorption cross section above the GDR, up to 140 MeV, was taken from QD model calculations.

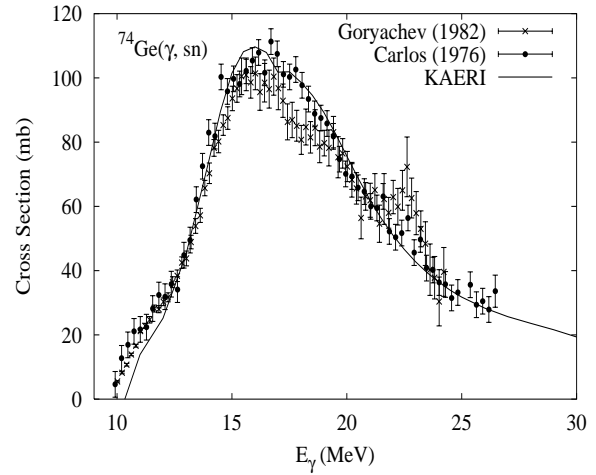
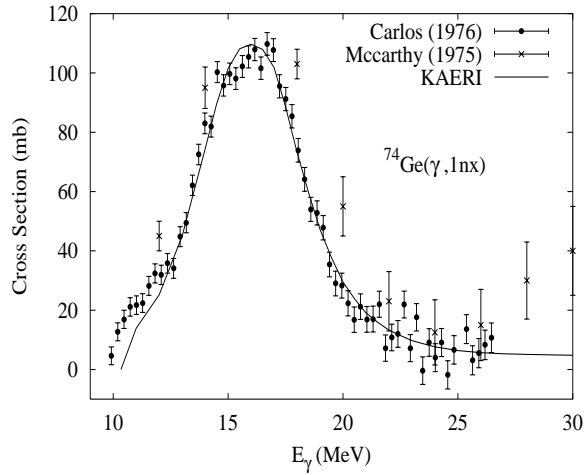
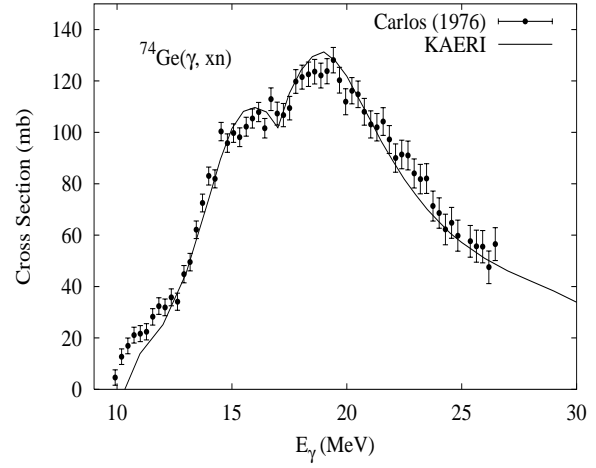
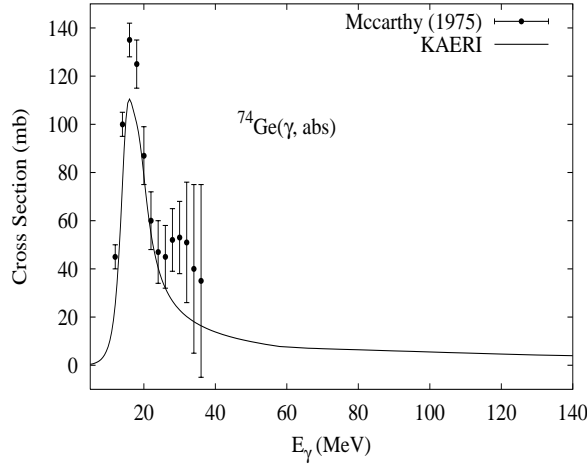
The calculated results of the emission channels by the GNASH code are in good agreement with the experimental data of Carlos.

Abundance (%)	Threshold Energies (MeV)								
	$\gamma, n$	$\gamma, p$	$\gamma, t$	$\gamma, \text{He-3}$	$\gamma, \alpha$	$\gamma, 2n$	$\gamma, np$	$\gamma, 2p$	$\gamma, 3n$
7.73	6.78	9.99	17.34	16.67	5.30	17.53	16.52	18.55	24.95



The photoabsorption cross section has not been measured. However, there are experimental data for the  $(\gamma, sn)$  reaction cross sections by Goryachev [Gor82]. By analyzing the Goryachev and Carlos's data for  ${}^{72,74}\text{Ge}$ , the cross sections for  $(\gamma, sn)$  reaction were scaled up to have 110 mb at 16 MeV. The GUNF and GNASH codes were used to infer the absorption cross section in the GDR regime, so as to model accurately the reconstructed  $(\gamma, sn)$  reaction of Goryachev. The photoabsorption cross section above the GDR, up to 140 MeV, was obtained from QD model calculations using the theory of Chadwick.

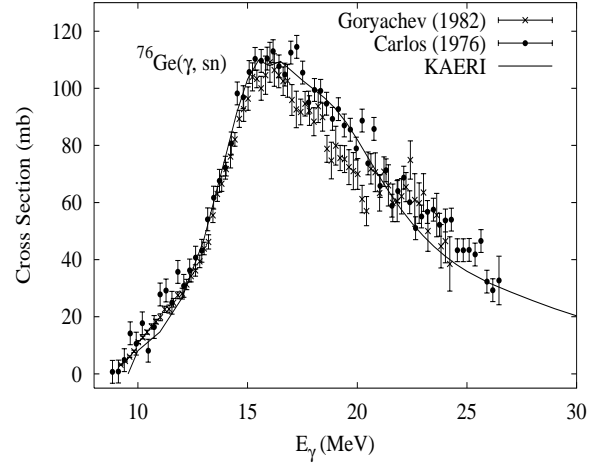
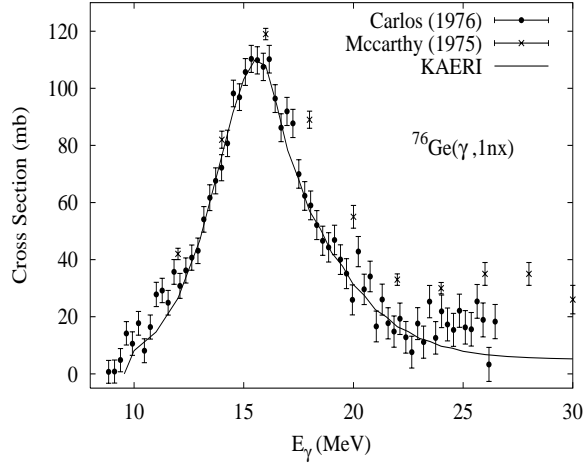
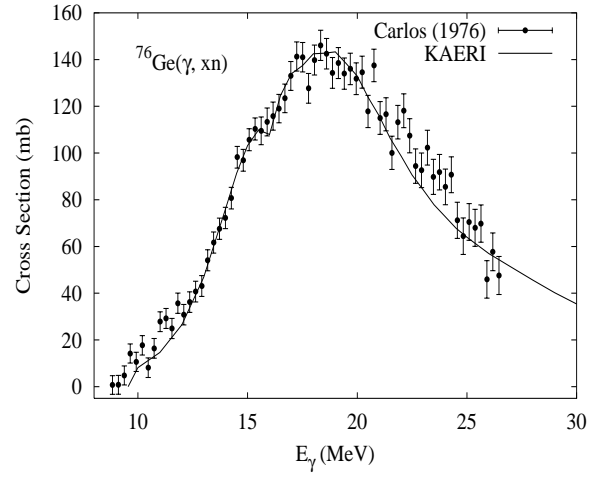
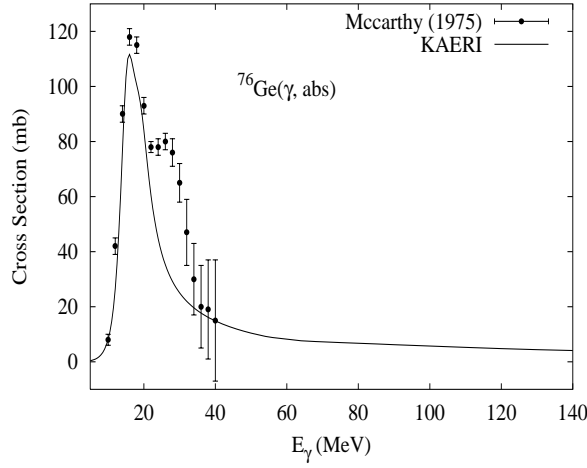
Abundance (%)	Threshold Energies (MeV)								
	$\gamma, n$	$\gamma, p$	$\gamma, t$	$\gamma, \text{He-3}$	$\gamma, \alpha$	$\gamma, 2n$	$\gamma, np$	$\gamma, 2p$	$\gamma, 3n$
35.94	10.20	11.01	18.23	21.03	6.29	16.98	20.19	19.87	27.73



The experimental data of absorption cross section and  $(\gamma, 1nx)$ ,  $(\gamma, 1p)$ ,  $(\gamma, np)$ ,  $(\gamma, 2nx)$  reaction cross sections were given by McCarthy [McC75]. However, his absorption cross section has a small number of data points and a peak with large errors above 30 MeV, and his  $(\gamma, 1nx)$  cross section has different threshold, shape, and magnitude than the others. The experimental data of Carlos [Car76] and Goryachev [Gor82] were also given for  $(\gamma, 1nx)$ ,  $(\gamma, 2nx)$ ,  $(\gamma, sn)$  and  $(\gamma, xn)$  reaction cross sections. We relied on the GUNF and GNASH codes to infer the absorption cross section in the GDR regime, so as to model accurately the  $(\gamma, sn)$  reaction measured data. The absorption cross section above the GDR, up to 140 MeV, was taken from QD model calculations.

The calculated results of the emission channels by the GNASH code are in good agreement with the experimental data of Carlos and Goryachev.

Abundance (%)	Threshold Energies (MeV)								
	$\gamma, n$	$\gamma, p$	$\gamma, t$	$\gamma, \text{He-3}$	$\gamma, \alpha$	$\gamma, 2n$	$\gamma, np$	$\gamma, 2p$	$\gamma, 3n$
7.44	9.43	12.04	18.46	22.74	7.51	15.93	20.52	22.08	26.13

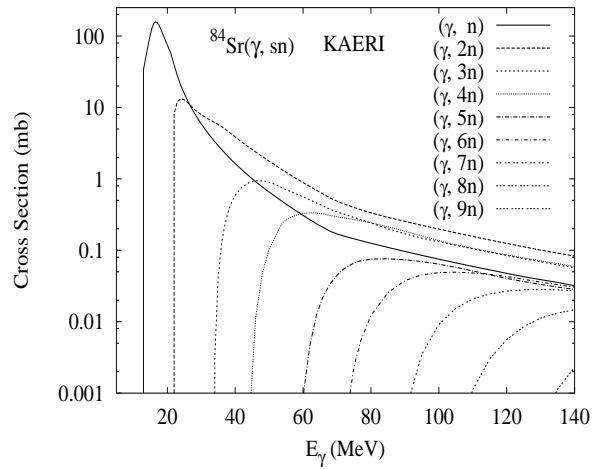
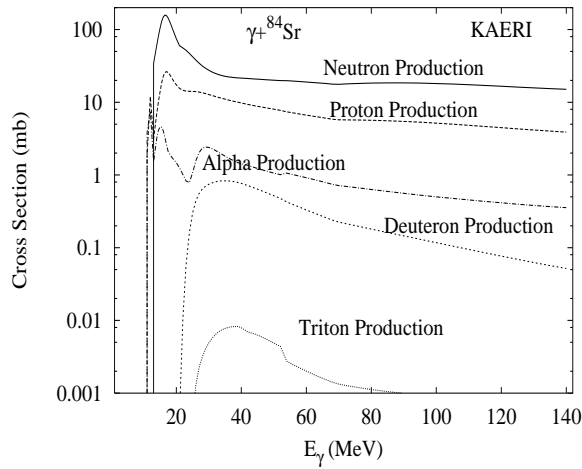
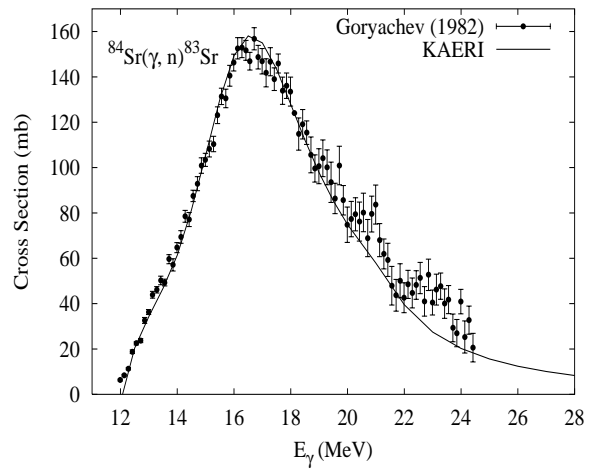
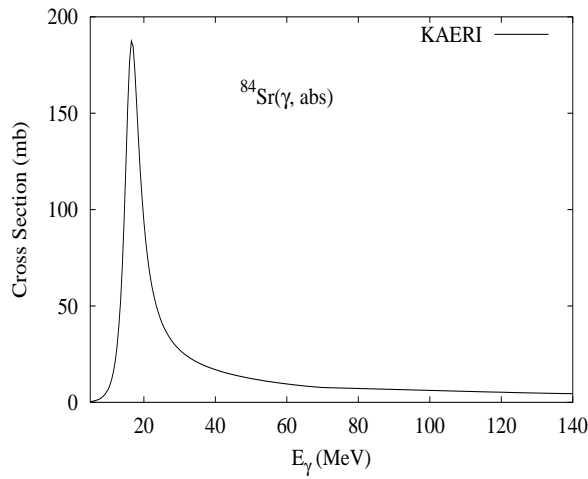


The experimental data of absorption cross section and  $(\gamma, 1nx)$ ,  $(\gamma, 1p)$ ,  $(\gamma, np)$ ,  $(\gamma, 2nx)$  reaction cross sections were given by McCarthy [McC75]. However, his absorption cross section has a small number of data points and a peak with large errors above 30 MeV, and his  $(\gamma, 1nx)$  cross section has different threshold, shape, and magnitude than the others. The experimental data of Carlos [Car76] and Goryachev [Gor82] were also given for  $(\gamma, 1nx)$ ,  $(\gamma, 2nx)$ ,  $(\gamma, sn)$  and  $(\gamma, xn)$  reaction cross sections. We relied on the GUNF and GNASH codes to infer the absorption cross section in the GDR regime, so as to model accurately the  $(\gamma, sn)$  reaction measured data. The absorption cross section above the GDR, up to 140 MeV, was taken from QD model calculations.

The calculated results of the emission channels by the GNASH code are in good agreement with the experimental data of Carlos and Goryachev.

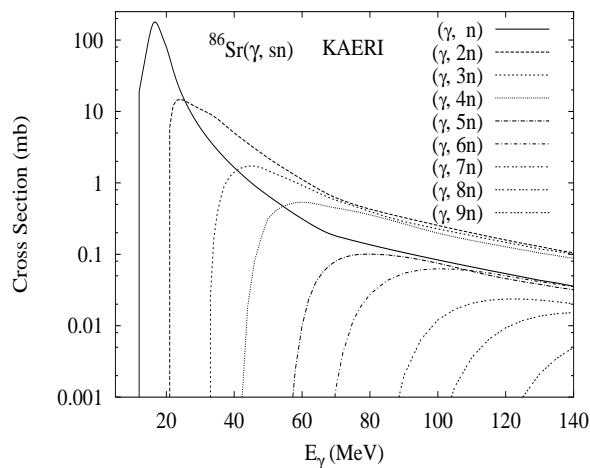
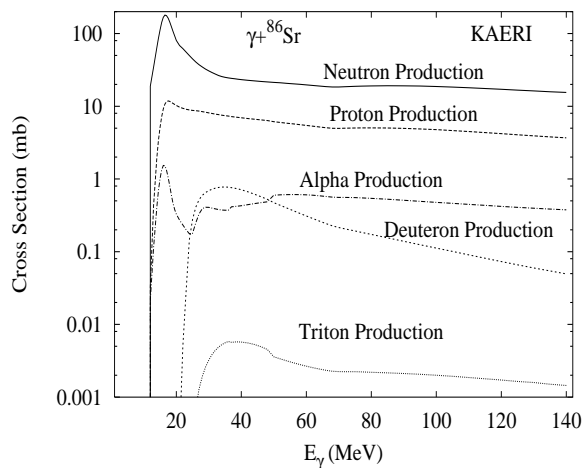
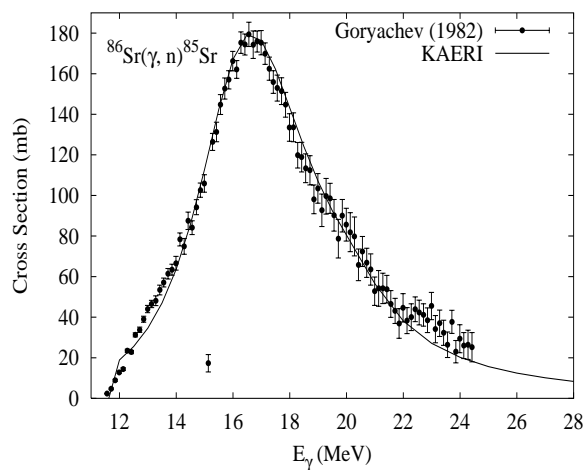
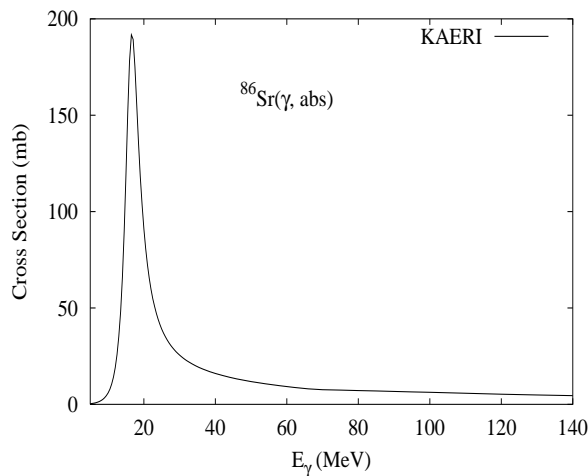


Abundance (%)	Threshold Energies (MeV)								
	$\gamma, n$	$\gamma, p$	$\gamma, t$	$\gamma, \text{He-3}$	$\gamma, \alpha$	$\gamma, 2n$	$\gamma, np$	$\gamma, 2p$	$\gamma, 3n$
0.56	11.93	8.88	20.13	17.88	5.17	20.79	19.80	14.63	33.39



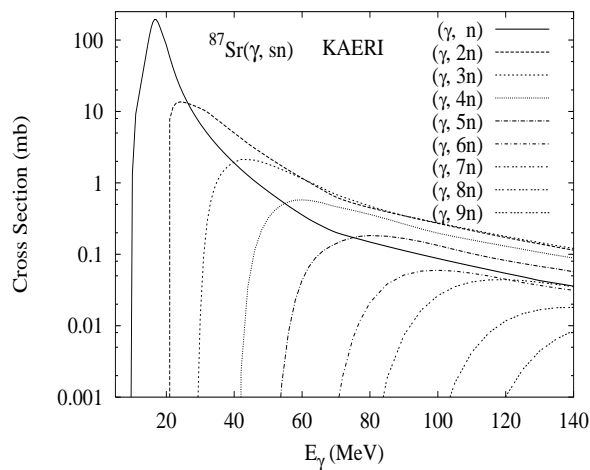
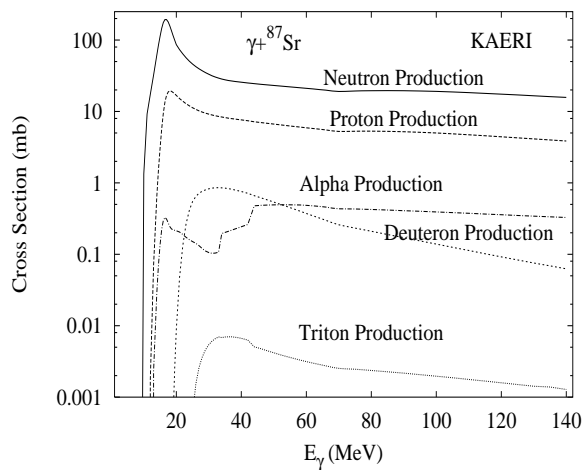
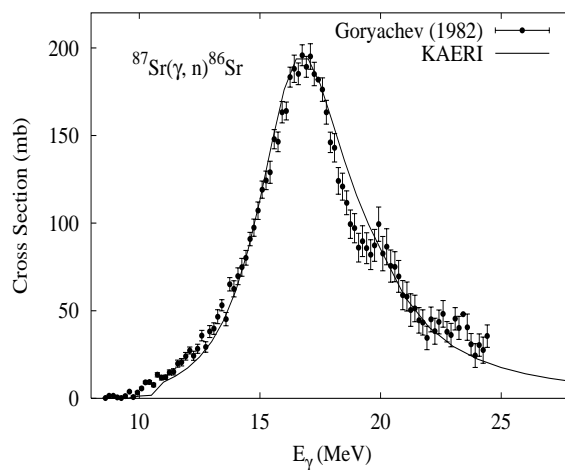
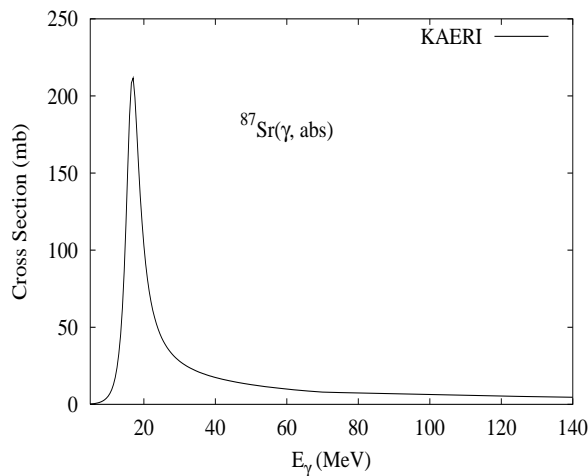
The photoabsorption cross section has not been measured. However, there are experimental data for the  $(\gamma, 1n)$  reaction cross section [Gor82]. We relied on the GUNF and GNASH codes to infer the photoabsorption cross section in the GDR regime, in order to model accurately the  $(\gamma, 1n)$  data. The photoabsorption cross section above the GDR, up to 140 MeV, was obtained from QD model calculations using the theory of Chadwick.

Abundance (%)	Threshold Energies (MeV)								
	$\gamma, n$	$\gamma, p$	$\gamma, t$	$\gamma, \text{He-3}$	$\gamma, \alpha$	$\gamma, 2n$	$\gamma, np$	$\gamma, 2p$	$\gamma, 3n$
9.86	11.49	9.64	20.42	19.47	6.35	20.02	20.13	16.67	31.95



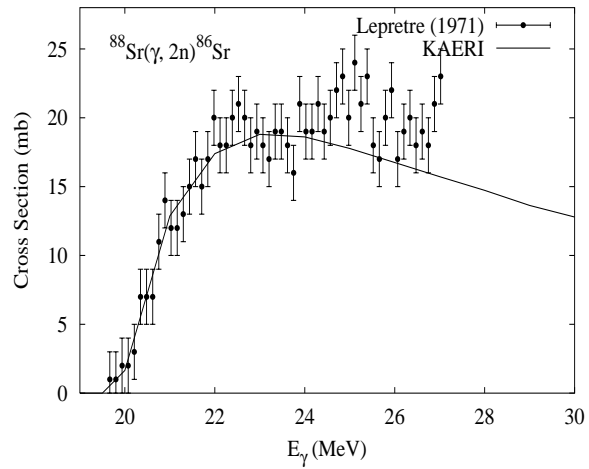
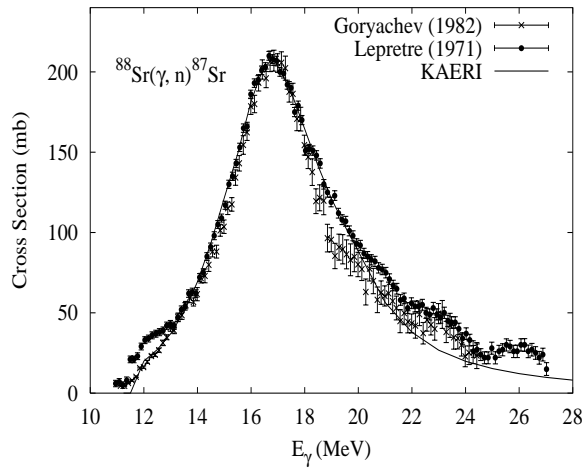
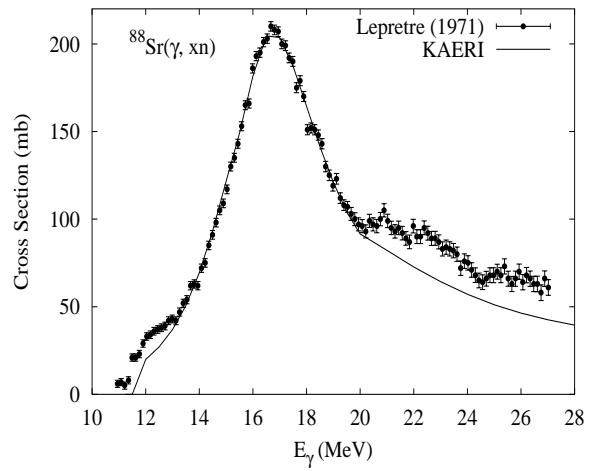
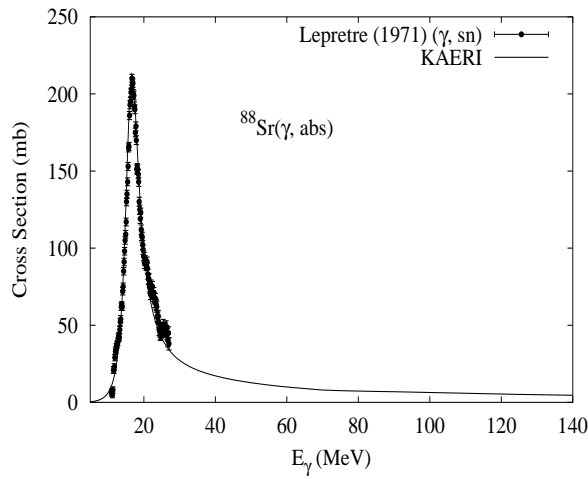
The photoabsorption cross section has not been measured. However, there are experimental data for the  $(\gamma, 1n)$  reaction cross section [Gor82]. We relied on the GUNF and GNASH codes to infer the photoabsorption cross section in the GDR regime, in order to model accurately the  $(\gamma, 1n)$  data. The photoabsorption cross section above the GDR, up to 140 MeV, was obtained from QD model calculations using the theory of Chadwick.

Abundance (%)	Threshold Energies (MeV)								
	$\gamma, n$	$\gamma, p$	$\gamma, t$	$\gamma, \text{He-3}$	$\gamma, \alpha$	$\gamma, 2n$	$\gamma, np$	$\gamma, 2p$	$\gamma, 3n$
7.00	8.43	9.42	20.08	17.38	7.32	19.92	18.07	17.98	28.45



The photoabsorption cross section has not been measured. However, there are experimental data for the  $(\gamma, 1n)$  reaction cross section [Gor82]. We relied on the GUNF and GNASH codes to infer the photoabsorption cross section in the GDR regime, in order to model accurately the  $(\gamma, 1n)$  data. The photoabsorption cross section above the GDR, up to 140 MeV, was obtained from QD model calculations using the theory of Chadwick.

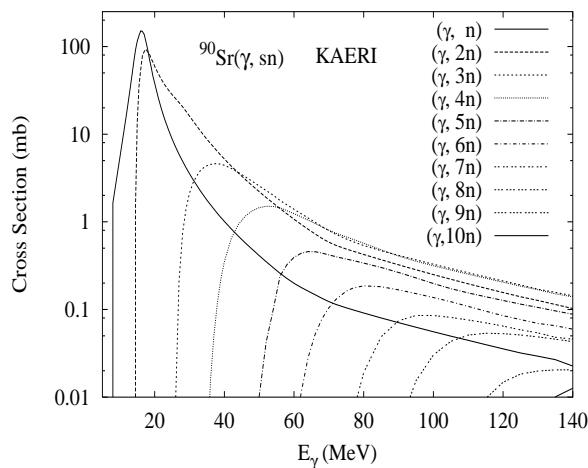
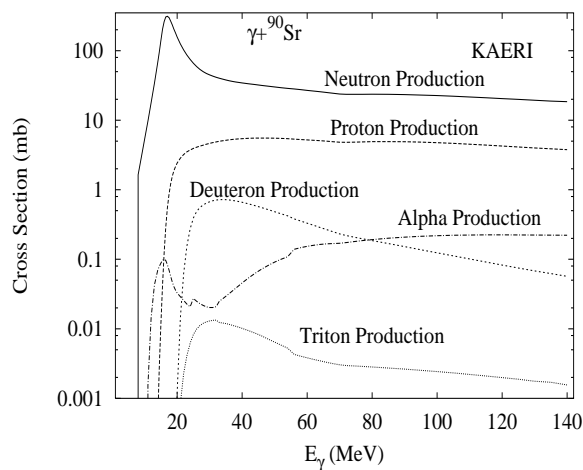
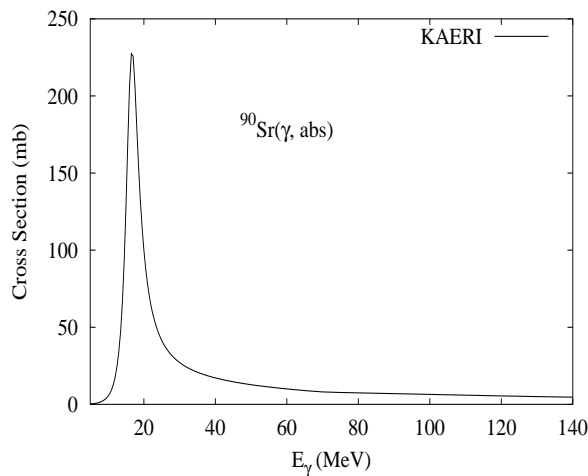
Abundance (%)	Threshold Energies (MeV)								
	$\gamma, n$	$\gamma, p$	$\gamma, t$	$\gamma, \text{He-3}$	$\gamma, \alpha$	$\gamma, 2n$	$\gamma, np$	$\gamma, 2p$	$\gamma, 3n$
82.58	11.11	10.61	20.70	21.37	7.91	19.54	20.53	19.23	31.03



The photoabsorption cross section has not been measured. However, for  ${}^{nat}\text{Sr}$ , there are experimental data for the  $(\gamma, 1nx)$ ,  $(\gamma, 2nx)$ ,  $(\gamma, sn)$  and  $(\gamma, xn)$  reaction cross sections [Lep71]. Experimental data were also reported [Gor82] for the  $(\gamma, 1n)$  cross section of  ${}^{88}\text{Sr}$ . We relied on the GUNF and GNASH codes to infer the photoabsorption cross section in the GDR regime, in order to model accurately Lepretre's  $(\gamma, sn)$  data. The photoabsorption cross section above the GDR, up to 140 MeV, was obtained from QD model calculations using the theory of Chadwick.

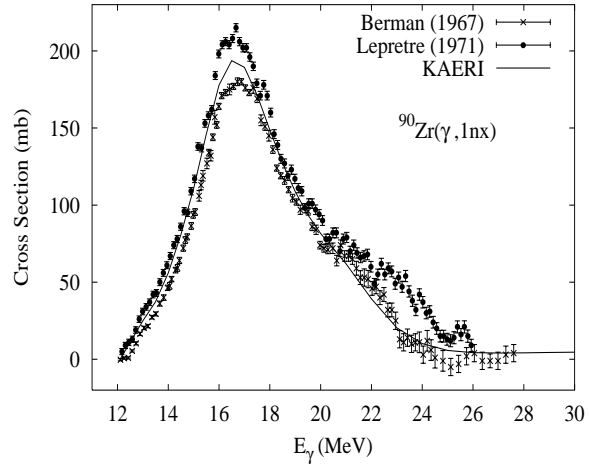
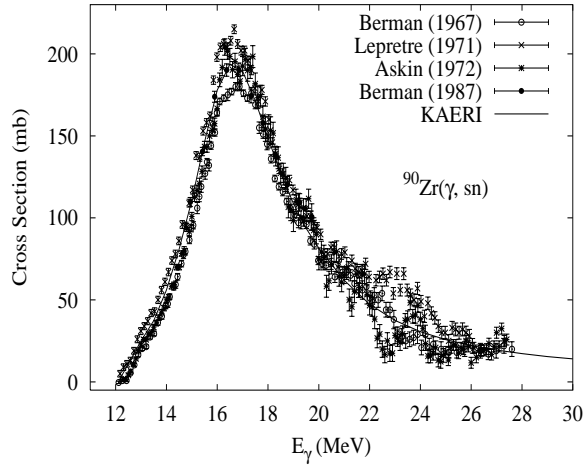
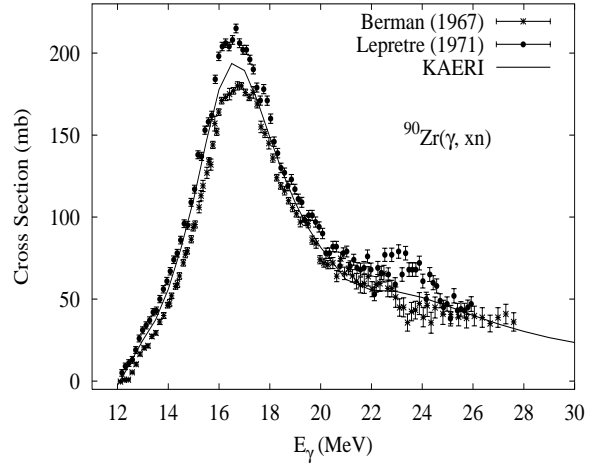
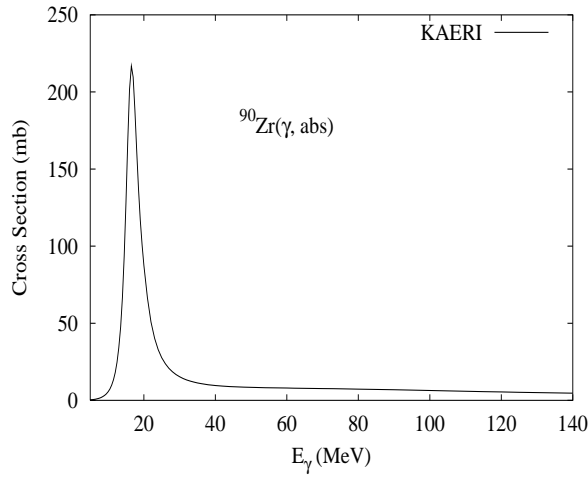
The calculated results of the emission channels by the GNASH code are in good agreement with the experimental data.

Abundance (%)	Threshold Energies (MeV)								
	$\gamma, n$	$\gamma, p$	$\gamma, t$	$\gamma, \text{He-3}$	$\gamma, \alpha$	$\gamma, 2n$	$\gamma, np$	$\gamma, 2p$	$\gamma, 3n$
0.00	7.80	11.52	16.30	20.17	5.11	14.17	18.70	20.83	25.28



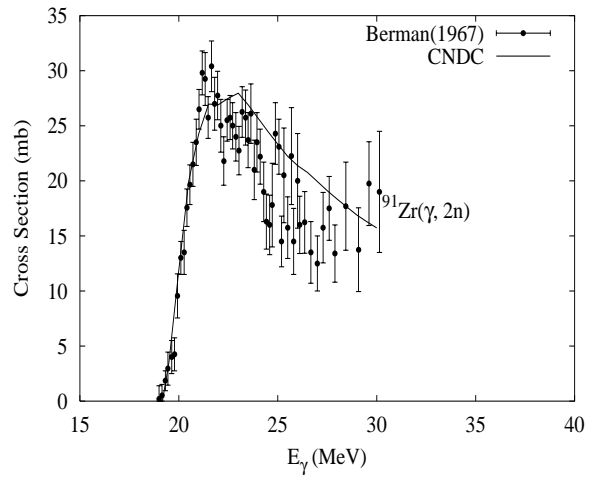
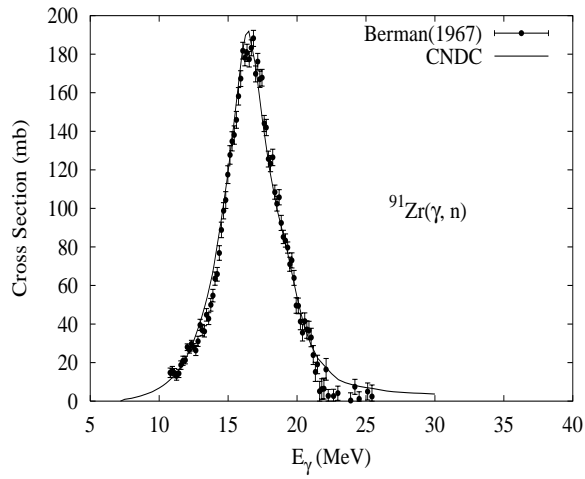
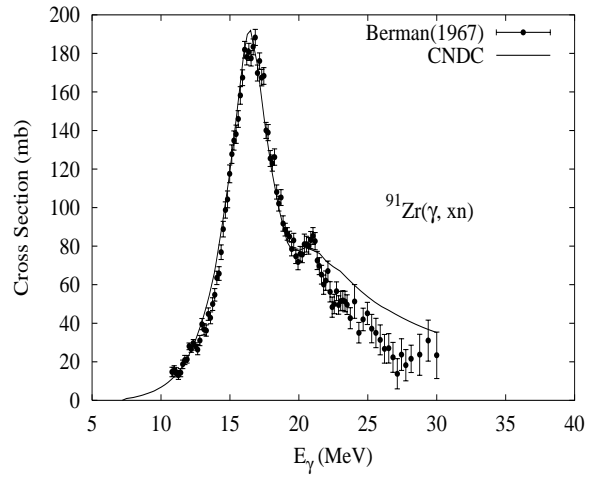
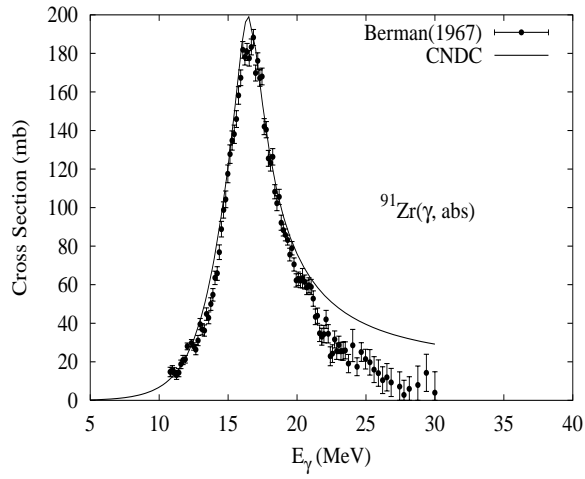
There are no experimental data available. The photoabsorption cross section was obtained from GDR and QD model calculations, adopting the GDR parameters of  ${}^{88}\text{Sr}$ . The neutron, proton, deuteron, triton and alpha emission cross sections, as well as production cross sections, were calculated by the GNASH code.

Abundance (%)	Threshold Energies (MeV)								
	$\gamma, n$	$\gamma, p$	$\gamma, t$	$\gamma, \text{He-3}$	$\gamma, \alpha$	$\gamma, 2n$	$\gamma, np$	$\gamma, 2p$	$\gamma, 3n$
51.45	11.97	8.36	20.71	18.83	6.68	21.29	19.84	15.43	33.64



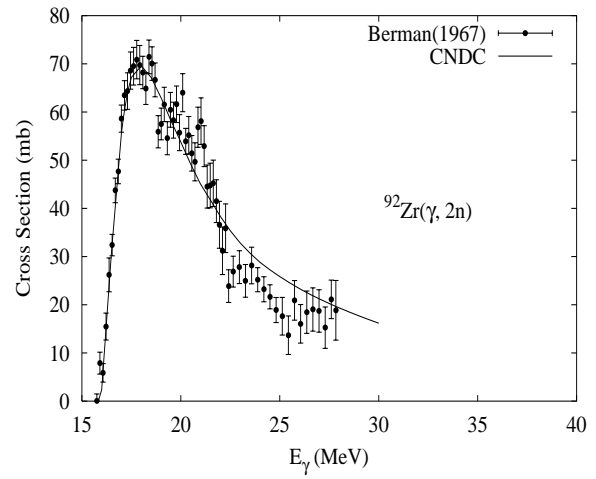
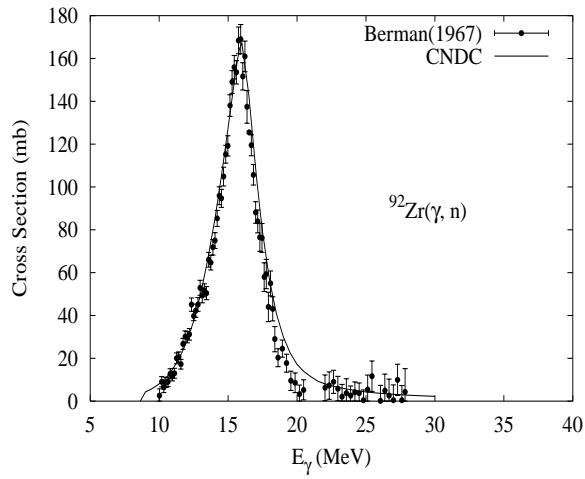
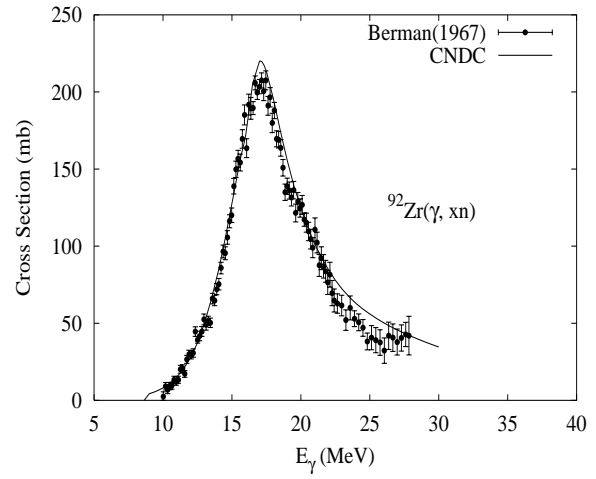
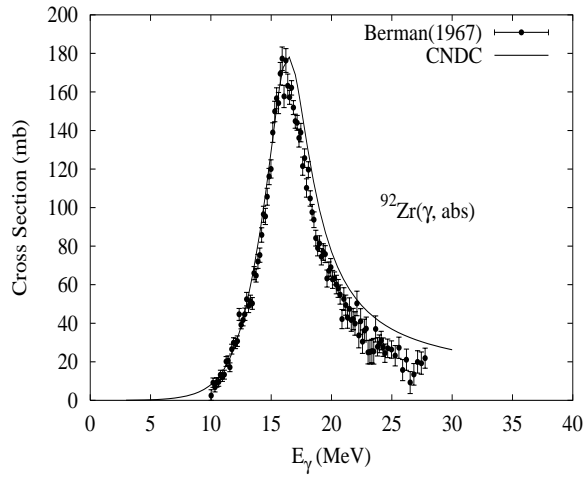
The photoabsorption cross section has not been measured. However, there are experimental data for  $(\gamma, 1nx)$ ,  $(\gamma, 2nx)$ ,  $(\gamma, sn)$  and  $(\gamma, xn)$  reaction cross sections by Berman [Ber67] and Lepretre [Lep71], and for  $(\gamma, sn)$  by Ashkin [Ask72]. Lepretre's data is different from Berman's and Askin's data in the magnitudes. Berman [Ber87] remeasured the  $(\gamma, sn)$  reaction cross section near the peak of the giant dipole resonance for natural Zr in 1987. We relied on the GUNF and GNASH codes to infer the photoabsorption cross section in the GDR regime, in order to model accurately the  $(\gamma, sn)$  data of Berman measured in 1987. The photoabsorption cross section above the GDR, up to 140 MeV, was obtained from QD model calculations using the theory of Chadwick. The calculated results of the emission channels by the GNASH code are in overall agreement with the experimental data of  $(\gamma, 1nx)$ ,  $(\gamma, 2nx)$  and  $(\gamma, xn)$  reaction cross sections.

Abundance (%)	Threshold Energies (MeV)								
	$\gamma, n$	$\gamma, p$	$\gamma, t$	$\gamma, \text{He-3}$	$\gamma, \alpha$	$\gamma, 2n$	$\gamma, np$	$\gamma, 2p$	$\gamma, 3n$
11.22	7.19	8.69	18.55	14.91	5.44	19.17	15.55	16.26	28.48



The photoabsorption cross section has not been measured. However, there are experimental data for the  $(\gamma, 1nx)$ ,  $(\gamma, 2nx)$  and  $(\gamma, xn)$  reaction cross sections [Ber67]. We relied on GUNF code [Zha98] to infer the photoabsorption cross section in the GDR regime, in order to model accurately the available experimental data.

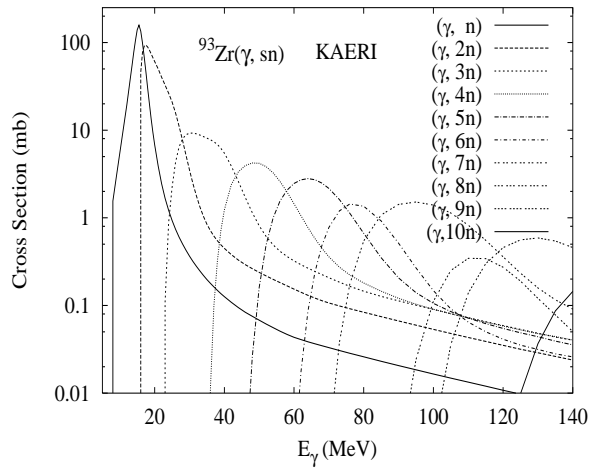
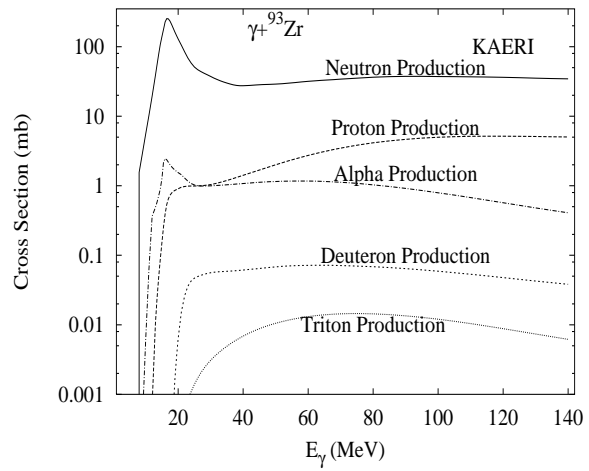
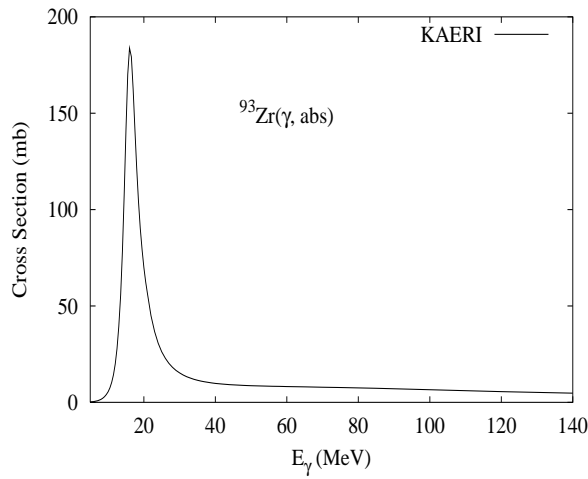
Abundance (%)	Threshold Energies (MeV)								
	$\gamma, n$	$\gamma, p$	$\gamma, t$	$\gamma, \text{He-3}$	$\gamma, \alpha$	$\gamma, 2n$	$\gamma, np$	$\gamma, 2p$	$\gamma, 3n$
17.15	8.64	9.40	15.70	17.18	2.97	15.83	17.33	17.09	27.80



The photoabsorption cross section has not been measured. However, there are experimental data for the  $(\gamma, 1nx)$ ,  $(\gamma, 2nx)$  and  $(\gamma, xn)$  reaction cross sections [Ber67]. We relied on GUNF code [Zha98] to infer the photoabsorption cross section in the GDR regime, in order to model accurately the available experimental data.

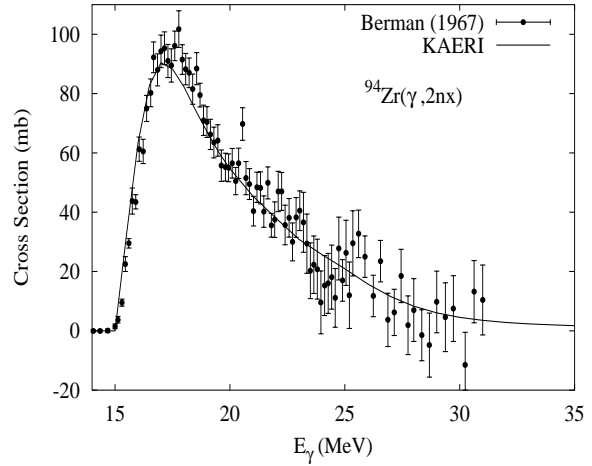
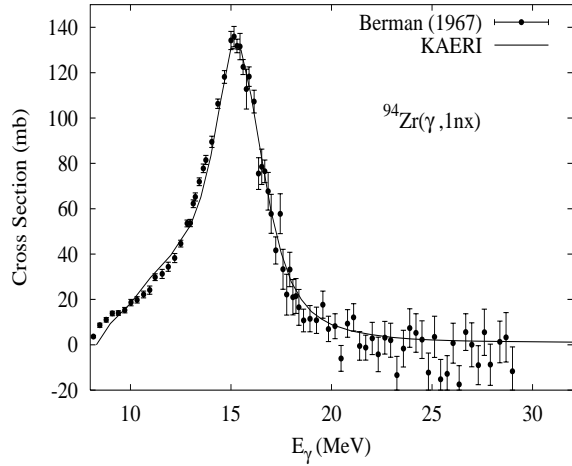
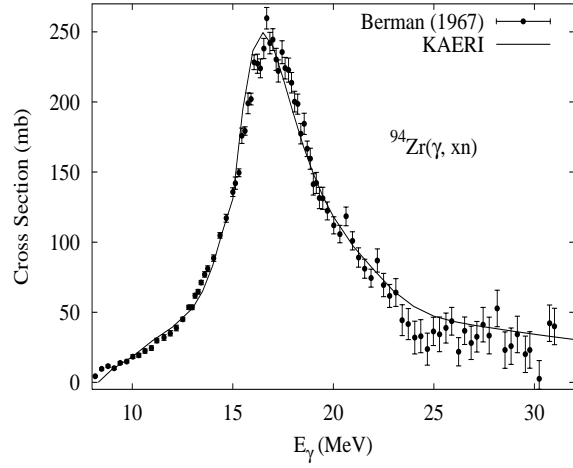
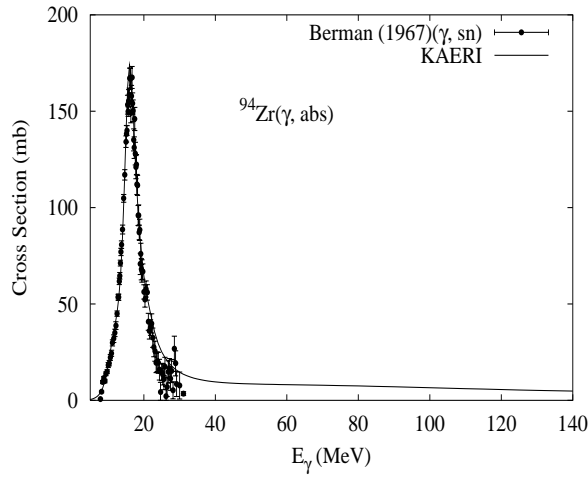


Abundance (%)	Threshold Energies (MeV)								
	$\gamma, n$	$\gamma, p$	$\gamma, t$	$\gamma, \text{He-3}$	$\gamma, \alpha$	$\gamma, 2n$	$\gamma, np$	$\gamma, 2p$	$\gamma, 3n$
0.00	6.73	9.58	15.58	16.11	3.33	15.37	16.13	18.05	22.56



There are no experimental data available. The photoabsorption cross section was obtained from GDR and QD model calculations, adopting the GDR parameters of  ${}^{94}\text{Zr}$ . The neutron, proton, deuteron, triton and alpha emission cross sections, as well as production cross sections, were calculated by the GNASH code.

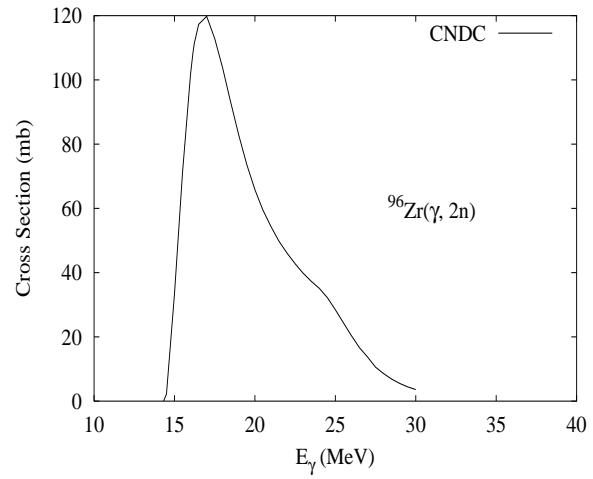
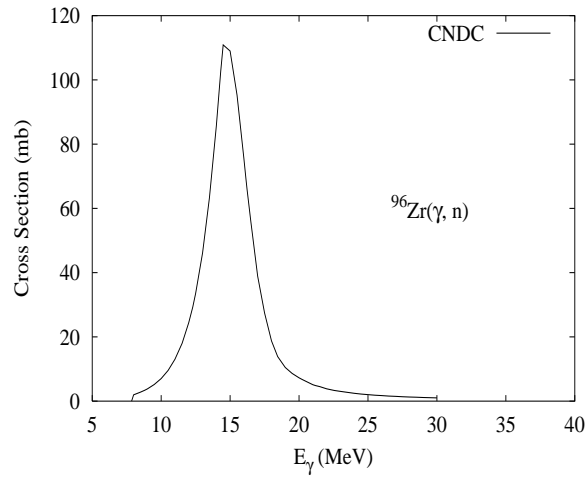
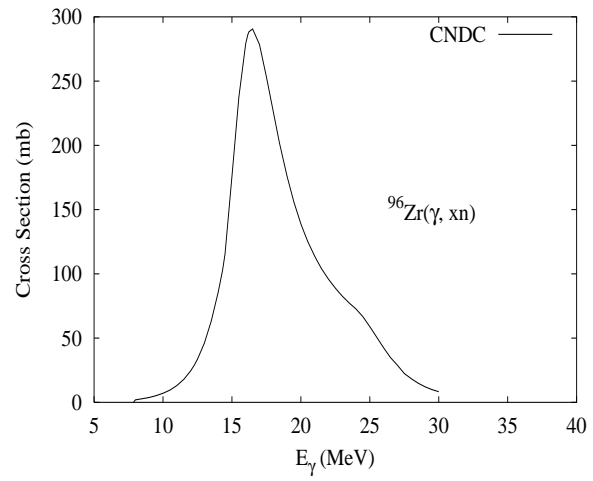
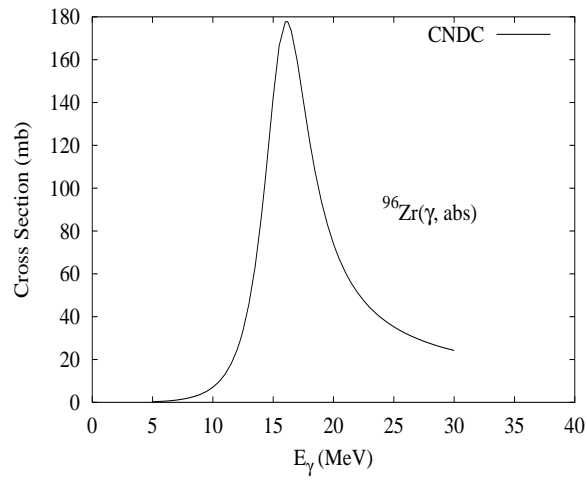
Abundance (%)	Threshold Energies (MeV)								
	$\gamma, n$	$\gamma, p$	$\gamma, t$	$\gamma, \text{He-3}$	$\gamma, \alpha$	$\gamma, 2n$	$\gamma, np$	$\gamma, 2p$	$\gamma, 3n$
17.38	8.22	10.31	15.87	18.55	3.75	14.95	17.80	18.92	23.59



The photoabsorption cross section has not been measured. However, there are experimental data for the  $(\gamma, 1nx)$ ,  $(\gamma, 2nx)$ ,  $(\gamma, sn)$ , and  $(\gamma, xn)$  reaction cross sections [Ber67]. We relied on the GUNF and GNASH codes to infer the photoabsorption cross section in the GDR regime, in order to model accurately the  $(\gamma, sn)$  data. The photoabsorption cross section above the GDR, up to 140 MeV, was obtained from QD model calculations using the theory of Chadwick.

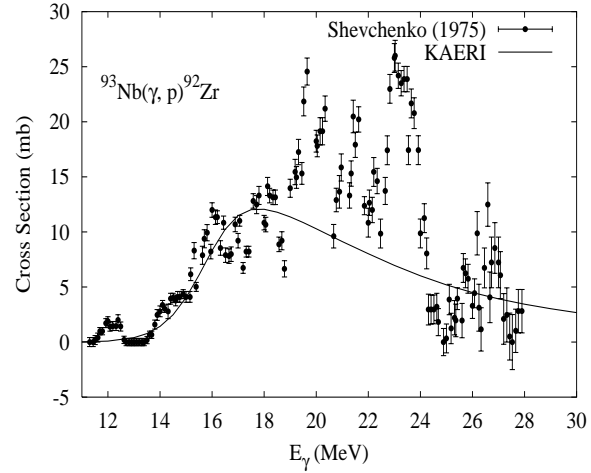
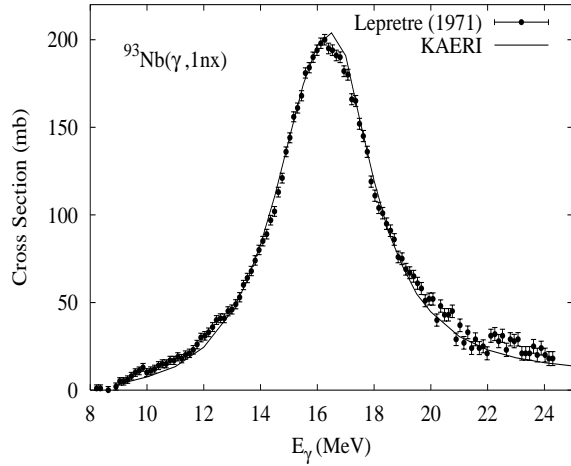
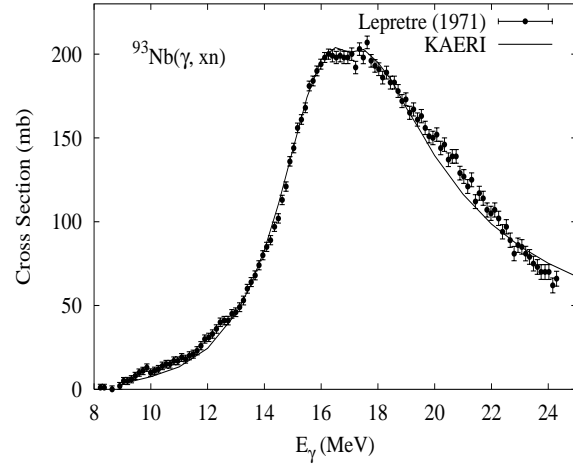
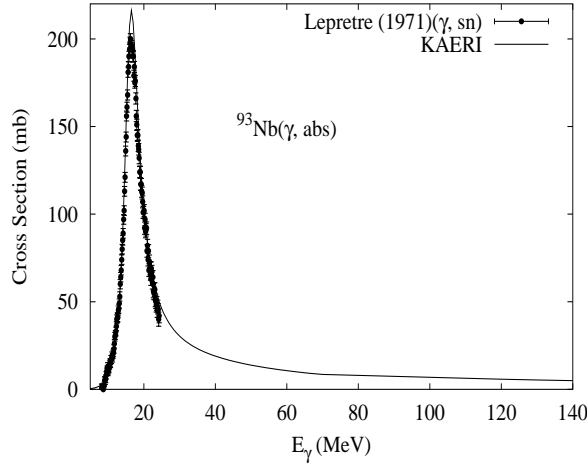
The calculated results of the emission channels by the GNASH code are in good agreement with the experimental data for  $(\gamma, 1nx)$ ,  $(\gamma, 2nx)$  and  $(\gamma, xn)$  reaction cross sections.

Abundance (%)	Threshold Energies (MeV)								
	$\gamma, n$	$\gamma, p$	$\gamma, t$	$\gamma, \text{He-3}$	$\gamma, \alpha$	$\gamma, 2n$	$\gamma, np$	$\gamma, 2p$	$\gamma, 3n$
2.80	7.85	11.52	16.15	20.21	4.94	14.32	18.45	21.18	22.54



There are no experimental data available. The photoabsorption cross section was obtained from GDR model calculations using the GUNF code [Zha98], adopting the same model parameters as for the  $\gamma + {}^{90,91,92,94}\text{Zr}$  reactions.

Abundance (%)	Threshold Energies (MeV)								
	$\gamma, n$	$\gamma, p$	$\gamma, t$	$\gamma, \text{He-3}$	$\gamma, \alpha$	$\gamma, 2n$	$\gamma, np$	$\gamma, 2p$	$\gamma, 3n$
100.00	8.83	6.04	13.39	15.65	1.93	16.71	14.68	15.44	28.77

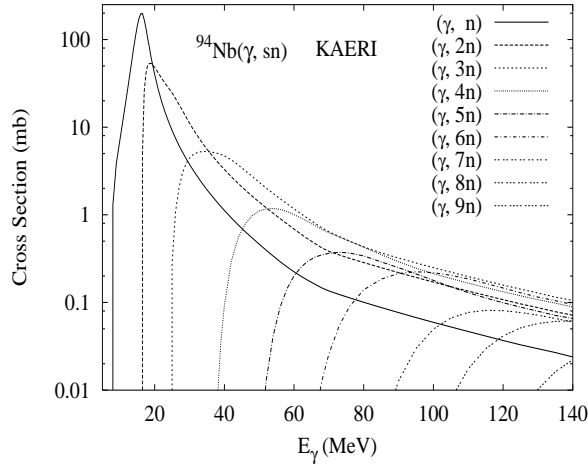
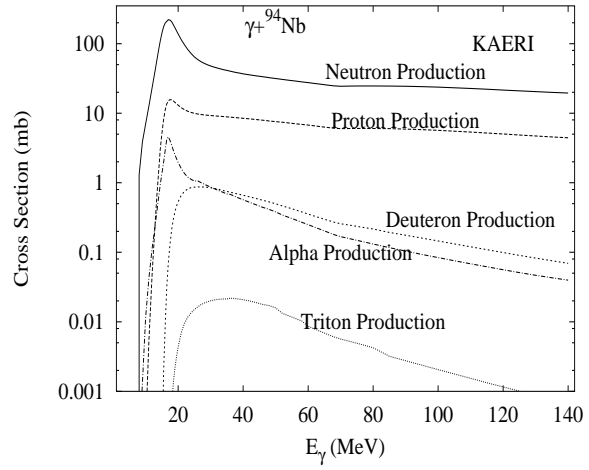
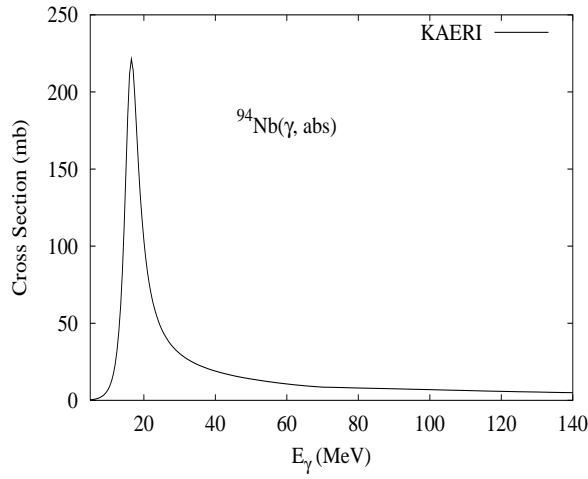


The photoabsorption cross section has not been measured. However, there are experimental data for the  $(\gamma, 1nx)$ ,  $(\gamma, 2nx)$ ,  $(\gamma, sn)$  and  $(\gamma, xn)$  reaction cross sections by Lepretre [Lep71], and  $(\gamma, 1p)$  reaction cross section by Shevchenko [She75]. We relied on the GUNF and GNASH codes to infer the photoabsorption cross section in the GDR regime, in order to model accurately the  $(\gamma, sn)$  data. The photoabsorption cross section above the GDR, up to 140 MeV, was obtained from QD model calculations using the theory of Chadwick.

The calculated results of the emission channels by the GNASH code are in good agreement with the experimental data for  $(\gamma, 1nx)$  and  $(\gamma, xn)$  reaction cross sections. For the  $(\gamma, 1p)$  reaction cross section, the calculated results are in good agreement with the experimental data below 18 MeV, but are lower than the experiment above that. A possible explanation is that the experiment may include the  $(\gamma, np)$  channel.

$\gamma + {}^{94}\text{Nb}$ 

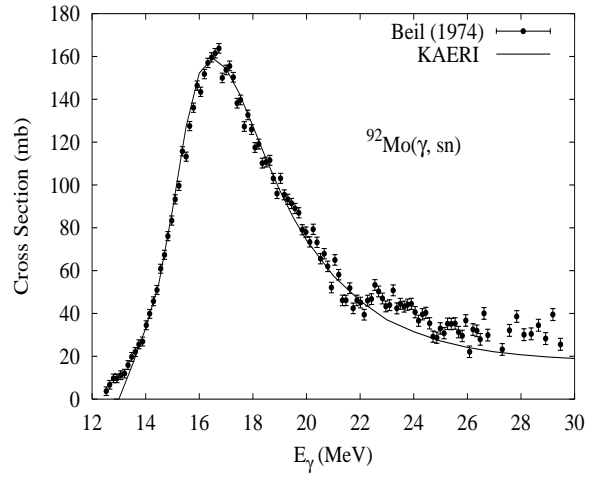
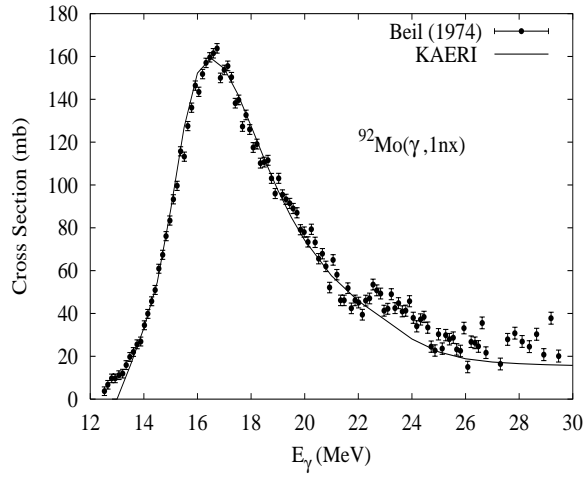
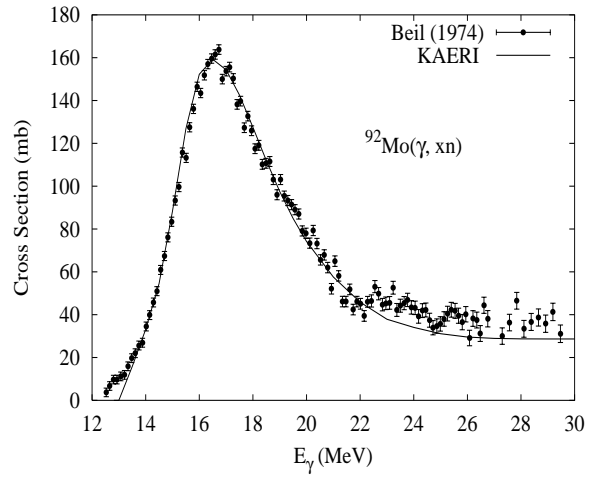
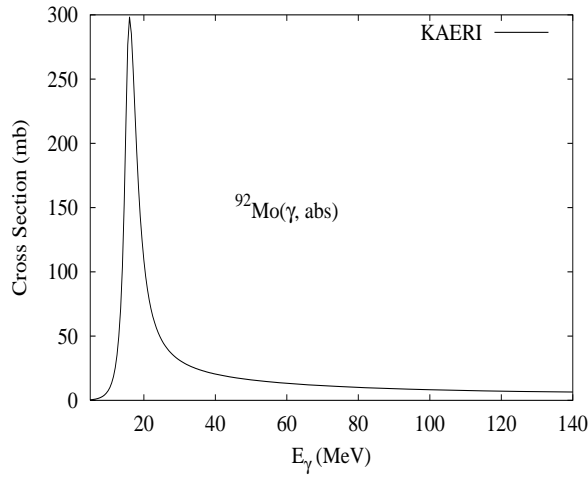
Abundance (%)	Threshold Energies (MeV)								
	$\gamma, n$	$\gamma, p$	$\gamma, t$	$\gamma, \text{He-3}$	$\gamma, \alpha$	$\gamma, 2n$	$\gamma, np$	$\gamma, 2p$	$\gamma, 3n$
0.00	7.23	6.54	13.42	14.95	2.30	16.06	13.27	16.11	23.94



There are no experimental data available. The photoabsorption cross section was obtained from GDR and QD model calculations, adopting the GDR parameters of  ${}^{93}\text{Nb}$ . The neutron, proton, deuteron, triton and alpha emission cross sections, as well as production cross sections, were calculated by the GNASH code.

# $\gamma + {}^{92}\text{Mo}$

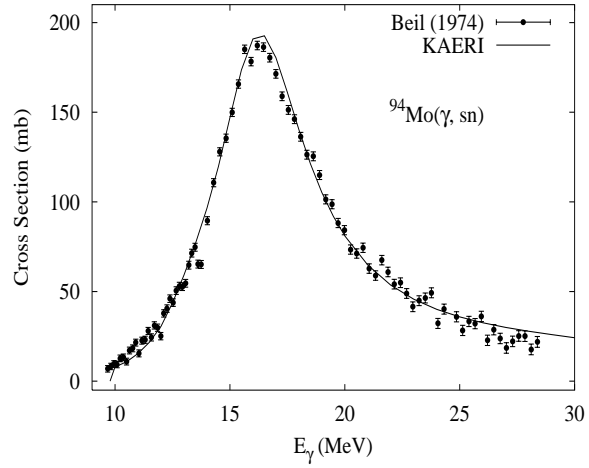
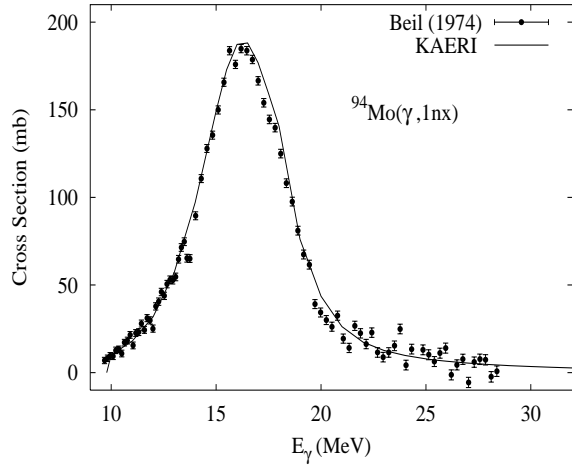
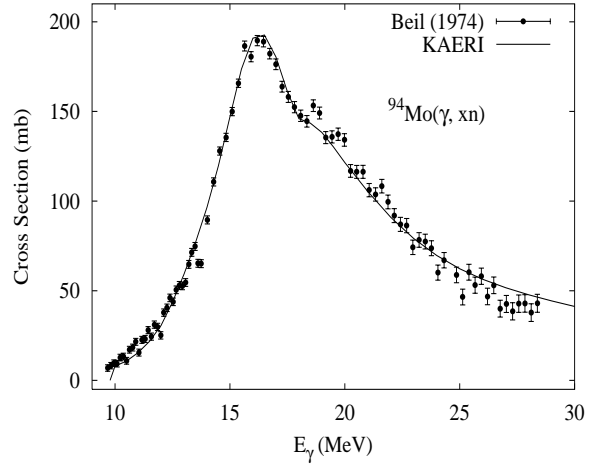
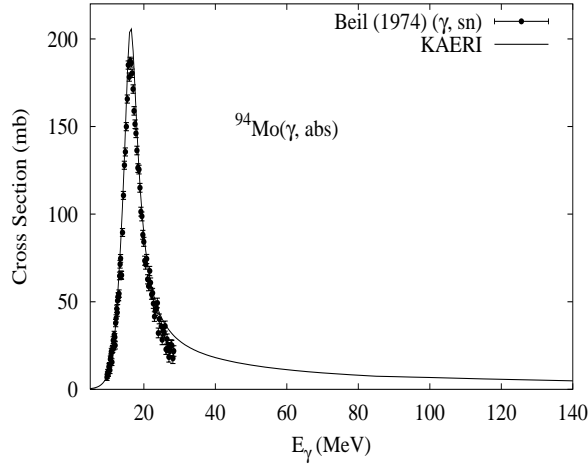
Abundance (%)	Threshold Energies (MeV)								
	$\gamma, n$	$\gamma, p$	$\gamma, t$	$\gamma, \text{He-3}$	$\gamma, \alpha$	$\gamma, 2n$	$\gamma, np$	$\gamma, 2p$	$\gamma, 3n$
14.84	12.67	7.46	21.18	16.87	5.61	22.78	19.51	12.62	36.02



The photoabsorption cross section has not been measured. However, there are experimental data for the  $(\gamma, 1nx)$ ,  $(\gamma, 2nx)$ ,  $(\gamma, sn)$ , and  $(\gamma, xn)$  reaction cross sections [Bei74]. We relied on the GUNF and GNASH codes to infer the photoabsorption cross section in the GDR regime, in order to model accurately the  $(\gamma, sn)$  data. The photoabsorption cross section above the GDR, up to 140 MeV, was obtained from QD model calculations using the theory of Chadwick.

The calculated results of the emission channels by the GNASH code are in good agreement with the experimental data.

Abundance (%)	Threshold Energies (MeV)								
	$\gamma, n$	$\gamma, p$	$\gamma, t$	$\gamma, \text{He-3}$	$\gamma, \alpha$	$\gamma, 2n$	$\gamma, np$	$\gamma, 2p$	$\gamma, 3n$
9.25	9.68	8.49	16.72	15.45	2.07	17.75	17.32	14.53	30.42

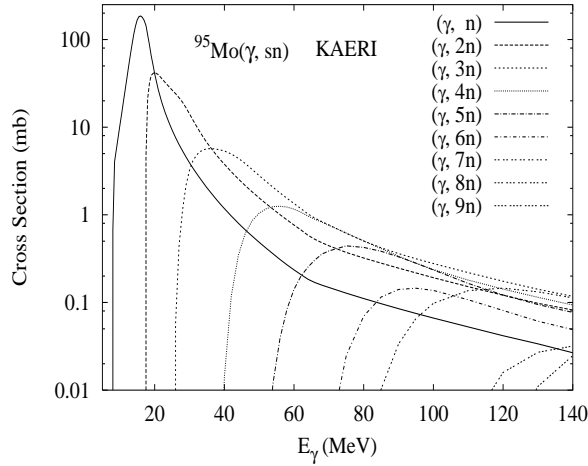
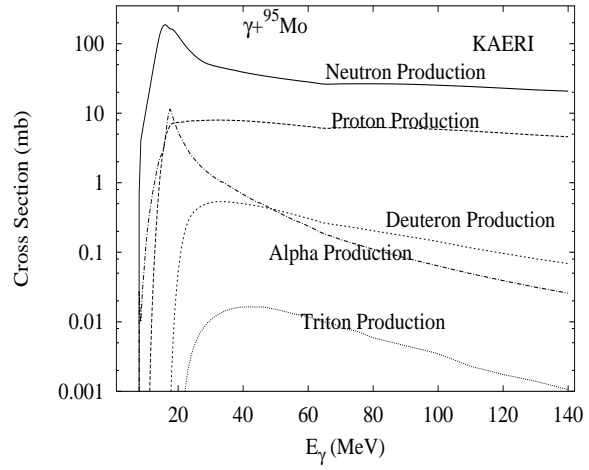
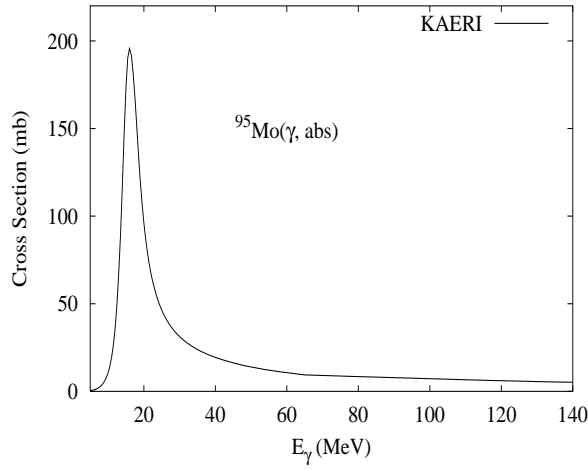


The photoabsorption cross section has not been measured. However, there are experimental data for the  $(\gamma, 1nx)$ ,  $(\gamma, 2nx)$ ,  $(\gamma, sn)$ , and  $(\gamma, xn)$  reaction cross sections [Bei74]. We relied on the GUNF and GNASH codes to infer the photoabsorption cross section in the GDR regime, in order to model accurately the  $(\gamma, sn)$  data. The photoabsorption cross section above the GDR, up to 140 MeV, was obtained from QD model calculations using the theory of Chadwick.

The calculated results of the emission channels by the GNASH code are in good agreement with the experimental data.

$\gamma + {}^{95}\text{Mo}$ 

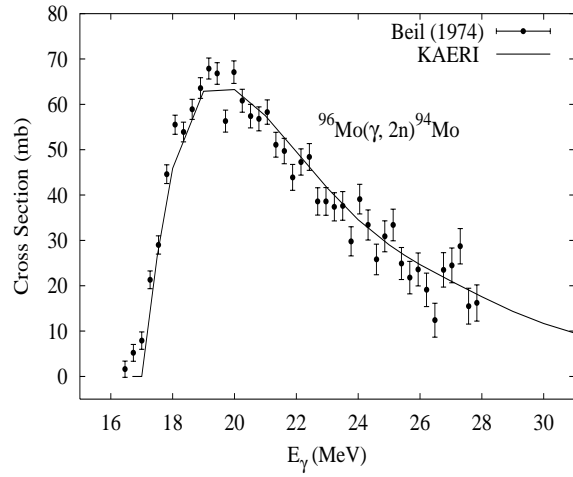
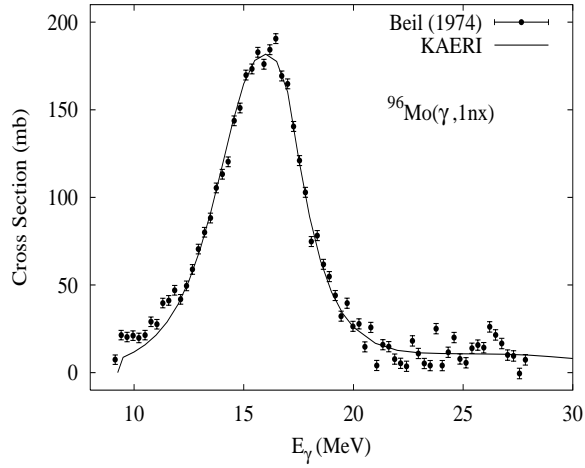
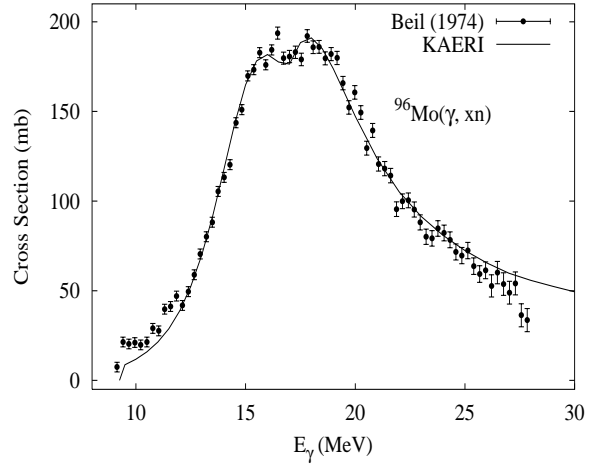
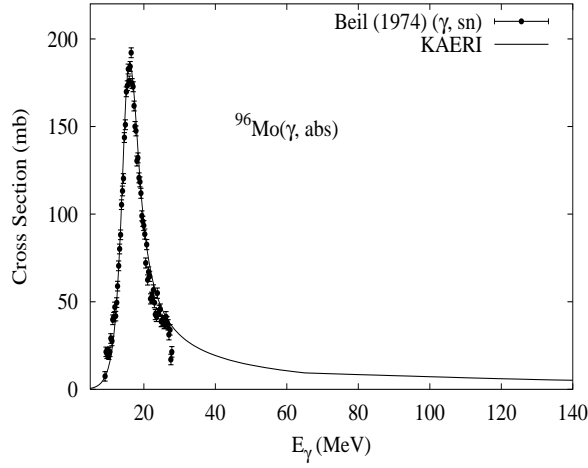
Abundance (%)	Threshold Energies (MeV)								
	$\gamma, n$	$\gamma, p$	$\gamma, t$	$\gamma, \text{He-3}$	$\gamma, \alpha$	$\gamma, 2n$	$\gamma, np$	$\gamma, 2p$	$\gamma, 3n$
15.92	7.37	8.63	16.21	14.18	2.24	17.05	15.86	15.17	25.11



There are no experimental data available. The photoabsorption cross section was obtained from GDR and QD model calculations, adopting the GDR parameters of  ${}^{96}\text{Mo}$ . The neutron, proton, deuteron, triton and alpha emission cross sections, as well as production cross sections, were calculated by the GNASH code.



Abundance (%)	Threshold Energies (MeV)								
	$\gamma, n$	$\gamma, p$	$\gamma, t$	$\gamma, \text{He-3}$	$\gamma, \alpha$	$\gamma, 2n$	$\gamma, np$	$\gamma, 2p$	$\gamma, 3n$
16.68	9.15	9.30	16.53	16.60	2.76	16.52	17.78	16.10	26.20

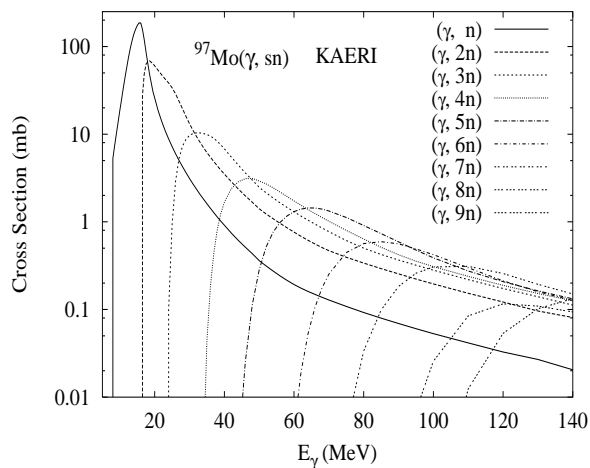
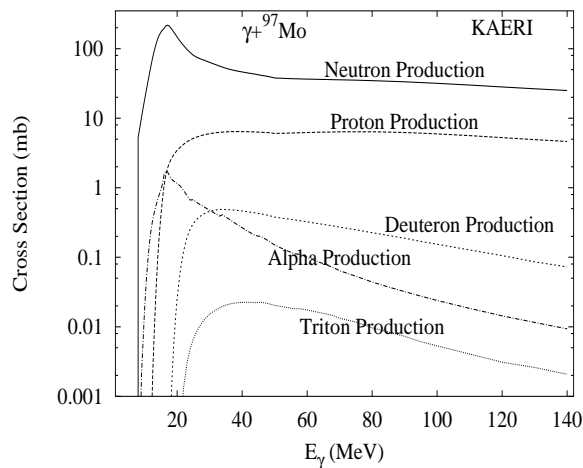
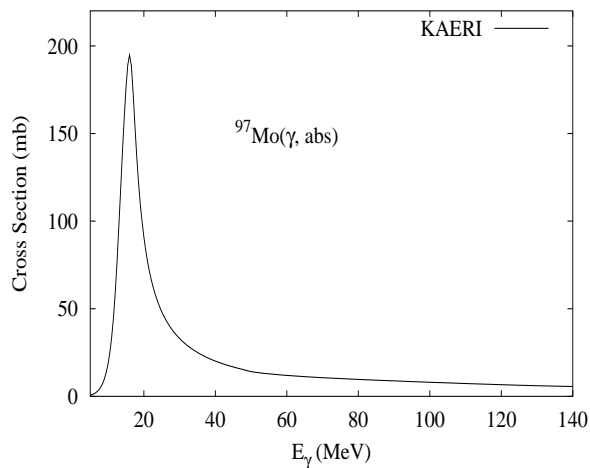


The photoabsorption cross section has not been measured. However, there are experimental data for the  $(\gamma, 1nx)$ ,  $(\gamma, 2nx)$ ,  $(\gamma, sn)$ , and  $(\gamma, xn)$  reaction cross sections [Bei74]. We relied on the GUNF and GNASH codes to infer the photoabsorption cross section in the GDR regime, in order to model accurately the  $(\gamma, sn)$  data. The photoabsorption cross section above the GDR, up to 140 MeV, was obtained from QD model calculations using the theory of Chadwick.

The calculated results of the emission channels by the GNASH code are in good agreement with the experimental data.

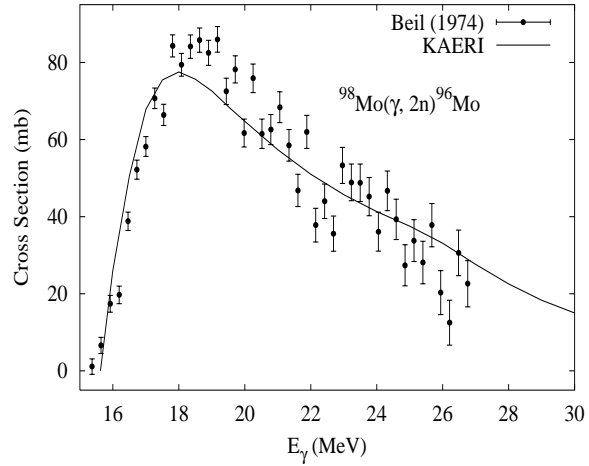
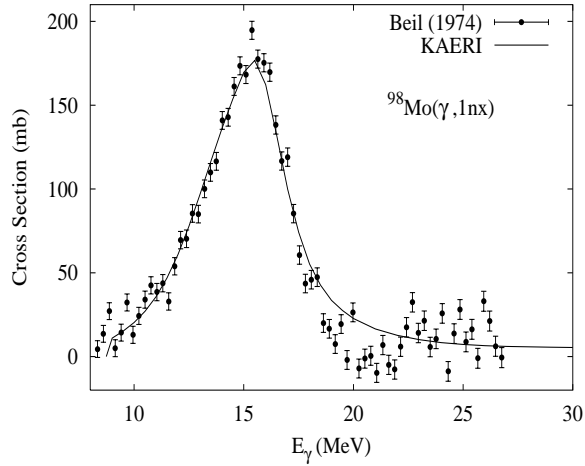
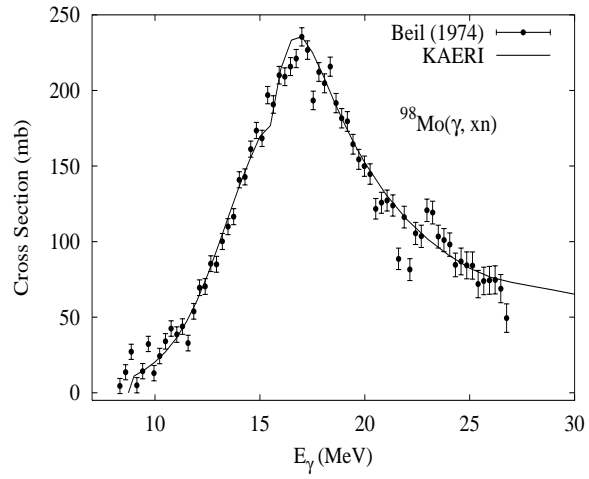
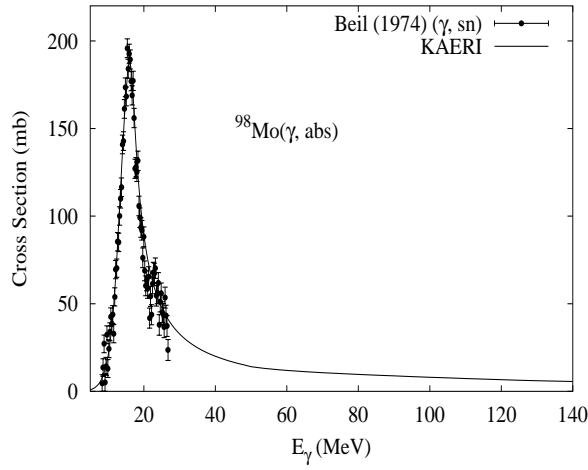
# $\gamma + {}^{97}\text{Mo}$

Abundance (%)	Threshold Energies (MeV)								
	$\gamma, n$	$\gamma, p$	$\gamma, t$	$\gamma, \text{He-3}$	$\gamma, \alpha$	$\gamma, 2n$	$\gamma, np$	$\gamma, 2p$	$\gamma, 3n$
9.55	6.82	9.23	16.12	15.21	2.85	15.98	16.12	16.46	23.34



There are no experimental data available. The photoabsorption cross section was obtained from GDR and QD model calculations, adopting the GDR parameters of  ${}^{98}\text{Mo}$ . The neutron, proton, deuteron, triton and alpha emission cross sections, as well as production cross sections, were calculated by the GNASH code.

Abundance (%)	Threshold Energies (MeV)								
	$\gamma, n$	$\gamma, p$	$\gamma, t$	$\gamma, \text{He-3}$	$\gamma, \alpha$	$\gamma, 2n$	$\gamma, np$	$\gamma, 2p$	$\gamma, 3n$
24.13	8.64	9.79	16.28	17.39	3.27	15.46	17.87	17.25	24.62

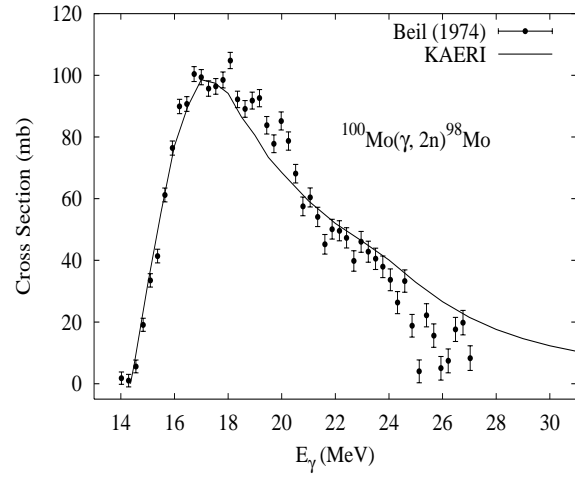
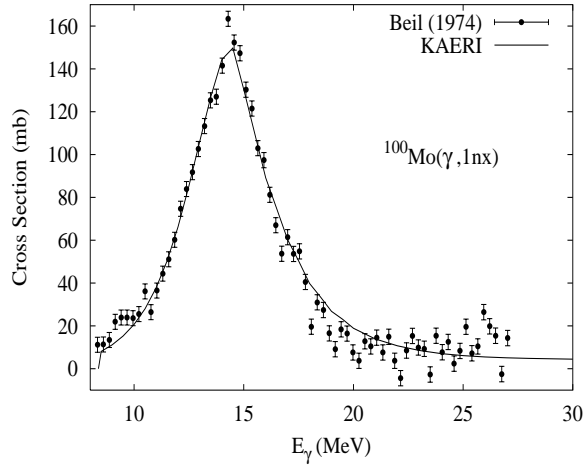
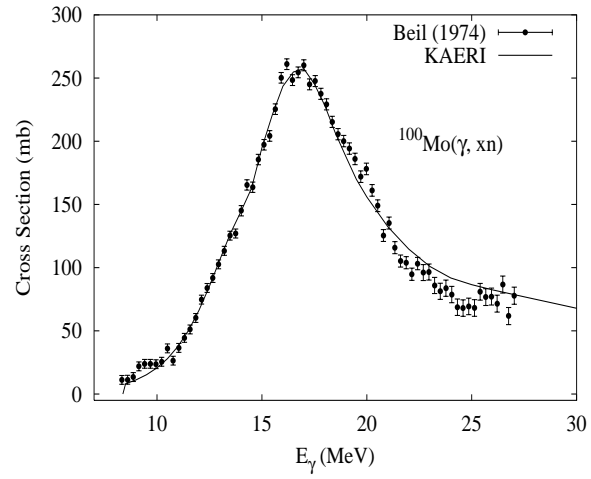
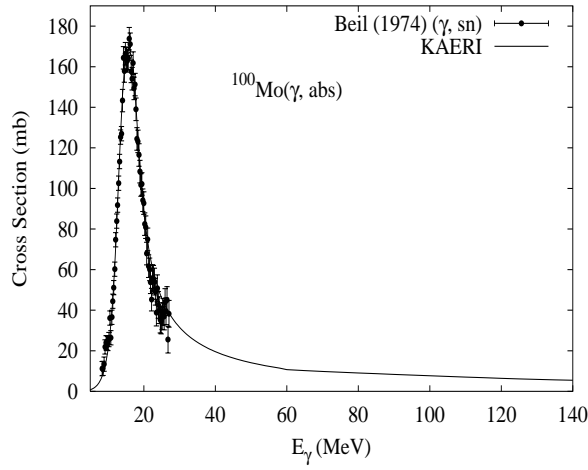


The photoabsorption cross section has not been measured. However, there are experimental data for the  $(\gamma, 1nx)$ ,  $(\gamma, 2nx)$ ,  $(\gamma, 3nx)$ ,  $(\gamma, sn)$ , and  $(\gamma, xn)$  reaction cross sections [Bei74]. We relied on the GUNF and GNASH codes to infer the photoabsorption cross section in the GDR regime, in order to model accurately the  $(\gamma, sn)$  data. The photoabsorption cross section above the GDR, up to 140 MeV, was obtained from QD model calculations using the theory of Chadwick.

The calculated results of the emission channels by the GNASH code are in good agreement with the experimental data.

# $\gamma + {}^{100}\text{Mo}$

Abundance (%)	Threshold Energies (MeV)								
	$\gamma, n$	$\gamma, p$	$\gamma, t$	$\gamma, \text{He-3}$	$\gamma, \alpha$	$\gamma, 2n$	$\gamma, np$	$\gamma, 2p$	$\gamma, 3n$
9.63	8.29	11.15	15.53	18.17	3.17	14.22	18.02	19.48	22.86

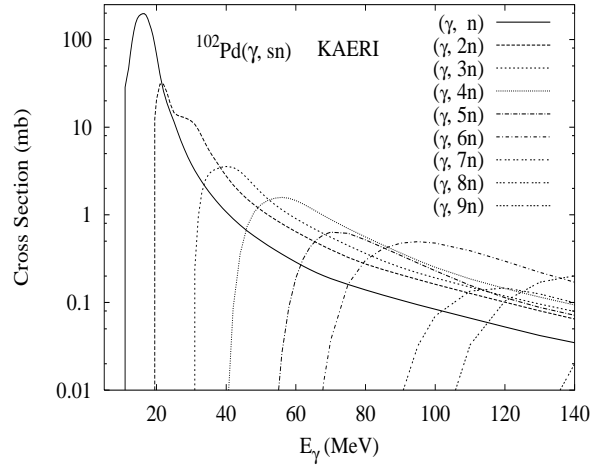
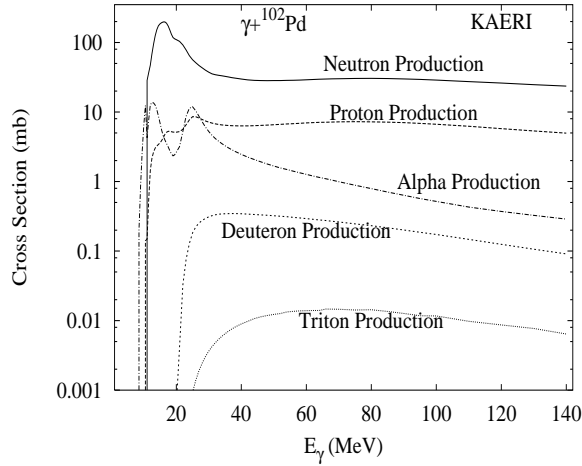
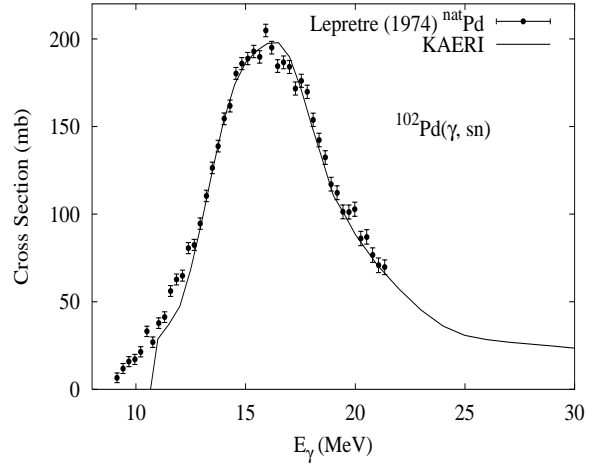
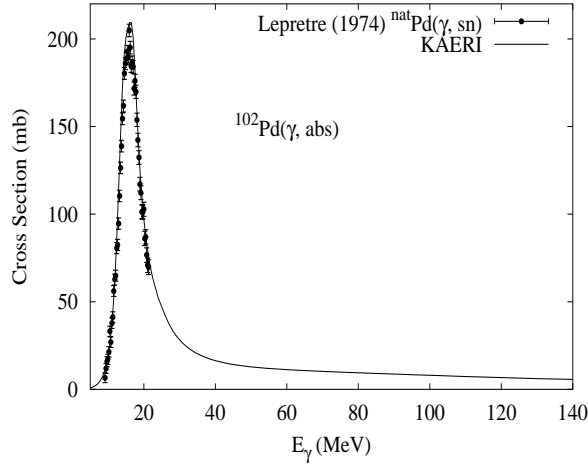


The photoabsorption cross section has not been measured. However, there are experimental data for the  $(\gamma, 1nx)$ ,  $(\gamma, 2nx)$ ,  $(\gamma, 3nx)$ ,  $(\gamma, sn)$ , and  $(\gamma, xn)$  reaction cross sections [Bei74]. We relied on the GUNF and GNASH codes to infer the photoabsorption cross section in the GDR regime, in order to model accurately the  $(\gamma, sn)$  data. The photoabsorption cross section above the GDR, up to 140 MeV, was obtained from QD model calculations using the theory of Chadwick.

The calculated results of the emission channels by the GNASH code are in good agreement with the experimental data.

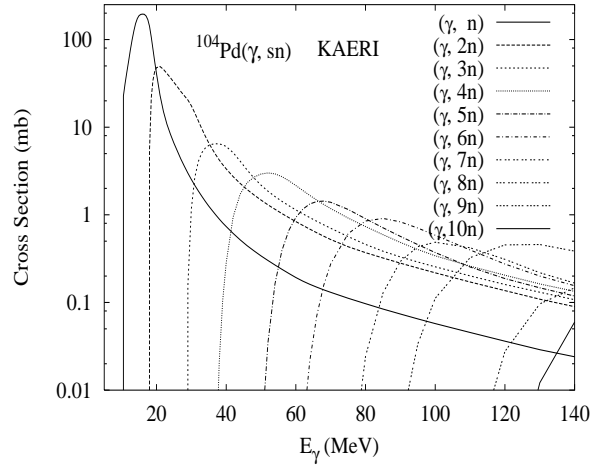
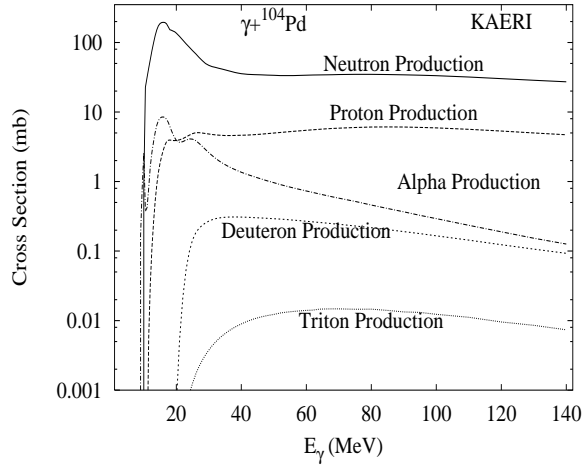
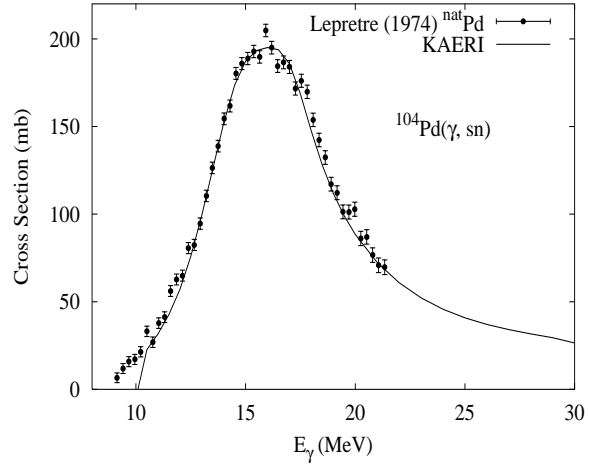
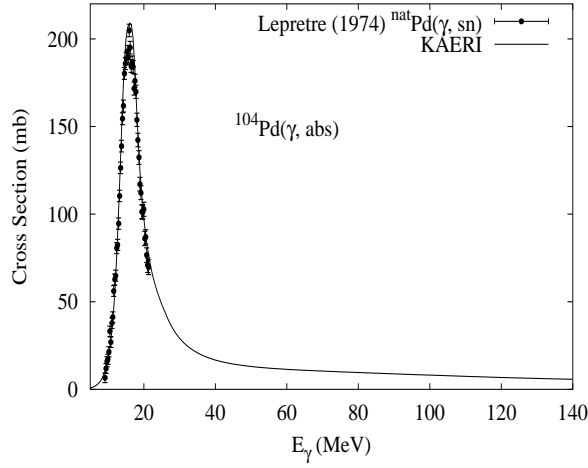
# $\gamma + {}^{102}\text{Pd}$

Abundance (%)	Threshold Energies (MeV)								
	$\gamma, n$	$\gamma, p$	$\gamma, t$	$\gamma, \text{He-3}$	$\gamma, \alpha$	$\gamma, 2n$	$\gamma, np$	$\gamma, 2p$	$\gamma, 3n$
1.02	10.56	7.80	17.35	15.23	2.12	18.84	17.69	13.28	29.94



The photoabsorption cross section has not been measured. However, for  ${}^{nat}\text{Pd}$ , there are experimental data for the  $(\gamma, 1nx)$ ,  $(\gamma, 2nx)$ ,  $(\gamma, sn)$  and  $(\gamma, xn)$  reaction cross sections [Lep74]. We relied on the GUNF and GNASH codes to infer the photoabsorption cross section in the GDR regime, in order to model accurately the  $(\gamma, sn)$  data. The photoabsorption cross section above the GDR, up to 140 MeV, was obtained from QD model calculations using the theory of Chadwick. The neutron, proton, deuteron, triton and alpha emission cross sections, as well as production cross sections, were calculated by the GNASH code.

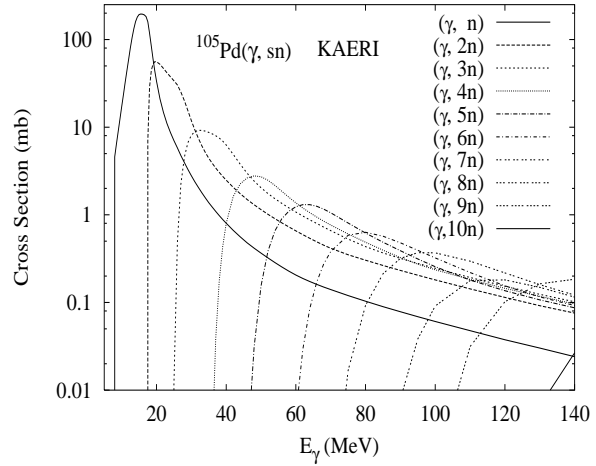
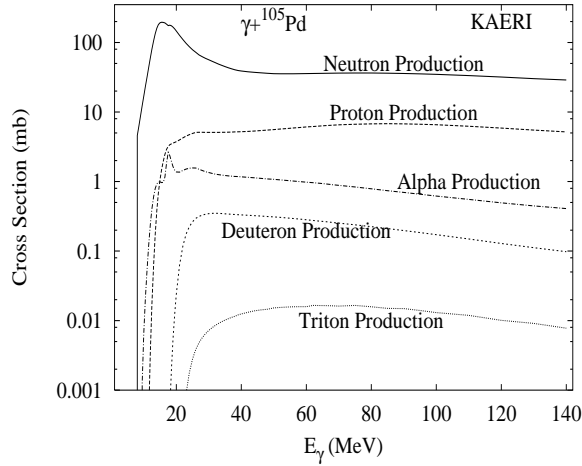
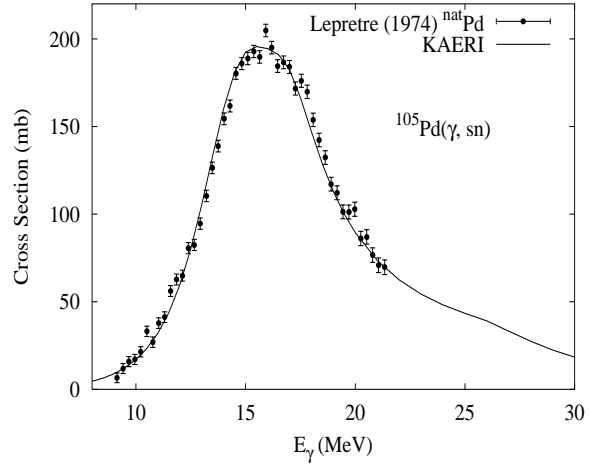
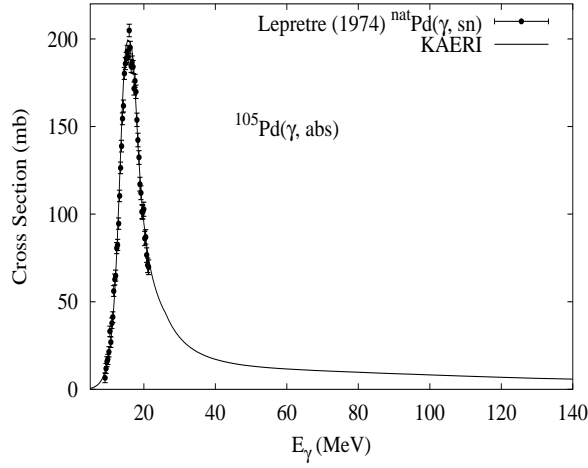
Abundance (%)	Threshold Energies (MeV)								
	$\gamma, n$	$\gamma, p$	$\gamma, t$	$\gamma, \text{He-3}$	$\gamma, \alpha$	$\gamma, 2n$	$\gamma, np$	$\gamma, 2p$	$\gamma, 3n$
11.14	9.99	8.66	16.93	16.37	2.60	17.62	17.93	14.87	28.18



The photoabsorption cross section has not been measured. However, for  ${}^{nat}\text{Pd}$ , there are experimental data for the  $(\gamma, 1nx)$ ,  $(\gamma, 2nx)$ ,  $(\gamma, sn)$  and  $(\gamma, xn)$  reaction cross sections [Lep74]. We relied on the GUNF and GNASH codes to infer the photoabsorption cross section in the GDR regime, in order to model accurately the  $(\gamma, sn)$  data. The photoabsorption cross section above the GDR, up to 140 MeV, was obtained from QD model calculations using the theory of Chadwick. The neutron, proton, deuteron, triton and alpha emission cross sections, as well as production cross sections, were calculated by the GNASH code.

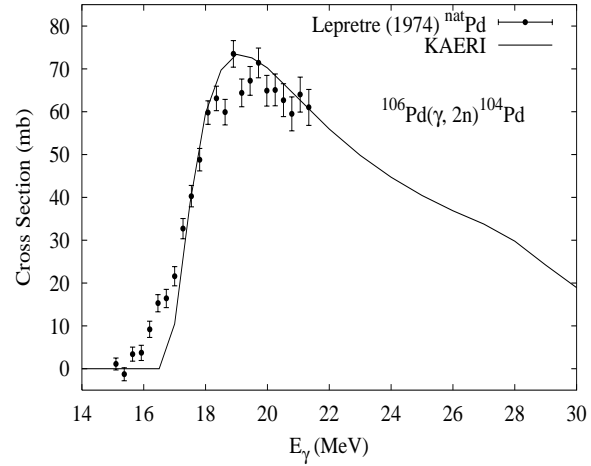
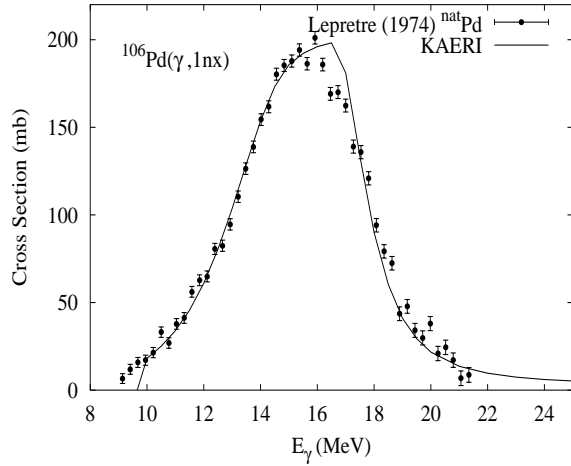
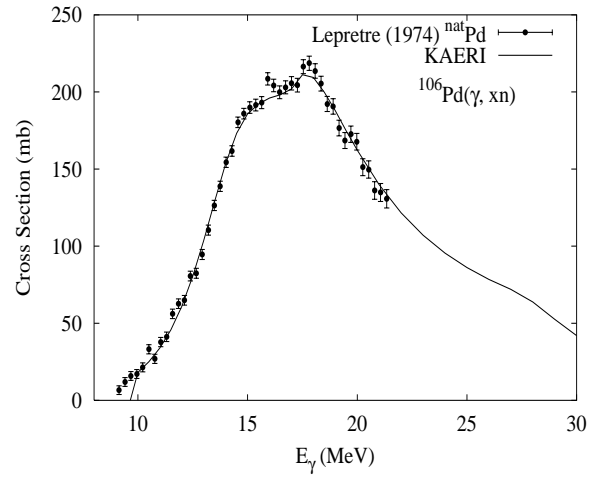
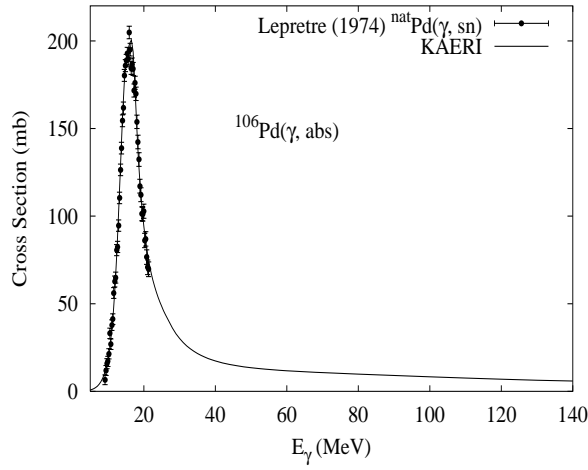
# $\gamma + {}^{105}\text{Pd}$

Abundance (%)	Threshold Energies (MeV)								
	$\gamma, n$	$\gamma, p$	$\gamma, t$	$\gamma, \text{He-3}$	$\gamma, \alpha$	$\gamma, 2n$	$\gamma, np$	$\gamma, 2p$	$\gamma, 3n$
22.33	7.09	8.75	16.54	14.25	2.89	17.09	15.75	15.73	24.71



The photoabsorption cross section has not been measured. However, for  ${}^{nat}\text{Pd}$ , there are experimental data for the  $(\gamma, 1nx)$ ,  $(\gamma, 2nx)$ ,  $(\gamma, sn)$  and  $(\gamma, xn)$  reaction cross sections [Lep74]. We relied on the GUNF and GNASH codes to infer the photoabsorption cross section in the GDR regime, in order to model accurately the  $(\gamma, sn)$  data. The photoabsorption cross section above the GDR, up to 140 MeV, was obtained from QD model calculations using the theory of Chadwick. The neutron, proton, deuteron, triton and alpha emission cross sections, as well as production cross sections, were calculated by the GNASH code.

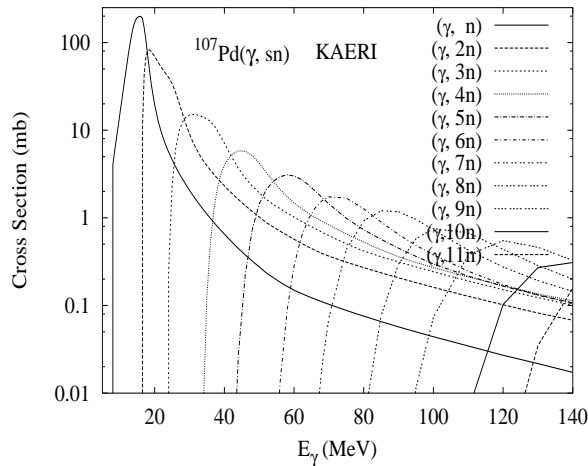
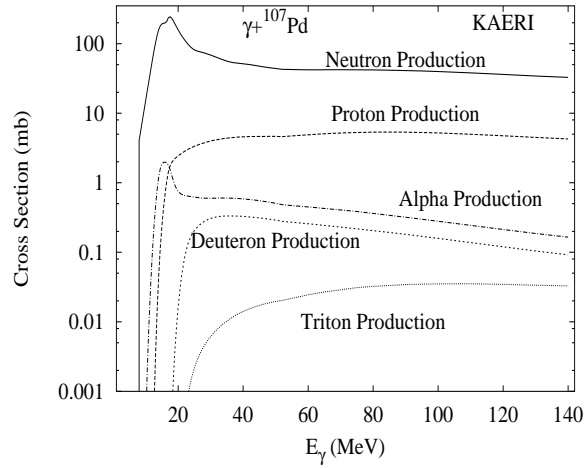
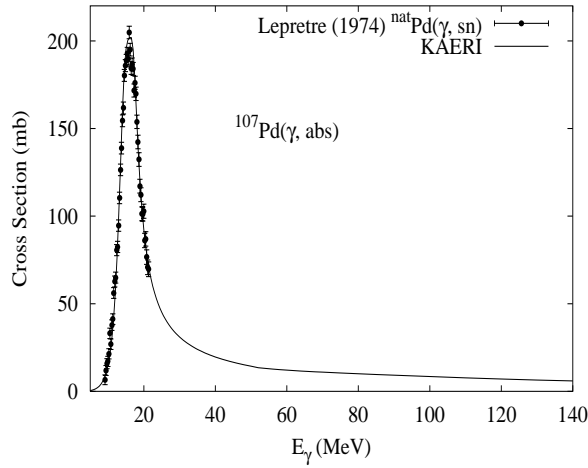
Abundance (%)	Threshold Energies (MeV)								
	$\gamma, n$	$\gamma, p$	$\gamma, t$	$\gamma, \text{He-3}$	$\gamma, \alpha$	$\gamma, 2n$	$\gamma, np$	$\gamma, 2p$	$\gamma, 3n$
27.33	9.56	9.35	16.83	17.58	3.23	16.66	18.32	16.39	26.65



The photoabsorption cross section has not been measured. However, for  ${}^{nat}\text{Pd}$ , there are experimental data for the  $(\gamma, 1nx)$ ,  $(\gamma, 2nx)$ ,  $(\gamma, sn)$  and  $(\gamma, xn)$  reaction cross sections [Lep74]. We relied on the GUNF and GNASH codes to infer the photoabsorption cross section in the GDR regime, in order to model accurately the  $(\gamma, sn)$  data. The photoabsorption cross section above the GDR, up to 140 MeV, was obtained from QD model calculations using the theory of Chadwick. The neutron, proton, deuteron, triton and alpha emission cross sections, as well as production cross sections, were calculated by the GNASH code.

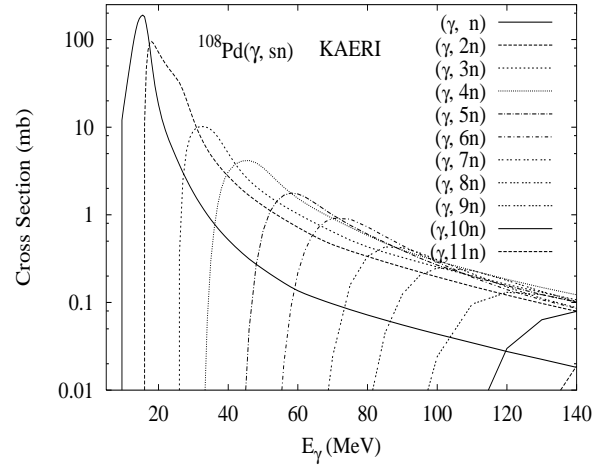
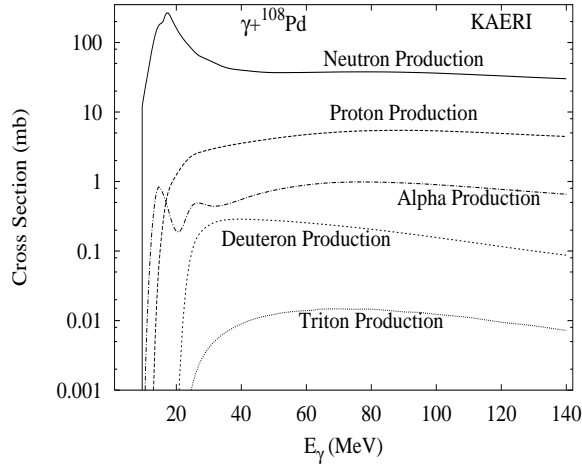
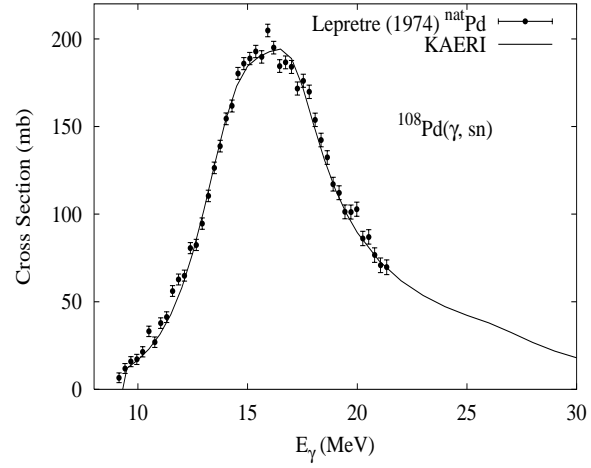
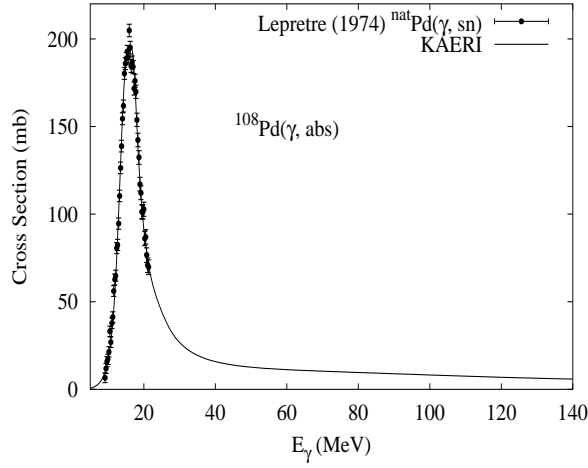


Abundance (%)	Threshold Energies (MeV)								
	$\gamma, n$	$\gamma, p$	$\gamma, t$	$\gamma, \text{He-3}$	$\gamma, \alpha$	$\gamma, 2n$	$\gamma, np$	$\gamma, 2p$	$\gamma, 3n$
0.00	6.54	9.30	16.37	15.21	3.54	16.10	15.89	17.02	23.20



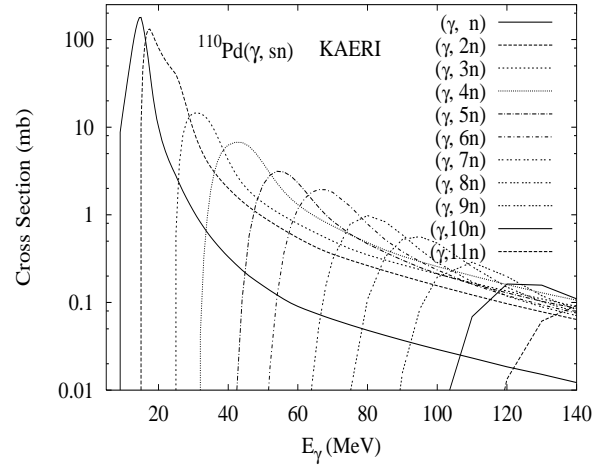
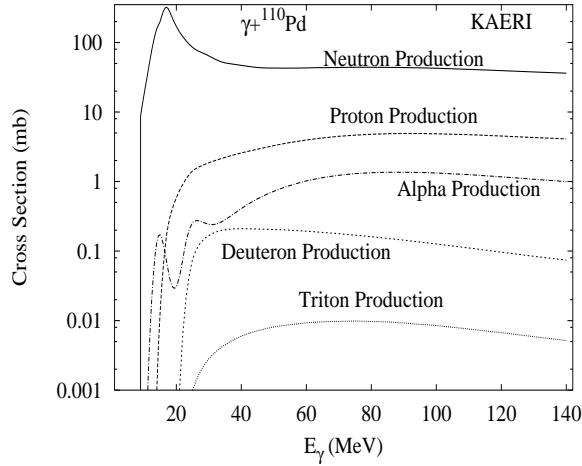
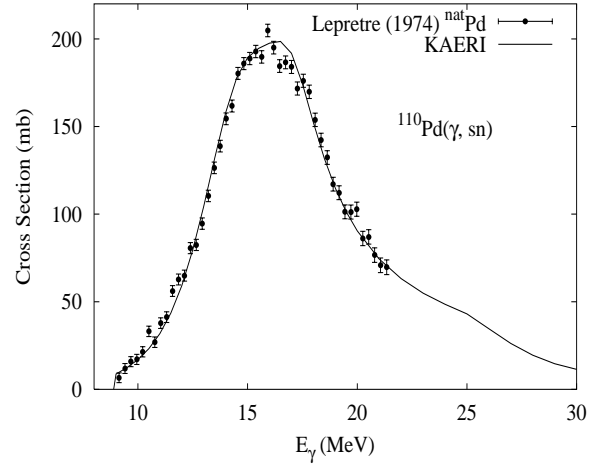
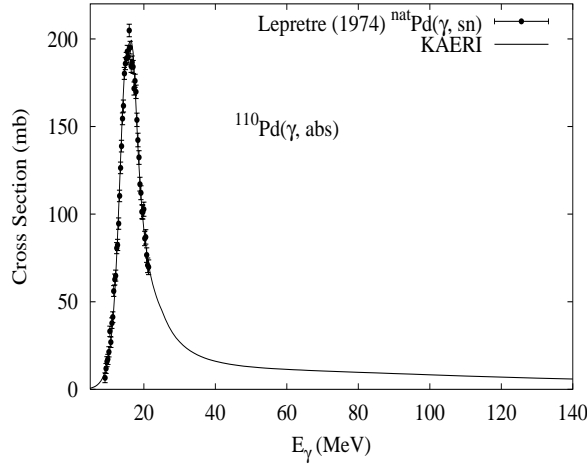
The photoabsorption cross section has not been measured. However, for  ${}^{nat}\text{Pd}$ , there are experimental data for the  $(\gamma, 1nx)$ ,  $(\gamma, 2nx)$ ,  $(\gamma, sn)$  and  $(\gamma, xn)$  reaction cross sections [Lep74]. We relied on the GUNF and GNASH codes to infer the photoabsorption cross section in the GDR regime, in order to model accurately the  $(\gamma, sn)$  data. The photoabsorption cross section above the GDR, up to 140 MeV, was obtained from QD model calculations using the theory of Chadwick. The neutron, proton, deuteron, triton and alpha emission cross sections, as well as production cross sections, were calculated by the GNASH code.

Abundance (%)	Threshold Energies (MeV)								
	$\gamma, n$	$\gamma, p$	$\gamma, t$	$\gamma, \text{He-3}$	$\gamma, \alpha$	$\gamma, 2n$	$\gamma, np$	$\gamma, 2p$	$\gamma, 3n$
26.46	9.22	9.95	16.62	18.52	3.85	15.76	18.52	17.78	25.32



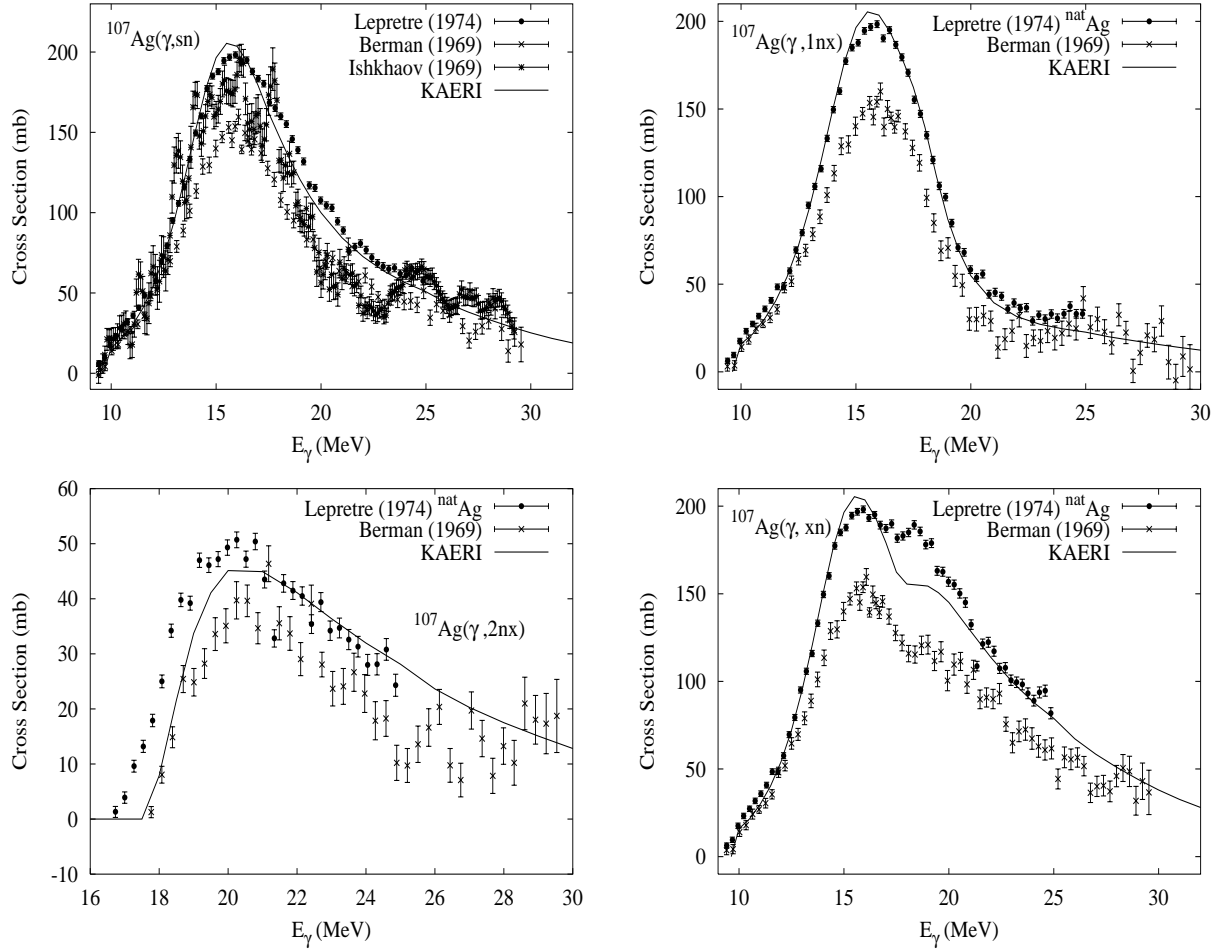
The photoabsorption cross section has not been measured. However, for  ${}^{nat}\text{Pd}$ , there are experimental data for the  $(\gamma, 1nx)$ ,  $(\gamma, 2nx)$ ,  $(\gamma, sn)$  and  $(\gamma, xn)$  reaction cross sections [Lep74]. We relied on the GUNF and GNASH codes to infer the photoabsorption cross section in the GDR regime, in order to model accurately the  $(\gamma, sn)$  data. The photoabsorption cross section above the GDR, up to 140 MeV, was obtained from QD model calculations using the theory of Chadwick. The neutron, proton, deuteron, triton and alpha emission cross sections, as well as production cross sections, were calculated by the GNASH code.

Abundance (%)	Threshold Energies (MeV)								
	$\gamma, n$	$\gamma, p$	$\gamma, t$	$\gamma, \text{He-3}$	$\gamma, \alpha$	$\gamma, 2n$	$\gamma, np$	$\gamma, 2p$	$\gamma, 3n$
11.72	8.81	10.61	16.43	19.57	4.44	14.96	18.63	19.16	24.19



The photoabsorption cross section has not been measured. However, for  ${}^{nat}\text{Pd}$ , there are experimental data for the  $(\gamma, 1nx)$ ,  $(\gamma, 2nx)$ ,  $(\gamma, sn)$  and  $(\gamma, xn)$  reaction cross sections [Lep74]. We relied on the GUNF and GNASH codes to infer the photoabsorption cross section in the GDR regime, in order to model accurately the  $(\gamma, sn)$  data. The photoabsorption cross section above the GDR, up to 140 MeV, was obtained from QD model calculations using the theory of Chadwick. The neutron, proton, deuteron, triton and alpha emission cross sections, as well as production cross sections, were calculated by the GNASH code.

Abundance (%)	Threshold Energies (MeV)								
	$\gamma, n$	$\gamma, p$	$\gamma, t$	$\gamma, \text{He-3}$	$\gamma, \alpha$	$\gamma, 2n$	$\gamma, np$	$\gamma, 2p$	$\gamma, 3n$
51.84	9.54	5.79	13.96	16.39	2.81	17.47	15.35	15.14	27.51

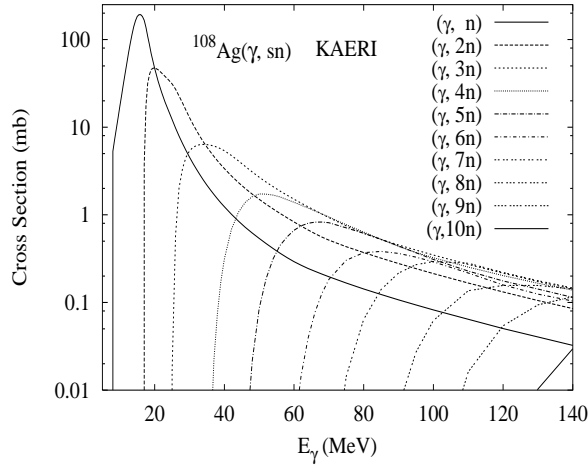
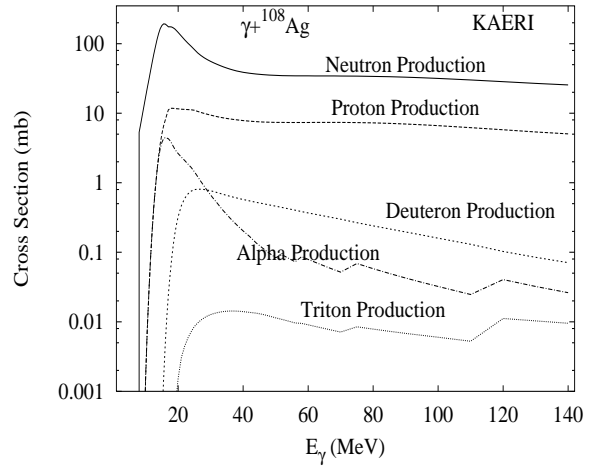
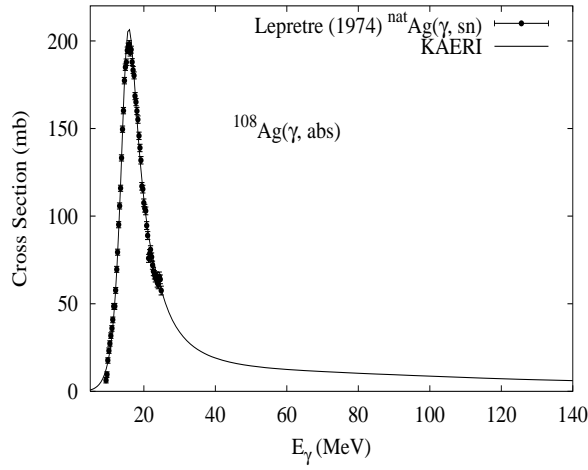


The photoabsorption cross section has not been measured. However, there are experimental data for the  $(\gamma, 1\text{nx})$ ,  $(\gamma, 2\text{nx})$ ,  $(\gamma, \text{sn})$ , and  $(\gamma, \text{xn})$  reaction cross sections from [Ber69b], and for the  $(\gamma, \text{sn})$  from [Ish69]. Experimental data for  ${}^{nat}\text{Ag}$  were reported for the  $(\gamma, 1\text{nx})$ ,  $(\gamma, 2\text{nx})$ ,  $(\gamma, \text{sn})$  and  $(\gamma, \text{xn})$  cross sections [Lep74]. Ishkhanov's and Lepretre's data agree fairly well in magnitude. By comparing those with that of neighboring nuclei such as Pd and Cd, the results of Lepretre were selected as reference. We relied on the GUNF and GNASH codes to infer the photoabsorption cross section in the GDR regime, in order to model accurately Lepretre's  $(\gamma, \text{sn})$  data. The photoabsorption cross section above the GDR, up to 140 MeV, was obtained from QD model calculations using the theory of Chadwick.

The calculated results of the emission channels by the GNASH code are in good agreement with all the experimental data of Lepretre.

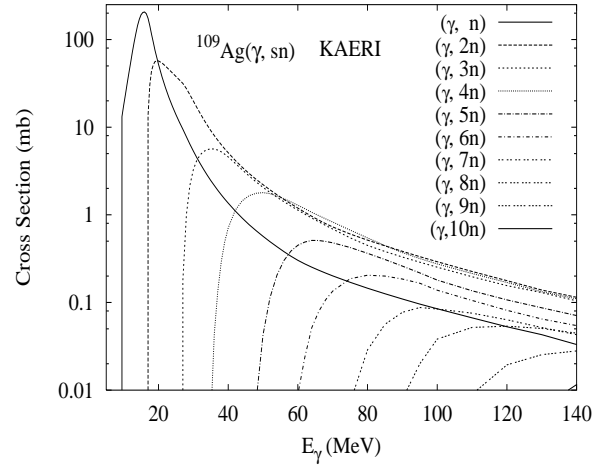
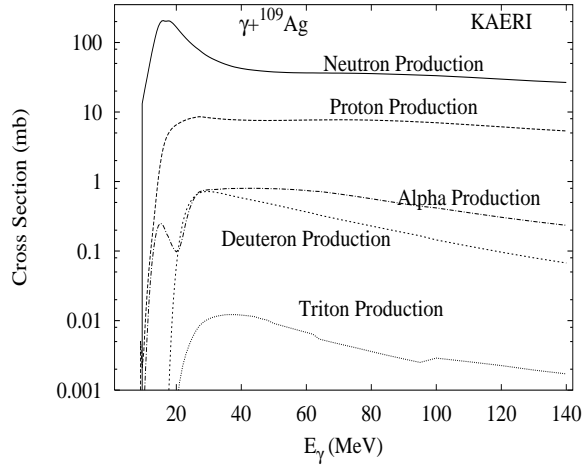
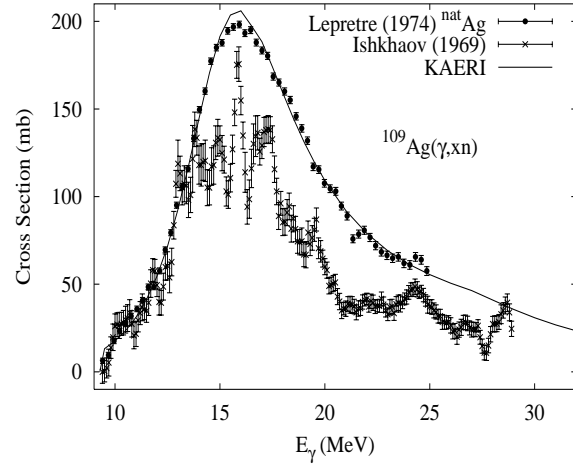
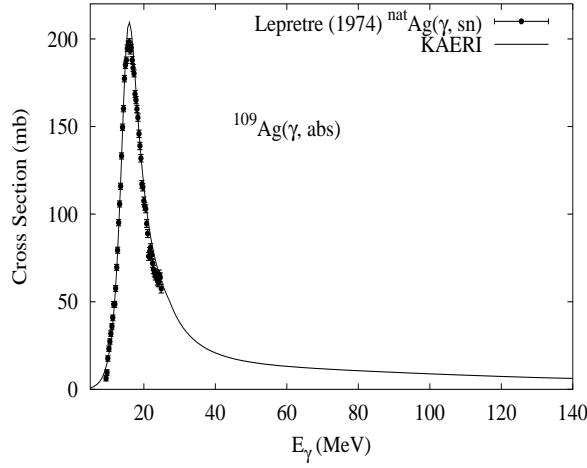
# $\gamma + {}^{108}\text{Ag}$

Abundance (%)	Threshold Energies (MeV)								
	$\gamma, n$	$\gamma, p$	$\gamma, t$	$\gamma, \text{He-3}$	$\gamma, \alpha$	$\gamma, 2n$	$\gamma, np$	$\gamma, 2p$	$\gamma, 3n$
0.00	7.27	6.52	14.14	14.69	3.08	16.81	13.06	15.82	24.74



The photoabsorption cross section has not been measured. However, there are experimental data, for  ${}^{nat}\text{Ag}$ , for the  $(\gamma, 1nx)$ ,  $(\gamma, 2nx)$ ,  $(\gamma, sn)$ , and  $(\gamma, xn)$  reaction cross sections [Lep74]. The photoabsorption cross section was obtained from GDR and QD model calculations, adopting the GDR parameters of  ${}^{109}\text{Ag}$ . The neutron, proton, deuteron, triton and alpha emission cross sections, as well as production cross sections, were calculated by the GNASH code.

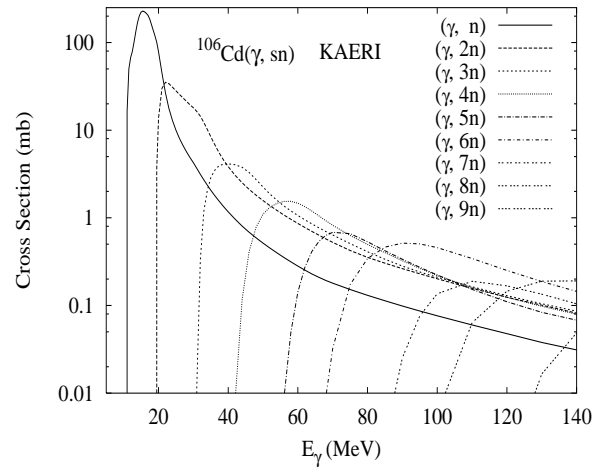
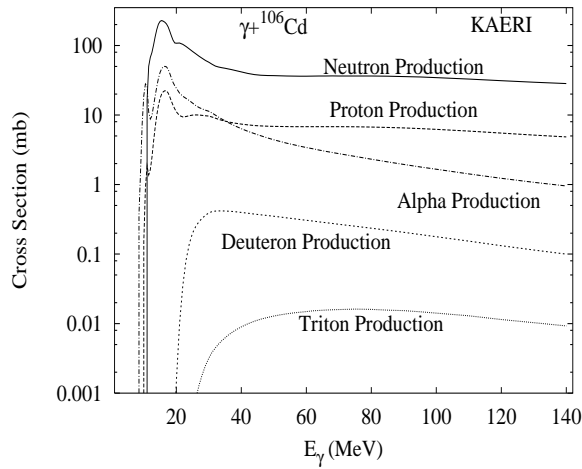
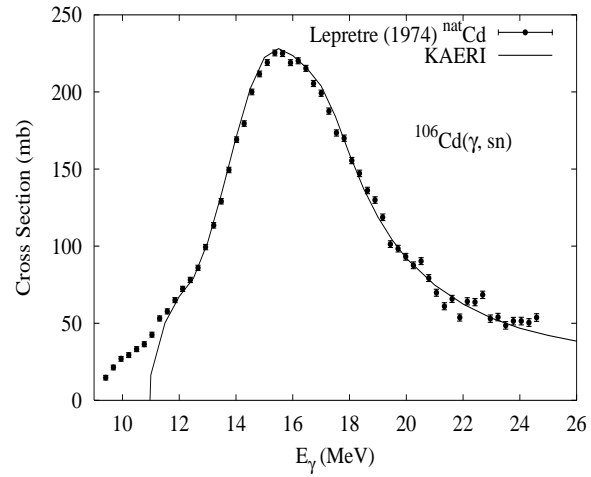
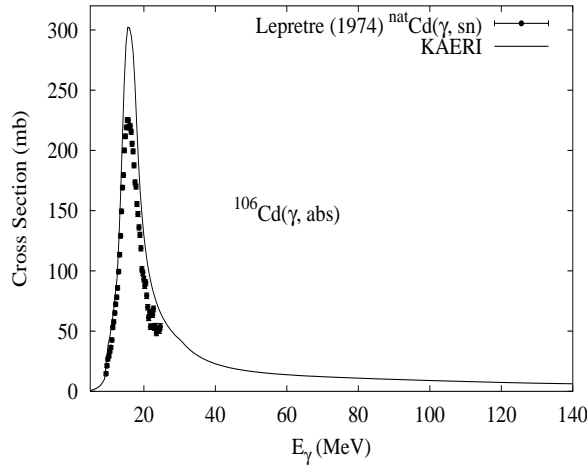
Abundance (%)	Threshold Energies (MeV)								
	$\gamma, n$	$\gamma, p$	$\gamma, t$	$\gamma, \text{He-3}$	$\gamma, \alpha$	$\gamma, 2n$	$\gamma, np$	$\gamma, 2p$	$\gamma, 3n$
48.16	9.19	6.49	13.76	17.29	3.30	16.46	15.71	16.44	25.99



The photoabsorption cross section has not been measured. However, there are experimental data, for  ${}^{nat}\text{Ag}$ , for the  $(\gamma, 1nx)$ ,  $(\gamma, 2nx)$ ,  $(\gamma, sn)$ , and  $(\gamma, xn)$  reaction cross sections [Lep74], which were used as reference. We relied on the GUNF and GNASH codes to infer the photoabsorption cross section in the GDR regime, in order to model accurately Lepretre's  $(\gamma, sn)$  data. The photoabsorption cross section above the GDR, up to 140 MeV, was obtained from QD model calculations using the theory of Chadwick.

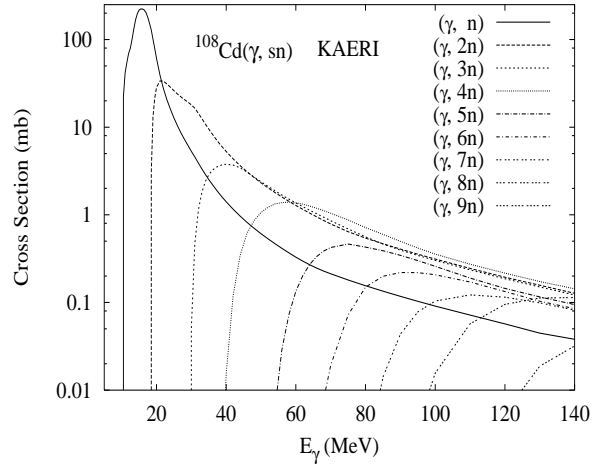
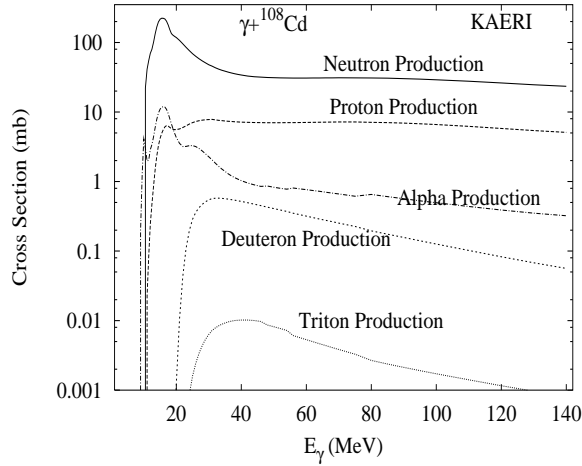
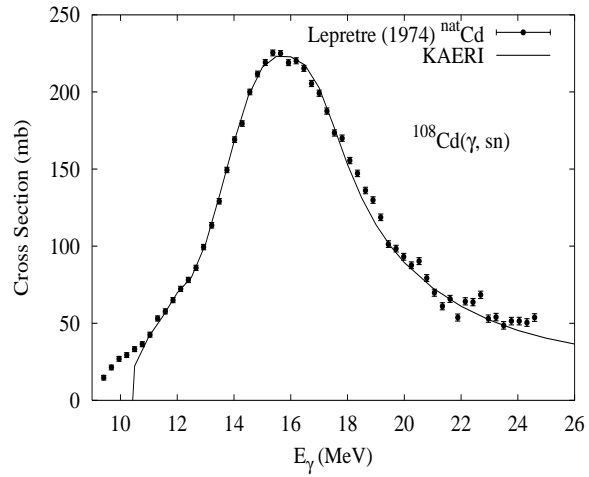
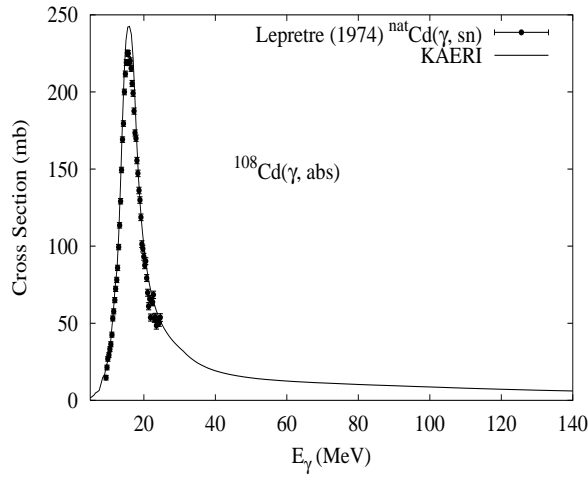
The calculated results of the emission channels by the GNASH code are in good agreement with all the experimental data of Lepretre.

Abundance (%)	Threshold Energies (MeV)								
	$\gamma, n$	$\gamma, p$	$\gamma, t$	$\gamma, \text{He-3}$	$\gamma, \alpha$	$\gamma, 2n$	$\gamma, np$	$\gamma, 2p$	$\gamma, 3n$
1.25	10.87	7.35	17.30	14.60	1.64	19.30	17.38	12.32	30.70



The photoabsorption cross section has not been measured. However, for  ${}^{nat}\text{Cd}$ , there are experimental data for the  $(\gamma, 1nx)$ ,  $(\gamma, 2nx)$ ,  $(\gamma, sn)$  and  $(\gamma, xn)$  reaction cross sections [Lep74]. We relied on the GUNF and GNASH codes to infer the photoabsorption cross section in the GDR regime, in order to model accurately the  $(\gamma, sn)$  data. The photoabsorption cross section above the GDR, up to 140 MeV, was obtained from QD model calculations using the theory of Chadwick. The neutron, proton, deuteron, triton and alpha emission cross sections, as well as production cross sections, were calculated by the GNASH code.

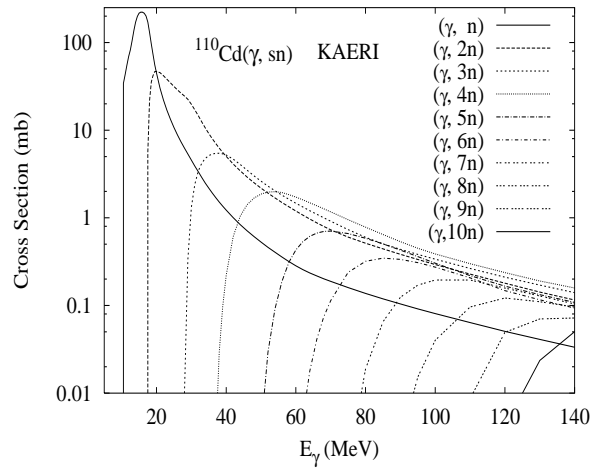
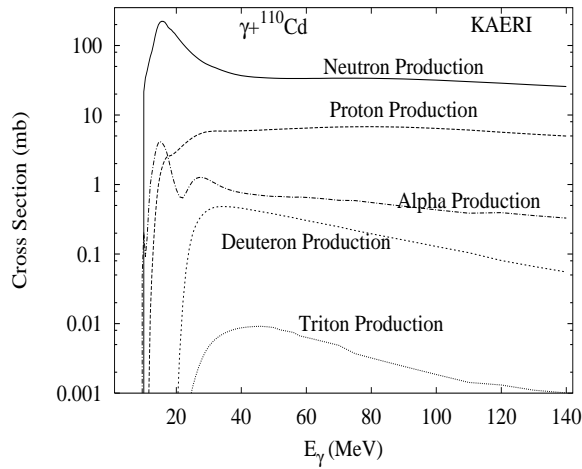
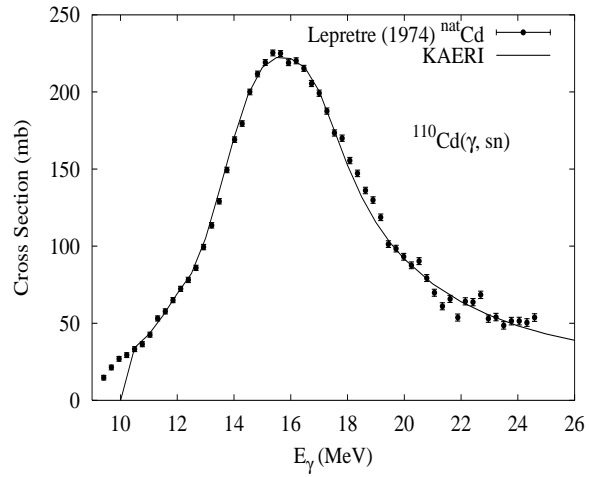
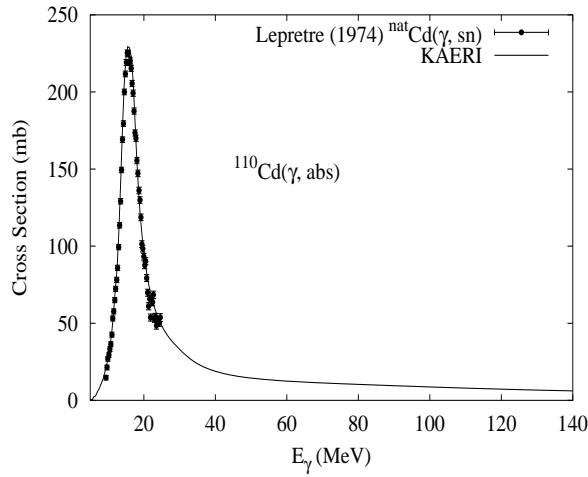
Abundance (%)	Threshold Energies (MeV)								
	$\gamma, n$	$\gamma, p$	$\gamma, t$	$\gamma, \text{He-3}$	$\gamma, \alpha$	$\gamma, 2n$	$\gamma, np$	$\gamma, 2p$	$\gamma, 3n$
0.89	10.33	8.14	17.12	15.77	2.28	18.26	17.67	13.92	29.13



The photoabsorption cross section has not been measured. However, for  ${}^{nat}\text{Cd}$ , there are experimental data for the  $(\gamma, 1nx)$ ,  $(\gamma, 2nx)$ ,  $(\gamma, sn)$  and  $(\gamma, xn)$  reaction cross sections [Lep74]. We relied on the GUNF and GNASH codes to infer the photoabsorption cross section in the GDR regime, in order to model accurately the  $(\gamma, sn)$  data. The photoabsorption cross section above the GDR, up to 140 MeV, was obtained from QD model calculations using the theory of Chadwick. The neutron, proton, deuteron, triton and alpha emission cross sections, as well as production cross sections, were calculated by the GNASH code.

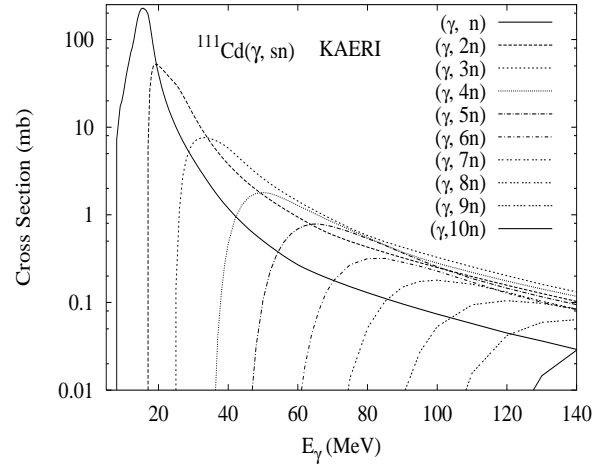
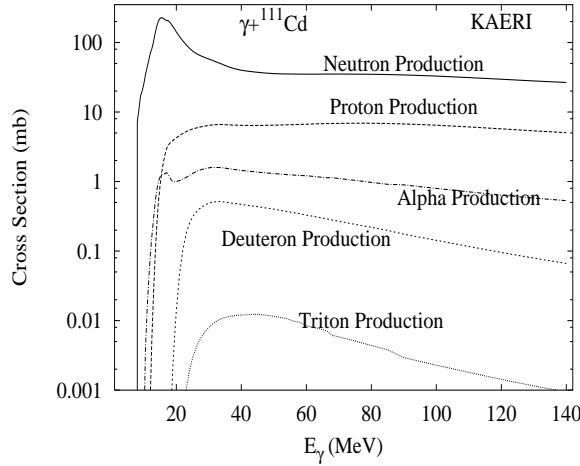
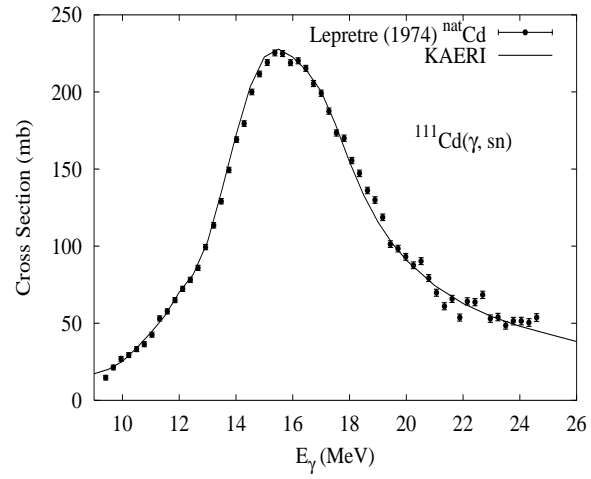
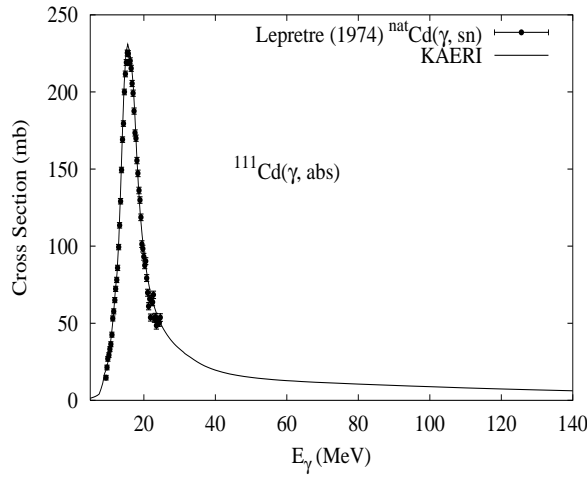


Abundance (%)	Threshold Energies (MeV)								
	$\gamma, n$	$\gamma, p$	$\gamma, t$	$\gamma, \text{He-3}$	$\gamma, \alpha$	$\gamma, 2n$	$\gamma, np$	$\gamma, 2p$	$\gamma, 3n$
12.49	9.92	8.92	16.89	16.91	2.87	17.24	18.11	15.41	27.58



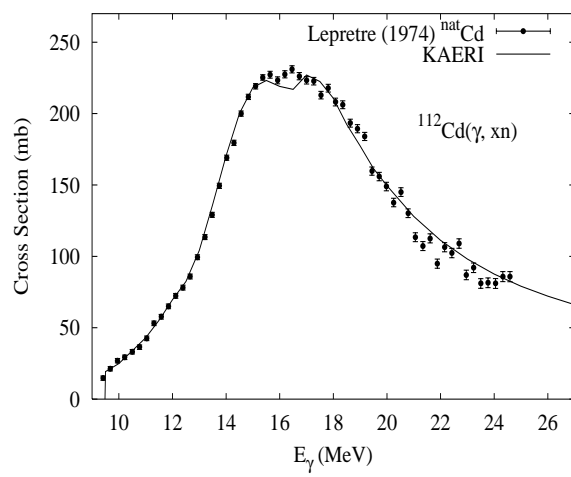
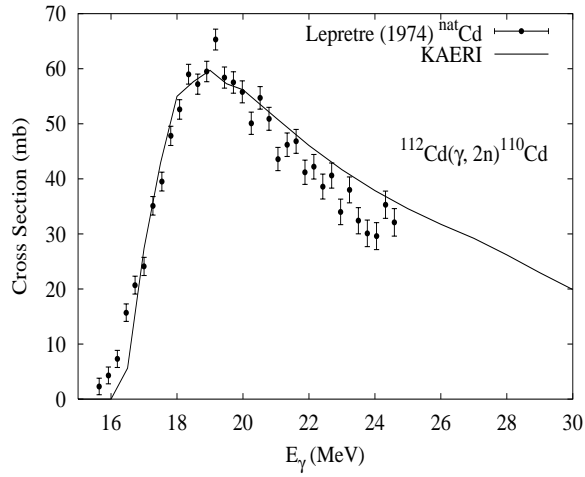
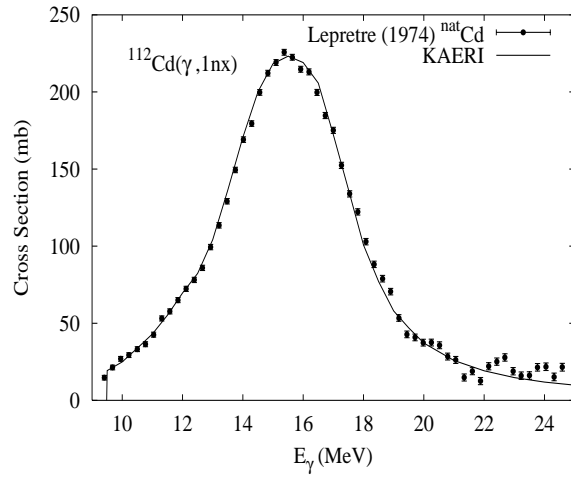
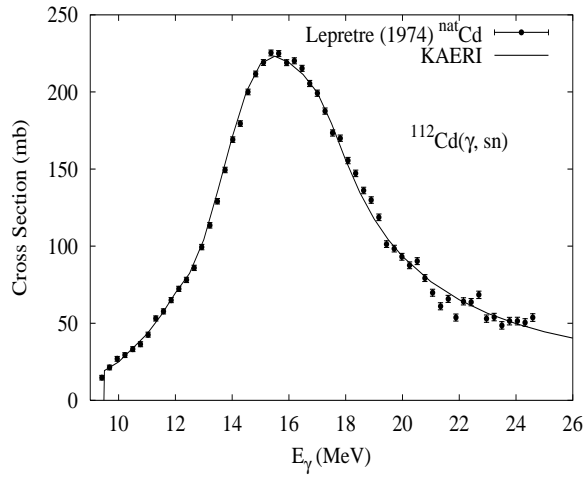
The photoabsorption cross section has not been measured. However, for  ${}^{nat}\text{Cd}$ , there are experimental data for the  $(\gamma, 1nx)$ ,  $(\gamma, 2nx)$ ,  $(\gamma, sn)$  and  $(\gamma, xn)$  reaction cross sections [Lep74]. We relied on the GUNF and GNASH codes to infer the photoabsorption cross section in the GDR regime, in order to model accurately the  $(\gamma, sn)$  data. The photoabsorption cross section above the GDR, up to 140 MeV, was obtained from QD model calculations using the theory of Chadwick. The neutron, proton, deuteron, triton and alpha emission cross sections, as well as production cross sections, were calculated by the GNASH code.

Abundance (%)	Threshold Energies (MeV)								
	$\gamma, n$	$\gamma, p$	$\gamma, t$	$\gamma, \text{He-3}$	$\gamma, \alpha$	$\gamma, 2n$	$\gamma, np$	$\gamma, 2p$	$\gamma, 3n$
12.80	6.97	9.08	16.60	14.66	3.30	16.89	15.89	16.23	24.22



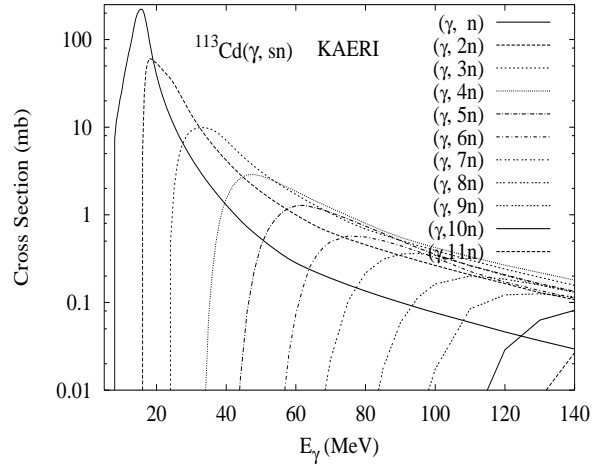
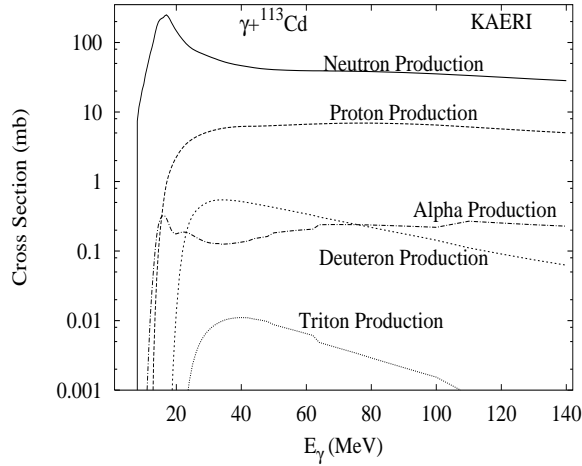
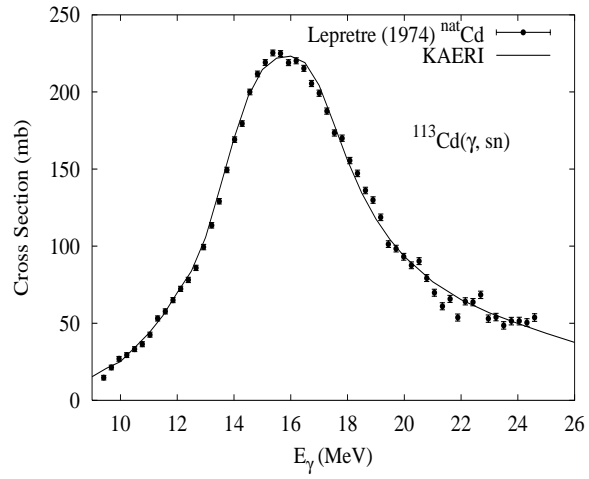
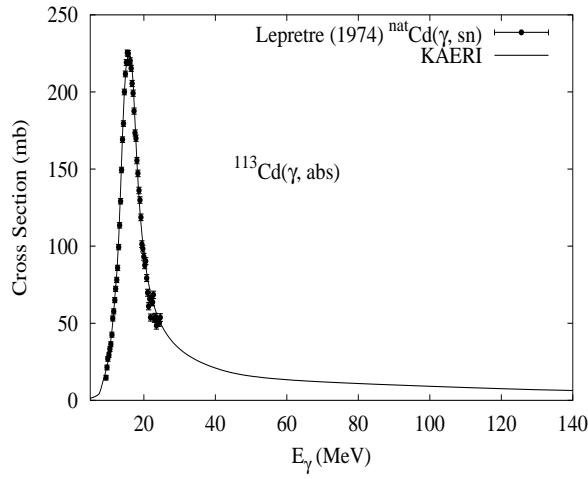
The photoabsorption cross section has not been measured. However, for  ${}^{nat}\text{Cd}$ , there are experimental data for the  $(\gamma, 1nx)$ ,  $(\gamma, 2nx)$ ,  $(\gamma, sn)$  and  $(\gamma, xn)$  reaction cross sections [Lep74]. We relied on the GUNF and GNASH codes to infer the photoabsorption cross section in the GDR regime, in order to model accurately the  $(\gamma, sn)$  data. The photoabsorption cross section above the GDR, up to 140 MeV, was obtained from QD model calculations using the theory of Chadwick. The neutron, proton, deuteron, triton and alpha emission cross sections, as well as production cross sections, were calculated by the GNASH code.

Abundance (%)	Threshold Energies (MeV)								
	$\gamma, n$	$\gamma, p$	$\gamma, t$	$\gamma, \text{He-3}$	$\gamma, \alpha$	$\gamma, 2n$	$\gamma, np$	$\gamma, 2p$	$\gamma, 3n$
24.13	9.40	9.65	16.81	17.91	3.48	16.37	18.48	16.81	26.29



The photoabsorption cross section has not been measured. However, for  ${}^{nat}\text{Cd}$ , there are experimental data for the  $(\gamma, 1nx)$ ,  $(\gamma, 2nx)$ ,  $(\gamma, sn)$  and  $(\gamma, xn)$  reaction cross sections [Lep74]. We relied on the GUNF and GNASH codes to infer the photoabsorption cross section in the GDR regime, in order to model accurately the  $(\gamma, sn)$  data. The photoabsorption cross section above the GDR, up to 140 MeV, was obtained from QD model calculations using the theory of Chadwick. The neutron, proton, deuteron, triton and alpha emission cross sections, as well as production cross sections, were calculated by the GNASH code.

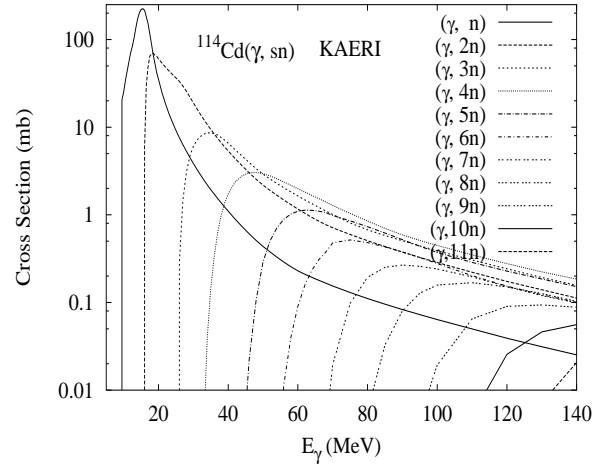
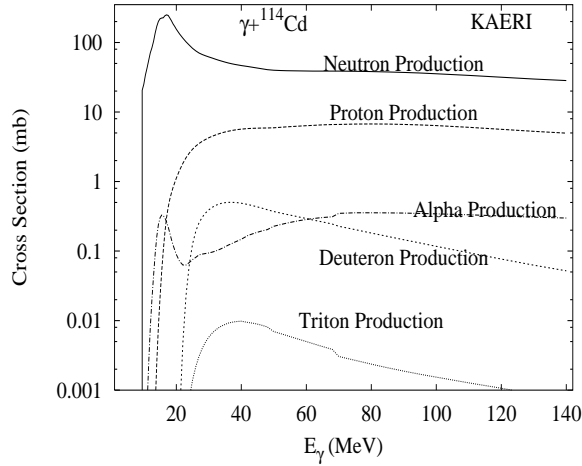
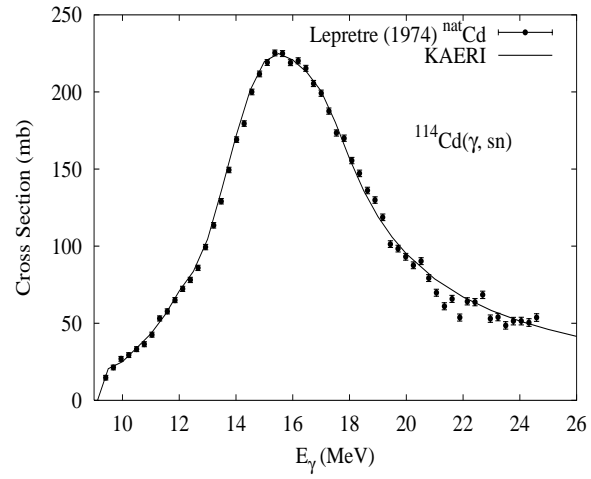
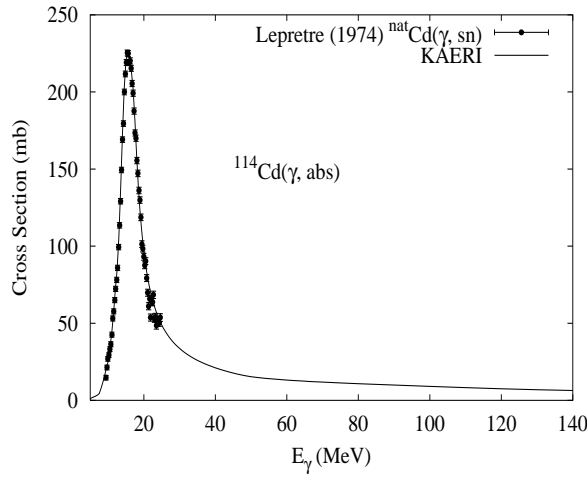
Abundance (%)	Threshold Energies (MeV)								
	$\gamma, n$	$\gamma, p$	$\gamma, t$	$\gamma, \text{He-3}$	$\gamma, \alpha$	$\gamma, 2n$	$\gamma, np$	$\gamma, 2p$	$\gamma, 3n$
12.22	6.54	9.72	16.54	15.64	3.87	15.94	16.19	17.60	22.91



The photoabsorption cross section has not been measured. However, for  ${}^{nat}\text{Cd}$ , there are experimental data for the  $(\gamma, 1nx)$ ,  $(\gamma, 2nx)$ ,  $(\gamma, sn)$  and  $(\gamma, xn)$  reaction cross sections [Lep74]. We relied on the GUNF and GNASH codes to infer the photoabsorption cross section in the GDR regime, in order to model accurately the  $(\gamma, sn)$  data. The photoabsorption cross section above the GDR, up to 140 MeV, was obtained from QD model calculations using the theory of Chadwick. The neutron, proton, deuteron, triton and alpha emission cross sections, as well as production cross sections, were calculated by the GNASH code.

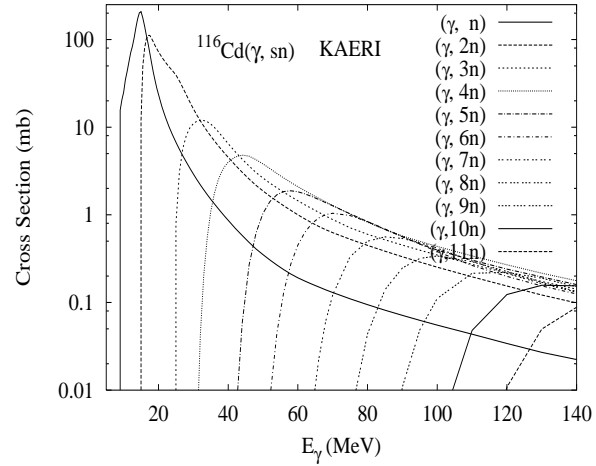
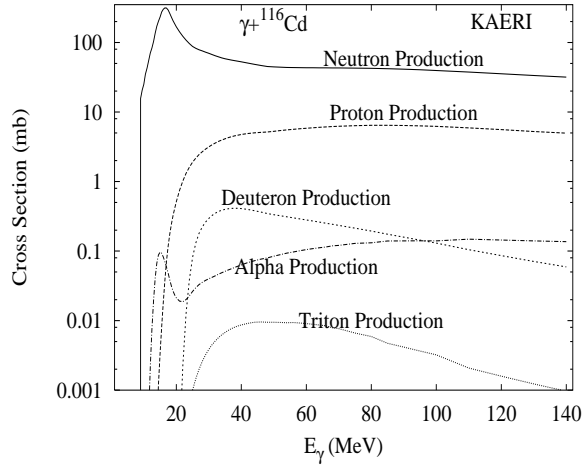
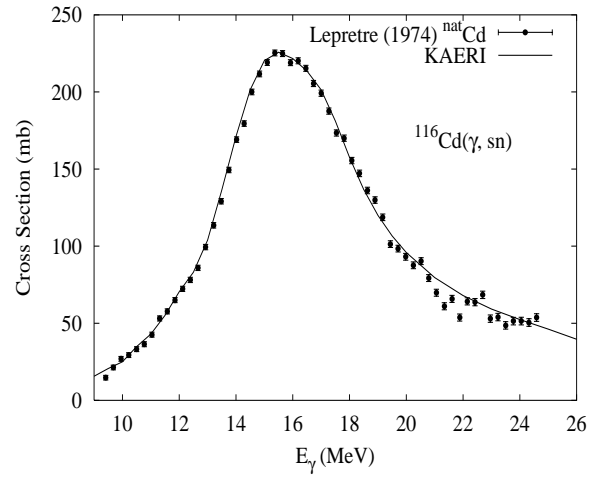
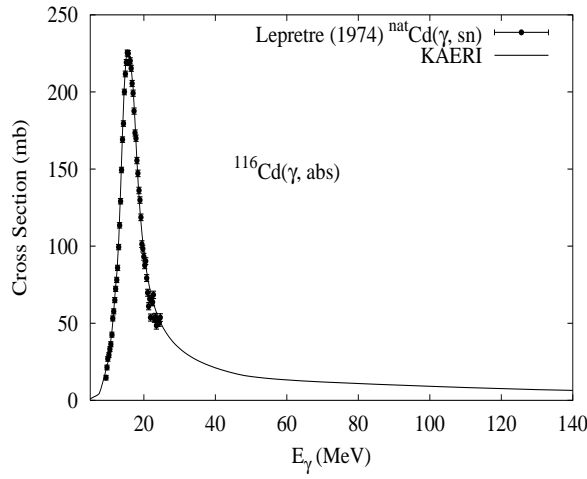
# $\gamma + {}^{114}\text{Cd}$

Abundance (%)	Threshold Energies (MeV)								
	$\gamma, n$	$\gamma, p$	$\gamma, t$	$\gamma, \text{He-3}$	$\gamma, \alpha$	$\gamma, 2n$	$\gamma, np$	$\gamma, 2p$	$\gamma, 3n$
28.73	9.04	10.27	16.75	18.92	4.10	15.58	18.76	18.27	24.98



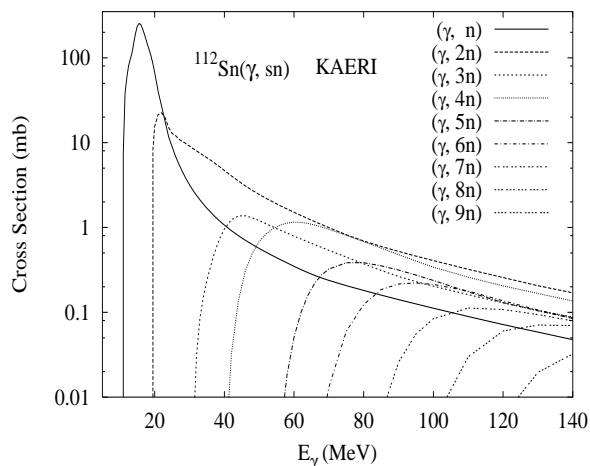
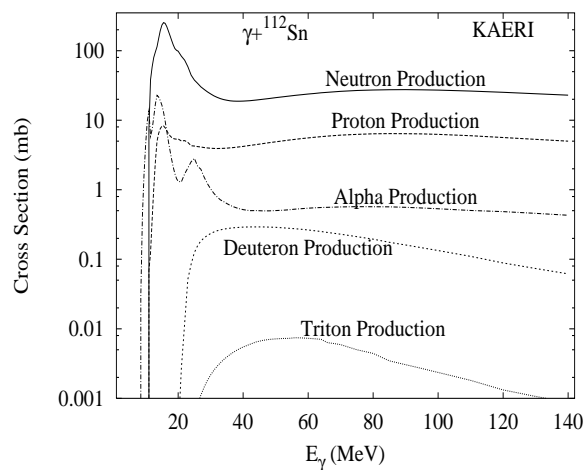
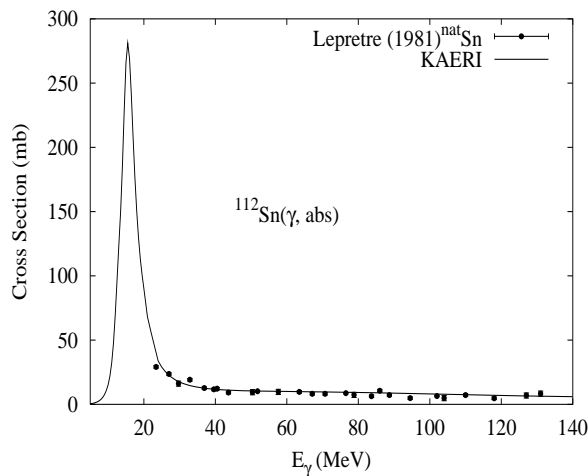
The photoabsorption cross section has not been measured. However, for  ${}^{nat}\text{Cd}$ , there are experimental data for the  $(\gamma, 1nx)$ ,  $(\gamma, 2nx)$ ,  $(\gamma, sn)$  and  $(\gamma, xn)$  reaction cross sections [Lep74]. We relied on the GUNF and GNASH codes to infer the photoabsorption cross section in the GDR regime, in order to model accurately the  $(\gamma, sn)$  data. The photoabsorption cross section above the GDR, up to 140 MeV, was obtained from QD model calculations using the theory of Chadwick. The neutron, proton, deuteron, triton and alpha emission cross sections, as well as production cross sections, were calculated by the GNASH code.

Abundance (%)	Threshold Energies (MeV)								
	$\gamma, n$	$\gamma, p$	$\gamma, t$	$\gamma, \text{He-3}$	$\gamma, \alpha$	$\gamma, 2n$	$\gamma, np$	$\gamma, 2p$	$\gamma, 3n$
7.49	8.70	11.06	16.63	19.97	4.81	14.84	19.12	19.84	23.88



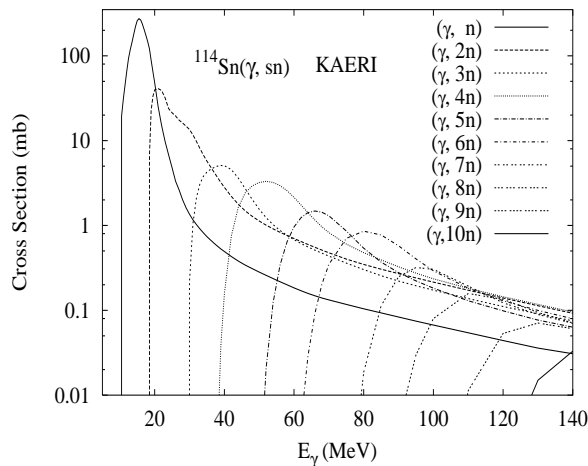
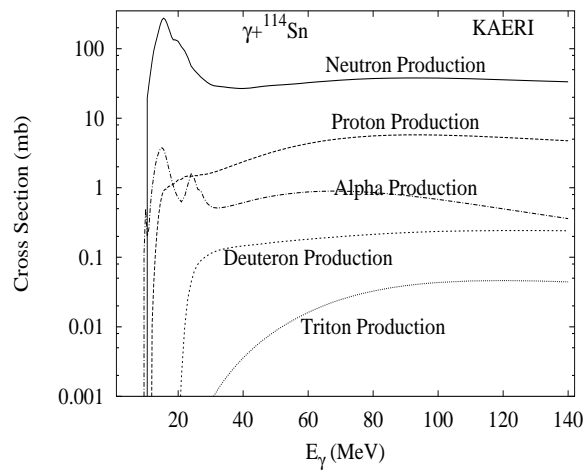
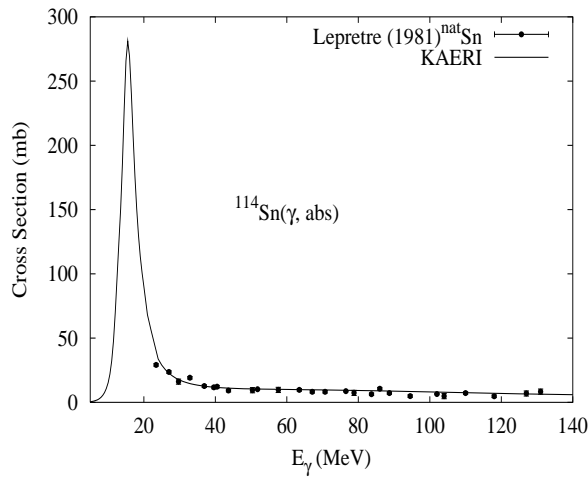
The photoabsorption cross section has not been measured. However, for  ${}^{nat}\text{Cd}$ , there are experimental data for the  $(\gamma, 1nx)$ ,  $(\gamma, 2nx)$ ,  $(\gamma, sn)$  and  $(\gamma, xn)$  reaction cross sections [Lep74]. We relied on the GUNF and GNASH codes to infer the photoabsorption cross section in the GDR regime, in order to model accurately the  $(\gamma, sn)$  data. The photoabsorption cross section above the GDR, up to 140 MeV, was obtained from QD model calculations using the theory of Chadwick. The neutron, proton, deuteron, triton and alpha emission cross sections, as well as production cross sections, were calculated by the GNASH code.

Abundance (%)	Threshold Energies (MeV)								
	$\gamma, n$	$\gamma, p$	$\gamma, t$	$\gamma, \text{He-3}$	$\gamma, \alpha$	$\gamma, 2n$	$\gamma, np$	$\gamma, 2p$	$\gamma, 3n$
0.97	10.79	7.56	17.12	15.08	1.83	18.97	17.61	12.89	30.24



Measurements of the photoabsorption cross section, above 25 MeV, are available for  ${}^{nat}\text{Sn}$  [Lep81]. The GUNF code was used to infer the photoabsorption cross section in the GDR regime, adopting the GDR parameters of  ${}^{116}\text{Sn}$ . The photoabsorption cross section above the GDR, up to 140 MeV, was obtained from QD model calculations using the theory of Chadwick. The neutron, proton, deuteron, triton and alpha emission cross sections, as well as production cross sections, were calculated by the GNASH code.

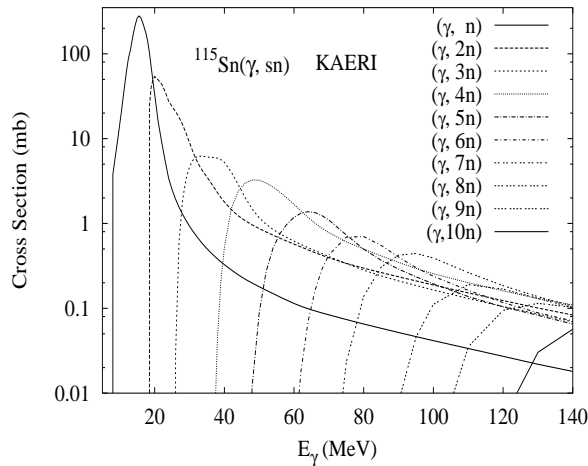
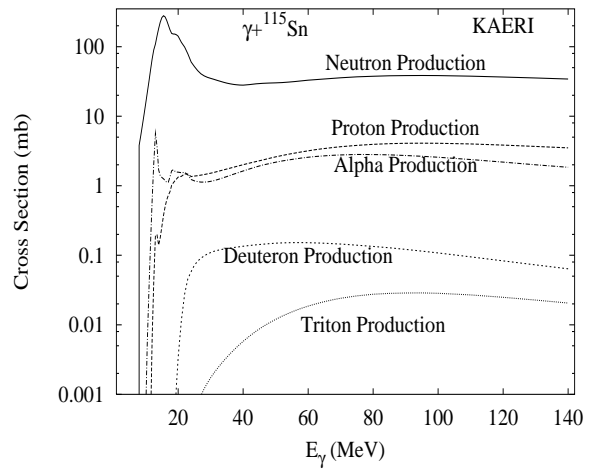
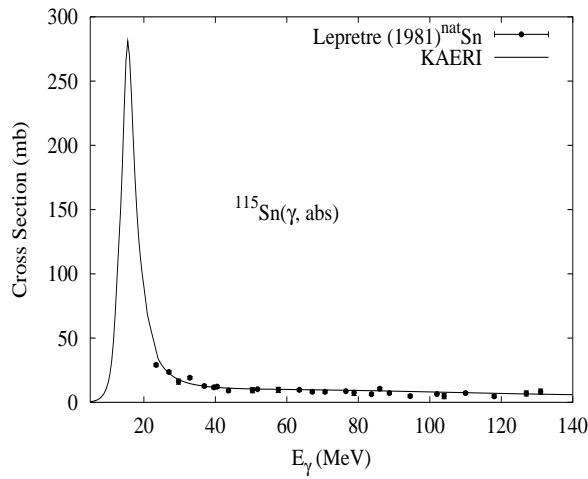
Abundance (%)	Threshold Energies (MeV)								
	$\gamma, n$	$\gamma, p$	$\gamma, t$	$\gamma, \text{He-3}$	$\gamma, \alpha$	$\gamma, 2n$	$\gamma, np$	$\gamma, 2p$	$\gamma, 3n$
0.65	10.30	8.48	17.12	16.24	2.63	18.04	17.93	14.56	28.83



Measurements of the photoabsorption cross section, above 25 MeV, are available for  ${}^{nat}\text{Sn}$  [Lep81]. The GUNF code was used to infer the photoabsorption cross section in the GDR regime, adopting the GDR parameters of  ${}^{116}\text{Sn}$ . The photoabsorption cross section above the GDR, up to 140 MeV, was obtained from QD model calculations using the theory of Chadwick. The neutron, proton, deuteron, triton and alpha emission cross sections, as well as production cross sections, were calculated by the GNASH code.

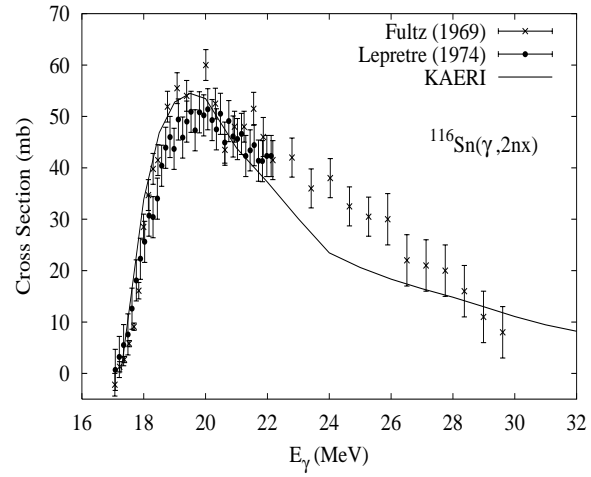
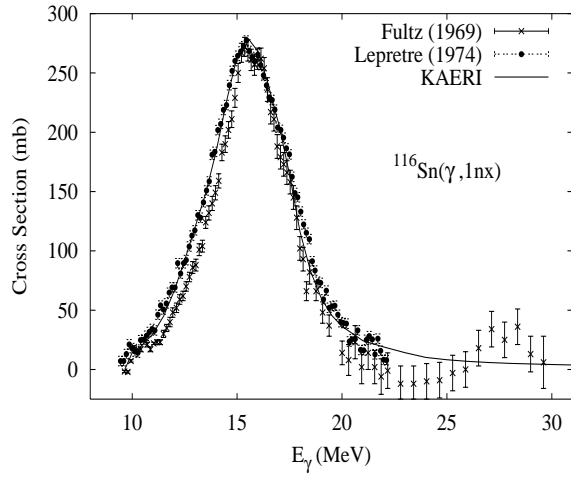
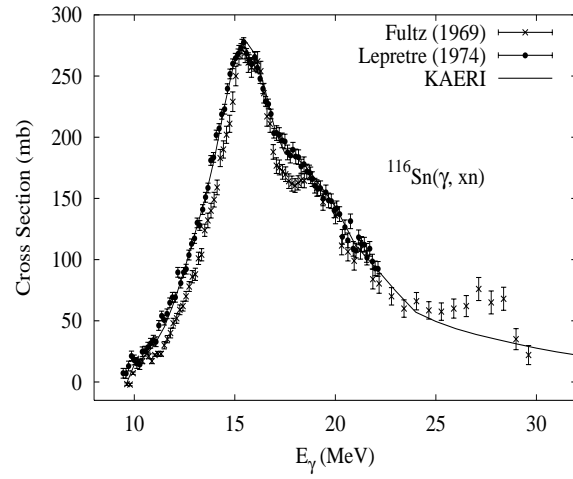
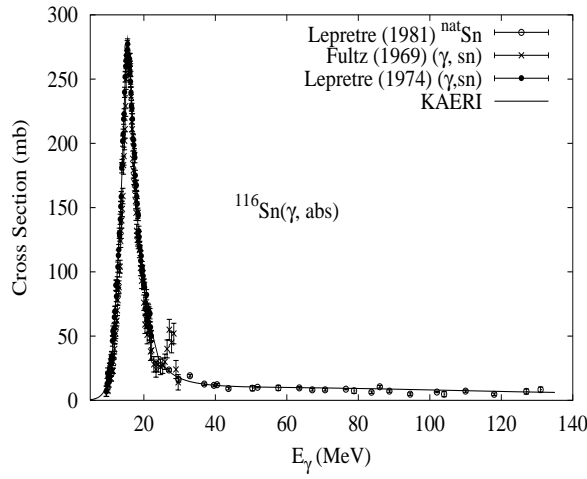


Abundance (%)	Threshold Energies (MeV)								
	$\gamma, n$	$\gamma, p$	$\gamma, t$	$\gamma, \text{He-3}$	$\gamma, \alpha$	$\gamma, 2n$	$\gamma, np$	$\gamma, 2p$	$\gamma, 3n$
0.36	7.55	8.75	16.99	14.38	3.21	17.85	16.03	15.56	25.59



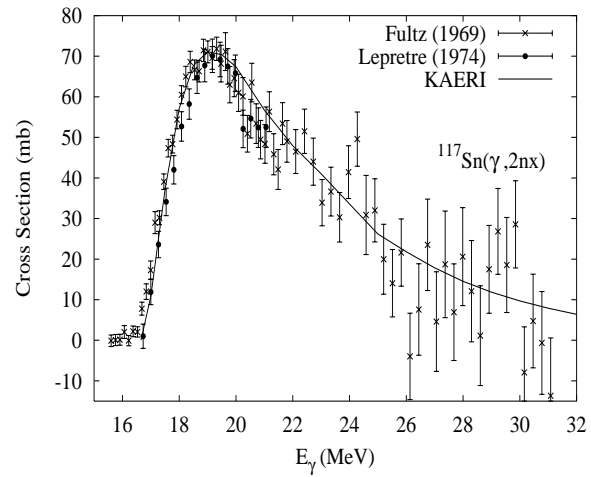
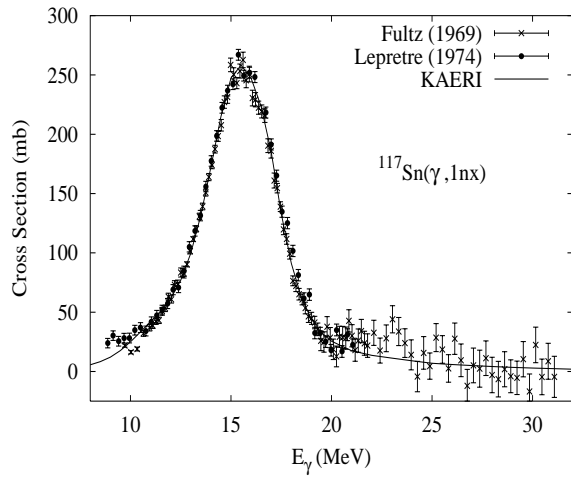
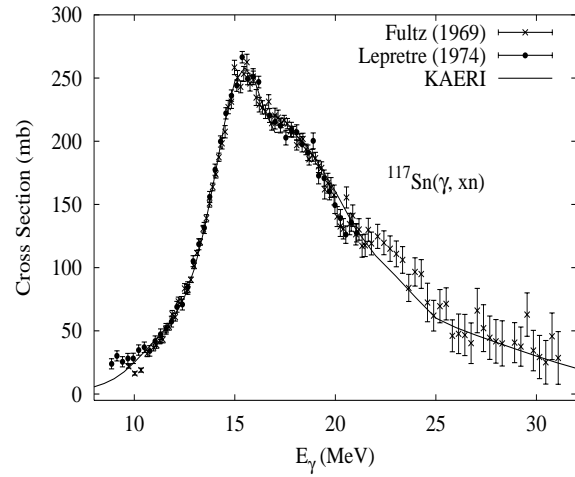
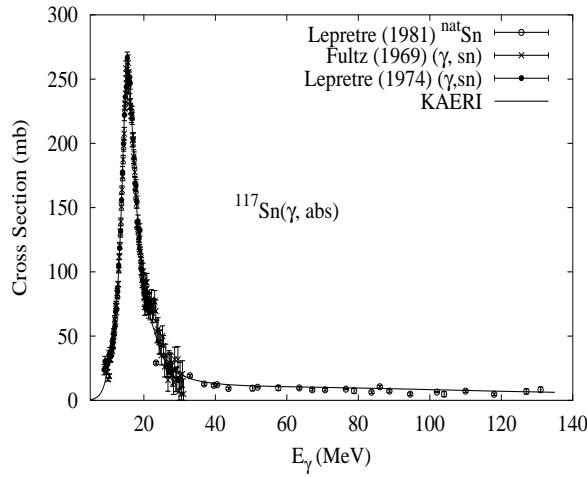
Measurements of the photoabsorption cross section, above 25 MeV, are available for  ${}^{nat}\text{Sn}$  [Lep81]. The GUNF code was used to infer the photoabsorption cross section in the GDR regime, adopting the GDR parameters of  ${}^{116}\text{Sn}$ . The photoabsorption cross section above the GDR, up to 140 MeV, was obtained from QD model calculations using the theory of Chadwick. The neutron, proton, deuteron, triton and alpha emission cross sections, as well as production cross sections, were calculated by the GNASH code.

Abundance (%)	Threshold Energies (MeV)								
	$\gamma, n$	$\gamma, p$	$\gamma, t$	$\gamma, \text{He-3}$	$\gamma, \alpha$	$\gamma, 2n$	$\gamma, np$	$\gamma, 2p$	$\gamma, 3n$
14.53	9.56	9.28	17.11	17.41	3.37	17.11	18.32	16.08	27.41



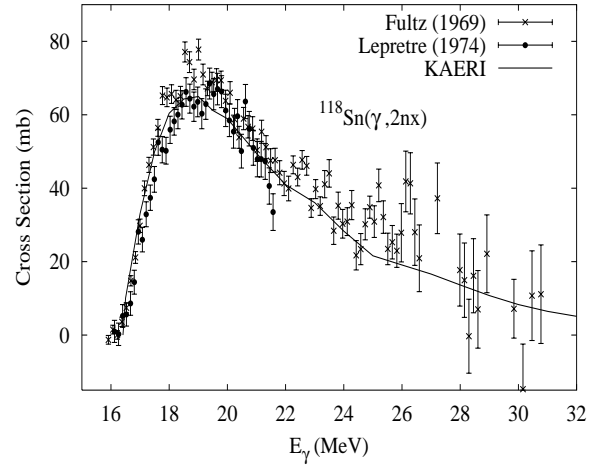
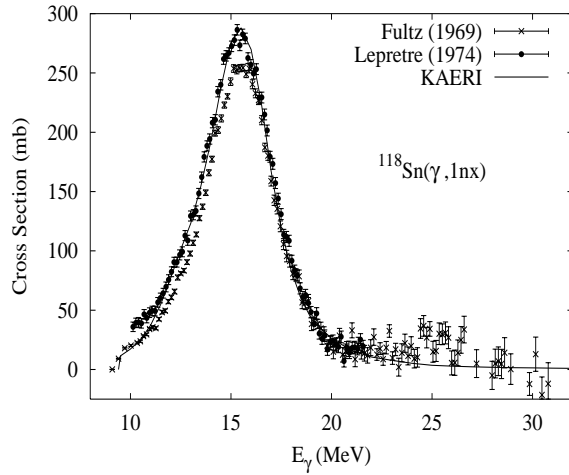
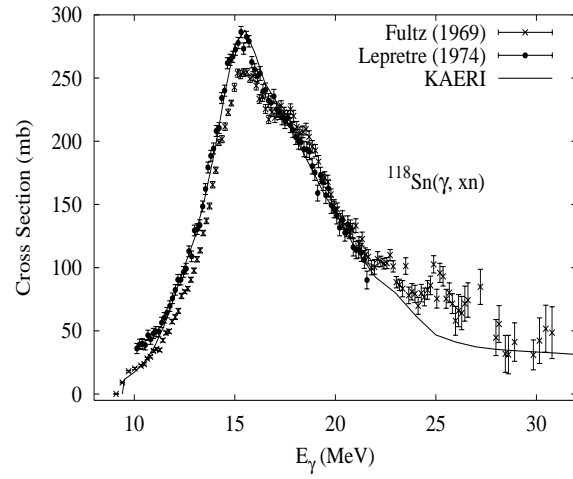
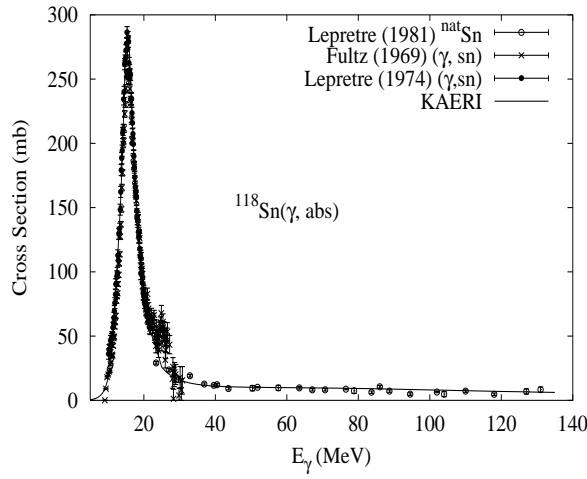
There are no measurements of the photoabsorption cross section in the GDR energy region. Lepretre [Lep74] and Fultz [Ful69] measured the  $(\gamma, 1nx)$ ,  $(\gamma, 2nx)$ ,  $(\gamma, sn)$  and  $(\gamma, xn)$  reaction cross sections. Lepretre [Lep81] also measured the photoabsorption cross section for  ${}^{nat}\text{Sn}$  from 25 MeV to 135 MeV. We relied on the GUNF and GNASH codes to infer the photoabsorption cross section in the GDR regime, using Lepretre's two measurements [Lep81, Lep74], in order to model all the photonuclear cross sections consistently. The photoabsorption cross section above the GDR, up to 140 MeV, was obtained from QD model calculations using the theory of Chadwick. The neutron, proton, deuteron, triton and alpha emission cross sections, as well as production cross sections, were calculated by the GNASH code.

Abundance (%)	Threshold Energies (MeV)								
	$\gamma, n$	$\gamma, p$	$\gamma, t$	$\gamma, \text{He-3}$	$\gamma, \alpha$	$\gamma, 2n$	$\gamma, np$	$\gamma, 2p$	$\gamma, 3n$
7.68	6.94	9.44	16.78	15.31	3.77	16.51	16.22	16.89	24.05



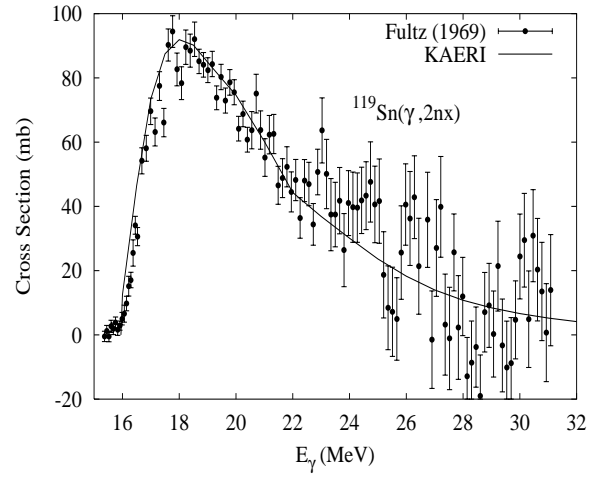
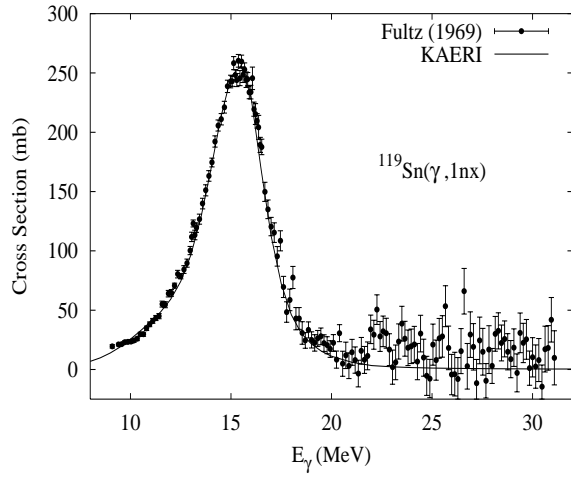
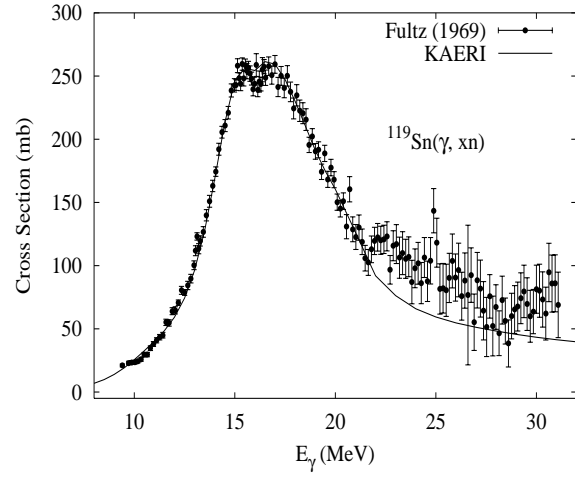
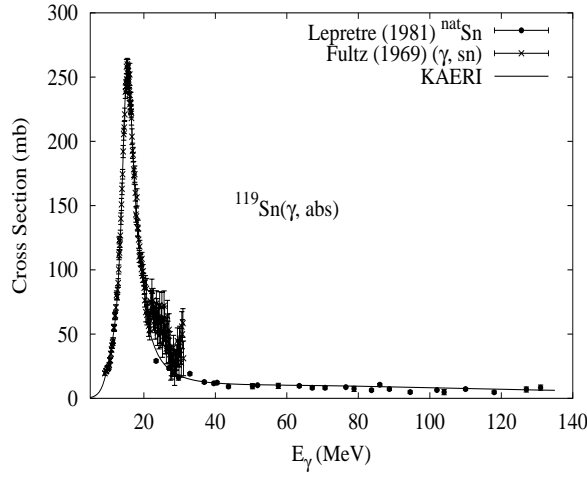
There are no measurements of the photoabsorption cross section in the GDR energy region. Lepretre [Lep74] and Fultz [Ful69] measured the  $(\gamma, 1nx)$ ,  $(\gamma, 2nx)$ ,  $(\gamma, sn)$  and  $(\gamma, xn)$  reaction cross sections. Lepretre [Lep81] also measured the photoabsorption cross section for  ${}^{nat}\text{Sn}$  from 25 MeV to 135 MeV. We relied on the GUNF and GNASH codes to infer the photoabsorption cross section in the GDR regime, using Lepretre's two measurements [Lep81, Lep74], in order to model all the photonuclear cross sections consistently. The photoabsorption cross section above the GDR, up to 140 MeV, was obtained from QD model calculations using the theory of Chadwick. The neutron, proton, deuteron, triton and alpha emission cross sections, as well as production cross sections, were calculated by the GNASH code.

Abundance (%)	Threshold Energies (MeV)								
	$\gamma, n$	$\gamma, p$	$\gamma, t$	$\gamma, \text{He-3}$	$\gamma, \alpha$	$\gamma, 2n$	$\gamma, np$	$\gamma, 2p$	$\gamma, 3n$
24.22	9.33	10.00	17.07	18.49	4.06	16.27	18.76	17.51	25.83



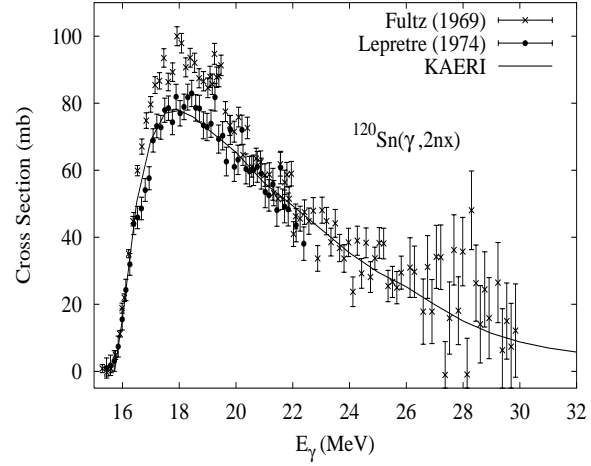
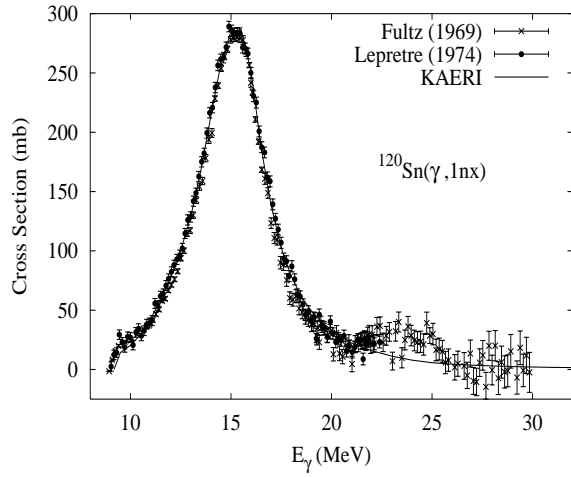
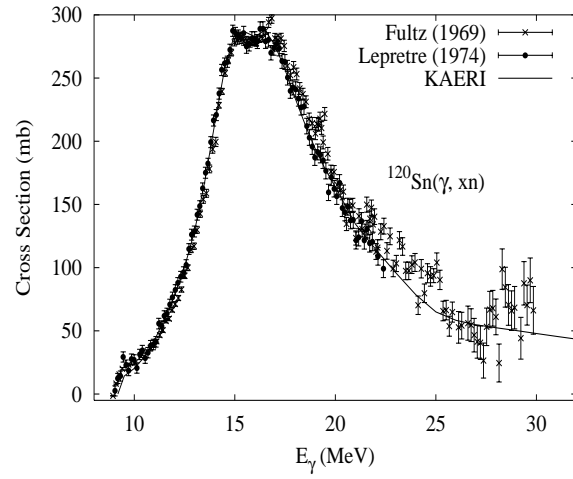
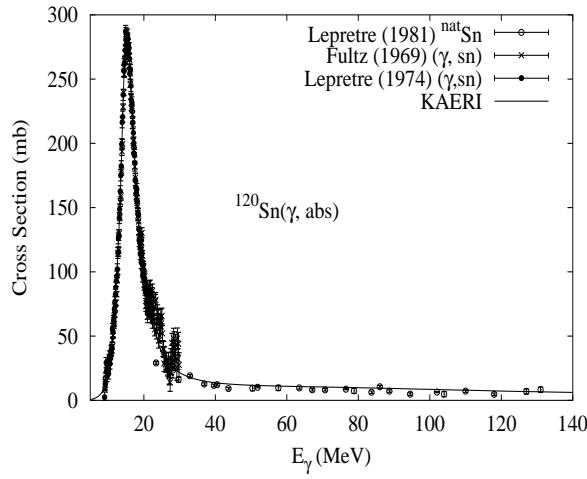
There are no measurements of the photoabsorption cross section in the GDR energy region. Lepretre [Lep74] and Fultz [Ful69] measured the  $(\gamma, 1nx)$ ,  $(\gamma, 2nx)$ ,  $(\gamma, sn)$  and  $(\gamma, xn)$  reaction cross sections. Lepretre [Lep81] also measured the photoabsorption cross section for  ${}^{nat}\text{Sn}$  from 25 MeV to 135 MeV. We relied on the GUNF and GNASH codes to infer the photoabsorption cross section in the GDR regime, using Lepretre's two measurements [Lep81, Lep74], in order to model all the photonuclear cross sections consistently. The photoabsorption cross section above the GDR, up to 140 MeV, was obtained from QD model calculations using the theory of Chadwick. The neutron, proton, deuteron, triton and alpha emission cross sections, as well as production cross sections, were calculated by the GNASH code.

Abundance (%)	Threshold Energies (MeV)								
	$\gamma, n$	$\gamma, p$	$\gamma, t$	$\gamma, \text{He-3}$	$\gamma, \alpha$	$\gamma, 2n$	$\gamma, np$	$\gamma, 2p$	$\gamma, 3n$
8.58	6.49	10.13	16.77	16.28	4.40	15.81	16.48	18.23	22.76



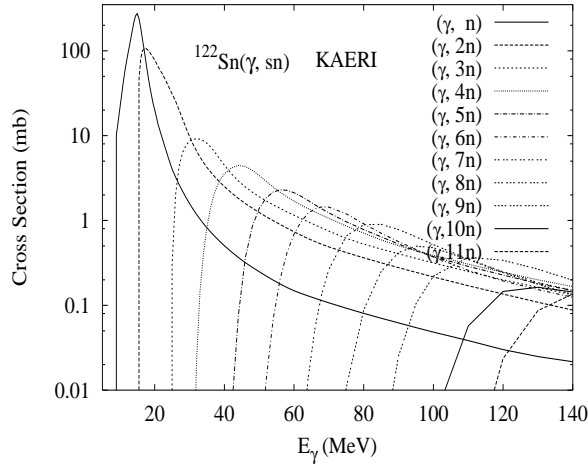
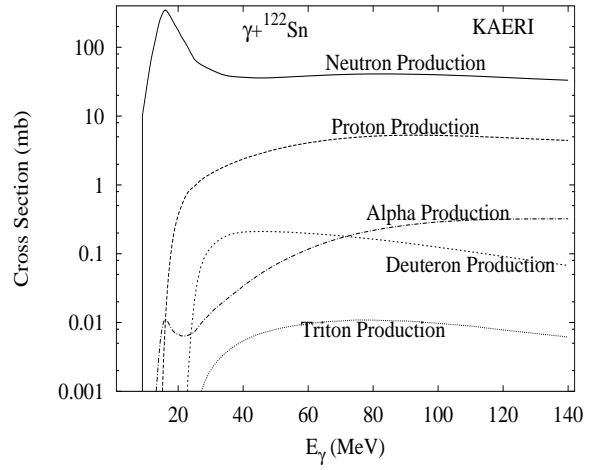
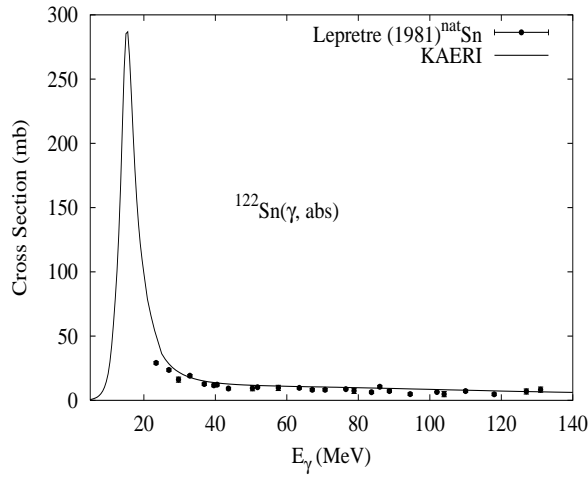
There are no measurements of the photoabsorption cross section in the GDR energy region. Fultz [Ful69] measured the  $(\gamma, 1nx)$ ,  $(\gamma, 2nx)$ ,  $(\gamma, sn)$  and  $(\gamma, xn)$  reaction cross sections. Lepretre [Lep81] measured the photoabsorption cross section for  ${}^{nat}\text{Sn}$  from 25 MeV to 135 MeV. We relied on the GUNF and GNASH codes to infer the photoabsorption cross section in the GDR regime, using Fultz's and Lepretre's measurements [Ful69, Lep81], in order to model all the photonuclear cross sections consistently. The photoabsorption cross section above the GDR, up to 140 MeV, was obtained from QD model calculations using the theory of Chadwick. The neutron, proton, deuteron, triton and alpha emission cross sections, as well as production cross sections, were calculated by the GNASH code.

Abundance (%)	Threshold Energies (MeV)								
	$\gamma, n$	$\gamma, p$	$\gamma, t$	$\gamma, \text{He-3}$	$\gamma, \alpha$	$\gamma, 2n$	$\gamma, np$	$\gamma, 2p$	$\gamma, 3n$
32.59	9.11	10.66	17.11	19.62	4.81	15.59	19.23	18.97	24.92



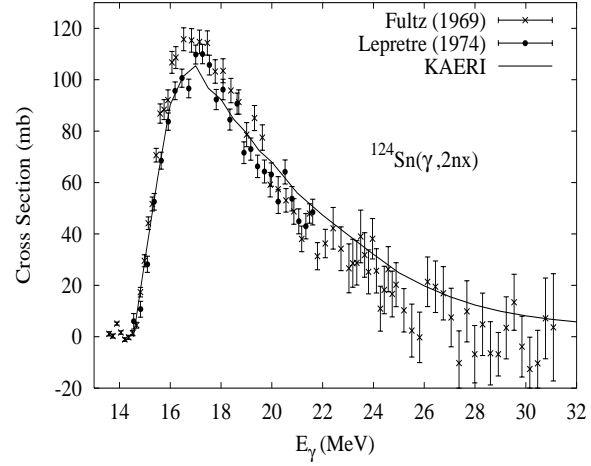
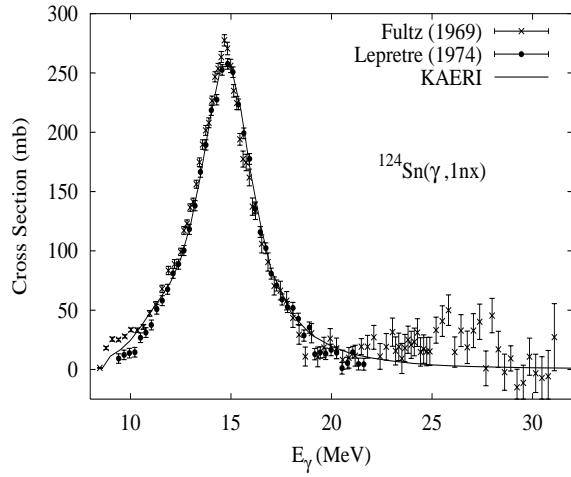
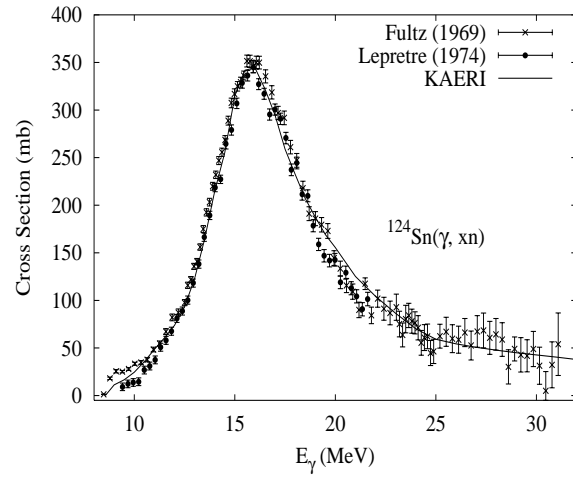
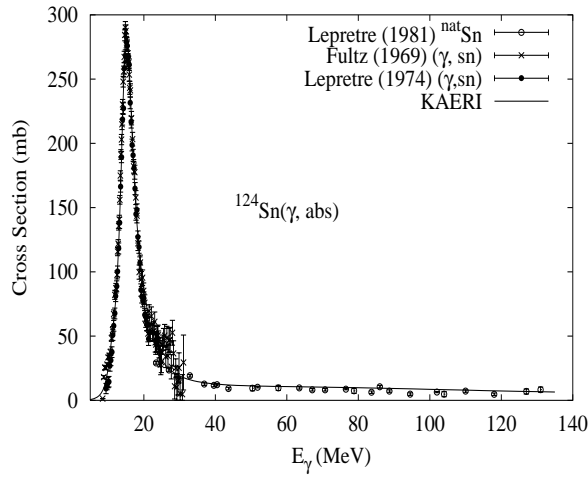
There are no measurements of the photoabsorption cross section in the GDR energy region. Lepretre [Lep74] and Fultz [Ful69] measured the  $(\gamma, 1nx)$ ,  $(\gamma, 2nx)$ ,  $(\gamma, sn)$  and  $(\gamma, xn)$  reaction cross sections. Lepretre [Lep81] also measured the photoabsorption cross section for  ${}^{nat}\text{Sn}$  from 25 MeV to 135 MeV. We relied on the GUNF and GNASH codes to infer the photoabsorption cross section in the GDR regime, using Lepretre's two measurements [Lep81, Lep74], in order to model all the photonuclear cross sections consistently. The photoabsorption cross section above the GDR, up to 140 MeV, was obtained from QD model calculations using the theory of Chadwick. The neutron, proton, deuteron, triton and alpha emission cross sections, as well as production cross sections, were calculated by the GNASH code.

Abundance (%)	Threshold Energies (MeV)								
	$\gamma, n$	$\gamma, p$	$\gamma, t$	$\gamma, \text{He-3}$	$\gamma, \alpha$	$\gamma, 2n$	$\gamma, np$	$\gamma, 2p$	$\gamma, 3n$
4.63	8.81	11.39	17.16	20.94	5.66	14.98	19.51	20.55	24.09



Measurements of the photoabsorption cross section, above 25 MeV, are available for  ${}^{nat}\text{Sn}$  [Lep81]. The GUNF code was used to infer the photoabsorption cross section in the GDR regime, adopting the GDR parameters of  ${}^{116}\text{Sn}$ . The photoabsorption cross section above the GDR, up to 140 MeV, was obtained from QD model calculations using the theory of Chadwick. The neutron, proton, deuteron, triton and alpha emission cross sections, as well as production cross sections, were calculated by the GNASH code.

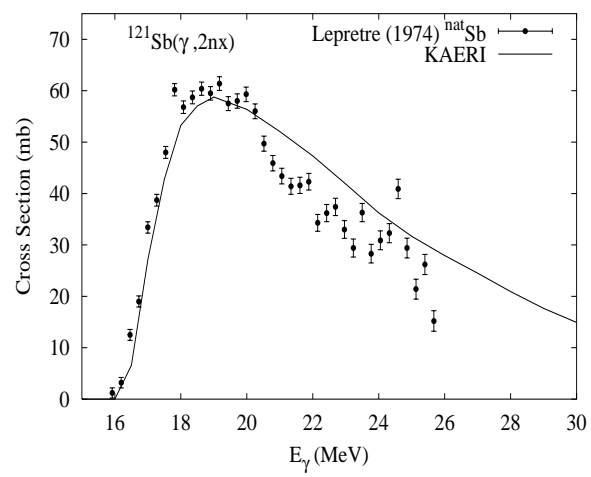
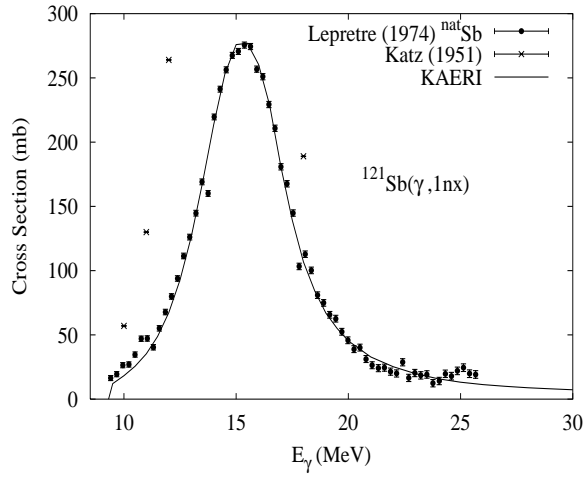
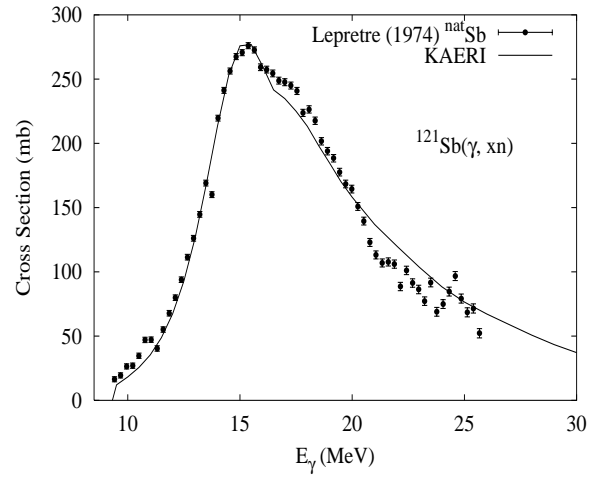
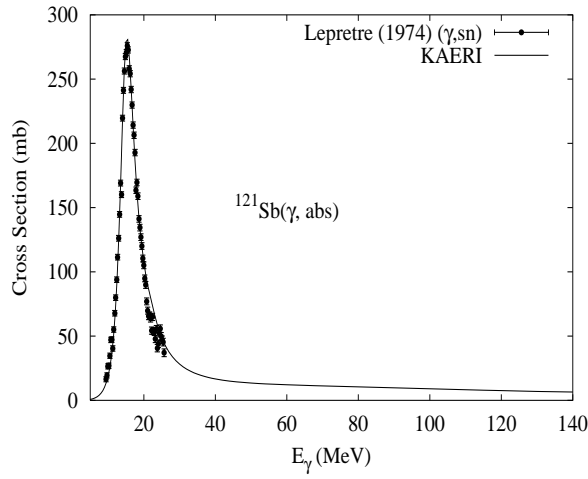
Abundance (%)	Threshold Energies (MeV)								
	$\gamma, n$	$\gamma, p$	$\gamma, t$	$\gamma, \text{He-3}$	$\gamma, \alpha$	$\gamma, 2n$	$\gamma, np$	$\gamma, 2p$	$\gamma, 3n$
5.79	8.49	12.11	17.35	22.22	6.69	14.43	20.02	21.83	23.25



There are no measurements of the photoabsorption cross section in the GDR energy region. Lepretre [Lep74] and Fultz [Ful69] measured the  $(\gamma, 1nx)$ ,  $(\gamma, 2nx)$ ,  $(\gamma, sn)$  and  $(\gamma, xn)$  reaction cross sections. Lepretre [Lep81] also measured the photoabsorption cross section for  ${}^{nat}\text{Sn}$  from 25 MeV to 135 MeV. We relied on the GUNF and GNASH codes to infer the photoabsorption cross section in the GDR regime, using Lepretre's two measurements [Lep81, Lep74], in order to model all the photonuclear cross sections consistently. The photoabsorption cross section above the GDR, up to 140 MeV, was obtained from QD model calculations using the theory of Chadwick. The neutron, proton, deuteron, triton and alpha emission cross sections, as well as production cross sections, were calculated by the GNASH code.



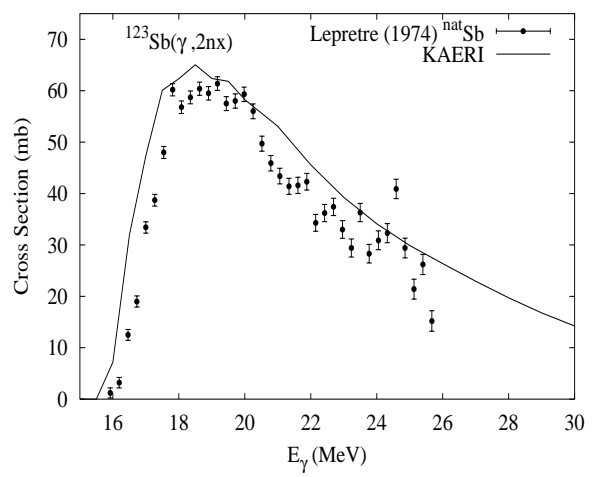
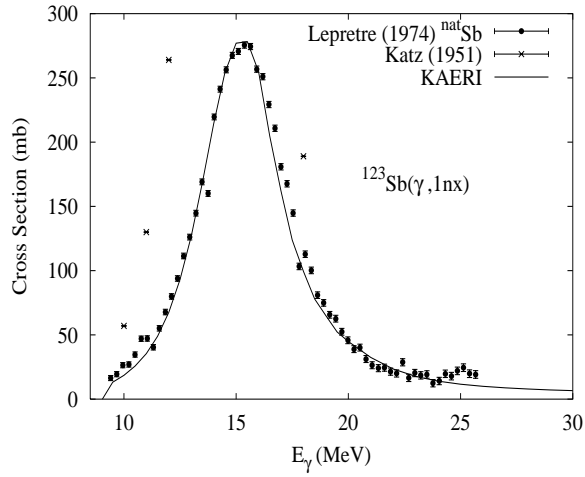
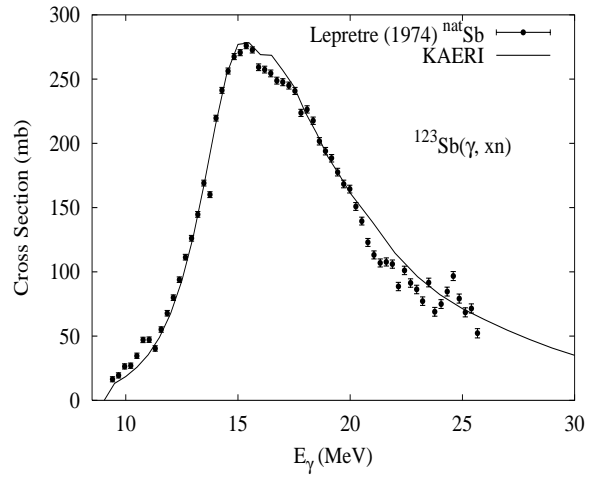
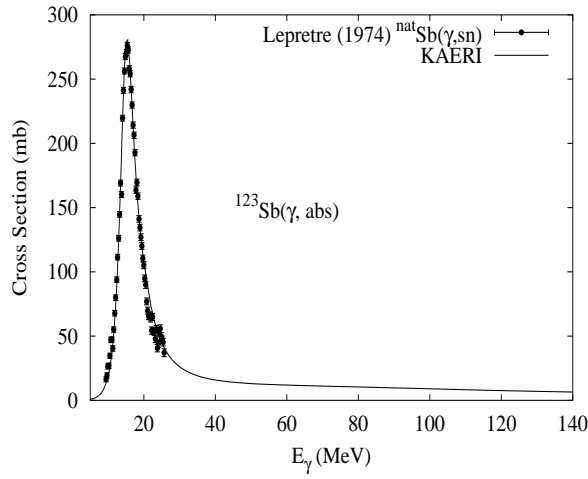
Abundance (%)	Threshold Energies (MeV)								
	$\gamma, n$	$\gamma, p$	$\gamma, t$	$\gamma, \text{He-3}$	$\gamma, \alpha$	$\gamma, 2n$	$\gamma, np$	$\gamma, 2p$	$\gamma, 3n$
57.36	9.24	5.78	12.89	17.29	3.07	16.26	14.88	16.44	25.81



The photoabsorption cross section has not been measured. However, for  ${}^{nat}\text{Sb}$ , there are experimental data for the  $(\gamma, 1nx)$ ,  $(\gamma, 2nx)$ ,  $(\gamma, sn)$  and  $(\gamma, xn)$  reaction cross sections [Lep74]. Katz reported a few points for the  $(\gamma, 1n)$  reaction cross section [Kat51]. We relied on the GUNF and GNASH codes to infer the photoabsorption cross section in the GDR regime, in order to model accurately the  $(\gamma, sn)$  data. The photoabsorption cross section above the GDR, up to 140 MeV, was obtained from QD model calculations using the theory of Chadwick.

The calculated results of the emission channels by the GNASH code are in good agreement with all the experimental data of Lepretre.

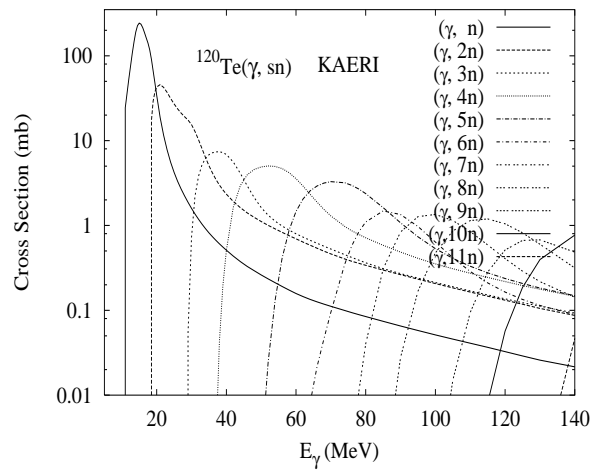
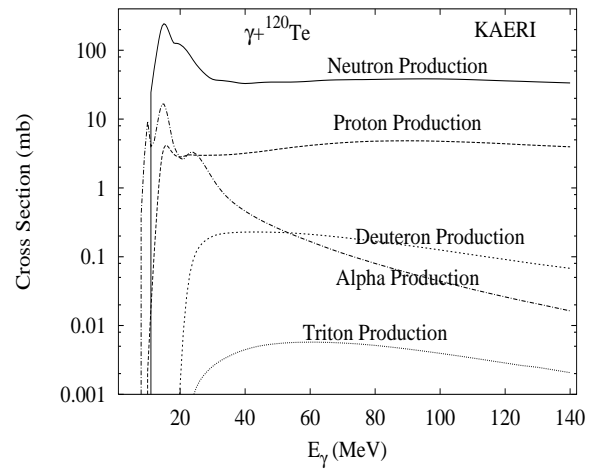
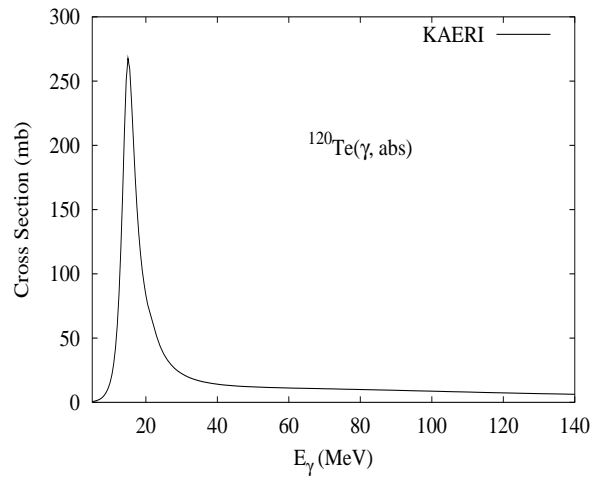
Abundance (%)	Threshold Energies (MeV)								
	$\gamma, n$	$\gamma, p$	$\gamma, t$	$\gamma, \text{He-3}$	$\gamma, \alpha$	$\gamma, 2n$	$\gamma, np$	$\gamma, 2p$	$\gamma, 3n$
42.64	8.97	6.57	13.07	18.36	3.92	15.77	15.38	17.96	25.01



The photoabsorption cross section has not been measured. However, for  ${}^{nat}\text{Sb}$ , there are experimental data for the  $(\gamma, 1nx)$ ,  $(\gamma, 2nx)$ ,  $(\gamma, sn)$  and  $(\gamma, xn)$  reaction cross sections [Lep74]. Katz reported a few points for the  $(\gamma, 1n)$  reaction cross section [Kat51]. We relied on the GUNF and GNASH codes to infer the photoabsorption cross section in the GDR regime, in order to model accurately the  $(\gamma, sn)$  data. The photoabsorption cross section above the GDR, up to 140 MeV, was obtained from QD model calculations using the theory of Chadwick.

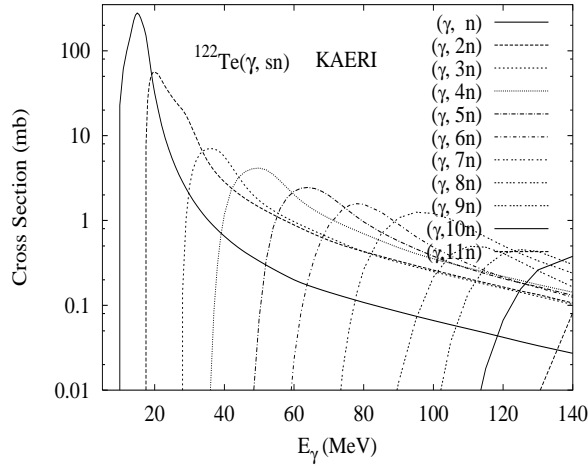
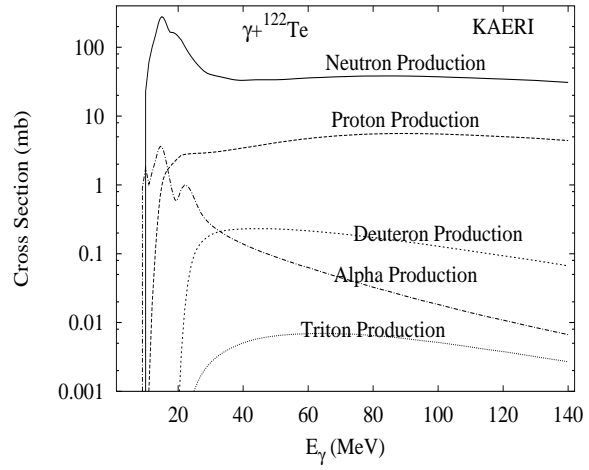
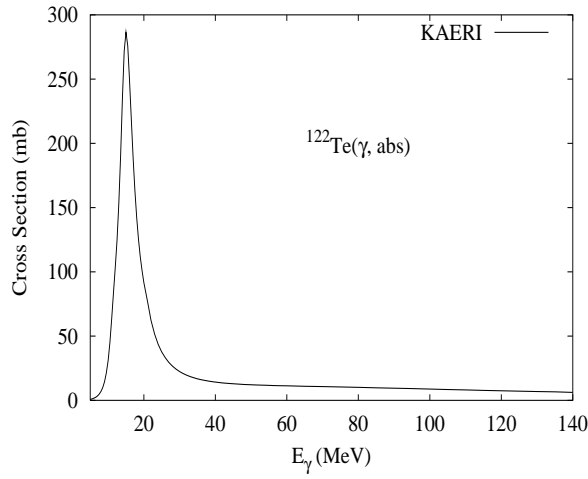
The calculated results of the emission channels by the GNASH code are in good agreement with all the experimental data of Lepretre.

Abundance (%)	Threshold Energies (MeV)								
	$\gamma, n$	$\gamma, p$	$\gamma, t$	$\gamma, \text{He-3}$	$\gamma, \alpha$	$\gamma, 2n$	$\gamma, np$	$\gamma, 2p$	$\gamma, 3n$
0.10	10.28	7.20	15.69	13.92	0.28	17.88	16.75	12.31	28.49



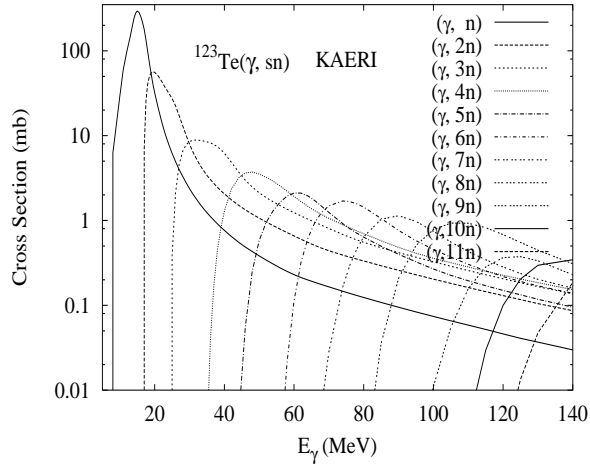
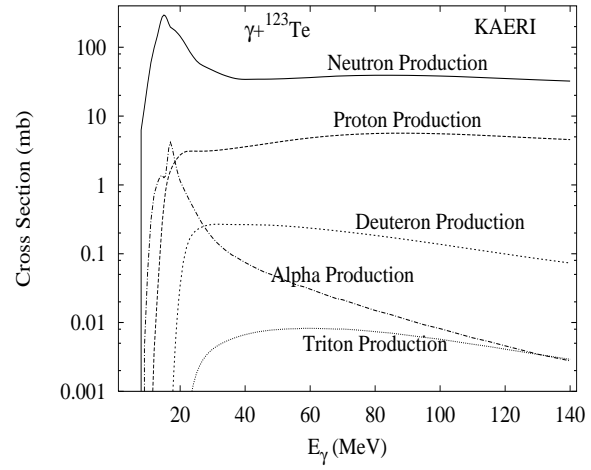
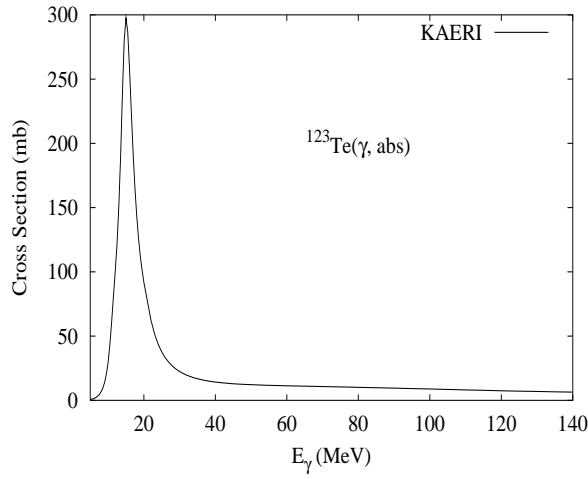
There are no experimental data available. The photoabsorption cross section was obtained from GDR and QD model calculations, adopting the GDR parameters of  ${}^{124}\text{Te}$ . The neutron, proton, deuteron, triton and alpha emission cross sections, as well as production cross sections, were calculated by the GNASH code.

Abundance (%)	Threshold Energies (MeV)								
	$\gamma, n$	$\gamma, p$	$\gamma, t$	$\gamma, \text{He-3}$	$\gamma, \alpha$	$\gamma, 2n$	$\gamma, np$	$\gamma, 2p$	$\gamma, 3n$
2.59	9.83	8.00	15.78	15.17	1.08	17.06	17.24	13.78	27.34



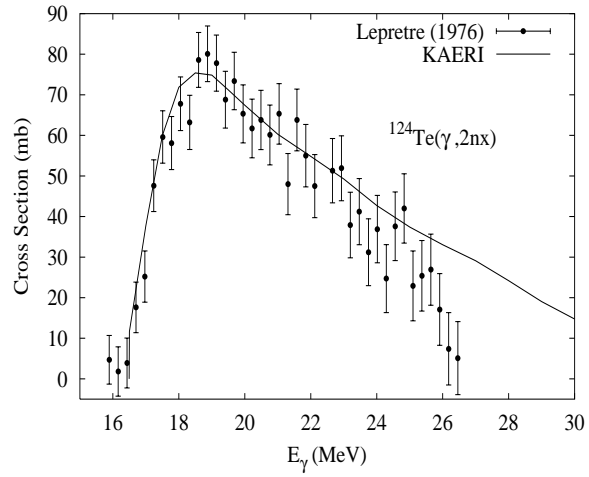
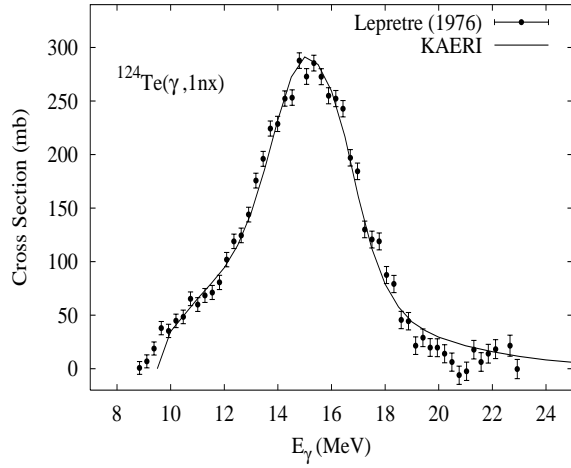
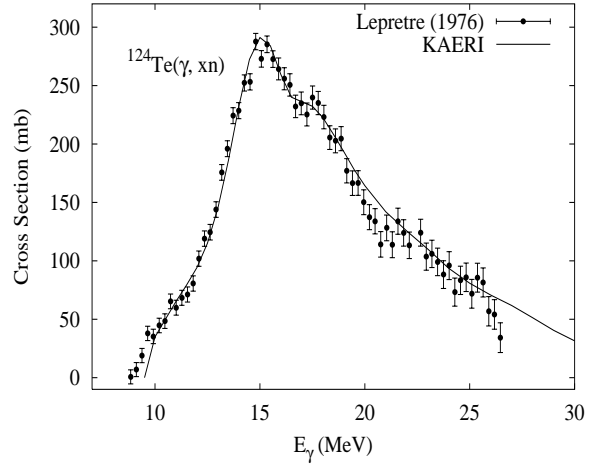
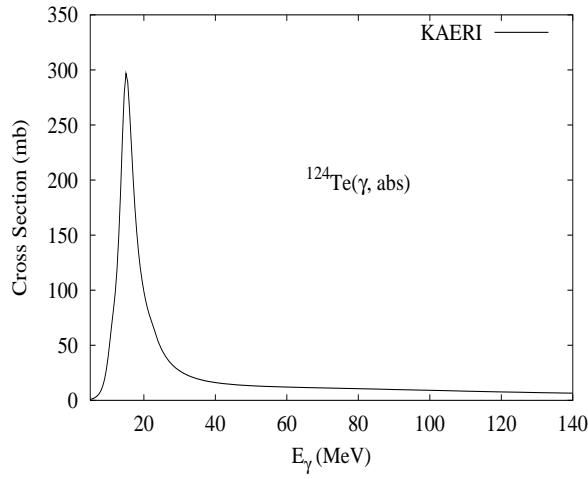
There are no experimental data available. The photoabsorption cross section was obtained from GDR and QD model calculations, adopting the GDR parameters of  ${}^{124}\text{Te}$ . The neutron, proton, deuteron, triton and alpha emission cross sections, as well as production cross sections, were calculated by the GNASH code.

Abundance (%)	Threshold Energies (MeV)								
	$\gamma, n$	$\gamma, p$	$\gamma, t$	$\gamma, \text{He-3}$	$\gamma, \alpha$	$\gamma, 2n$	$\gamma, np$	$\gamma, 2p$	$\gamma, 3n$
0.91	6.94	8.13	15.70	13.00	1.53	16.76	14.94	14.55	24.00



There are no experimental data available. The photoabsorption cross section was obtained from GDR and QD model calculations, adopting the GDR parameters of  ${}^{124}\text{Te}$ . The neutron, proton, deuteron, triton and alpha emission cross sections, as well as production cross sections, were calculated by the GNASH code.

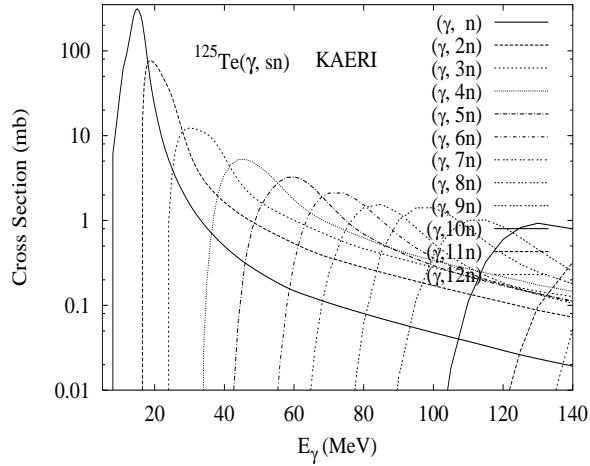
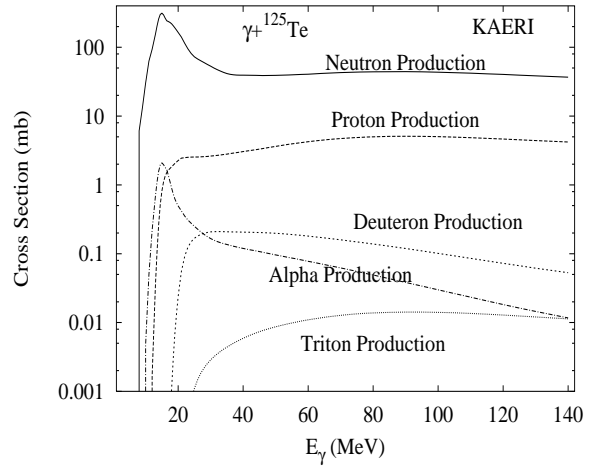
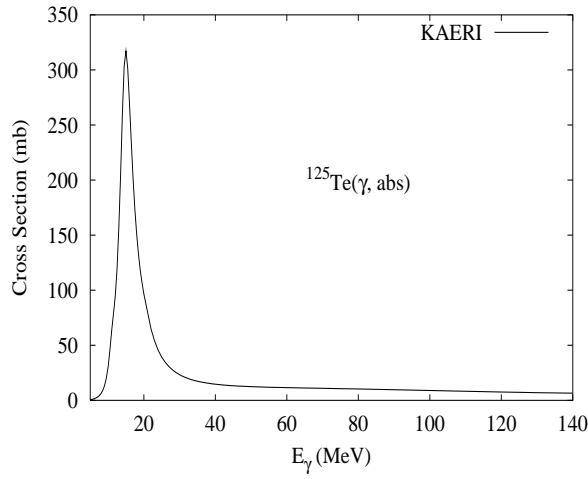
Abundance (%)	Threshold Energies (MeV)								
	$\gamma, n$	$\gamma, p$	$\gamma, t$	$\gamma, \text{He-3}$	$\gamma, \alpha$	$\gamma, 2n$	$\gamma, np$	$\gamma, 2p$	$\gamma, 3n$
4.79	9.43	8.59	15.88	16.25	1.85	16.36	17.56	15.16	26.19



The photoabsorption cross section has not been measured. However, there are experimental data for the  $(\gamma, 1nx)$ ,  $(\gamma, 2nx)$  and  $(\gamma, xn)$  reaction cross sections [Lep76]. We relied on the GUNF and GNASH codes to infer the photoabsorption cross section in the GDR regime, in order to model accurately the  $(\gamma, xn)$  channel data. The photoabsorption cross section above the GDR, up to 140 MeV, was obtained from QD model calculations using the theory of Chadwick.

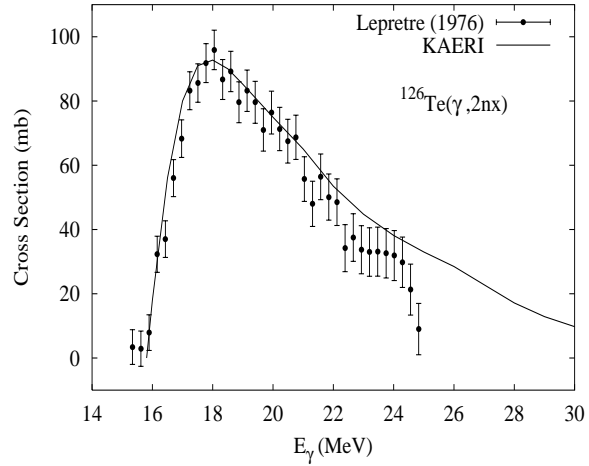
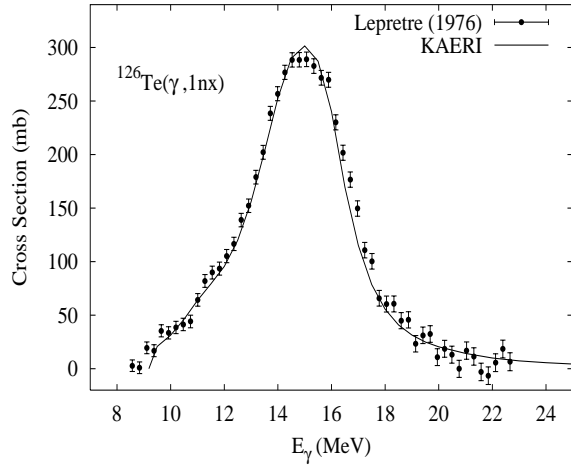
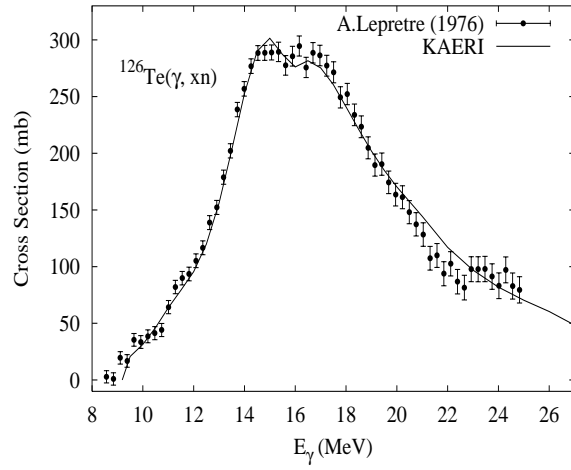
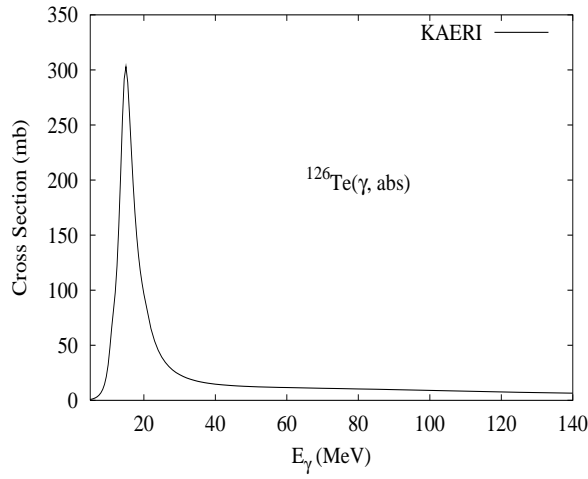
The calculated results of the emission channels by the GNASH code are in good agreement with the data for the  $(\gamma, 1nx)$ ,  $(\gamma, 2nx)$  and  $(\gamma, xn)$  cross sections.

Abundance (%)	Threshold Energies (MeV)								
	$\gamma, n$	$\gamma, p$	$\gamma, t$	$\gamma, \text{He-3}$	$\gamma, \alpha$	$\gamma, 2n$	$\gamma, np$	$\gamma, 2p$	$\gamma, 3n$
7.12	6.57	8.69	15.65	14.01	2.25	16.00	15.16	15.78	22.93



There are no experimental data available. The photoabsorption cross section was obtained from GDR and QD model calculations, adopting the GDR parameters of  ${}^{126}\text{Te}$ . The neutron, proton, deuteron, triton and alpha emission cross sections, as well as production cross sections, were calculated by the GNASH code.

Abundance (%)	Threshold Energies (MeV)								
	$\gamma, n$	$\gamma, p$	$\gamma, t$	$\gamma, \text{He-3}$	$\gamma, \alpha$	$\gamma, 2n$	$\gamma, np$	$\gamma, 2p$	$\gamma, 3n$
18.93	9.11	9.10	15.79	17.18	2.55	15.68	17.81	16.41	25.11

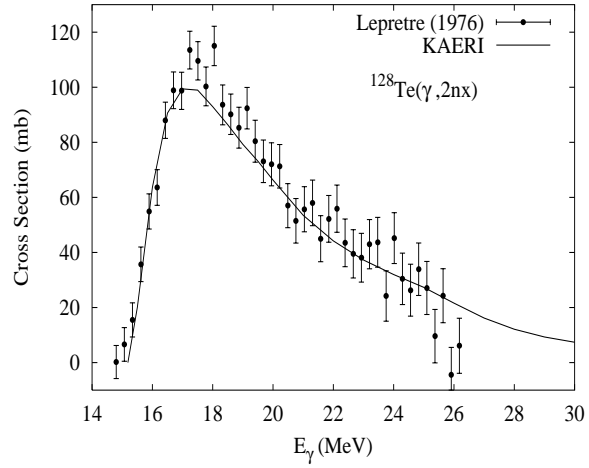
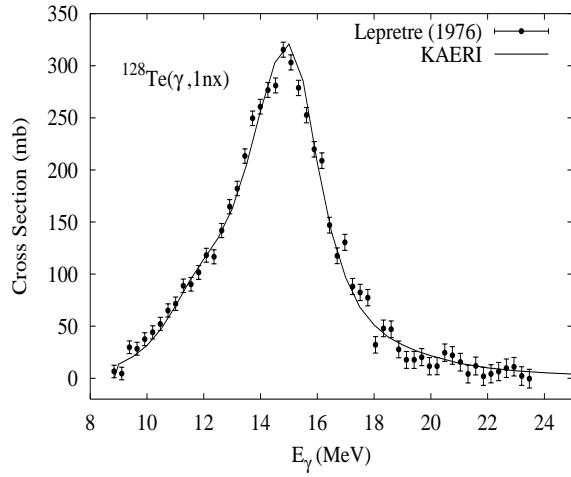
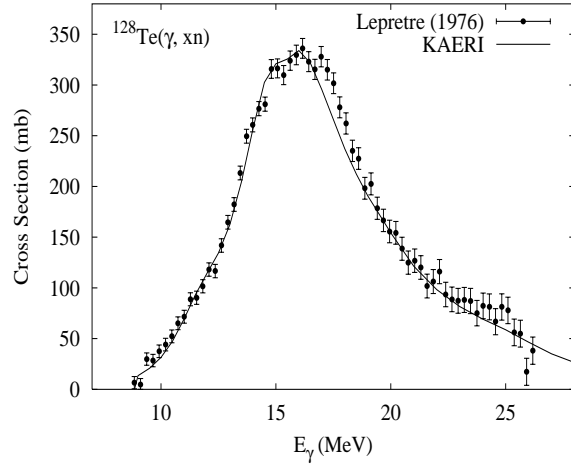
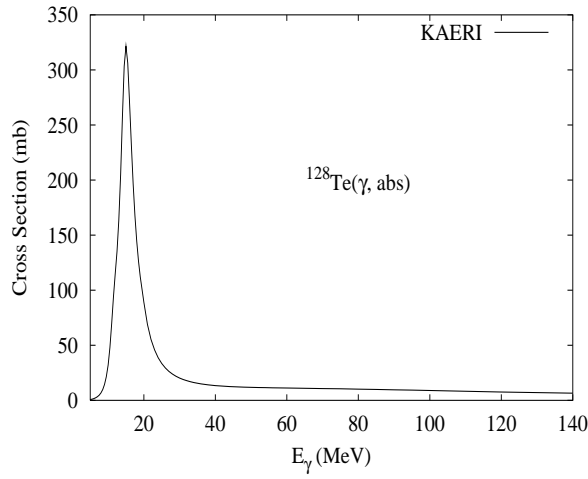


The photoabsorption cross section has not been measured. However, there are experimental data for the  $(\gamma, 1nx)$ ,  $(\gamma, 2nx)$  and  $(\gamma, xn)$  reaction cross sections [Lep76]. We relied on the GUNF and GNASH codes to infer the photoabsorption cross section in the GDR regime, in order to model accurately the  $(\gamma, xn)$  channel data. The photoabsorption cross section above the GDR, up to 140 MeV, was obtained from QD model calculations using the theory of Chadwick.

The calculated results of the emission channels by the GNASH code are in good agreement with the data for the  $(\gamma, 1nx)$ ,  $(\gamma, 2nx)$  and  $(\gamma, xn)$  cross sections.



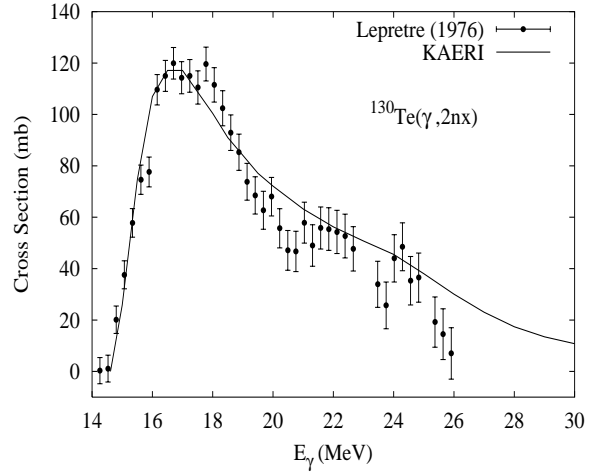
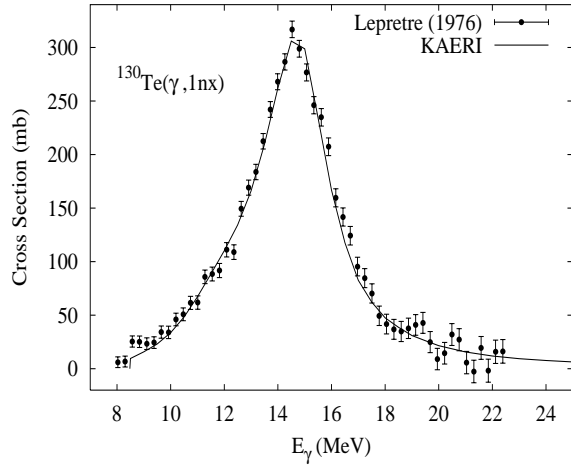
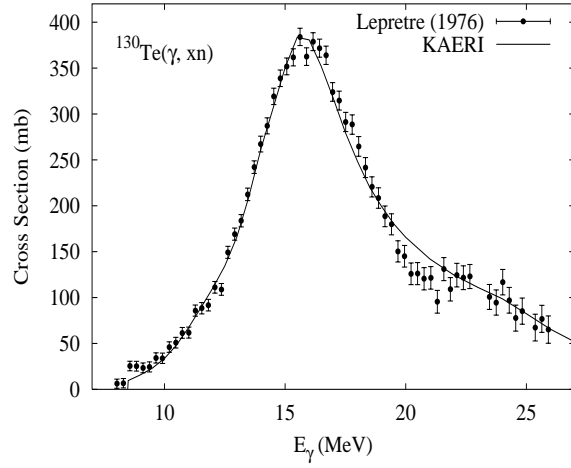
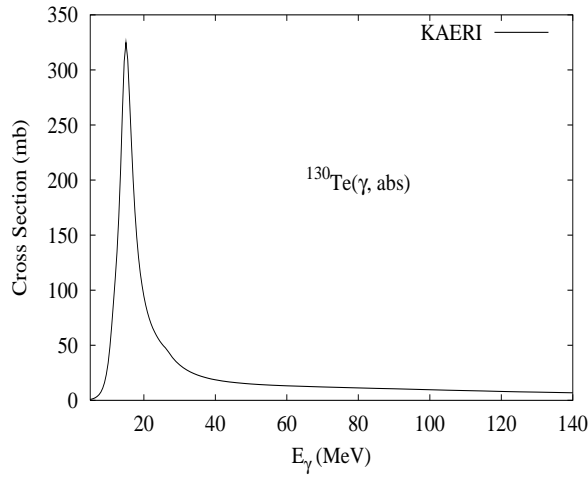
Abundance (%)	Threshold Energies (MeV)								
	$\gamma, n$	$\gamma, p$	$\gamma, t$	$\gamma, \text{He-3}$	$\gamma, \alpha$	$\gamma, 2n$	$\gamma, np$	$\gamma, 2p$	$\gamma, 3n$
31.70	8.78	9.58	15.68	18.02	3.18	15.07	17.95	17.55	24.18



The photoabsorption cross section has not been measured. However, there are experimental data for the  $(\gamma, 1nx)$ ,  $(\gamma, 2nx)$  and  $(\gamma, xn)$  reaction cross sections [Lep76]. We relied on the GUNF and GNASH codes to infer the photoabsorption cross section in the GDR regime, in order to model accurately the  $(\gamma, xn)$  channel data. The photoabsorption cross section above the GDR, up to 140 MeV, was obtained from QD model calculations using the theory of Chadwick.

The calculated results of the emission channels by the GNASH code are in good agreement with the data for the  $(\gamma, 1nx)$ ,  $(\gamma, 2nx)$  and  $(\gamma, xn)$  cross sections.

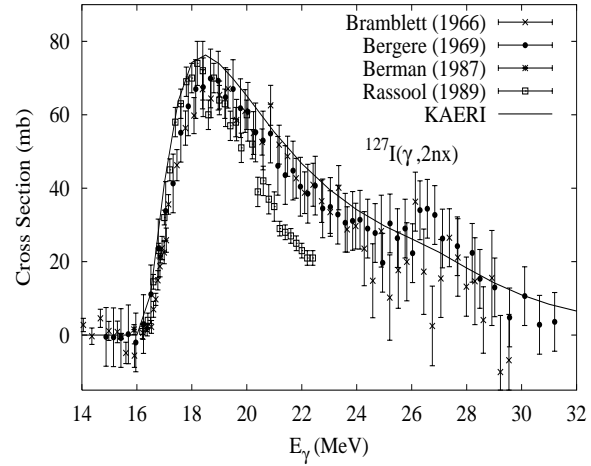
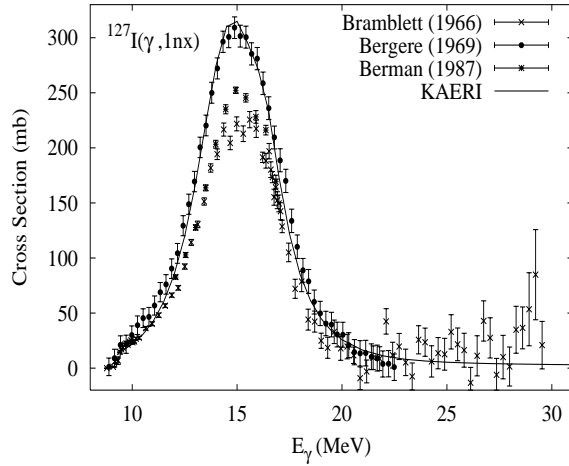
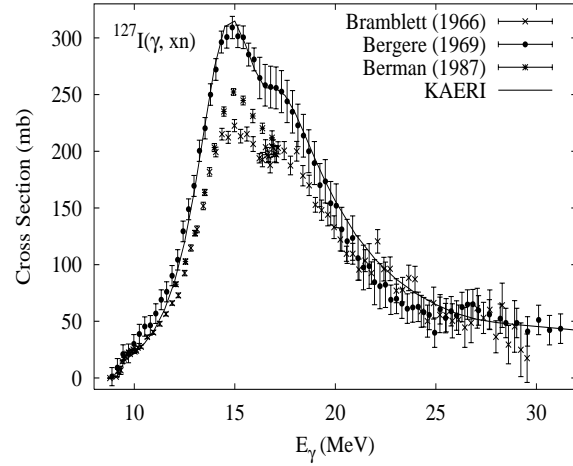
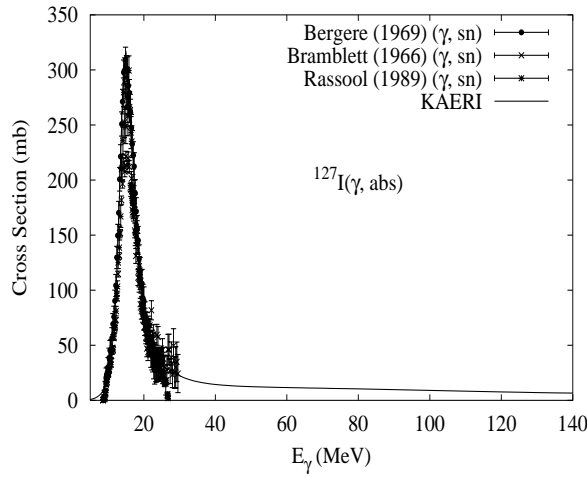
Abundance (%)	Threshold Energies (MeV)								
	$\gamma, n$	$\gamma, p$	$\gamma, t$	$\gamma, \text{He-3}$	$\gamma, \alpha$	$\gamma, 2n$	$\gamma, np$	$\gamma, 2p$	$\gamma, 3n$
33.87	8.41	10.01	15.59	18.78	3.75	14.50	18.10	18.60	23.28



The photoabsorption cross section has not been measured. However, there are experimental data for the  $(\gamma, 1nx)$ ,  $(\gamma, 2nx)$  and  $(\gamma, xn)$  reaction cross sections [Lep76]. We relied on the GUNF and GNASH codes to infer the photoabsorption cross section in the GDR regime, in order to model accurately the  $(\gamma, xn)$  channel data. The photoabsorption cross section above the GDR, up to 140 MeV, was obtained from QD model calculations using the theory of Chadwick.

The calculated results of the emission channels by the GNASH code are in good agreement with the data for the  $(\gamma, 1nx)$ ,  $(\gamma, 2nx)$  and  $(\gamma, xn)$  cross sections.

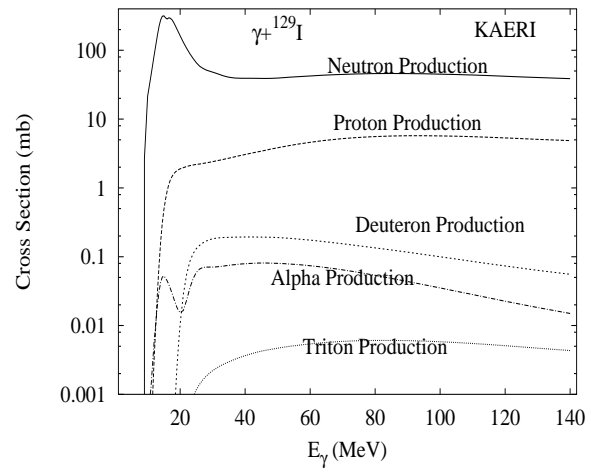
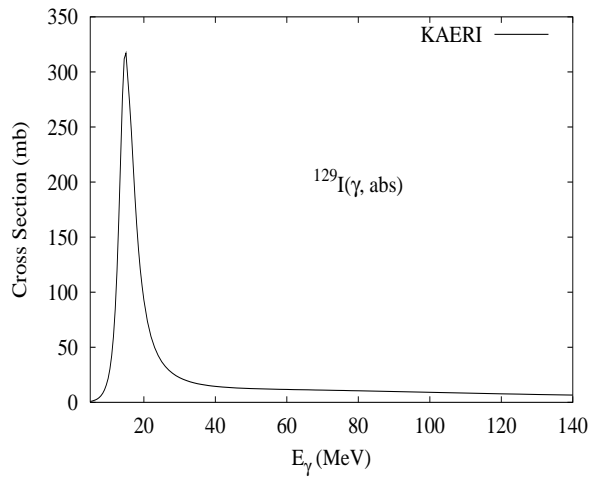
Abundance (%)	Threshold Energies (MeV)								
	$\gamma, n$	$\gamma, p$	$\gamma, t$	$\gamma, \text{He-3}$	$\gamma, \alpha$	$\gamma, 2n$	$\gamma, np$	$\gamma, 2p$	$\gamma, 3n$
100.00	9.14	6.20	13.41	16.29	2.18	16.28	15.32	15.30	25.83



The photoabsorption cross section has not been measured. However, there are experimental data for the  $(\gamma, 1nx)$ ,  $(\gamma, 2nx)$ ,  $(\gamma, sn)$  and  $(\gamma, xn)$  reaction cross sections, from Bramblett [Bra66], Bergere [Ber69a] and Berman [Ber87]. Bramblett also reported the  $(\gamma, 3nx)$  cross section, and Rassool [Ras89] the  $(\gamma, 2nx)$  and  $(\gamma, xn)$  cross sections. All the measurements present good agreement as the shapes of the cross sections are concerned, but not in their magnitudes. Bramblett's and Rassool's data have good agreement in the magnitude of the  $(\gamma, sn)$  cross section. We relied on the GUNF and GNASH codes to infer the photoabsorption cross section in the GDR regime, in order to model accurately Bramblett's  $(\gamma, sn)$  data. The photoabsorption cross section above the GDR, up to 140 MeV, was obtained from QD model calculations using the theory of Chadwick.

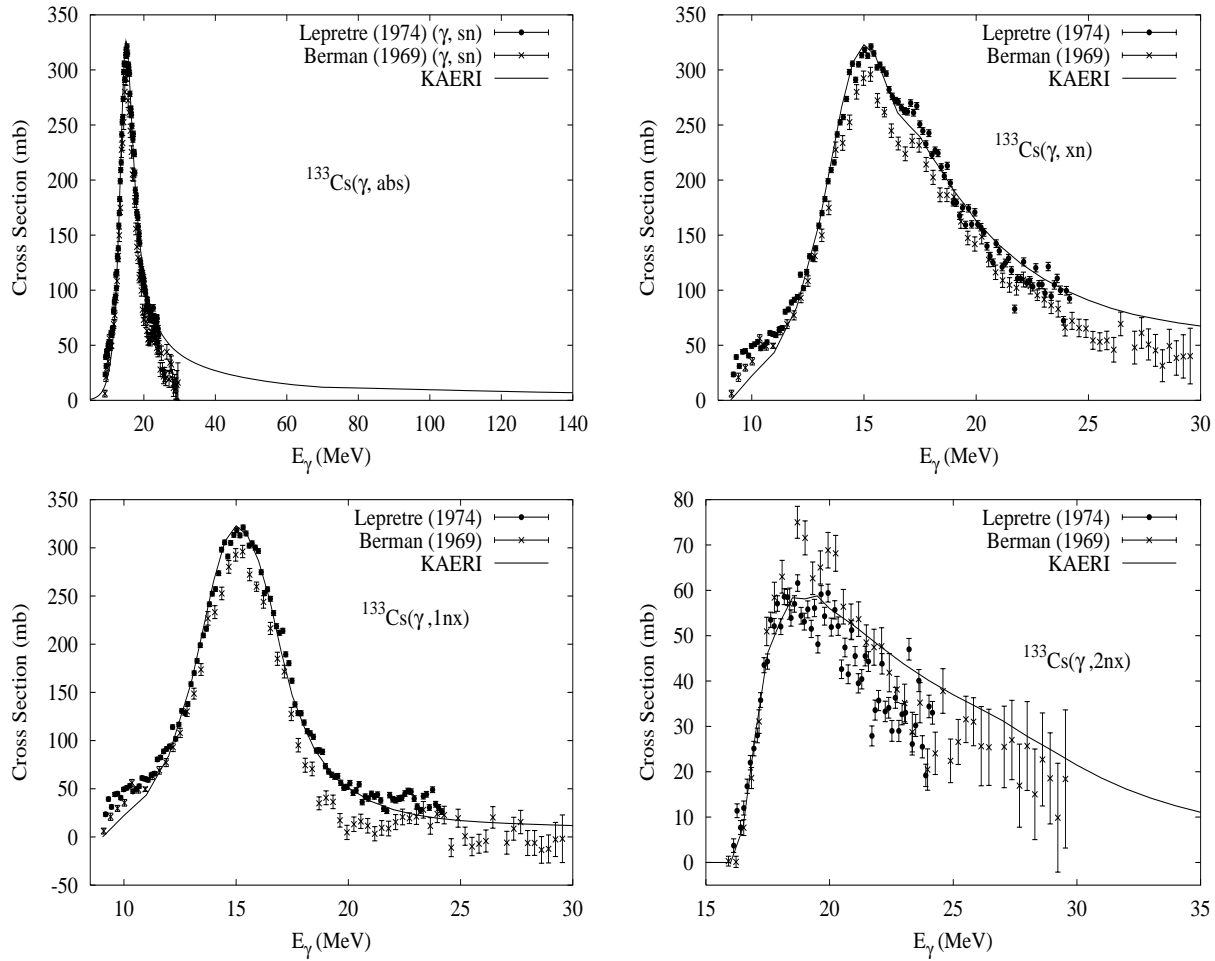
The calculated results of the emission channels by the GNASH code are in good agreement with Bramblett's experimental data for the  $(\gamma, 1nx)$ ,  $(\gamma, 2nx)$ , and  $(\gamma, xn)$  cross sections.

Abundance (%)	Threshold Energies (MeV)								
	$\gamma, n$	$\gamma, p$	$\gamma, t$	$\gamma, \text{He-3}$	$\gamma, \alpha$	$\gamma, 2n$	$\gamma, np$	$\gamma, 2p$	$\gamma, 3n$
0.00	8.84	6.80	13.39	17.04	2.67	15.67	15.58	16.38	24.81



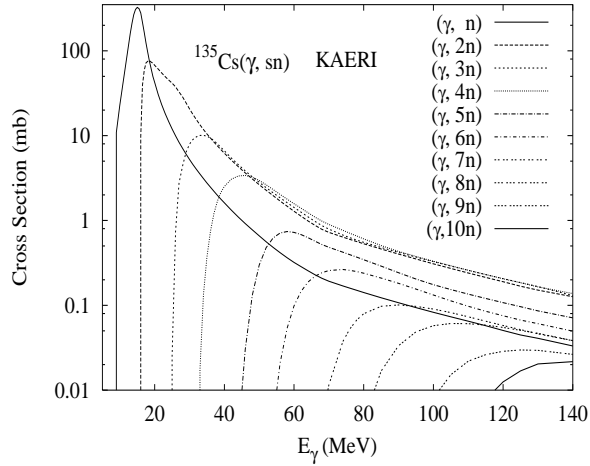
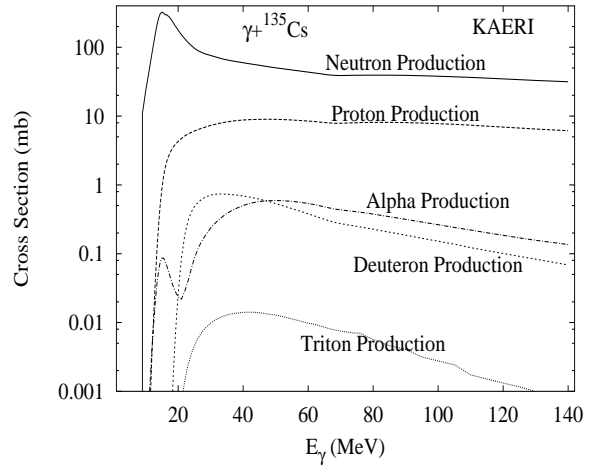
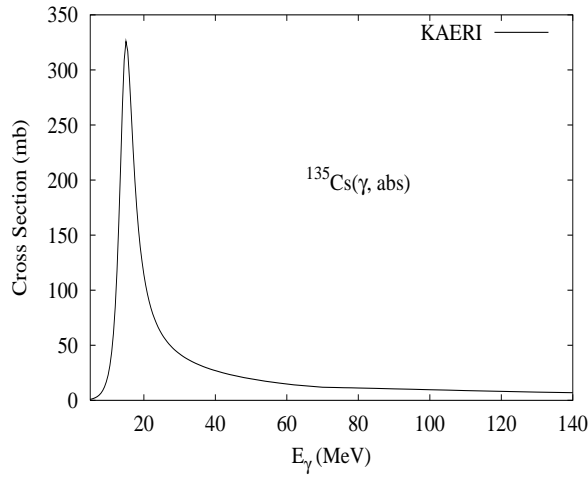
There are no experimental data available. The photoabsorption cross section was obtained from GDR and QD model calculations, adopting the GDR parameters of  ${}^{127}\text{I}$ . The neutron, proton, deuteron, triton and alpha emission cross sections, as well as production cross sections, were calculated by the GNASH code.

Abundance (%)	Threshold Energies (MeV)								
	$\gamma, n$	$\gamma, p$	$\gamma, t$	$\gamma, \text{He-3}$	$\gamma, \alpha$	$\gamma, 2n$	$\gamma, np$	$\gamma, 2p$	$\gamma, 3n$
100.00	8.99	6.08	13.15	16.12	2.00	16.15	15.02	15.21	25.45



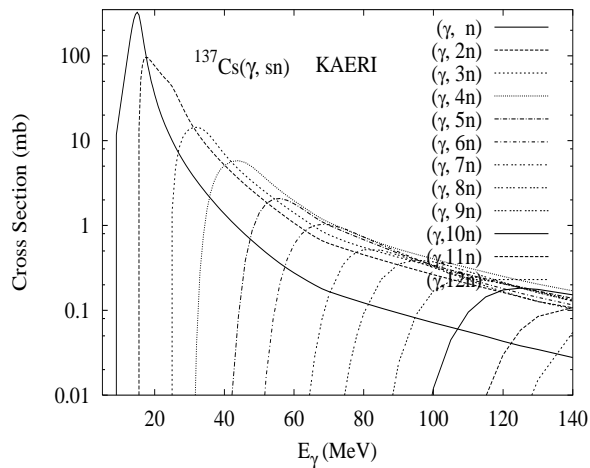
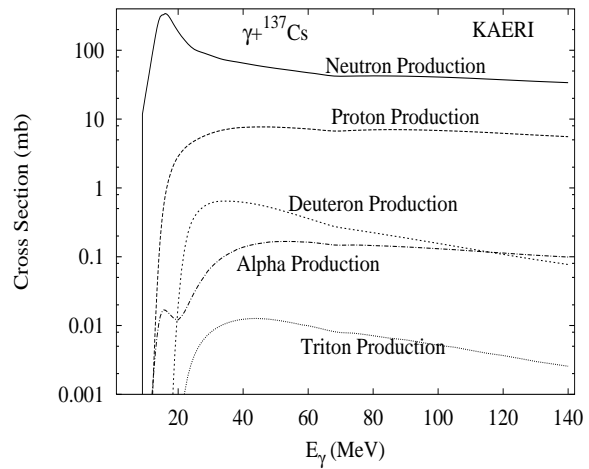
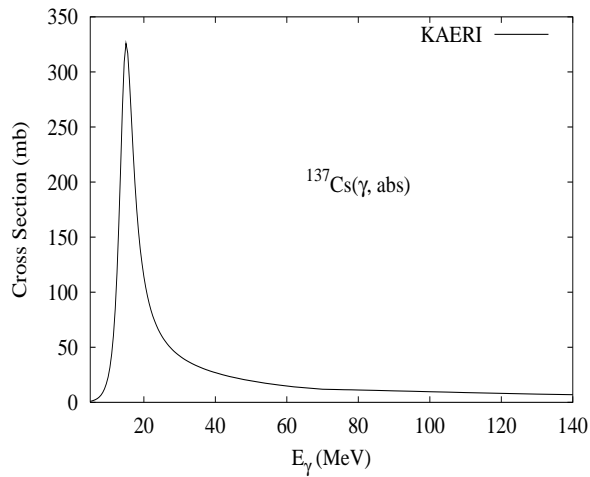
The photoabsorption cross section has not been measured. However, there are experimental data for the  $(\gamma, 1nx)$ ,  $(\gamma, 2nx)$ ,  $(\gamma, sn)$  and  $(\gamma, xn)$  reaction cross sections [Lep74, Ber69b]. Berman also reported the  $(\gamma, 3nx)$  cross section. All the measurements present good agreement as the shapes of the cross sections are concerned, but not in their magnitudes. However, based on the analysis [Mar97, Wol84] of the systematic differences between Saclay and Livermore data, Lepretre's measurements were used as reference. We relied on the GUNF and GNASH codes to infer the photoabsorption cross section in the GDR regime, in order to model accurately Lepretre's  $(\gamma, sn)$  data. The photoabsorption cross section above the GDR, up to 140 MeV, was obtained from QD model calculations using the theory of Chadwick. The calculated results of the emission channels by the GNASH code are in good agreement with the experimental data of Lepretre for  $(\gamma, 1nx)$ ,  $(\gamma, 2nx)$ , and  $(\gamma, xn)$  cross sections.

Abundance (%)	Threshold Energies (MeV)								
	$\gamma, n$	$\gamma, p$	$\gamma, t$	$\gamma, \text{He-3}$	$\gamma, \alpha$	$\gamma, 2n$	$\gamma, np$	$\gamma, 2p$	$\gamma, 3n$
0.00	8.83	6.83	13.32	16.88	2.63	15.72	15.36	16.35	24.71



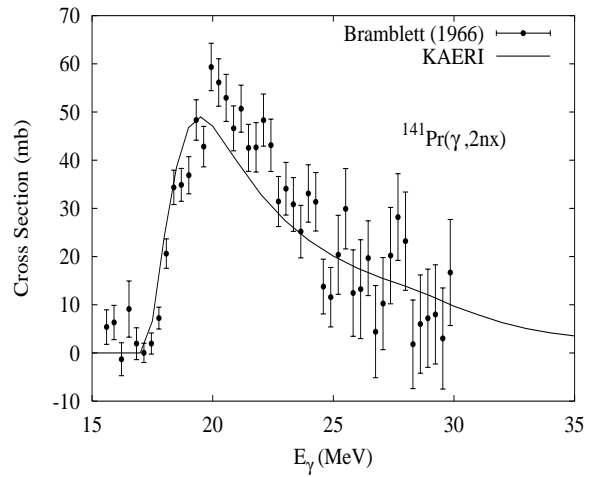
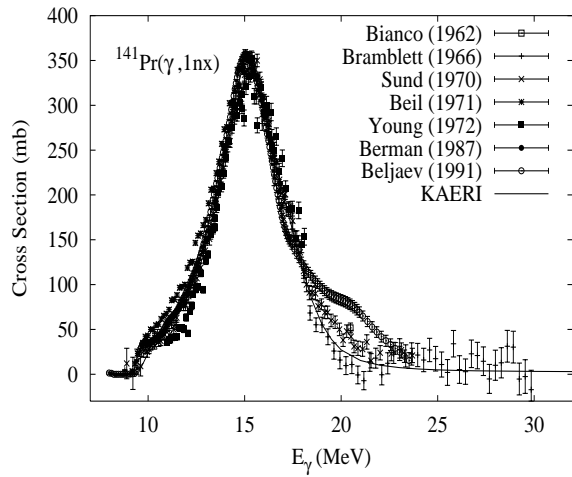
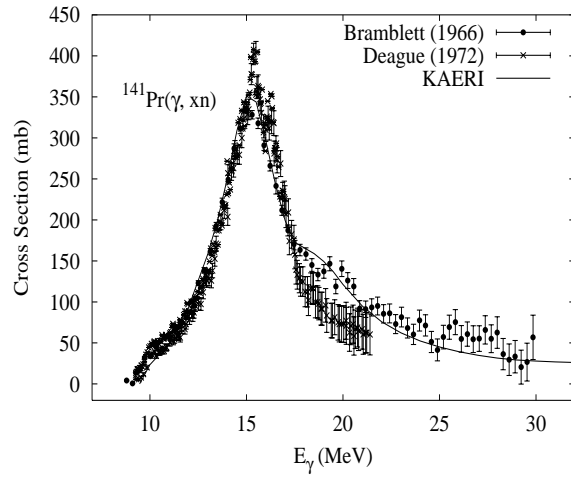
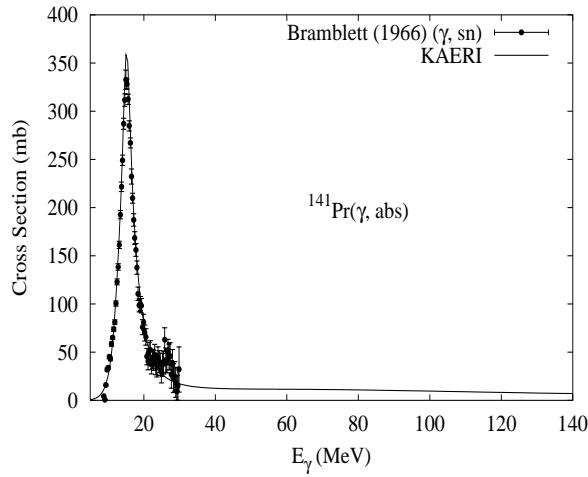
There are no experimental data available. The photoabsorption cross section was obtained from GDR and QD model calculations, adopting the GDR parameters of  ${}^{133}\text{Cs}$ . The neutron, proton, deuteron, triton and alpha emission cross sections, as well as production cross sections, were calculated by the GNASH code.

Abundance (%)	Threshold Energies (MeV)								
	$\gamma, n$	$\gamma, p$	$\gamma, t$	$\gamma, \text{He-3}$	$\gamma, \alpha$	$\gamma, 2n$	$\gamma, np$	$\gamma, 2p$	$\gamma, 3n$
0.00	8.27	7.42	13.38	17.50	3.09	15.04	15.41	17.31	23.86



There are no experimental data available. The photoabsorption cross section was obtained from GDR and QD model calculations, adopting the GDR parameters of  ${}^{133}\text{Cs}$ . The neutron, proton, deuteron, triton and alpha emission cross sections, as well as production cross sections, were calculated by the GNASH code.

Abundance (%)	Threshold Energies (MeV)								
	$\gamma, n$	$\gamma, p$	$\gamma, t$	$\gamma, \text{He-3}$	$\gamma, \alpha$	$\gamma, 2n$	$\gamma, np$	$\gamma, 2p$	$\gamma, 3n$
100.00	9.40	5.23	13.40	14.43	1.32	17.32	14.41	13.37	27.10

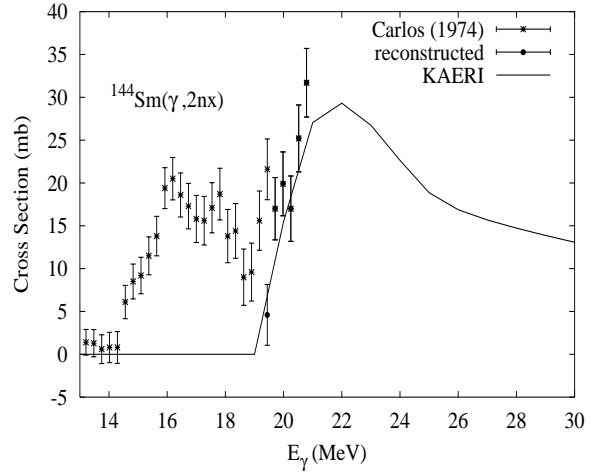
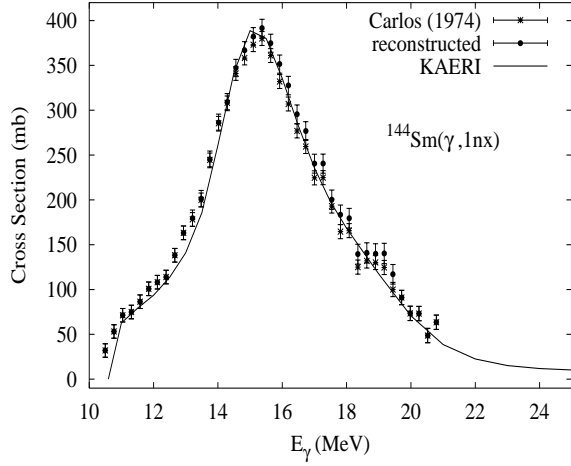
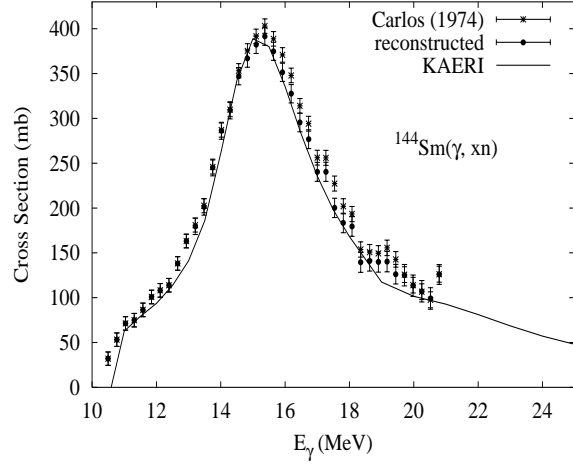
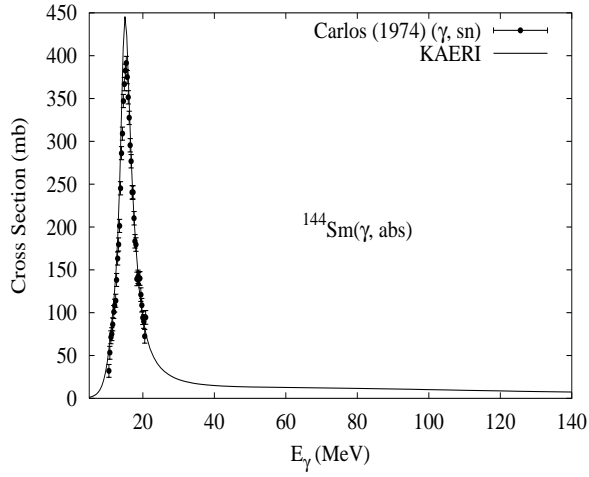


The photoabsorption cross section has not been measured. However, there are six different measurements of the  $(\gamma, 1nx)$  reaction cross section [Bia62, Bra66, Sun70, Bei71, You72, Ber87, Bel91]. Bramblett also measured the  $(\gamma, 2nx)$ ,  $(\gamma, 3nx)$ ,  $(\gamma, sn)$  and  $(\gamma, xn)$  cross sections. Deague [Dea72] measured the  $(\gamma, xn)$  reaction cross section [Dea72]. Bramblett's measurements were chosen as the reference data, since most of the photoneutron reactions were included. We relied on the GUNF and GNASH codes to infer the photoabsorption cross section in the GDR regime, in order to model accurately Bramblett's  $(\gamma, 1nx)$  data. The photoabsorption cross section above the GDR, up to 140 MeV, was obtained from QD model calculations using the theory of Chadwick.

The calculated results of the emission channels by the GNASH code are in good agreement with the Bramblett data for the  $(\gamma, 1nx)$ ,  $(\gamma, 2nx)$ ,  $(\gamma, sn)$ , and  $(\gamma, xn)$  cross sections.



Abundance (%)	Threshold Energies (MeV)								
	$\gamma, n$	$\gamma, p$	$\gamma, t$	$\gamma, \text{He-3}$	$\gamma, \alpha$	$\gamma, 2n$	$\gamma, np$	$\gamma, 2p$	$\gamma, 3n$
3.10	10.52	6.29	16.45	12.70	-0.07	19.13	16.25	10.59	30.25

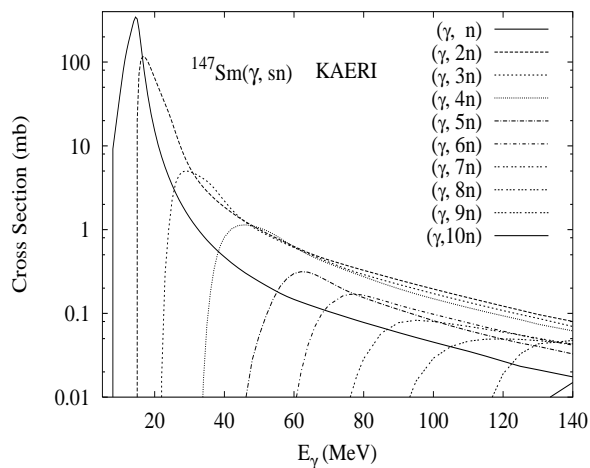
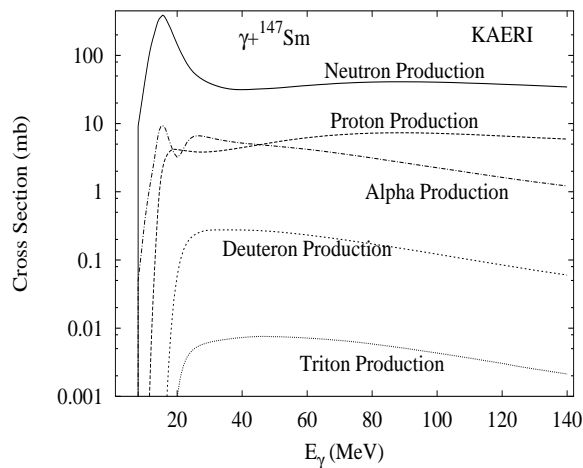
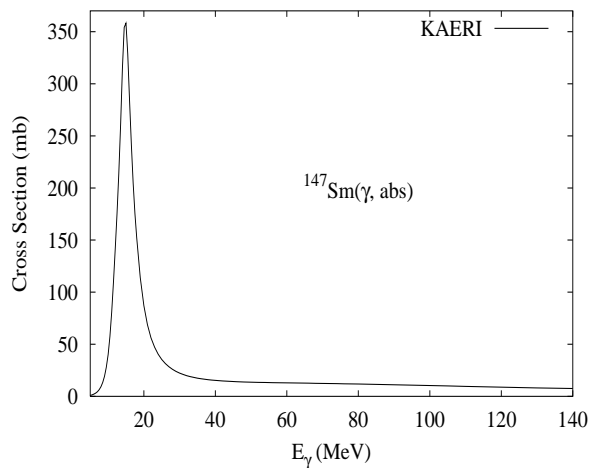


The photoabsorption cross section has not been measured. However, there are experimental data for the  $(\gamma, 1nx)$ ,  $(\gamma, 2nx)$ ,  $(\gamma, sn)$  and  $(\gamma, xn)$  reaction cross section [Car74]. However, the  $(\gamma, 2nx)$  reaction data do not correspond to the threshold energy of  $(\gamma, 2n+2np)$ , 19.13 MeV. The  $(\gamma, 1nx)$ ,  $(\gamma, 2nx)$  and  $(\gamma, xn)$  reaction data were fixed by converting  $(\gamma, 2nx)$  cross sections below the threshold energy into the  $(\gamma, 1nx)$  cross sections. We relied on the GUNF and GNASH codes to infer the photoabsorption cross section in the GDR regime, in order to model accurately the  $(\gamma, sn)$  reaction data. The photoabsorption cross section above the GDR, up to 140 MeV, was obtained from QD model calculations using the theory of Chadwick.

The calculated results of the emission channels by the GNASH code are in good agreement with the fixed experimental data for  $(\gamma, 1nx)$ ,  $(\gamma, 2nx)$  and  $(\gamma, xn)$  reaction cross sections.

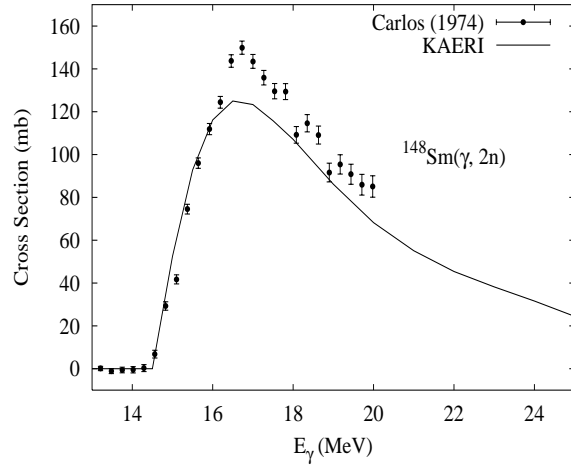
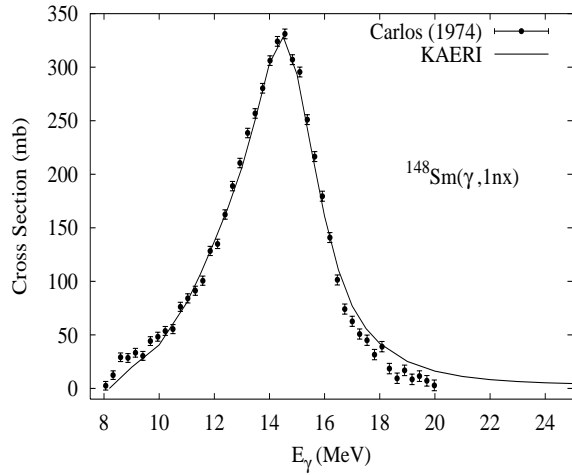
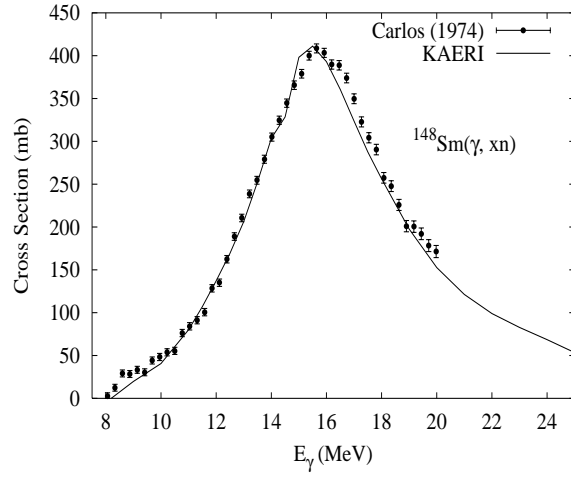
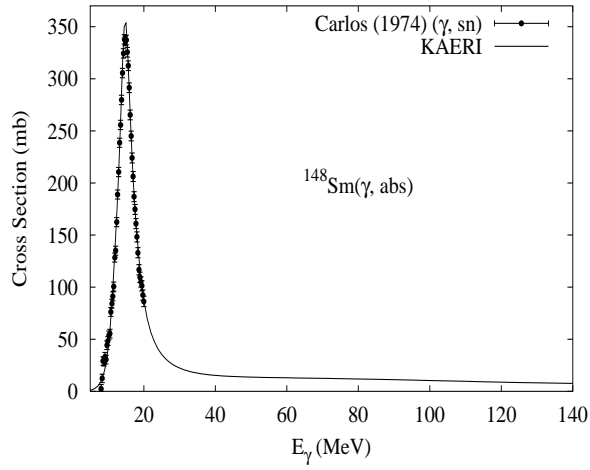
$\gamma + {}^{147}\text{Sm}$ 

Abundance (%)	Threshold Energies (MeV)								
	$\gamma, n$	$\gamma, p$	$\gamma, t$	$\gamma, \text{He-3}$	$\gamma, \alpha$	$\gamma, 2n$	$\gamma, np$	$\gamma, 2p$	$\gamma, 3n$
15.00	6.35	7.11	12.80	10.45	-2.31	14.76	13.36	12.41	21.52



There are no experimental data available. The photoabsorption cross section was obtained from GDR and QD model calculations, adopting the GDR parameters of  ${}^{148}\text{Sm}$ . The neutron, proton, deuteron, triton and alpha emission cross sections, as well as production cross sections, were calculated by the GNASH code.

Abundance (%)	Threshold Energies (MeV)								
	$\gamma, n$	$\gamma, p$	$\gamma, t$	$\gamma, \text{He-3}$	$\gamma, \alpha$	$\gamma, 2n$	$\gamma, np$	$\gamma, 2p$	$\gamma, 3n$
11.30	8.14	7.58	13.02	12.84	-1.99	14.49	15.25	12.99	22.90

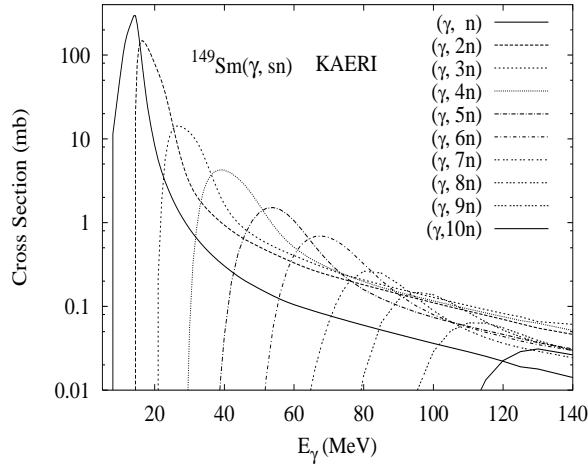
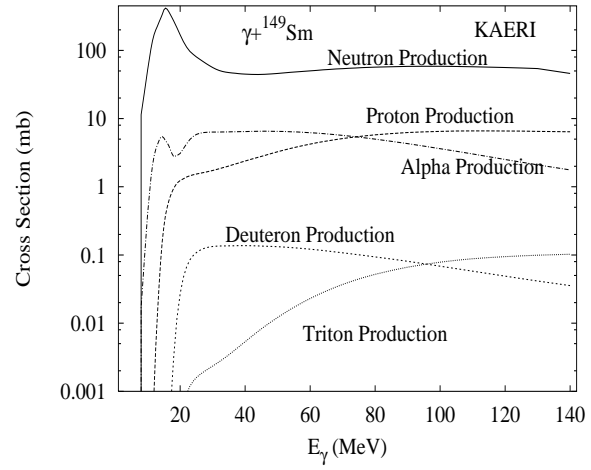
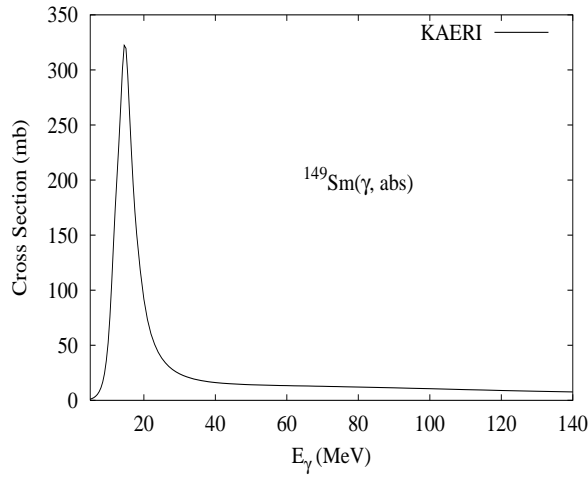


The photoabsorption cross section has not been measured. However, there are experimental data for the  $(\gamma, 1nx)$ ,  $(\gamma, 2nx)$ ,  $(\gamma, sn)$  and  $(\gamma, xn)$  reaction cross sections [Car74]. We relied on the GUNF and GNASH codes to infer the photoabsorption cross section in the GDR regime, in order to model accurately the  $(\gamma, sn)$  data. The photoabsorption cross section above the GDR, up to 140 MeV, was obtained from QD model calculations using the theory of Chadwick.

The calculated results of the emission channels by the GNASH code are in good agreement with the data for the  $(\gamma, 1nx)$ ,  $(\gamma, 2nx)$  and  $(\gamma, xn)$  cross sections.

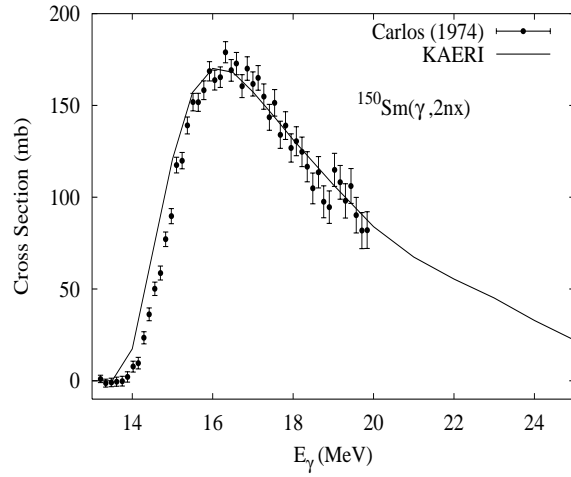
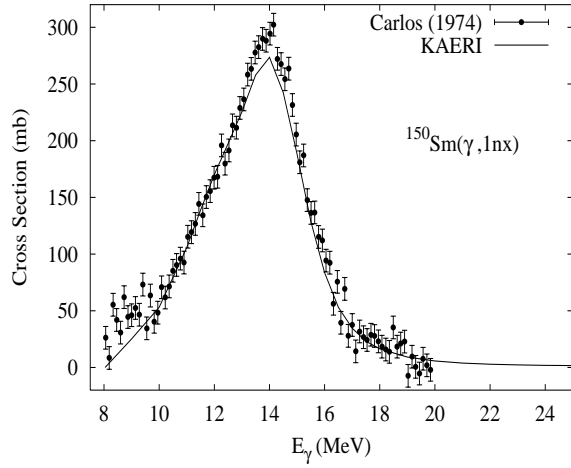
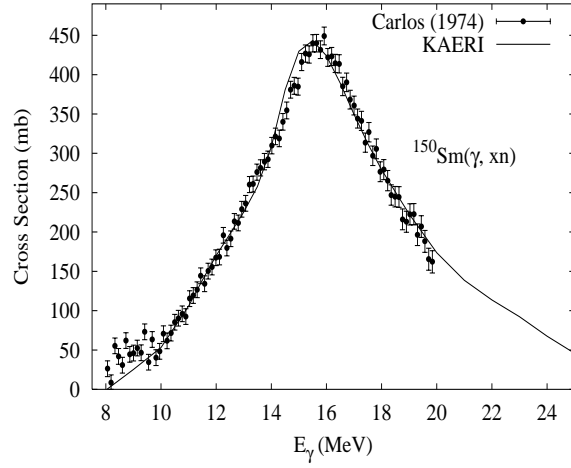
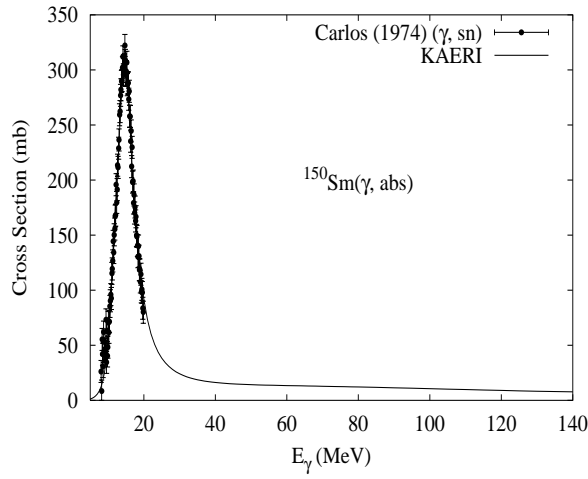
# $\gamma + {}^{149}\text{Sm}$

Abundance (%)	Threshold Energies (MeV)								
	$\gamma, n$	$\gamma, p$	$\gamma, t$	$\gamma, \text{He-3}$	$\gamma, \alpha$	$\gamma, 2n$	$\gamma, np$	$\gamma, 2p$	$\gamma, 3n$
13.80	5.87	7.56	12.64	11.14	-1.87	14.01	13.45	13.57	20.36



There are no experimental data available. The photoabsorption cross section was obtained from GDR and QD model calculations, adopting the GDR parameters of  ${}^{150}\text{Sm}$ . The neutron, proton, deuteron, triton and alpha emission cross sections, as well as production cross sections, were calculated by the GNASH code.

Abundance (%)	Threshold Energies (MeV)								
	$\gamma, n$	$\gamma, p$	$\gamma, t$	$\gamma, \text{He-3}$	$\gamma, \alpha$	$\gamma, 2n$	$\gamma, np$	$\gamma, 2p$	$\gamma, 3n$
7.40	7.99	8.28	12.96	13.84	-1.45	13.86	15.55	14.22	22.00

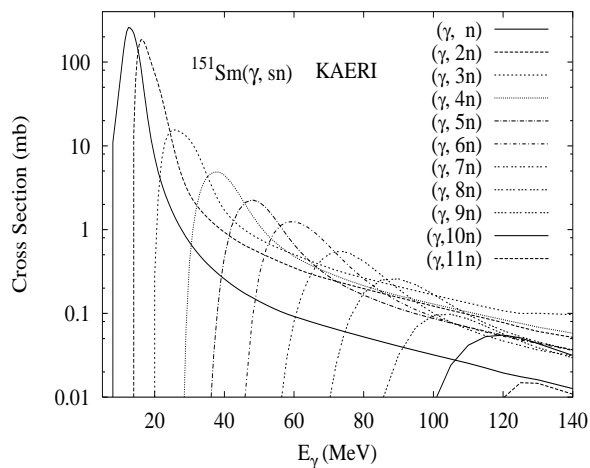
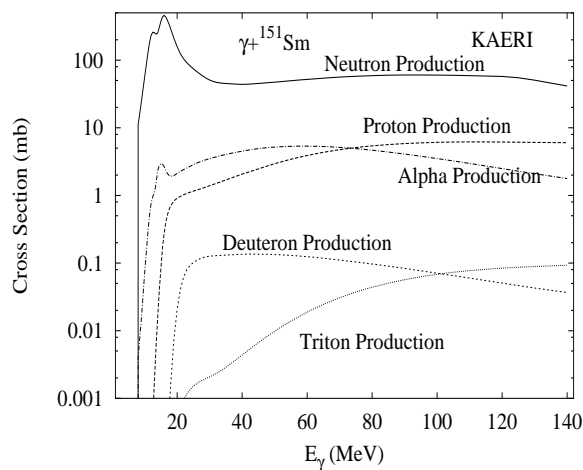
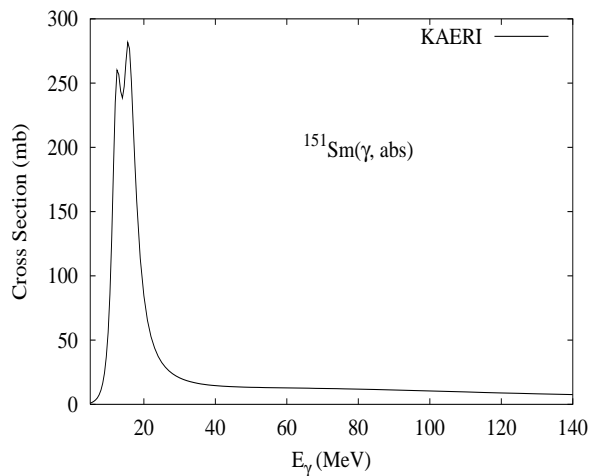


The photoabsorption cross section has not been measured. However, there are experimental data for the  $(\gamma, 1nx)$ ,  $(\gamma, 2nx)$ ,  $(\gamma, sn)$  and  $(\gamma, xn)$  reaction cross sections [Car74]. We relied on the GUNF and GNASH codes to infer the photoabsorption cross section in the GDR regime, in order to model accurately the  $(\gamma, sn)$  data. The photoabsorption cross section above the GDR, up to 140 MeV, was obtained from QD model calculations using the theory of Chadwick.

The calculated results of the emission channels by the GNASH code are in good agreement with the data for the  $(\gamma, 1nx)$ ,  $(\gamma, 2nx)$  and  $(\gamma, xn)$  cross sections.

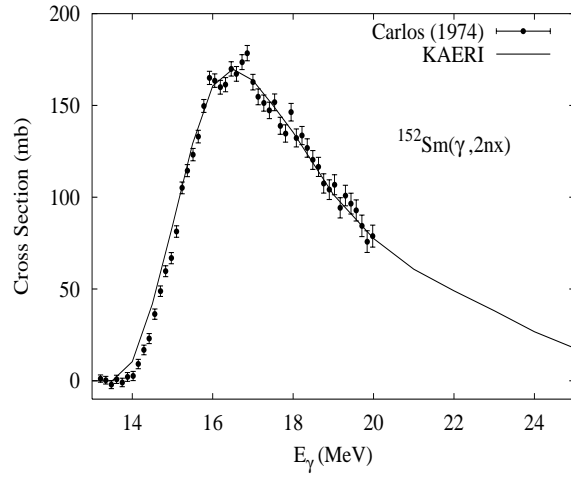
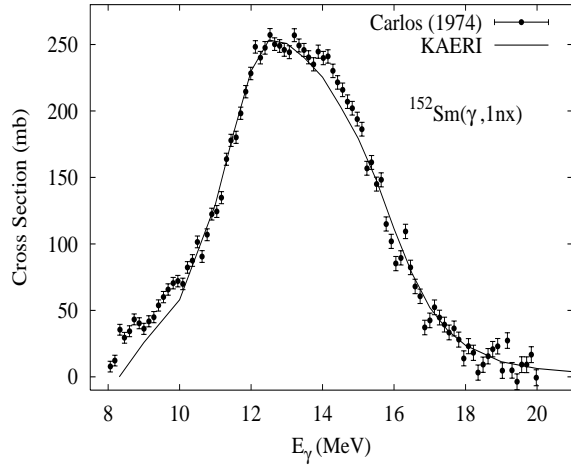
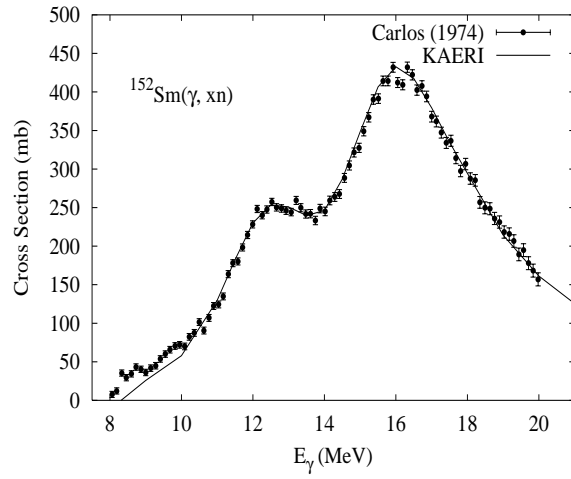
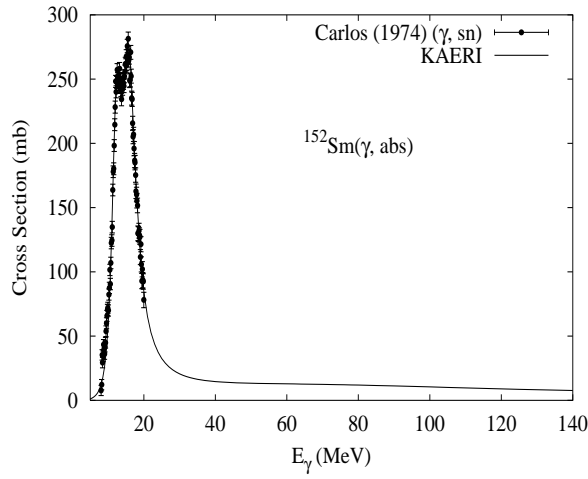
$\gamma + {}^{151}\text{Sm}$ 

Abundance (%)	Threshold Energies (MeV)								
	$\gamma, n$	$\gamma, p$	$\gamma, t$	$\gamma, \text{He-3}$	$\gamma, \alpha$	$\gamma, 2n$	$\gamma, np$	$\gamma, 2p$	$\gamma, 3n$
0.00	5.60	8.27	12.66	12.10	-1.14	13.58	13.87	14.78	19.46



There are no experimental data available. The photoabsorption cross section was obtained from GDR and QD model calculations, adopting the GDR parameters of  ${}^{152}\text{Sm}$ . The neutron, proton, deuteron, triton and alpha emission cross sections, as well as production cross sections, were calculated by the GNASH code.

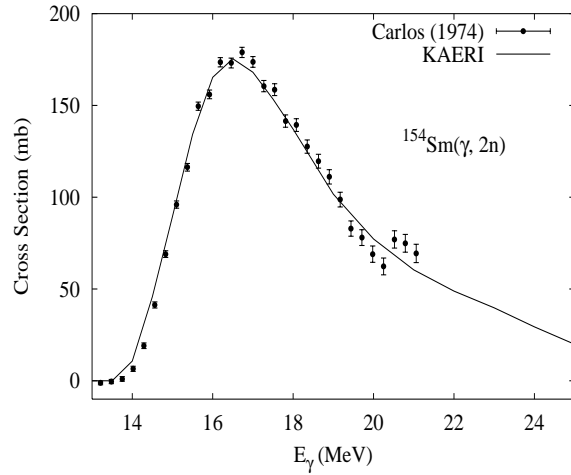
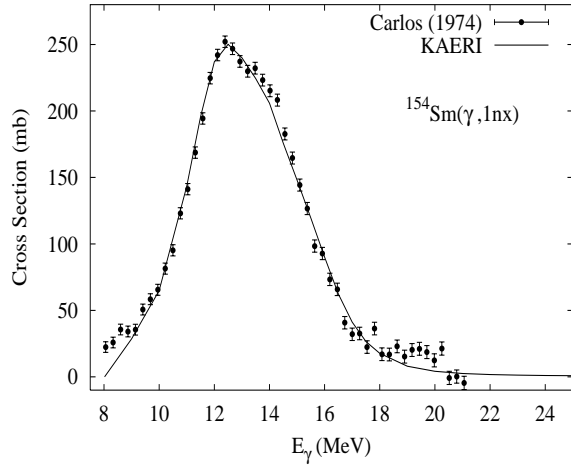
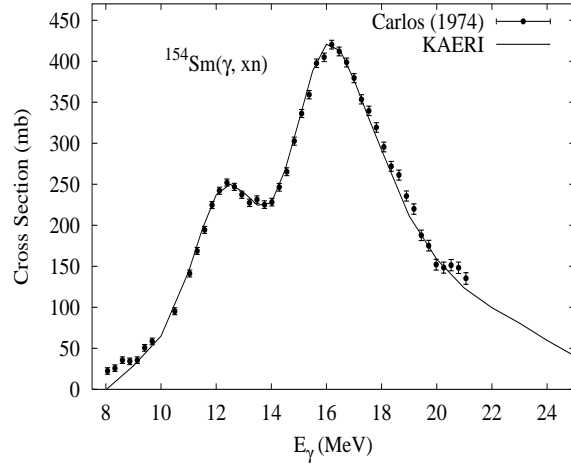
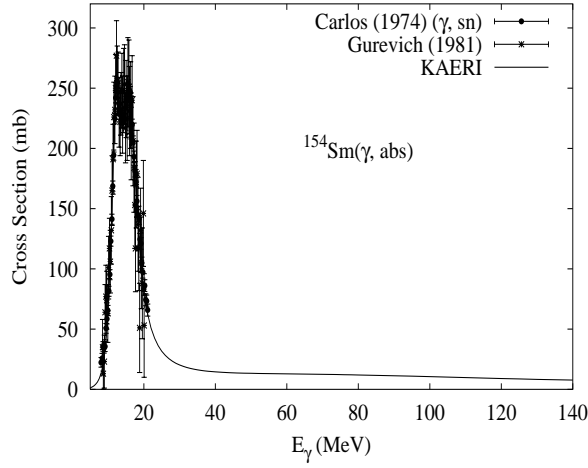
Abundance (%)	Threshold Energies (MeV)								
	$\gamma, n$	$\gamma, p$	$\gamma, t$	$\gamma, \text{He-3}$	$\gamma, \alpha$	$\gamma, 2n$	$\gamma, np$	$\gamma, 2p$	$\gamma, 3n$
26.70	8.26	8.66	13.65	15.32	-0.22	13.86	16.53	15.66	21.84



The photoabsorption cross section has not been measured. However, there are experimental data for the  $(\gamma, 1nx)$ ,  $(\gamma, 2nx)$ ,  $(\gamma, sn)$  and  $(\gamma, xn)$  reaction cross sections [Car74]. We relied on the GUNF and GNASH codes to infer the photoabsorption cross section in the GDR regime, in order to model accurately the  $(\gamma, sn)$  data. The photoabsorption cross section above the GDR, up to 140 MeV, was obtained from QD model calculations using the theory of Chadwick.

The calculated results of the emission channels by the GNASH code are in good agreement with the data for the  $(\gamma, 1nx)$ ,  $(\gamma, 2nx)$  and  $(\gamma, xn)$  cross sections.

Abundance (%)	Threshold Energies (MeV)								
	$\gamma, n$	$\gamma, p$	$\gamma, t$	$\gamma, \text{He-3}$	$\gamma, \alpha$	$\gamma, 2n$	$\gamma, np$	$\gamma, 2p$	$\gamma, 3n$
22.70	7.97	9.09	14.02	16.44	1.20	13.83	16.56	16.88	22.09

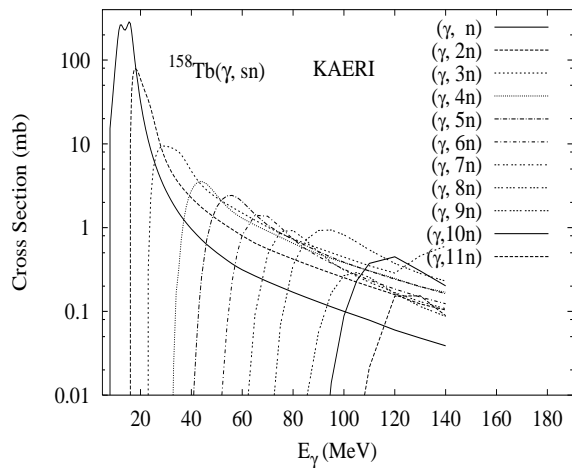
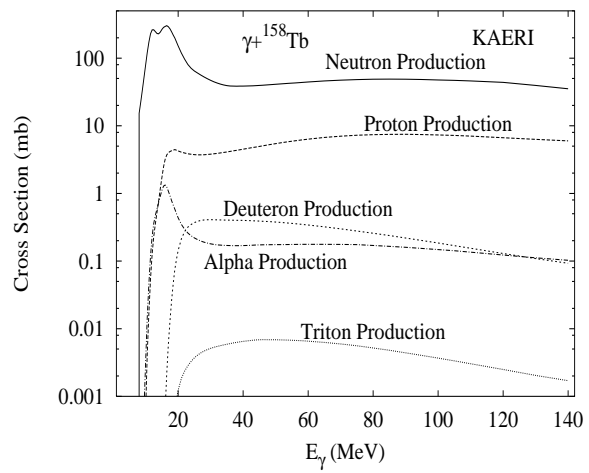
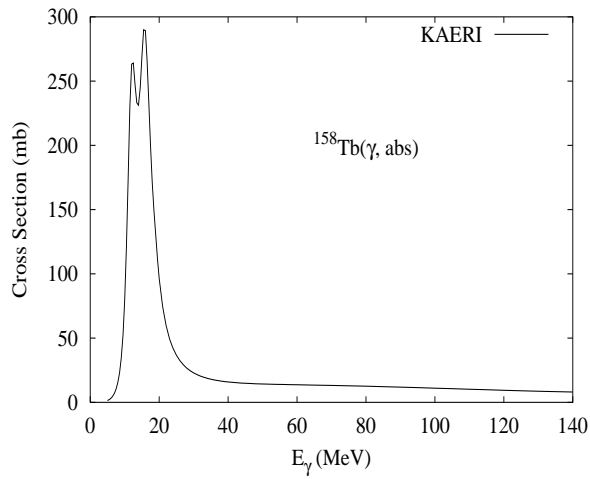


The experimental data for absorption cross section were given by Gurevich [Gur81]. Carlos [Car74] measured the  $(\gamma, 1nx)$ ,  $(\gamma, 2nx)$ ,  $(\gamma, sn)$  and  $(\gamma, xn)$  reaction cross section. Gurevich's absorption cross section has larger errors than Carlos's  $(\gamma, sn)$  data. We relied on the GUNF and GNASH codes to infer the photoabsorption cross section in the GDR regime, in order to model accurately Carlos's  $(\gamma, sn)$  data. The photoabsorption cross section above the GDR, up to 140 MeV, was taken from QD model calculations.

The calculated results of the emission channels by the GNASH code are in good agreement with the experimental data for  $(\gamma, 1nx)$ ,  $(\gamma, 2nx)$  and  $(\gamma, xn)$  reaction cross sections.

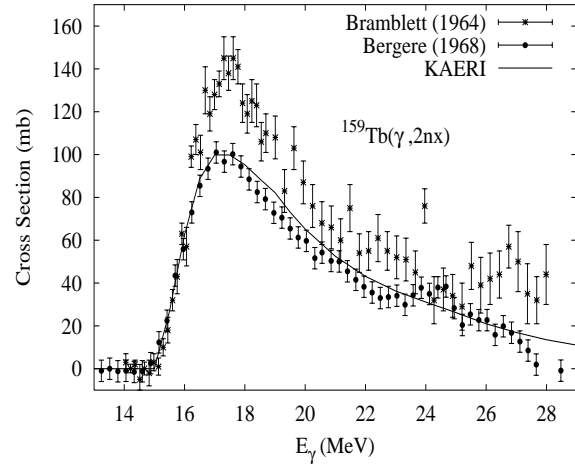
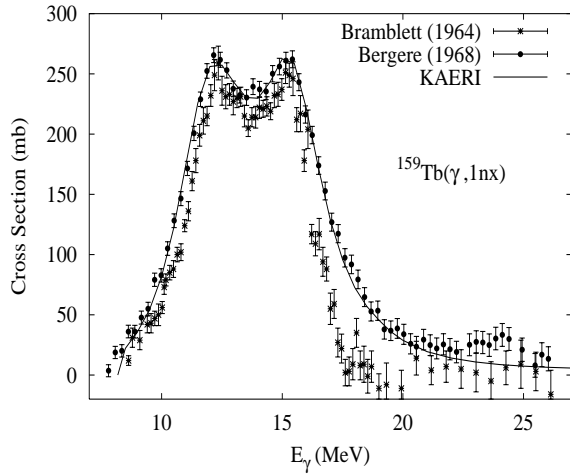
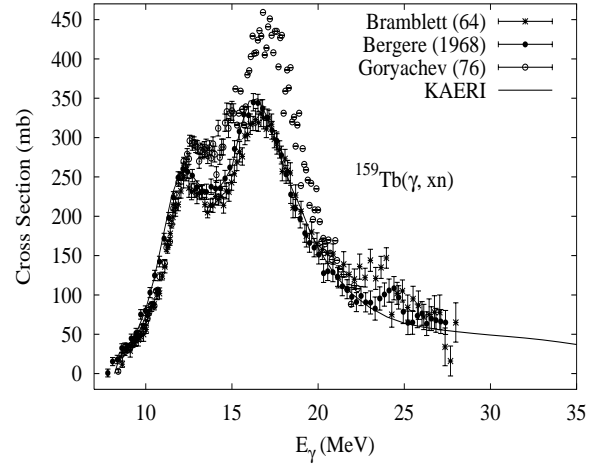
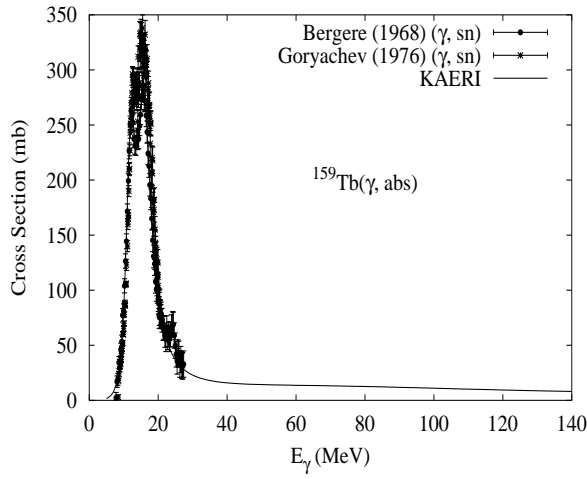


Abundance (%)	Threshold Energies (MeV)								
	$\gamma, n$	$\gamma, p$	$\gamma, t$	$\gamma, \text{He-3}$	$\gamma, \alpha$	$\gamma, 2n$	$\gamma, np$	$\gamma, 2p$	$\gamma, 3n$
0.00	6.78	5.94	12.35	12.58	0.16	15.52	12.29	13.96	22.43



There are no experimental data available. The photoabsorption cross section was obtained from GDR and QD model calculations, adopting the GDR parameters of  ${}^{159}\text{Tb}$ . The neutron, proton, deuteron, triton and alpha emission cross sections, as well as production cross sections, were calculated by the GNASH code.

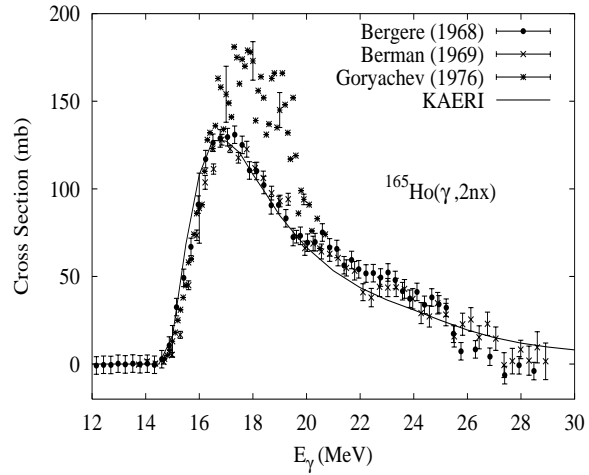
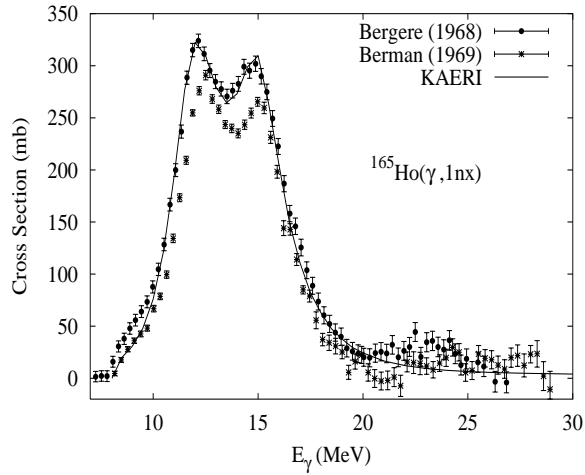
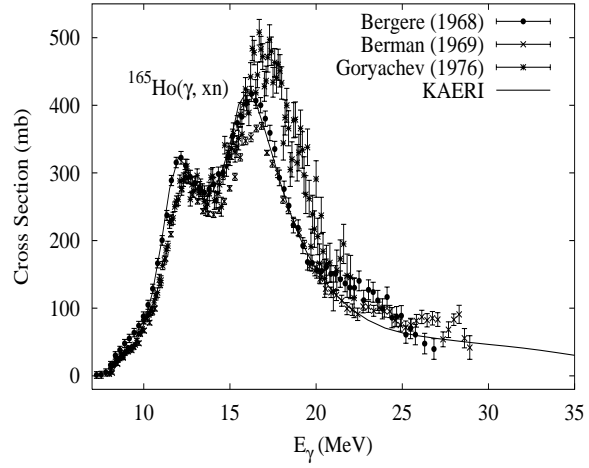
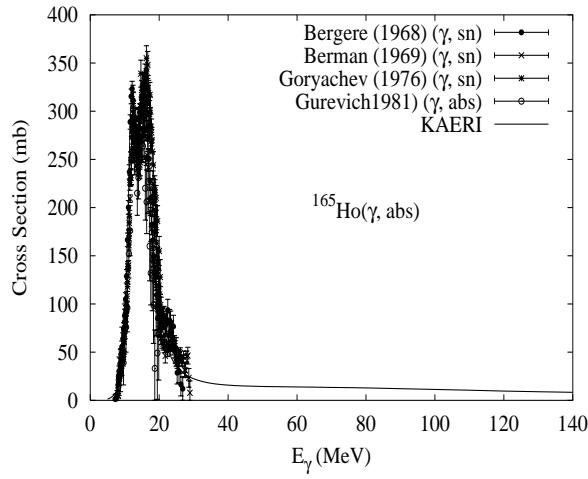
Abundance (%)	Threshold Energies (MeV)								
	$\gamma, n$	$\gamma, p$	$\gamma, t$	$\gamma, \text{He-3}$	$\gamma, \alpha$	$\gamma, 2n$	$\gamma, np$	$\gamma, 2p$	$\gamma, 3n$
100.00	8.13	6.13	11.95	14.38	0.14	14.91	14.07	14.65	23.65



The photoabsorption cross section has not been measured. However, there are experimental data for the  $(\gamma, 1nx)$ ,  $(\gamma, 2nx)$  and  $(\gamma, xn)$  reaction cross sections [Bra64, Ber68]. Bergere also reported the  $(\gamma, sn)$  cross section, and Goryachev [Gor76] reported both the  $(\gamma, sn)$  and  $(\gamma, xn)$  cross sections. The experiments present good agreement on the shape of the cross sections but their magnitudes are different. We relied on the GUNF and GNASH codes to infer the photoabsorption cross section in the GDR regime, in order to model accurately Bergere's  $(\gamma, sn)$  data. The photoabsorption cross section above the GDR, up to 140 MeV, was obtained from QD model calculations using the theory of Chadwick.

The calculated results of the emission channels by the GNASH code are in good agreement with the Bergere data for the  $(\gamma, 1nx)$ ,  $(\gamma, 2nx)$  and  $(\gamma, xn)$  cross sections.

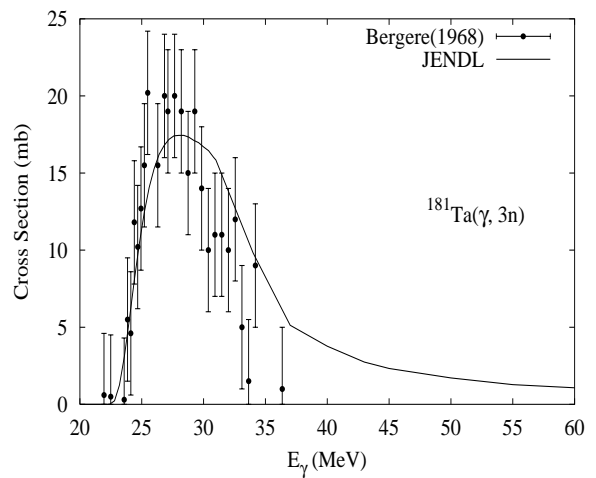
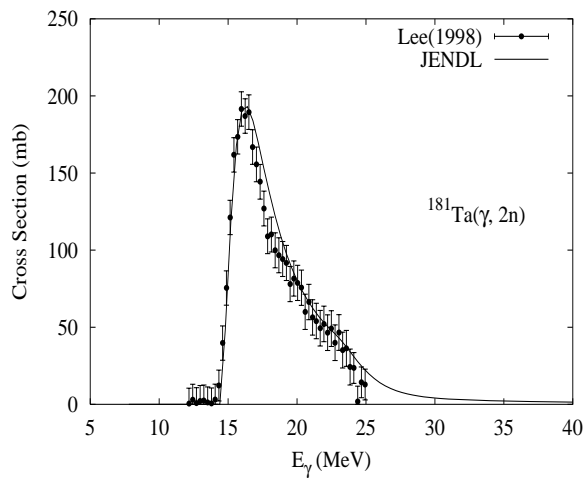
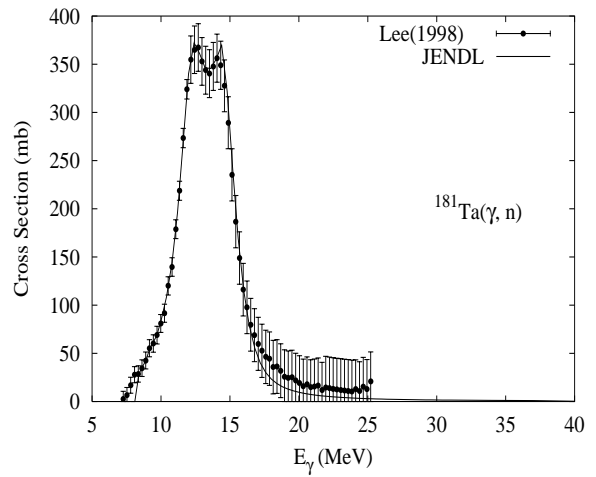
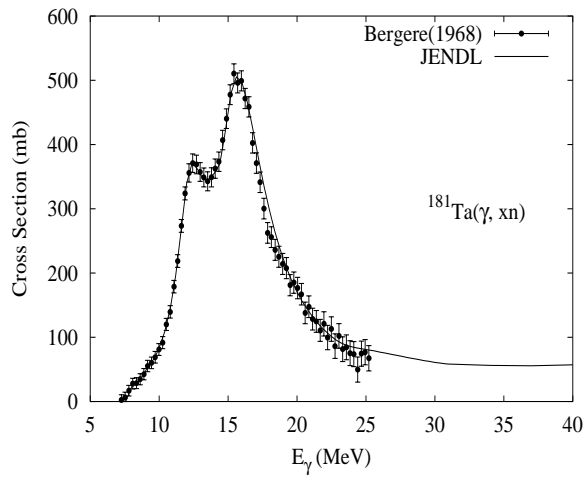
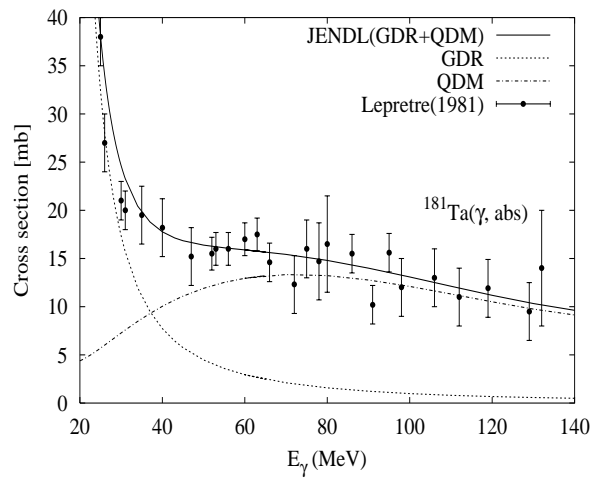
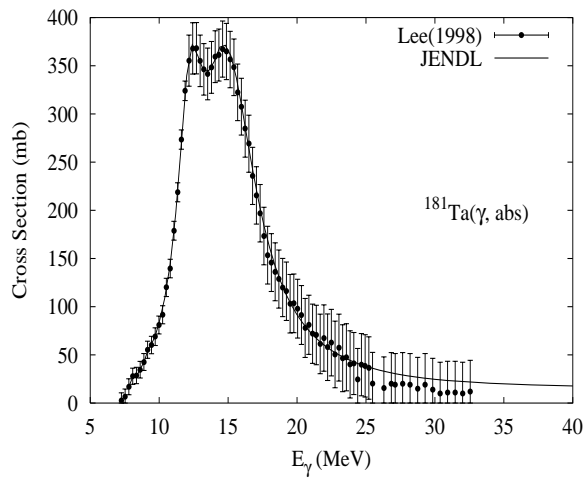
Abundance (%)	Threshold Energies (MeV)								
	$\gamma, n$	$\gamma, p$	$\gamma, t$	$\gamma, \text{He-3}$	$\gamma, \alpha$	$\gamma, 2n$	$\gamma, np$	$\gamma, 2p$	$\gamma, 3n$
100.00	7.99	6.22	11.67	14.16	-0.14	14.66	13.88	14.79	23.07



The photoabsorption cross section was measured by Gurevich [Gur76, Gur80]. Bergere [Ber68] and Berman [Ber69c] measured the  $(\gamma, 1nx)$ ,  $(\gamma, 2nx)$ ,  $(\gamma, 3nx)$ ,  $(\gamma, sn)$  and  $(\gamma, xn)$  reaction cross sections. Goryachev [Gor76] reported results for the  $(\gamma, 2nx)$ ,  $(\gamma, sn)$  and  $(\gamma, xn)$  cross sections. Gurevich's absorption cross sections are lower and have larger errors than the other  $(\gamma, sn)$  data above 10 MeV. We relied on the GUNF and GNASH codes to infer the photoabsorption cross section in the GDR regime, in order to model accurately Bergere's  $(\gamma, sn)$  data. The photoabsorption cross section above the GDR, up to 140 MeV, was obtained from QD model calculations using the theory of Chadwick.

The calculated results of the emission channels by the GNASH code are in good agreement with the Bergere data for the  $(\gamma, 1nx)$ ,  $(\gamma, 2nx)$  and  $(\gamma, xn)$  cross sections.

Abundance (%)	Threshold Energies (MeV)								
	$\gamma, n$	$\gamma, p$	$\gamma, t$	$\gamma, \text{He-3}$	$\gamma, \alpha$	$\gamma, 2n$	$\gamma, np$	$\gamma, 2p$	$\gamma, 3n$
99.99	7.58	5.94	10.95	13.04	-1.53	14.22	13.33	13.91	22.13

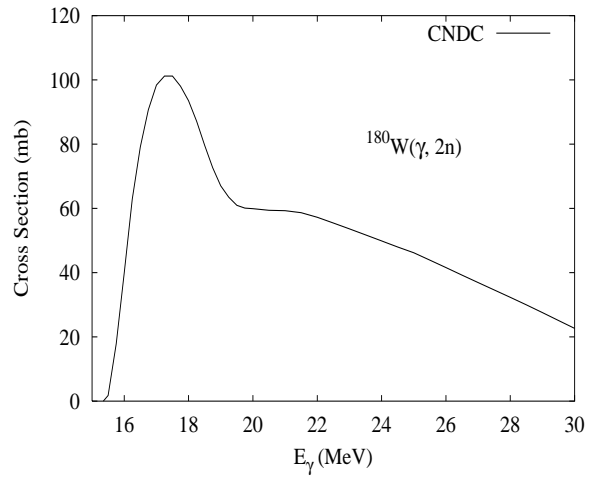
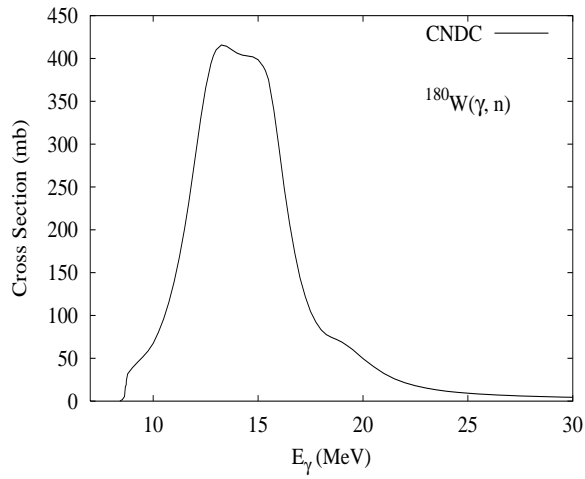
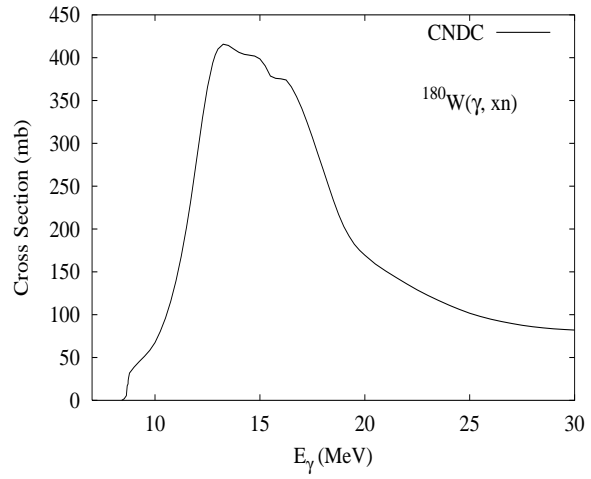
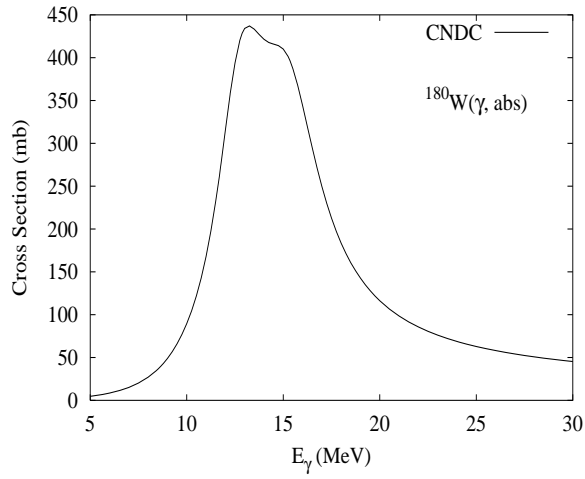


A study by Sao Paulo laboratory [Mar97, Wol84] showed that the differences between the Saclay [Ber68] and Livermore [Bra63] photoneutron cross sections arose from the incomplete separation of the partial cross section from the total neutron counts (neutron multiplicities sorting). It is noted that the neutron multiplicity sorting at Livermore is correct, while the excess ( $\gamma, n$ )

cross section in the Saclay measurement is caused by interpreting each  $(\gamma,2n)$  event as two  $(\gamma,n)$  events. However, the magnitude of the Livermore data is too low by a factor of 1.22. According to these arguments, new reference experimental data for  $(\gamma,n)$  and  $(\gamma,2n)$  are constructed as is  $(\gamma,abs)$  from Livermore measurements, but the  $(\gamma,3n)$  and  $(\gamma,xn)$  Saclay data remain unchanged [Lee98]. The reconstructed photoabsorption cross sections are fitted by the GDR below 40 MeV, and by Levinger parameter of  $L = 6.5$  with the Pauli-blocking effect [Cha91] which reproduces Lepretre's data [Lep81] well.

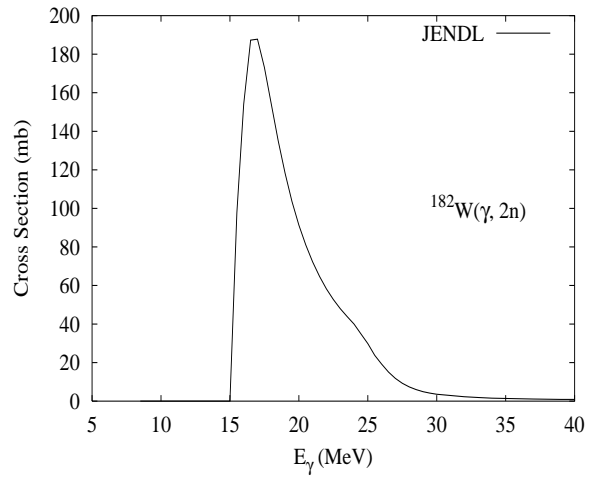
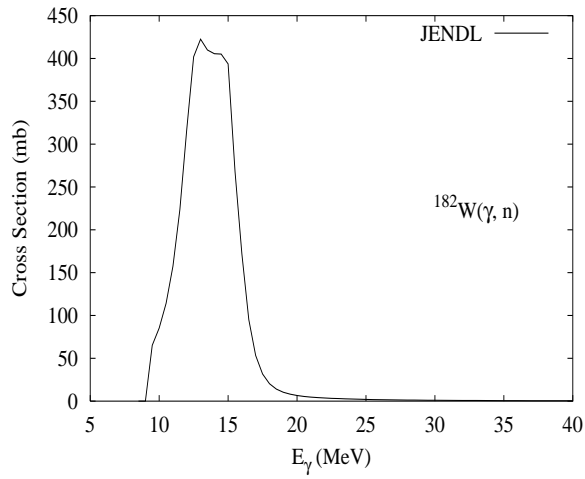
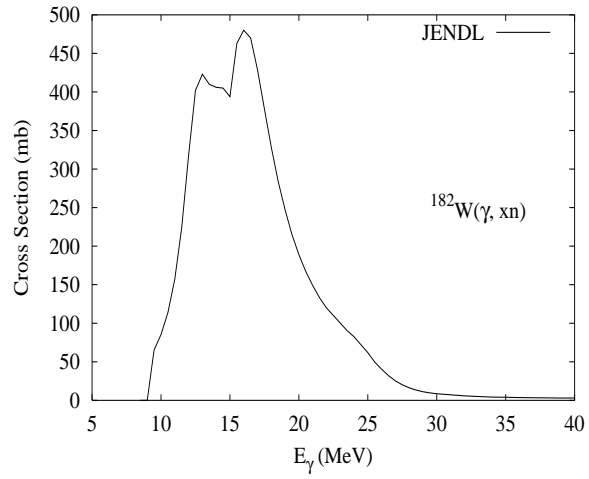
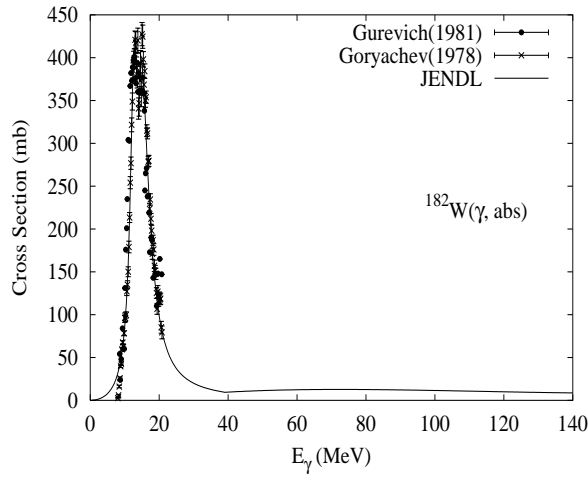
The ALICE-F [Fuk92] code was adopted for the theoretical evaluation of decaying processes by the use of the evaluated photoabsorption cross sections given as input, with the default parameters and options in principle except the level density parameter, which was adjusted as 11. The calculated results reproduce the experimental data of all the photoneutron cross sections consistently.

Abundance (%)	Threshold Energies (MeV)								
	$\gamma, n$	$\gamma, p$	$\gamma, t$	$\gamma, \text{He-3}$	$\gamma, \alpha$	$\gamma, 2n$	$\gamma, np$	$\gamma, 2p$	$\gamma, 3n$
0.12	8.41	6.57	12.87	11.69	-2.51	15.35	14.48	11.78	23.57



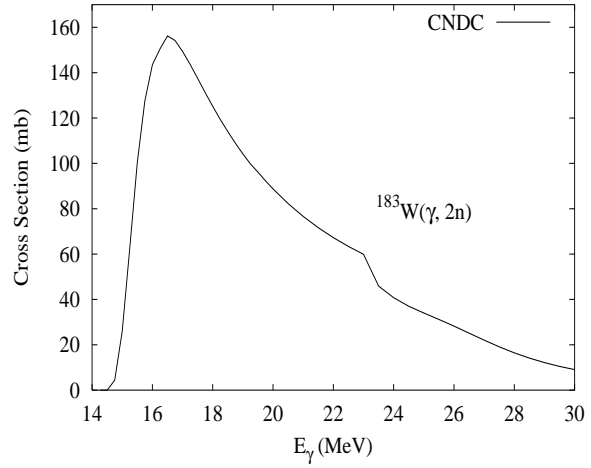
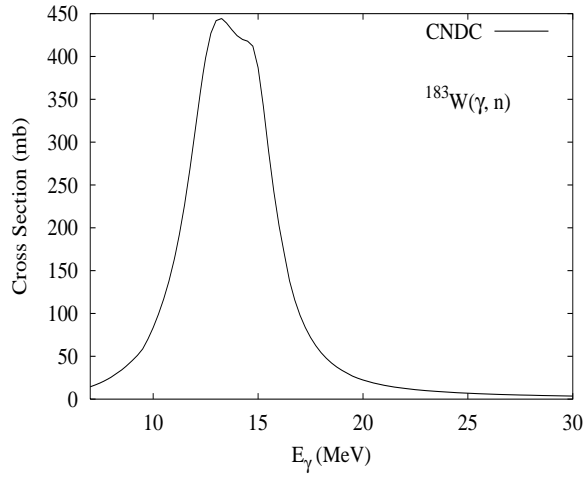
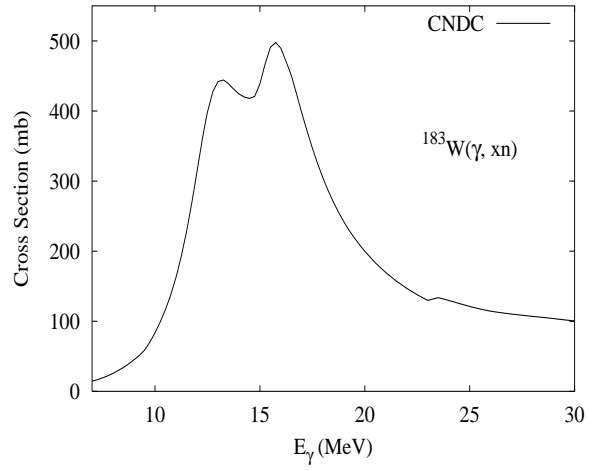
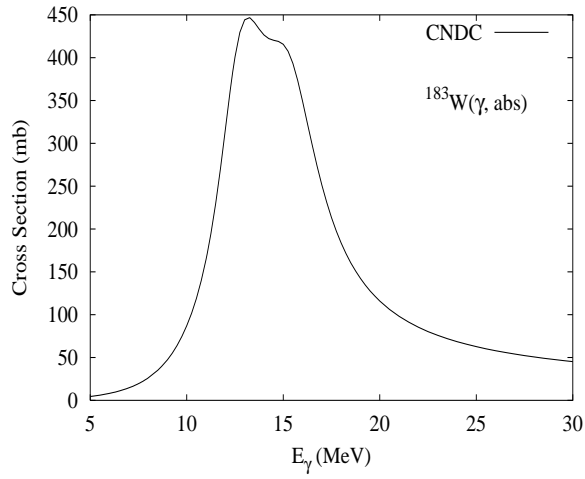
There are no experimental data available. The photoabsorption cross section was obtained from GDR model calculations using the GUNF code [Zha98], adopting the same model parameters of  ${}^{182,184,186}\text{W}$ .

Abundance (%)	Threshold Energies (MeV)								
	$\gamma, n$	$\gamma, p$	$\gamma, t$	$\gamma, \text{He-3}$	$\gamma, \alpha$	$\gamma, 2n$	$\gamma, np$	$\gamma, 2p$	$\gamma, 3n$
26.30	8.07	7.10	12.83	12.71	-1.77	14.75	14.67	13.04	23.16



Photonuclear reactions were evaluated using ALICE-F [Fuk93] code calculations together with experimental data. Input model parameters were adjusted so as to improve the quality of the calculated results compared with data [Gor78, Gur81]. Photoabsorption was modeled as a sum of GDR and QD components [Cha91].

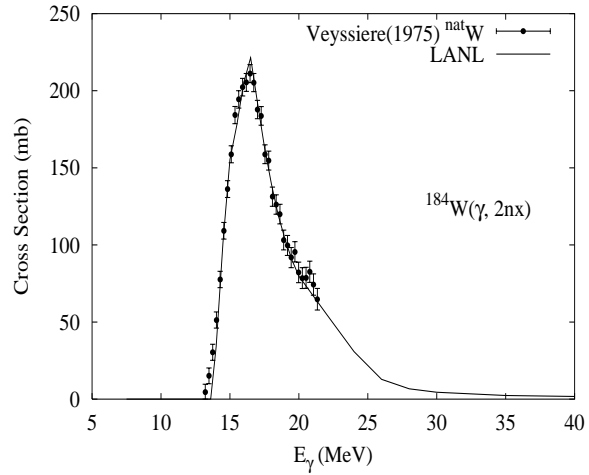
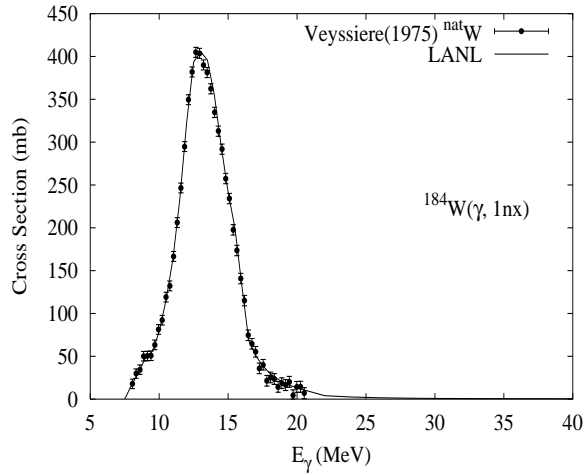
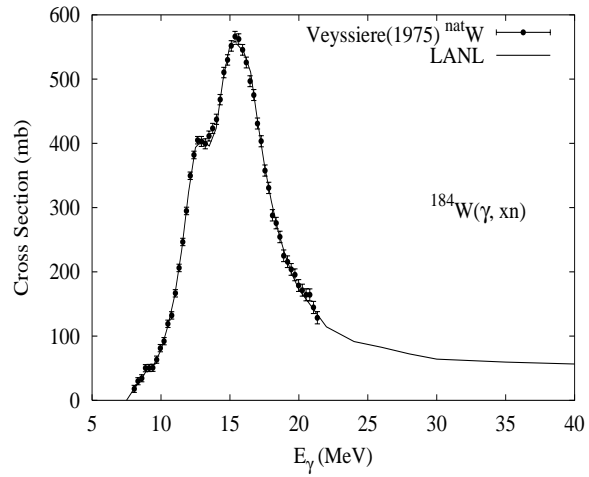
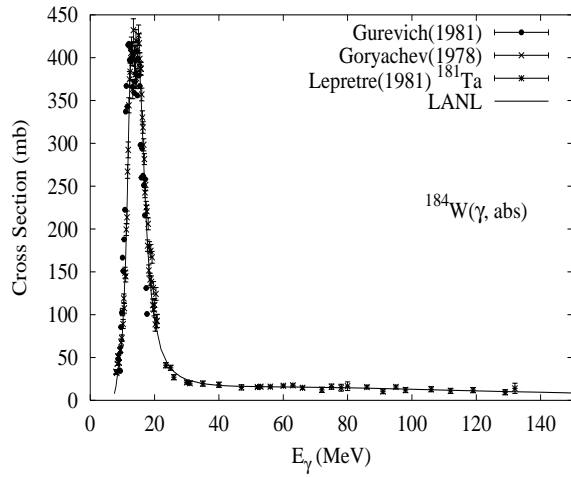
Abundance (%)	Threshold Energies (MeV)								
	$\gamma, n$	$\gamma, p$	$\gamma, t$	$\gamma, \text{He-3}$	$\gamma, \alpha$	$\gamma, 2n$	$\gamma, np$	$\gamma, 2p$	$\gamma, 3n$
14.28	6.19	7.22	12.38	11.51	-1.68	14.26	13.29	13.53	20.94



There are no experimental data available. The photoabsorption cross section was obtained from GDR model calculations using the GUNF code [Zha98], adopting the same model parameters of  ${}^{182,184,186}\text{W}$ .

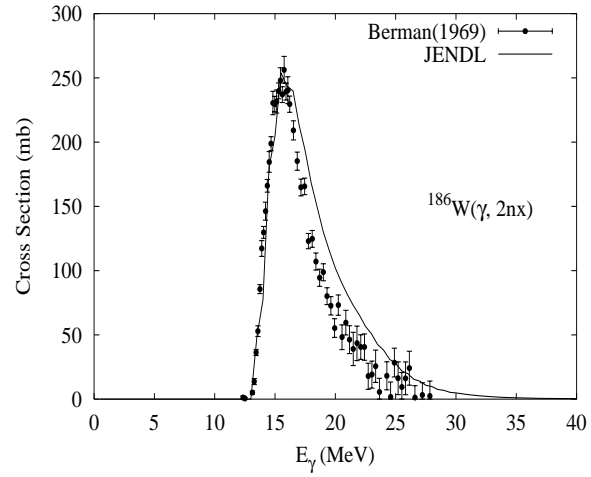
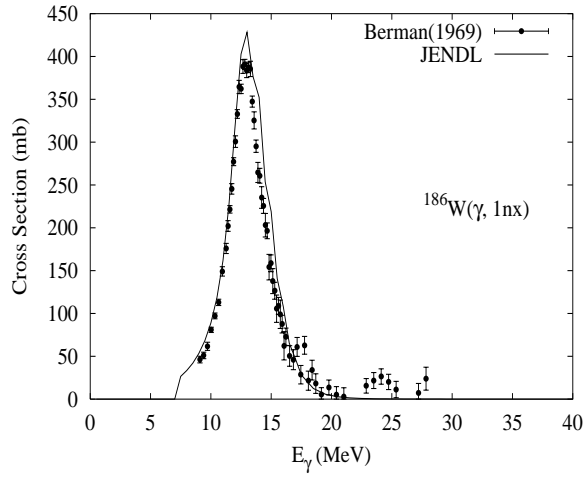
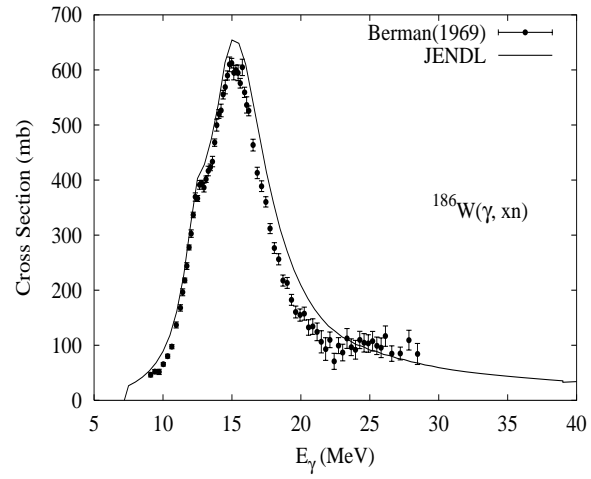
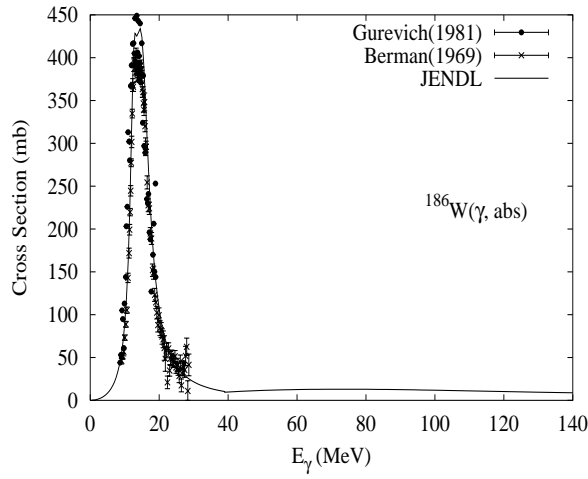


Abundance (%)	Threshold Energies (MeV)								
	$\gamma, n$	$\gamma, p$	$\gamma, t$	$\gamma, \text{He-3}$	$\gamma, \alpha$	$\gamma, 2n$	$\gamma, np$	$\gamma, 2p$	$\gamma, 3n$
30.70	7.41	7.70	12.22	13.22	-1.66	13.60	14.63	14.23	21.67



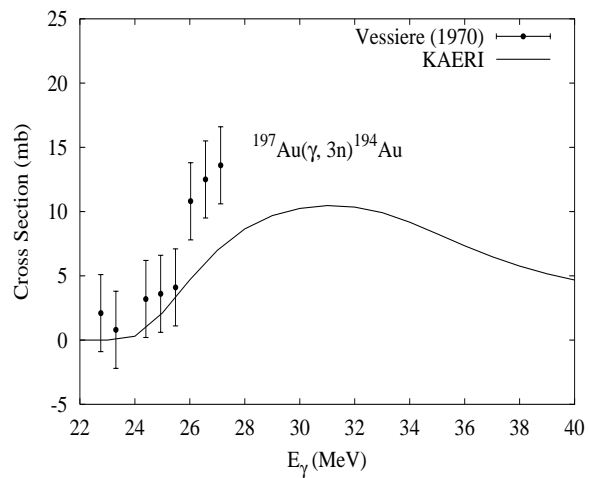
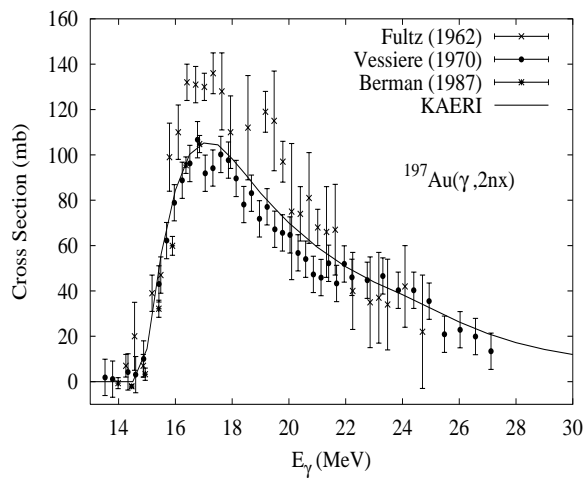
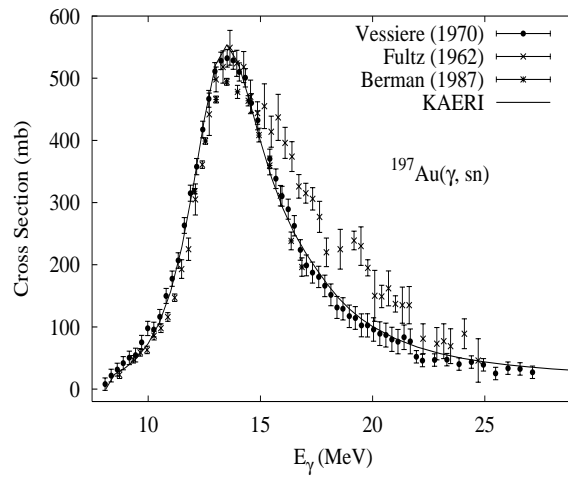
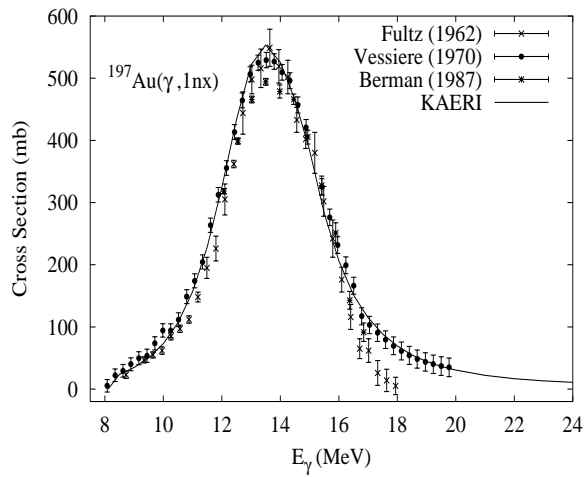
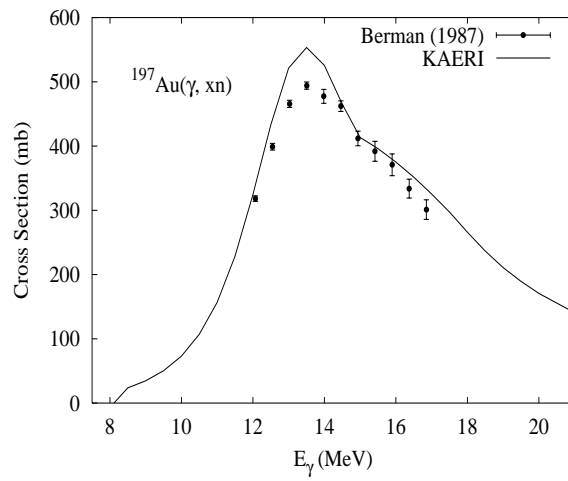
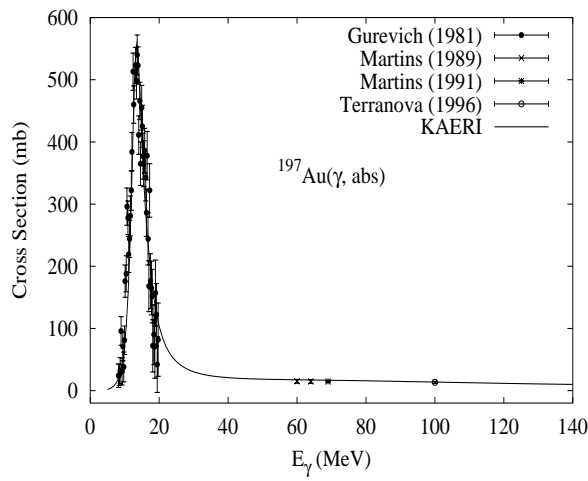
In the evaluation, the calculated photoabsorption cross section using GDR Lorentzian and QD parameters was modified slightly to better agree with the elemental tungsten photoabsorption cross section from Saclay [Vey75]. Use was made of the total Ta absorption cross section data of Lepretre et al [Lep81] to guide the QD model calculation of the absorption cross section, giving a Levinger parameter of  $L=6.7$ . (No such data exists for W, but we expect W and Ta experimental data to be similar). Good agreement was obtained with  $(\gamma, 1n)$  and  $(\gamma, 2n)$  elemental W experimental data from Saclay [Vey75], as well as neutron multiplicity data on Ta [Lep81]. The GNASH input parameter describing the preequilibrium exciton level density was modified to optimize agreement with the measured data.

Abundance (%)	Threshold Energies (MeV)								
	$\gamma, n$	$\gamma, p$	$\gamma, t$	$\gamma, \text{He-3}$	$\gamma, \alpha$	$\gamma, 2n$	$\gamma, np$	$\gamma, 2p$	$\gamma, 3n$
28.60	7.19	8.40	12.17	14.16	-1.12	12.95	15.03	15.59	20.36



Photonuclear reactions were evaluated using ALICE-F [Fuk93] code calculations together with experimental data. Input model parameters were adjusted so as to improve the quality of the calculated results compared with data [Gur81, Ber69b]. Photoabsorption was modeled as a sum of GDR and QD components [Cha91].

Abundance (%)	Threshold Energies (MeV)								
	$\gamma, n$	$\gamma, p$	$\gamma, t$	$\gamma, \text{He-3}$	$\gamma, \alpha$	$\gamma, 2n$	$\gamma, np$	$\gamma, 2p$	$\gamma, 3n$
100.00	8.07	5.78	11.33	13.56	-0.95	14.71	13.70	14.04	23.08

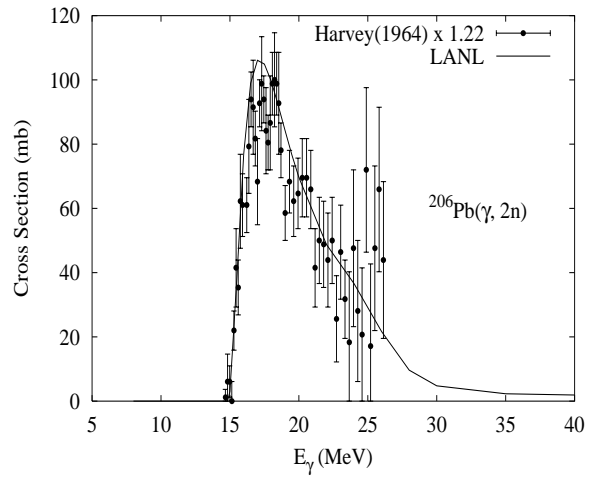
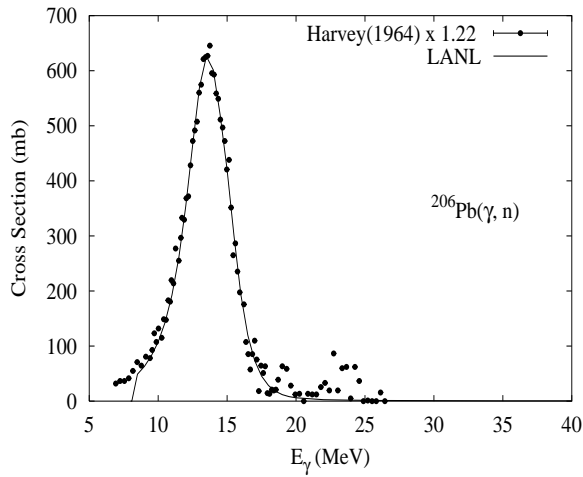
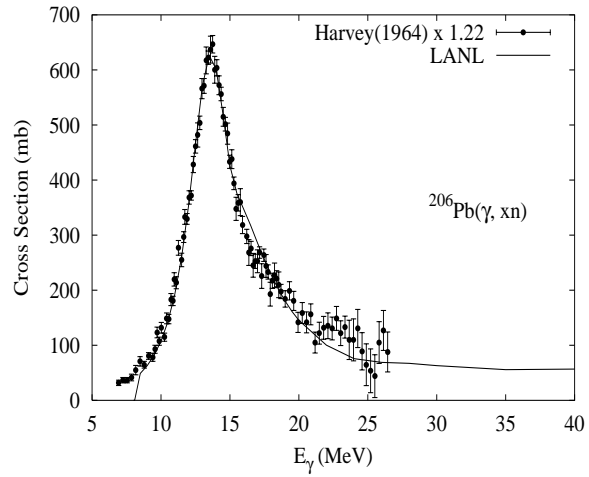
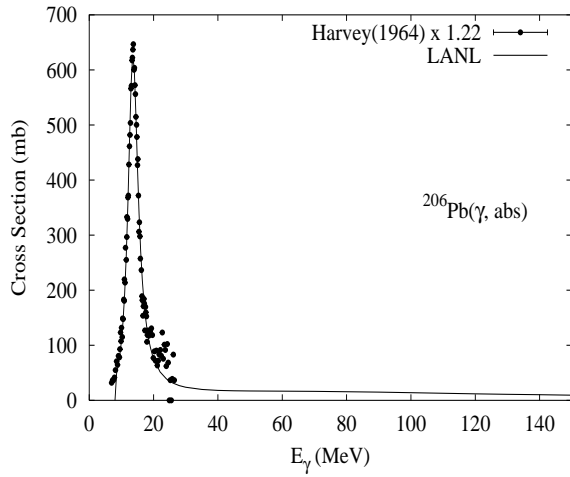


The experimental data for absorption cross section were given by Gurevich [Gur81], Terranova [Ter96] and Martins [Mar89, Mar91], respectively. Fultz [Ful62b], Veyssiere [Vey70] and Berman [Ber87] measured the  $(\gamma, 1nx)$ ,  $(\gamma, 2nx)$  and  $(\gamma, sn)$  reaction cross sections. Berman also gave the experimental data of  $(\gamma, sn)$  reaction cross section. Among these data, Veyssiere's and

Fultz's data have good agreement in their magnitudes of the  $(\gamma, \text{sn})$  cross sections. We relied on the GUNF and GNASH codes to infer the photoabsorption cross section in the GDR regime, in order to model accurately Veyssiere's  $(\gamma, \text{sn})$  data. The photoabsorption cross section above the GDR, up to 140 MeV, was obtained from QD model calculations using the theory of Chadwick.

The calculated results of the emission channels by the GNASH code are in overall agreement with the absorption cross sections data of Gurevich, Terranova and Martins, and in good agreement with the  $(\gamma, 1\text{nx})$ ,  $(\gamma, 2\text{nx})$  and  $(\gamma, 3\text{nx})$  data of Veyssiere.

Abundance (%)	Threshold Energies (MeV)								
	$\gamma, n$	$\gamma, p$	$\gamma, t$	$\gamma, \text{He-3}$	$\gamma, \alpha$	$\gamma, 2n$	$\gamma, np$	$\gamma, 2p$	$\gamma, 3n$
24.10	8.09	7.25	12.97	13.45	-1.14	14.82	14.80	13.67	23.21

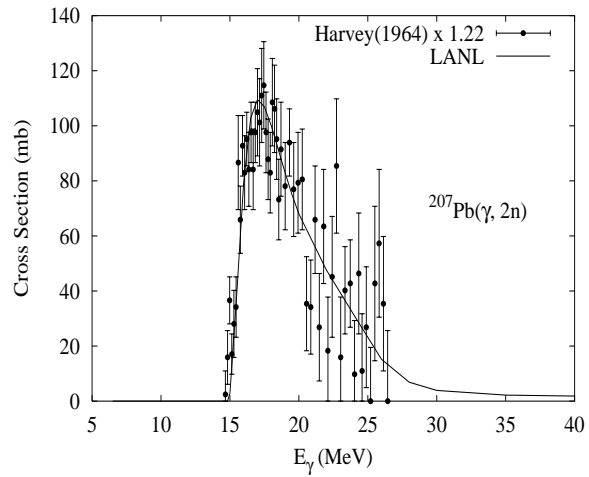
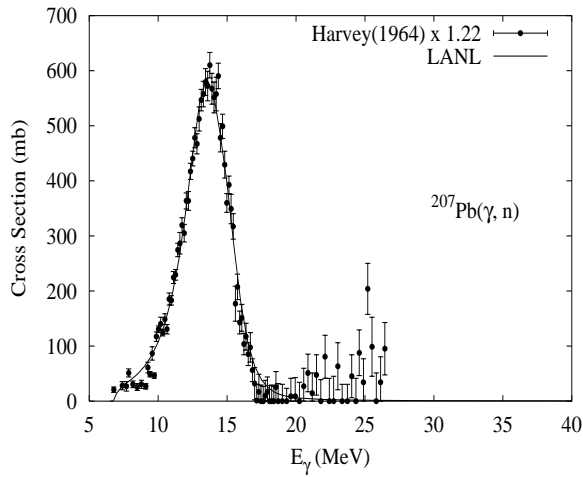
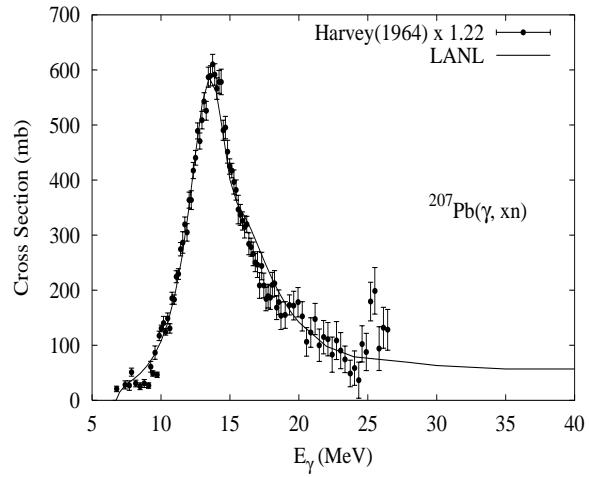
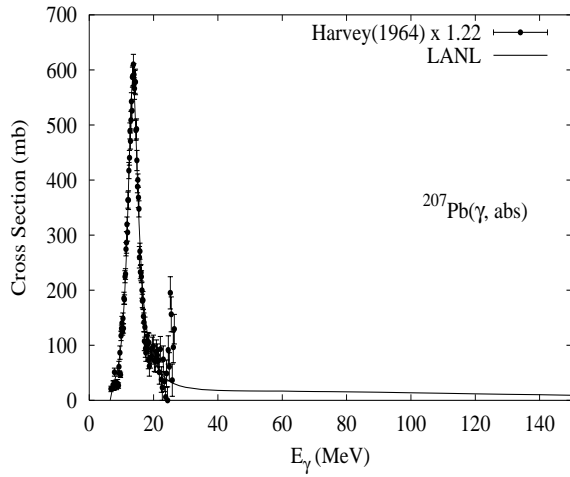


For photonuclear reactions on lead, there are systematic differences between some of the important measurements of neutron production. Specifically, the results from Saclay are significantly higher than those from Livermore. Berman [Ber87] concluded that the earlier Livermore measurements on lead [Har64] were too low. We have adopted Berman's view that the Livermore [Har64] data for  ${}^{206}\text{Pb}$  need to be renormalized up by 22%.

Thus, photoabsorption was evaluated based on the GDR parameters given by Dietrich and Berman [Die88], which were a fit to Harvey's data [Har64], but the peak was increased by 22%. Above the GDR, in the QD regime, we then evaluated the absorption cross section up to 150 MeV based on model calculations [Cha91].

The GNASH calculations gave results for the  $(\gamma, 1n)$ ,  $(\gamma, 2n)$ , and  $(\gamma, xn)$  cross sections that were in excellent agreement with the data [Har64], after it was also scaled by 22%.

Abundance (%)	Threshold Energies (MeV)								
	$\gamma, n$	$\gamma, p$	$\gamma, t$	$\gamma, \text{He-3}$	$\gamma, \alpha$	$\gamma, 2n$	$\gamma, np$	$\gamma, 2p$	$\gamma, 3n$
22.10	6.74	7.49	13.06	12.69	-0.39	14.83	13.99	14.74	21.56

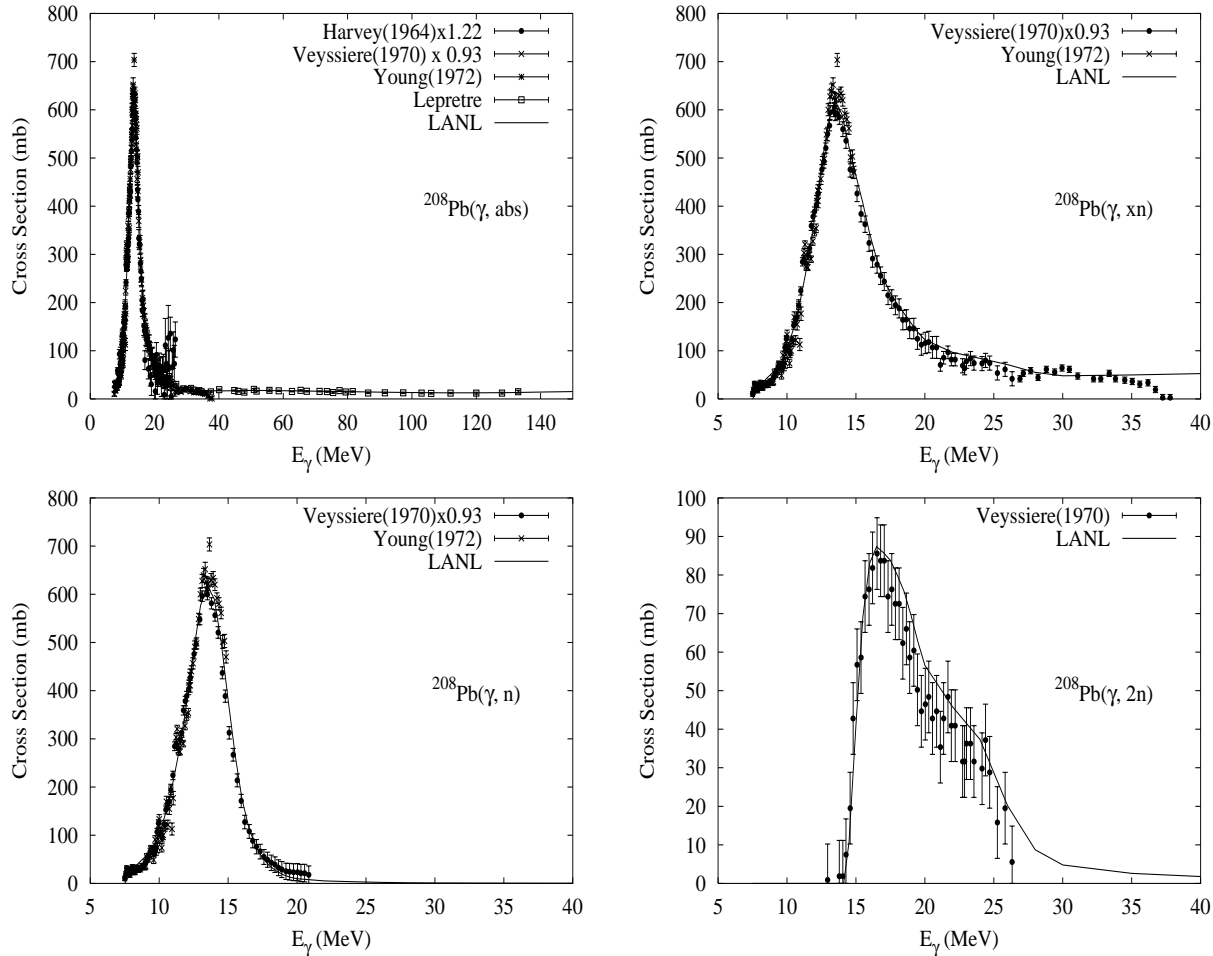


For photonuclear reactions on lead, there are systematical differences between some of the important measurements of neutron production. Specifically, the results from Saclay are significantly higher than those from Livermore. Berman [Ber87] concluded that the earlier Livermore measurements on lead [Har64] were too low. We have adopted Berman's view that the Livermore [Har64] data for  ${}^{207}\text{Pb}$  need to be renormalized up by 22%.

Thus, photoabsorption was evaluated based on the GDR parameters given by Dietrich and Berman [Die88] which were a fit to Harvey's data [Har64], but the peak was increased by 22%. Above the GDR, in the QD regime, we then evaluated the absorption cross section up to 150 MeV based on model calculations [Cha91].

The GNASH calculations gave results for the  $(\gamma, 1n)$ ,  $(\gamma, 2n)$ , and  $(\gamma, xn)$  cross sections that were in excellent agreement with the data [Har64], after it was also scaled by 22%.

Abundance (%)	Threshold Energies (MeV)								
	$\gamma, n$	$\gamma, p$	$\gamma, t$	$\gamma, \text{He-3}$	$\gamma, \alpha$	$\gamma, 2n$	$\gamma, np$	$\gamma, 2p$	$\gamma, 3n$
52.40	7.37	8.01	12.88	14.39	-0.52	14.11	14.85	15.38	22.19



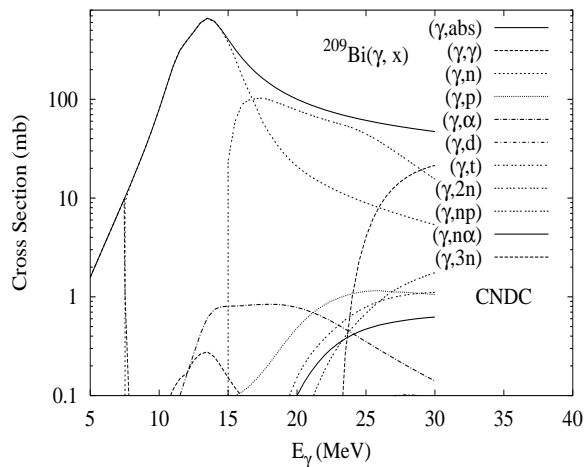
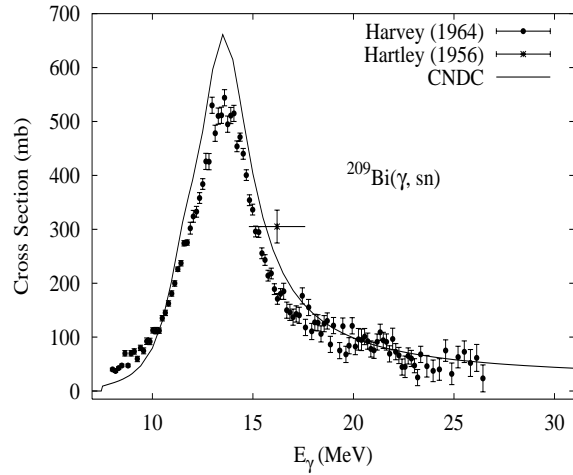
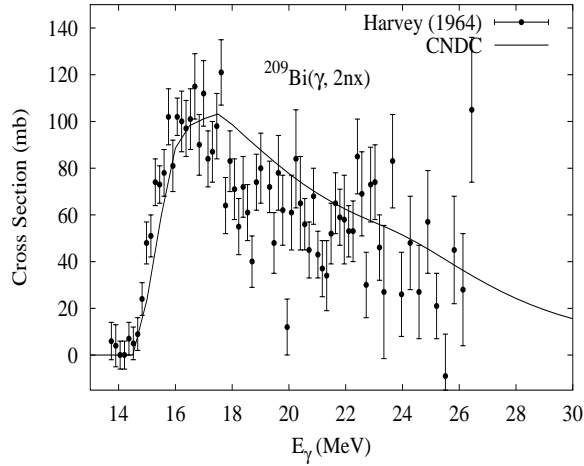
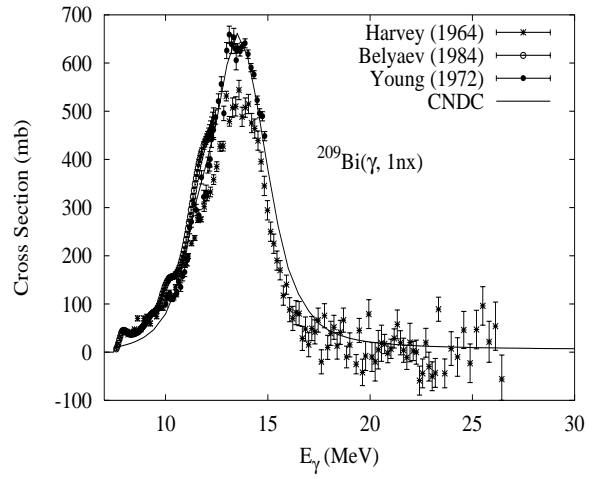
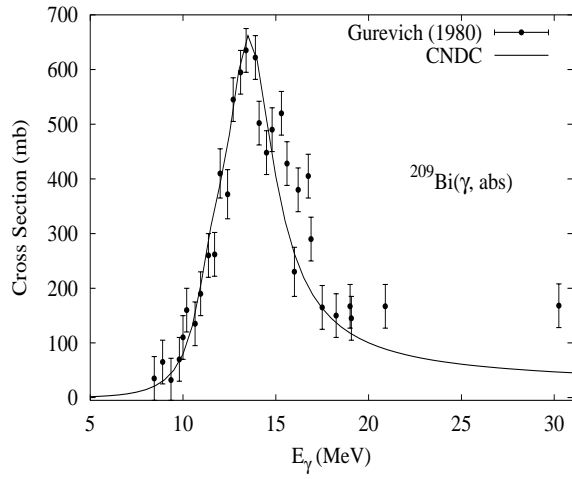
For photonuclear reactions on lead, there are systematic differences between some of the important measurements of neutron production. Specifically, the results from Saclay are significantly higher than those from Livermore. Berman [Ber87] concluded that the earlier Livermore measurements on lead [Har64] were too low. We have adopted Berman's view that the Saclay data [Vey70] need to be renormalized down by 7%, and the Livermore [Har64] data for  ${}^{208}\text{Pb}$  need to be renormalized up by 22%. The photoabsorption cross section was calculated from a Lorentzian line shape modified on the low-energy tail where deviations from experimental data are seen. Above the GDR, in the QD regime, we then evaluated the absorption cross section up to 150 MeV based on experimental data [Lep81] and model calculations [Cha91].

Our resulting evaluation is in good agreement with (renormalized) data [Har64, Vey70, You72, Lep81] for neutron production and for the photonuclear absorption cross section up to 150 MeV. Our results for  $(\gamma, 1n)$ ,  $(\gamma, 2n)$ ,  $(\gamma, 3n)$  reactions exhibit the following features:  $(\gamma, 1n)$  is in good agreement with data [Vey70, You72, Ber87];  $(\gamma, 2n)$  agrees reasonably with data [Vey70, You72] though appears somewhat high in the 17-25 MeV range;  $(\gamma, 3n)$  agrees reasonably with data [Vey70], though appears somewhat low in the 25-30 MeV range. We attempted to improve agreement with the  $(\gamma, 2n)$  and  $(\gamma, 3n)$  measurements but were unable to do so using a consistent set of input model parameters.

We have also compared [Cha95a] calculated multiplicities for neutron and proton emission with the measurements of Lepretre [Lep82](See Fig. 4.3 in Sec. 4.2.3). Our calculations describe the correct partitioning of ejectiles among preequilibrium and equilibrium emission, and between neutrons and protons. These measurements are invaluable for testing the preequilibrium modeling in our calculation, since direct measurements of the nucleon emission spectra from monoenergetic photons do not exist for lead. The large Coulomb barrier in lead is responsible for the excess of fast preequilibrium neutrons compared to protons; at the highest energies the differences are reduced. In general the slow neutron multiplicity is much larger than the fast reaction multiplicities, since preequilibrium decay accounts for at most the first two emissions, with the subsequent sequential particle decays coming from compound-nucleus emission.

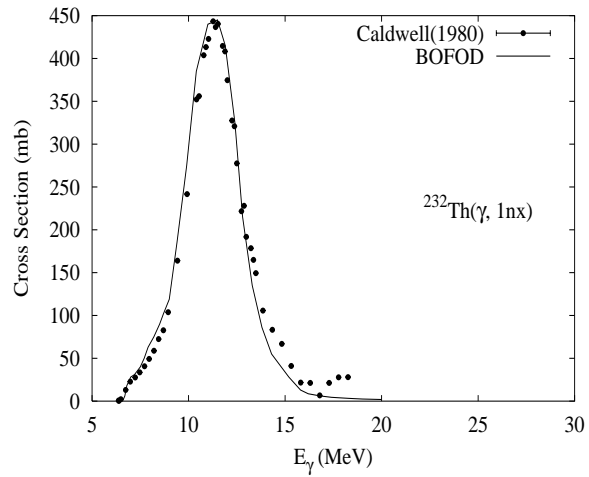
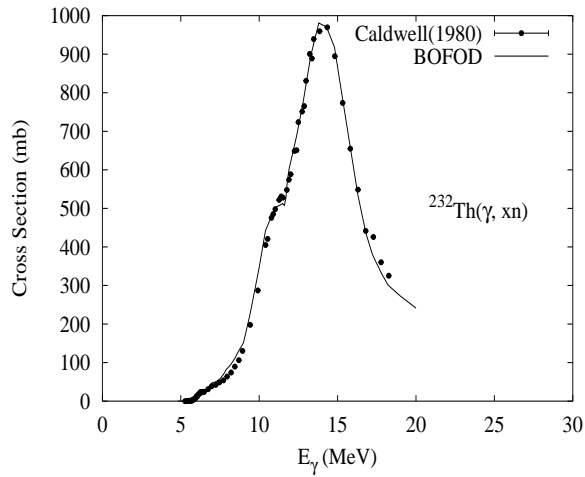
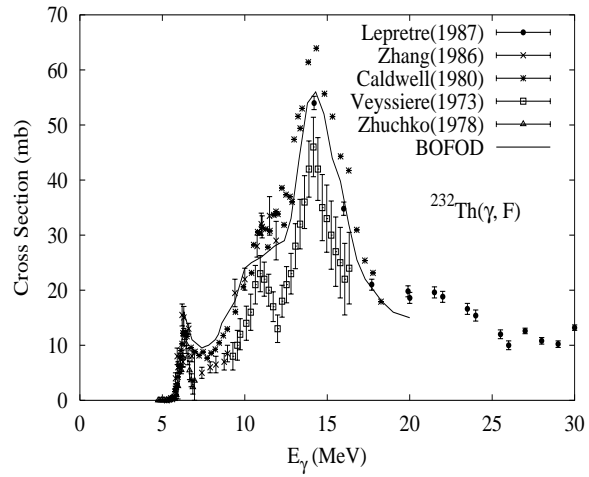
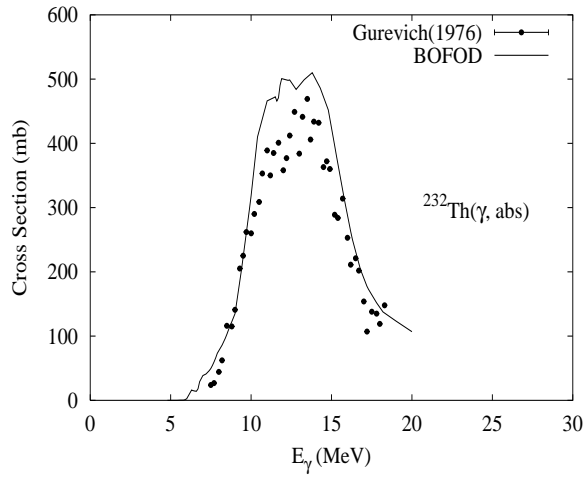


Abundance (%)	Threshold Energies (MeV)								
	$\gamma, n$	$\gamma, p$	$\gamma, t$	$\gamma, \text{He-3}$	$\gamma, \alpha$	$\gamma, 2n$	$\gamma, np$	$\gamma, 2p$	$\gamma, 3n$
100.00	7.46	3.80	9.42	10.94	-3.14	14.35	11.17	11.81	22.44



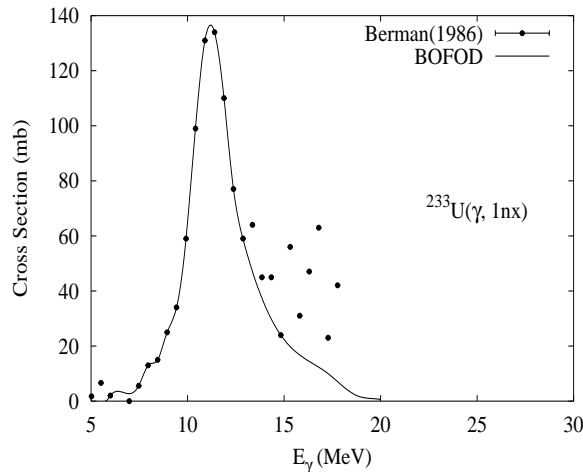
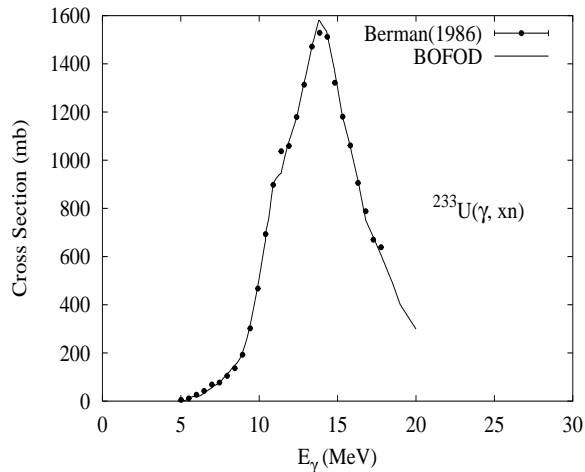
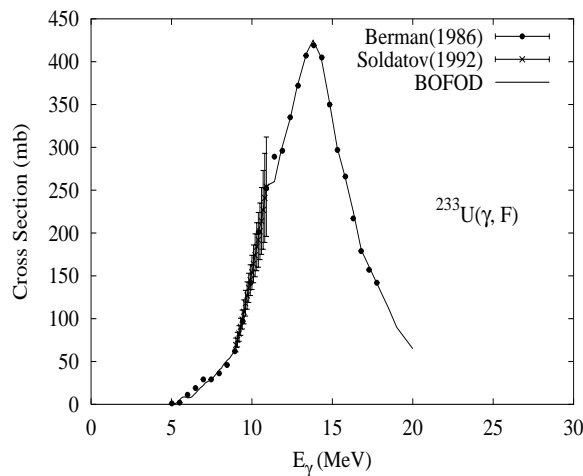
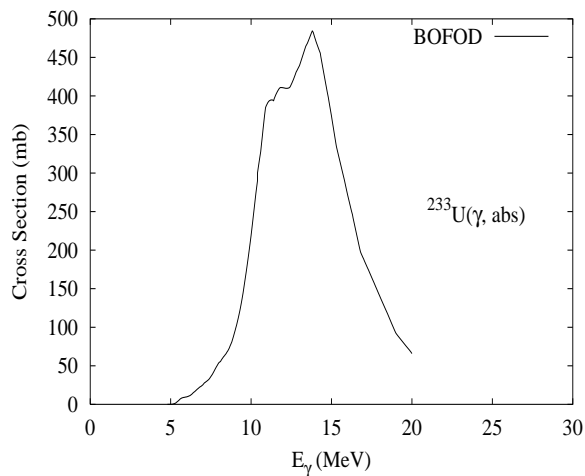
The photoabsorption [Gur80], as well as the photonuclear cross sections for  $(\gamma, 1nx)$ ,  $(\gamma, 2nx)$ ,  $(\gamma, xn)$ , and  $(\gamma, sn)$  reactions [Har64, Bel85, You72] were measured. We relied on GUNF code [Zha98] to infer the photoabsorption cross section in the GDR regime, in order to model accurately the experimental data [Gur80, Har64].

Abundance (%)	Threshold Energies (MeV)								
	$\gamma, n$	$\gamma, p$	$\gamma, t$	$\gamma, \text{He-3}$	$\gamma, \alpha$	$\gamma, 2n$	$\gamma, np$	$\gamma, 2p$	$\gamma, 3n$
100.00	6.44	7.75	10.41	12.15	-4.08	11.56	13.31	13.25	18.35



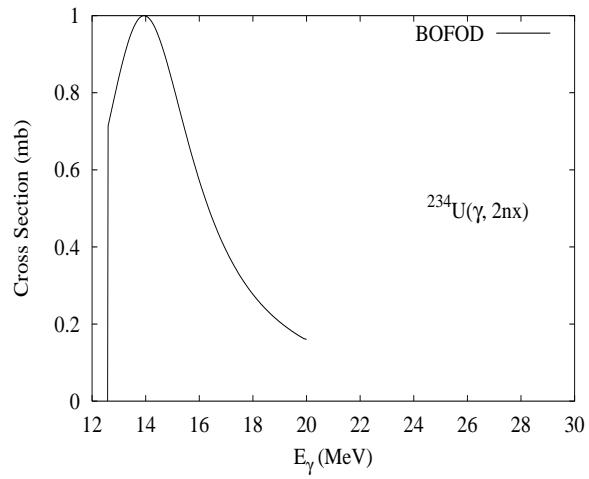
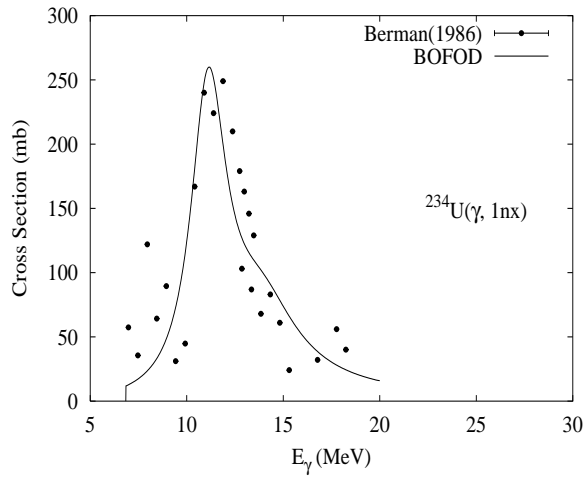
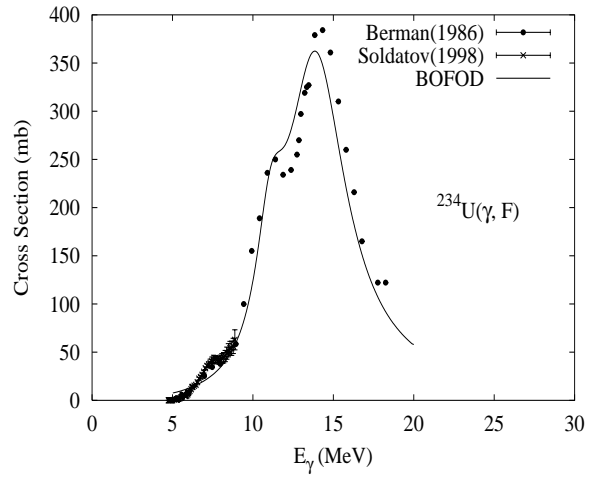
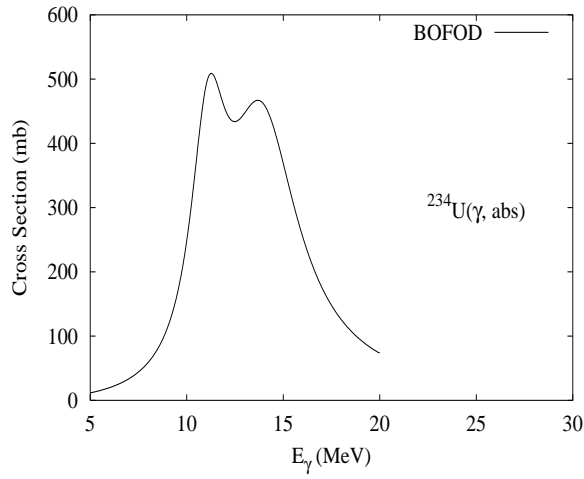
Experimental information is available for the photoabsorption [Gur76], photofission [Vey73, Cal80a, Zha86, Zhu78b, Lep87], and  $(\gamma, xn)$ ,  $(\gamma, 1nx)$ , and  $(\gamma, 2nx)$  cross sections [Cal80a, Vey73]. For a complete reference list of photofission cross sections see [Blo99a]. The photofission cross section presents large differences between some of the important measurements, in the energy range below 10 MeV. In the GDR range there are systematical differences between the Livermore [Cal80a] and the Saclay data [Vey73]. The evaluation adopted the Saclay data for photon-neutron production as reference, in order to obtain the relevant parameters of the statistical model [Blo99b]. The widths for radiative, neutron and fission decays were taken from the description of the photofission cross section below 6 MeV [Sto97]. The calculated results are in good agreement with the experimental data for  $(\gamma, xn)$ ,  $(\gamma, 1nx)$  and  $(\gamma, 2nx)$  reactions [Cal80a].

Abundance (%)	Threshold Energies (MeV)								
	$\gamma, n$	$\gamma, p$	$\gamma, t$	$\gamma, \text{He-3}$	$\gamma, \alpha$	$\gamma, 2n$	$\gamma, np$	$\gamma, 2p$	$\gamma, 3n$
0.00	5.74	6.30	10.20	8.88	-4.91	13.01	11.87	11.48	18.90



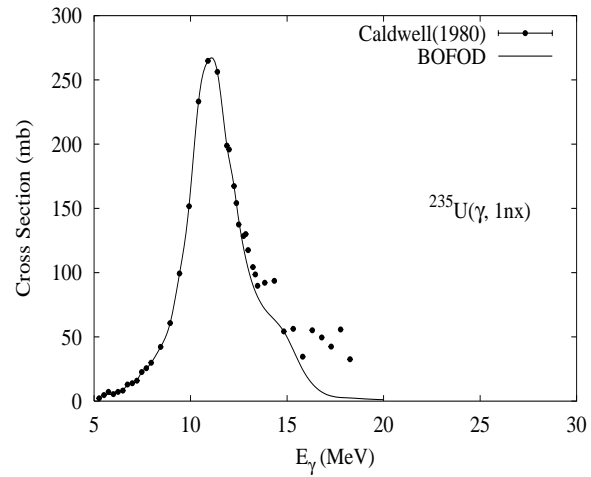
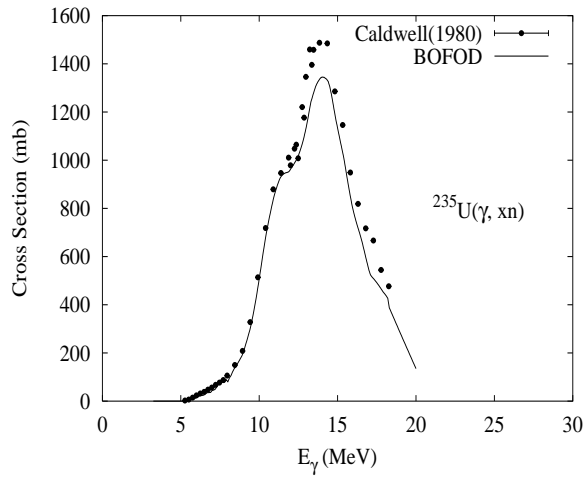
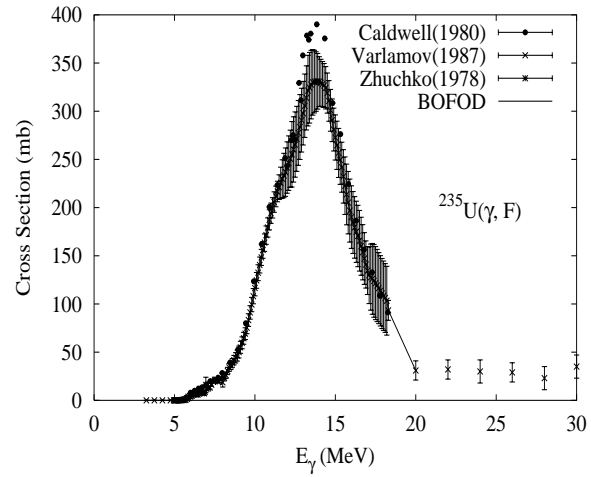
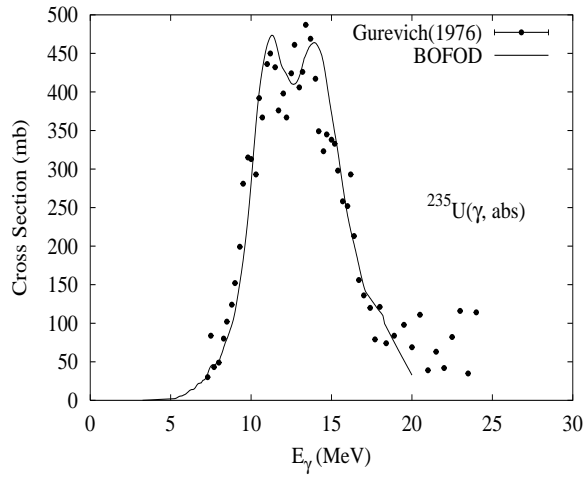
Experimental information is available for the photofission,  $(\gamma, xn)$ , and  $(\gamma, 1nx)$  cross sections [Ber86]. For a complete reference list of photofission cross sections see [Blo99a]. The evaluation adopted the Livermore data for photofission and photoneutron production as reference, in order to obtain the relevant parameters of the statistical model [Blo99b]. The widths for radiative, neutron and fission decays were taken from the description of the photofission cross section below 10 MeV [Sol92]. The calculated results are in good agreement with the experimental data for photofission and photoneutron production [Ber86] in the GDR region. Below 10 MeV the calculated results agree well with experimental data from [Sol92].

Abundance (%)	Threshold Energies (MeV)								
	$\gamma, n$	$\gamma, p$	$\gamma, t$	$\gamma, \text{He-3}$	$\gamma, \alpha$	$\gamma, 2n$	$\gamma, np$	$\gamma, 2p$	$\gamma, 3n$
0.01	6.84	6.63	10.23	10.60	-4.86	12.59	13.14	11.88	19.85



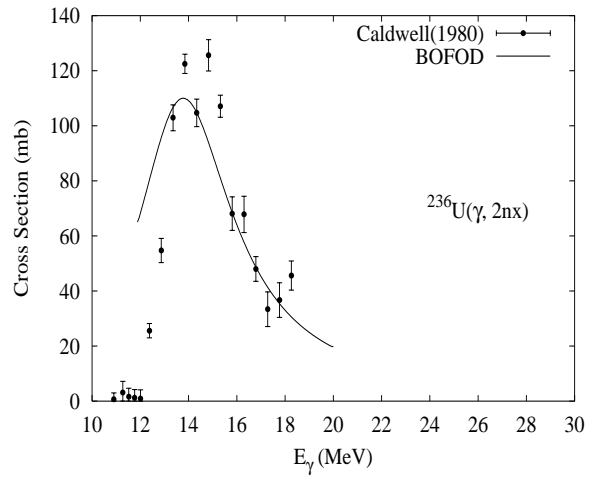
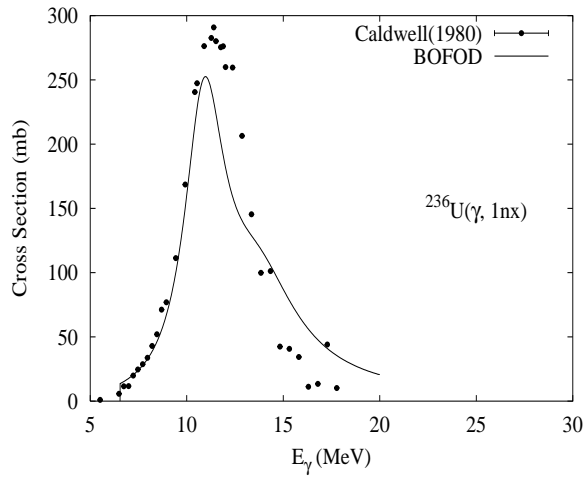
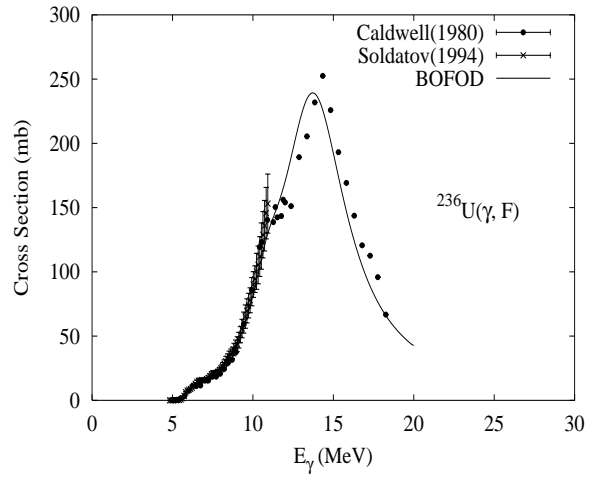
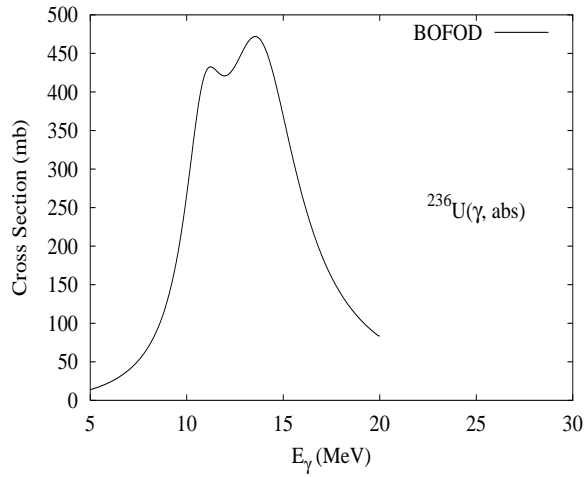
Experimental information is available for the photofission [Sol98, Ber86],  $(\gamma, xn)$ , and  $(\gamma, 1nx)$  cross sections [Ber86]. For a complete reference list of photofission cross sections see [Blo99a]. The evaluation adopted the Livermore data for photofission and photoneutron production as reference, in order to obtain the relevant parameters of the statistical model [Blo99b]. The widths for radiative, neutron and fission decays were taken from the description of the photofission cross section below 9 MeV [Sol98]. The calculated results are in good agreement with the experimental data for photofission and photoneutron production [Ber86] in the GDR region. Below 10 MeV the calculated results agree well with experimental data from [Sol98].

Abundance (%)	Threshold Energies (MeV)								
	$\gamma, n$	$\gamma, p$	$\gamma, t$	$\gamma, \text{He-3}$	$\gamma, \alpha$	$\gamma, 2n$	$\gamma, np$	$\gamma, 2p$	$\gamma, 3n$
0.72	5.30	6.71	9.96	9.46	-4.68	12.14	11.93	12.39	17.89



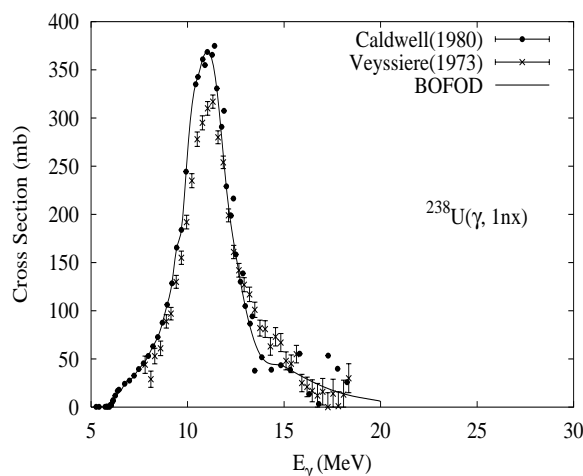
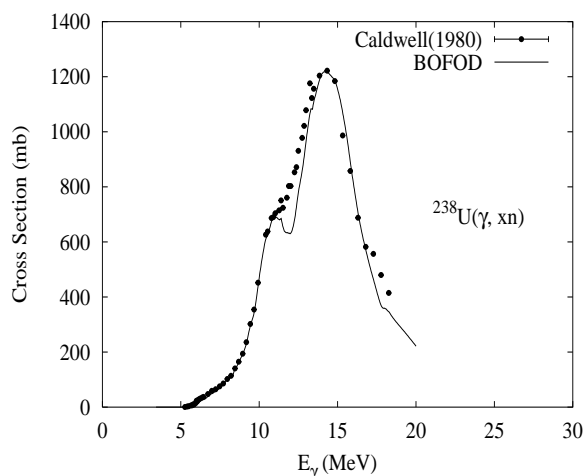
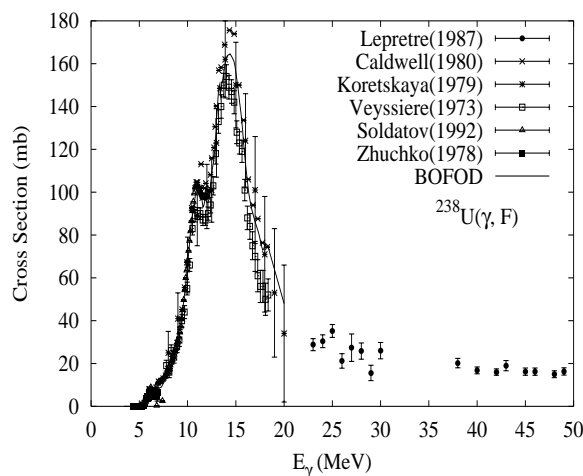
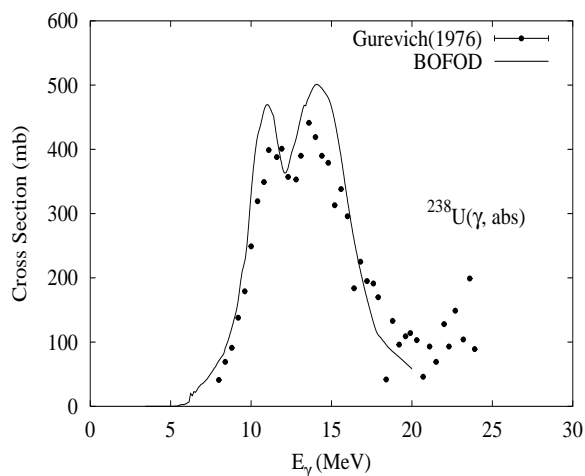
Experimental information is available for the photoabsorption [Gur76], photofission [Cal80b, Cal80a, Zhu78b],  $(\gamma, xn)$ , and  $(\gamma, 1nx)$  cross sections [Cal80a]. For a complete reference list of photofission cross sections see [Blo99a]. The evaluation adopted the Caldwell's data for the  $(\gamma, 1nx)$ , and Varlamov's photofission data as reference below 14 MeV, in order to obtain the relevant parameters of the statistical model [Blo99b]. The widths for radiative, neutron and fission decays were taken from the description of the  $(\gamma, 1nx)$  cross section below 14 MeV [Cal80a].

Abundance (%)	Threshold Energies (MeV)								
	$\gamma, n$	$\gamma, p$	$\gamma, t$	$\gamma, \text{He-3}$	$\gamma, \alpha$	$\gamma, 2n$	$\gamma, np$	$\gamma, 2p$	$\gamma, 3n$
0.00	6.55	7.18	9.99	11.22	-4.57	11.84	13.25	12.74	18.69



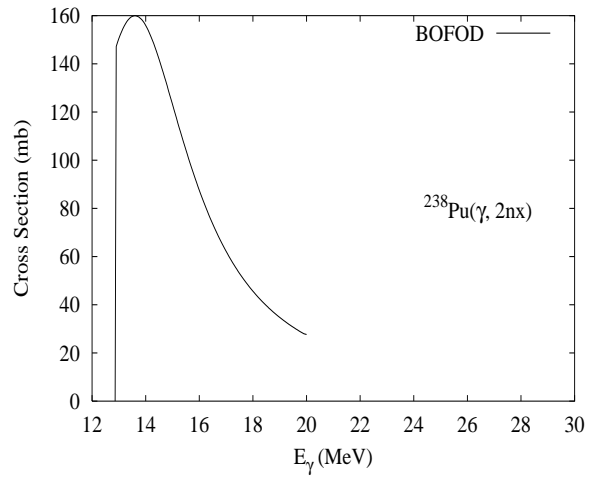
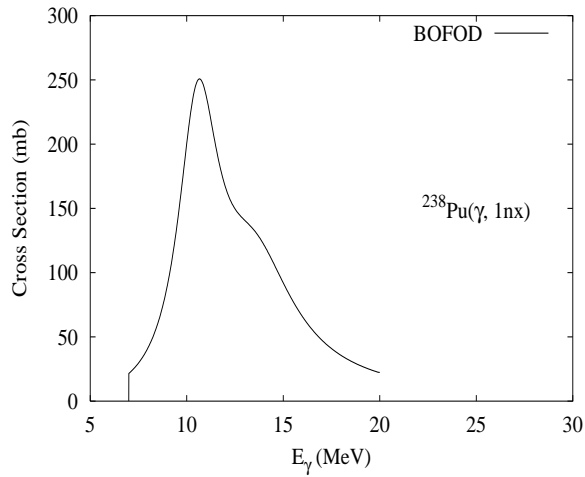
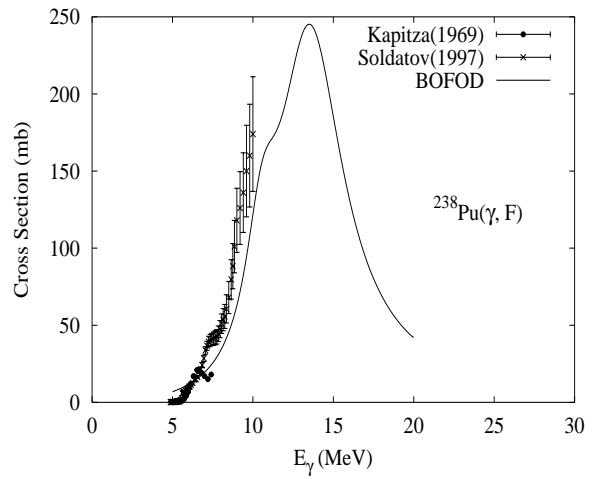
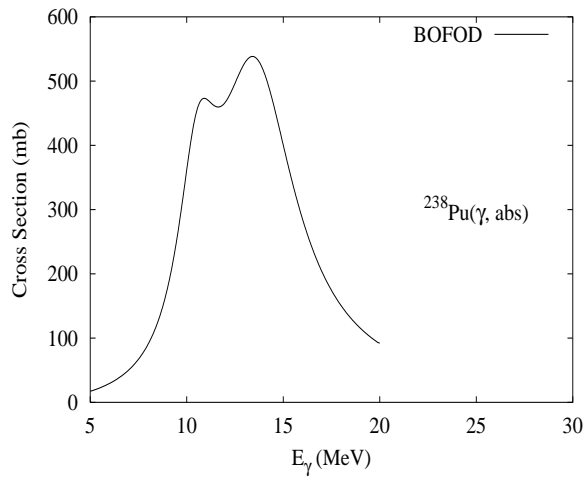
Experimental information is available for the photofission [Cal80b, Cal80a, Zhu78b, Zhu78a, Rud88, Sol94],  $(\gamma, xn)$ ,  $(\gamma, 1nx)$ , and  $(\gamma, 2nx)$  cross sections [Cal80a]. For a complete reference list of photofission cross sections see [Blo99a]. The evaluation adopted the Livermore data for  $(\gamma, 1nx)$  [Cal80a], and both the Livermore and Obninsk data for photofission [Cal80a, Sol94] as reference below 12 MeV, in order to obtain the relevant parameters of the statistical model [Blo99b]. The widths for radiative, neutron and fission decays were taken from the description of the photofission cross section below 10 MeV [Sol94]. The calculated results are in good agreement with the experimental data for photofission [Cal80a, Sol94], and for  $(\gamma, xn)$ ,  $(\gamma, 1nx)$ , and  $(\gamma, 2nx)$  cross sections below 12 MeV. In the 12 to 14 MeV range the evaluated data for the photoneutron production are lower than the experiment.

Abundance (%)	Threshold Energies (MeV)								
	$\gamma, n$	$\gamma, p$	$\gamma, t$	$\gamma, \text{He-3}$	$\gamma, \alpha$	$\gamma, 2n$	$\gamma, np$	$\gamma, 2p$	$\gamma, 3n$
99.27	6.15	7.62	9.97	11.88	-4.27	11.28	13.39	13.01	17.82



Experimental information is available for the photoabsorption [Gur76], photofission [Vey73, Cal80b, Cal80a, Zhu78b, Sol92], and  $(\gamma, xn)$ ,  $(\gamma, 1nx)$ , and  $(\gamma, 2nx)$  cross sections [Cal80a, Vey73]. For a complete reference list of reaction cross sections see [Blo99a]. The evaluation adopted the Livermore data for  $(\gamma, 1nx)$  and  $(\gamma, xn)$  [Cal80a], and both the Livermore and Obninsk data for photofission [Cal80a] and [Sol92] as reference below 14 MeV, in order to obtain the relevant parameters of the statistical model [Blo99b]. The widths for radiative, neutron and fission decays were taken from the description of the  $(\gamma, 1nx)$  cross section below 14 MeV [Cal80a], and the photofission cross section below 10 MeV [Sol92]. In general, the results are in reasonable agreement with experimental data [Gur76] for photoabsorption cross section and for  $(\gamma, xn)$ ,  $(\gamma, 1nx)$ ,  $(\gamma, 2nx)$  and  $(\gamma, F)$  reactions for gamma-ray energy below 20 MeV.

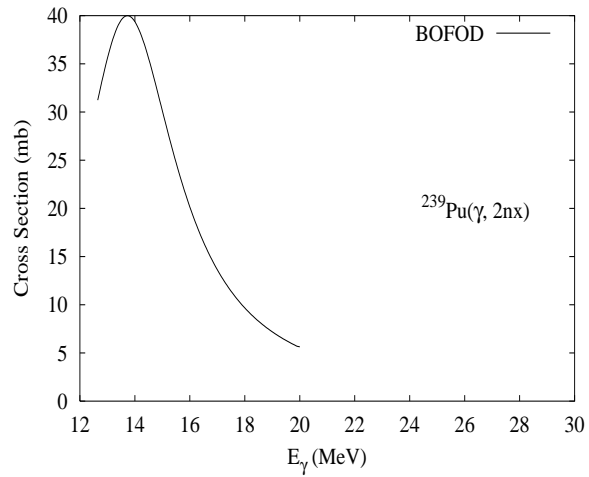
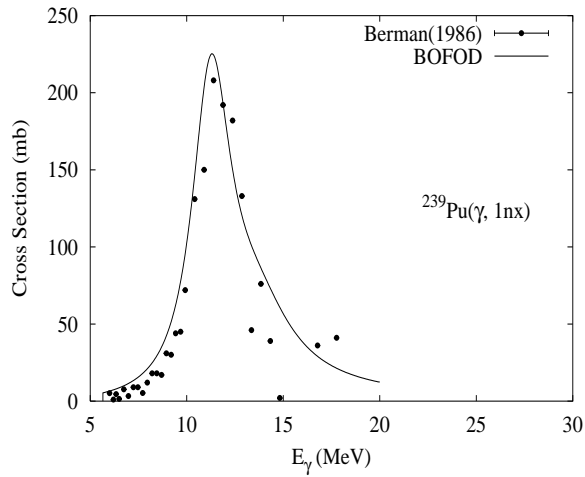
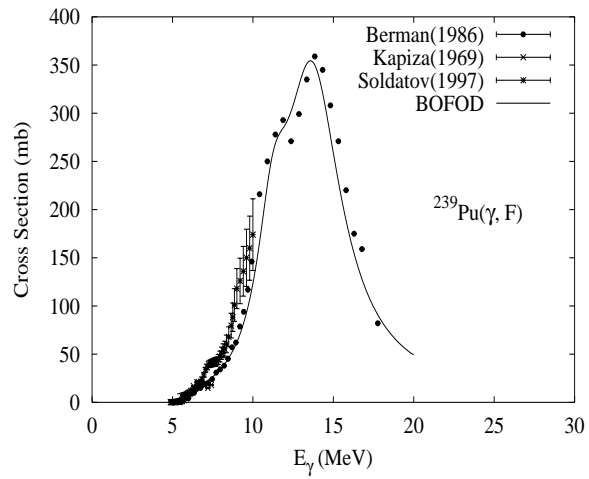
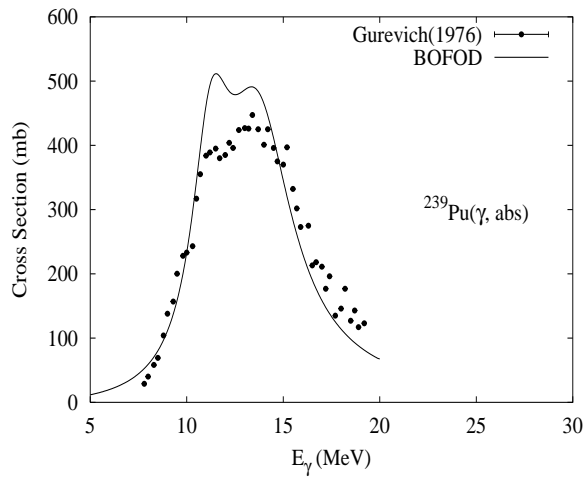
Abundance (%)	Threshold Energies (MeV)								
	$\gamma, n$	$\gamma, p$	$\gamma, t$	$\gamma, \text{He-3}$	$\gamma, \alpha$	$\gamma, 2n$	$\gamma, np$	$\gamma, 2p$	$\gamma, 3n$
0.00	7.00	6.00	9.83	9.69	-5.59	12.86	12.57	10.86	20.21



There are two measurements of the photofission cross sections [Kap69, Sol97]. The evaluation used statistical model parameters based on a systematics of neighboring nuclei [Blo99b]. The radiative-decay, neutron and fission widths were taken from description of  $(\gamma, F)$  reaction [Sol97] below 10 MeV.

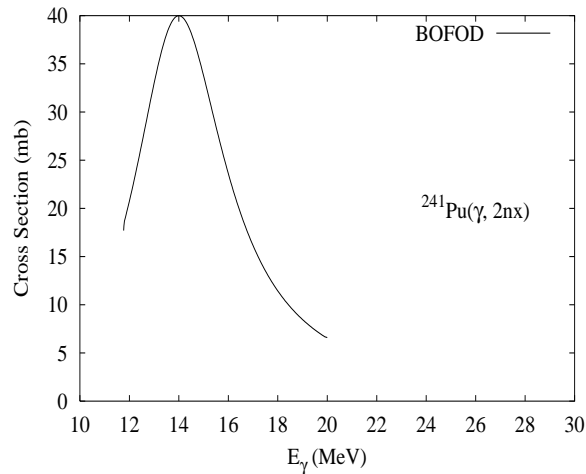
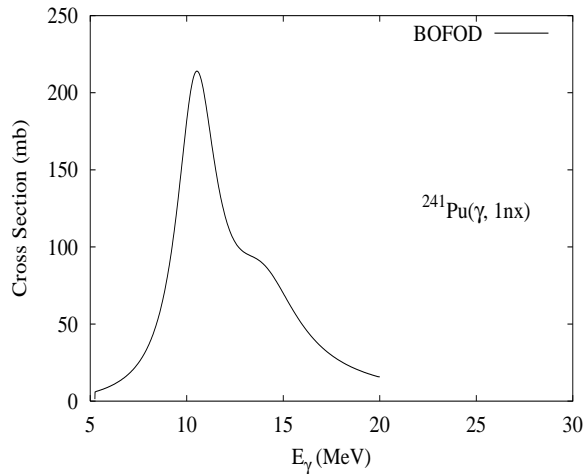
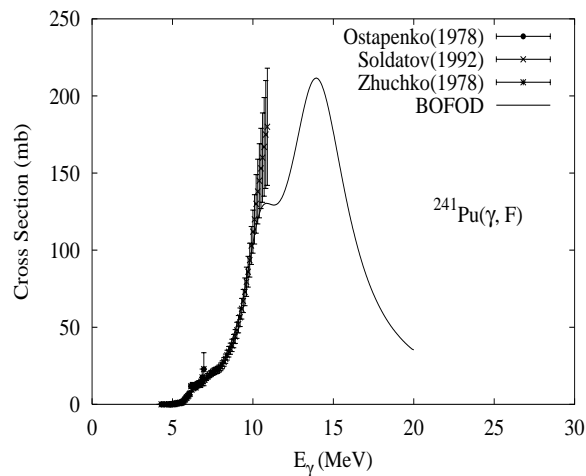
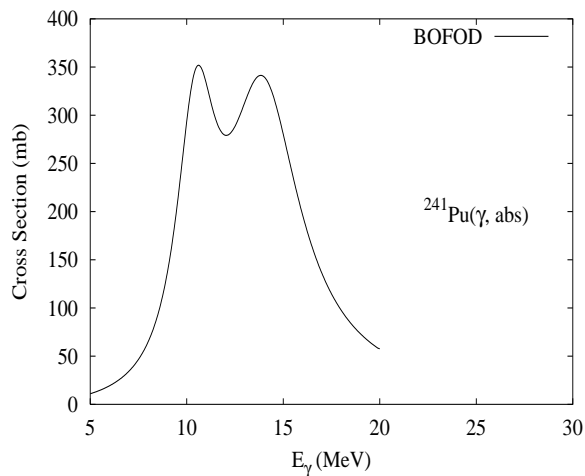


Abundance (%)	Threshold Energies (MeV)								
	$\gamma, n$	$\gamma, p$	$\gamma, t$	$\gamma, \text{He-3}$	$\gamma, \alpha$	$\gamma, 2n$	$\gamma, np$	$\gamma, 2p$	$\gamma, 3n$
0.00	5.65	6.16	9.74	8.79	-5.24	12.65	11.64	11.38	18.51



Experimental information is available for the photoabsorption [Gur76], photofission ([Ber86, Zhu78b, Sol92], and  $(\gamma, xn)$ ,  $(\gamma, 1nx)$ , and  $(\gamma, 2nx)$  cross sections [Ber86]. For a complete reference list of photofission cross sections see [Blo99a]. The evaluation adopted the Livermore data for photoneutron production as reference, in order to obtain the relevant parameters of the statistical model [Blo99b]. The widths for radiative, neutron and fission decays were taken from the description of the photofission cross section below 10 MeV [Sol92].

Abundance (%)	Threshold Energies (MeV)								
	$\gamma, n$	$\gamma, p$	$\gamma, t$	$\gamma, \text{He-3}$	$\gamma, \alpha$	$\gamma, 2n$	$\gamma, np$	$\gamma, 2p$	$\gamma, 3n$
0.00	5.24	6.66	9.45	9.29	-5.14	11.78	11.72	12.20	17.42



Experimental information is available only for the photofission cross section [Sol92, Zhu78a, Ost78]. The evaluation adopted both the Soldatov and Zhuchko data [Sol92, Zhu78a] for photofission below 12 MeV as reference, in order to obtain the relevant parameters of the statistical model [Blo99b]. The widths for radiative, neutron and fission decays were taken from the description of the photofission cross section below 10 MeV [Sol92].